Predictive cognition in dementia:

the case of music

A thesis submitted to University College London for the degree of

Doctor of Philosophy

Elia Benhamou

Dementia Research Centre

Institute of Neurology

University College London

2020

Declaration

I, Elia Benhamou, confirm that the work presented in this thesis is my own. Where information is derived from other sources, I confirm that this has been referenced appropriately.

Abstract and summary of experimental findings

The clinical complexity and pathological diversity of neurodegenerative diseases impose immense challenges for diagnosis and the design of rational interventions. To address these challenges, there is a need to identify new paradigms and biomarkers that capture shared pathophysiological processes and can be applied across a range of diseases. One core paradigm of brain function is predictive coding: the processes by which the brain establishes predictions and uses them to minimise prediction errors represented as the difference between predictions and actual sensory inputs. The processes involved in processing unexpected events and responding appropriately are vulnerable in common dementias but difficult to characterise. In my PhD work, I have exploited key properties of music – its universality, ecological relevance and structural regularity – to model and assess predictive cognition in patients representing major syndromes of frontotemporal dementia – non-fluent variant PPA (nfvPPA), semantic-variant PPA (svPPA) and behavioural-variant FTD (bvFTD) - and Alzheimer's disease relative to healthy older individuals.

In my first experiment, I presented patients with well-known melodies containing no deviants or one of three types of deviant - acoustic (white-noise burst), syntactic (key-violating pitch change) or semantic (key-preserving pitch change). I assessed accuracy detecting melodic deviants and simultaneously-recorded pupillary responses to these deviants. I used voxel-based morphometry to define neuroanatomical substrates for the behavioural and autonomic processing of these different types of deviants, and identified a posterior temporo-parietal network for detection of basic acoustic deviants and a more anterior fronto-temporo-striatal network for detection of syntactic pitch deviants. In my second chapter, I investigated the ability of patients to track the statistical structure of the same musical stimuli, using a computational model of the information dynamics of music to calculate the information-content of deviants (unexpectedness) and entropy of melodies (uncertainty). I related these information-theoretic metrics to performance for detection of deviants and to 'evoked' and 'integrative' pupil reactivity to deviants and melodies respectively and found neuroanatomical correlates in bilateral dorsal and ventral striatum, hippocampus, superior temporal gyri, right temporal pole and left inferior frontal gyrus. Together, chapters 3 and 4 revealed new hypotheses about the way FTD and AD pathologies disrupt the integration of predictive errors with predictions: a retained ability of AD patients to detect deviants at all levels of the hierarchy with a preserved autonomic sensitivity to information-theoretic properties of musical stimuli; a generalized impairment of surprise detection and statistical tracking of musical information at both a cognitive

and autonomic levels for svPPA patients underlying a diminished precision of predictions; the exact mirror profile of svPPA patients in nfvPPA patients with an abnormally high rate of false-alarms with up-regulated pupillary reactivity to deviants, interpreted as over-precise or inflexible predictions accompanied with normal cognitive and autonomic probabilistic tracking of information; an impaired behavioural and autonomic reactivity to unexpected events with a retained reactivity to environmental uncertainty in bvFTD patients.

Chapters 5 and 6 assessed the status of reward prediction error processing and updating via actions in bvFTD. I created pleasant and aversive musical stimuli by manipulating chord progressions and used a classic reinforcement-learning paradigm which asked participants to choose the visual cue with the highest probability of obtaining a musical 'reward'. bvFTD patients showed reduced sensitivity to the consequence of an action and lower learning rate in response to aversive stimuli compared to reward. These results correlated with neuroanatomical substrates in ventral and dorsal attention networks, dorsal striatum, parahippocampal gyrus and temporo-parietal junction. Deficits were governed by the level of environmental uncertainty with normal learning dynamics in a structured and binarized environment but exacerbated deficits in noisier environments. Impaired choice accuracy in noisy environments correlated with measures of ritualistic and compulsive behavioural changes and abnormally reduced learning dynamics correlated with behavioural changes related to empathy and theory-of-mind.

Together, these experiments represent the most comprehensive attempt to date to define the way neurodegenerative pathologies disrupts the perceptual, behavioural and physiological encoding of unexpected events in predictive coding terms.

Acknowledgments

First and foremost, I would like to thank all the patients and their families who participated in this research. Despite devastating illnesses, your dedication and your willingness to share your stories were extremely inspiring. I am also grateful to the healthy volunteers who kindly volunteered to participate in my studies.

I hold the deepest gratitude for my primary supervisor, Jason Warren, who was a constant, reliable and extremely kind source of support throughout this long and arduous journey. I cannot thank you enough for all the inspiring conversations we had and all the jewels of science, music, art and literature you helped me discover. I have learnt so much from you over the past few years and I really hope we will continue working together in the future. I would also like to thank my secondary supervisor, Gareth Barnes, who kindly introduced me to the MEG team, always made me feel welcome at the Functional Imaging Lab and offered invaluable advice on scientific methods and MEG experimental design and analysis. I am also very grateful for the informal mentorship and supervision of Dr Rimona Weil, Prof Jonathan Schott and Dr Bernadett Kalmar and a special thanks to Elizabeth Halton for her help at various stages of my PhD.

I could not have written this thesis without the support of my BBG colleagues and friends: Mai-Carmen Requena-Komuro, Janneke van Leuuwen, Harri Sivasathiaseelan, Chris Hardy, Jess Jiang and Jeremy Johnson. You are all incredible people, kind, curious, bright and always happy to help and give advice on all aspects of science or life. I consider myself extremely lucky to have met you all. I would also like to thank Lucy Russell, Caroline Greaves and Annabel Nelson who have worked tirelessly to ensure the smooth running of research visits. Many other colleagues at the Dementia Research Centre, the MEG lab, Monash University or the ICM in Paris have enriched my PhD experience, Dr Adeel Razi, Dr Tim Tierney, Dr Antonius Wiehler, Daniel Bates, Maggie Fraser, and I am grateful to all of them.

I would like to thank my friends outside of work for all their support. I am so lucky to have you here in London, Marie, Roshan, Maxime, Mathilde, Sara, Kate, Shane, Soco, Chris, Becca and outside of London, Eleonore, Lucile, Alice, Lauren, Hamza, Sara and Anne-Juliette. Thank you so much for your patience and your invaluable source of advice and love.

Finally, none of this would have been possible without my partner and my family. Jeremy, thank you for everything. My sisters, Yael, Anna and Talia, you are models of integrity and I am so proud of you. Ely, Jill, Solal, Boaz and Noa, thank you for constantly filling me with amazement and admiration. I owe my deepest gratitude to my parents who have supported me unconditionally during this PhD and before, through all my endeavours. This thesis is dedicated to you.

Funding

I was supported for the duration of this work by a Brain Research UK PhD studentship in Clinical Neurosciences. This work was additionally funded by the Alzheimer's Society and supported by the National Institute for Health Research University College London Hospitals Biomedical Research Centre and the Wellcome Trust. The Dementia Research Centre is supported by Alzheimer's Research UK, the Brain Research UK, the Medical Research Council and the Wolfson Foundation. This work was undertaken at University College London Hospital/University College London, which receives a proportion of its funding from the Department of Health's NIHR Biomedical Research Centres funding scheme.

Table of Contents

List of figures

List of tables

Abbreviations

AD – Alzheimer's disease

AG – angular gyrus

BMRQ – Barcelona Music Reward Questionnaire

BPVS – British Picture Vocabulary Scale

bvFTD – behavioural variant frontotemporal dementia

C9orf72 – chromosome 9 open reading frame 72

CI – confidence interval

CSF – cerebrospinal fluid

DARTEL – diffeomorphic anatomical registration through exponentiated lie algebra

D-KEFS – Delis-Kaplan Executive Function System

EPI – echoplanar imaging

EX – sensitivity to the emotions of others component of RSMS

fMRI – functional magnetic resonance imaging

FTD – frontotemporal dementia

FTLD – frontotemporal lobar degeneration

FUS – fused in sarcoma

FWE – family-wise error

GDA – Graded Difficulty Arithmetic

GNT – Graded Naming Test

GRN – progranulin

HC – Healthy controls

IFG – inferior frontal gyrus

MAPT – microtubule associated protein tau

mIRI – modified Interpersonal Reactivity Index

MMSE – Mini Mental State Examination

MNI – Montreal Neurological Institute

MRI – magnetic resonance imaging

MTG – middle temporal gyrus

MTL – medial temporal lobe

NAc – nucleus accumbens

nfvPPA – nonfluent variant primary progressive aphasia

OFC – orbitofrontal cortex

PAL – Paired Associate Learning test

PPA – primary progressive aphasia

RMT – Recognition Memory Test

ROI – region of interest

RSMS – Revised Self-Monitoring Scale

SD – standard deviation

SMA – supplementary motor area

SMG – supramargincal gyrus

STG – superior temporal gyrus

svPPA – semantic variant primary progressive aphasia

TDP-43 – transactive response DNA binding protein 43

TIV – total intracranial volume

VBM – voxel-based morphometry

VOSP – Visual Object and Spatial Perception battery

WASI – Wechsler Abbreviated Scale of Intelligence

WMS – Wechsler Memory Scale

Epigraph

'This is what happens to us in music: first one has to learn to hear a figure and melody at all, to detect and distinguish it, to isolate it and delimit it as a separate life; then it requires some exertion and good will to tolerate it in spite of its strangeness, to be patient with its appearance and expression, and kind-hearted about its oddity; finally there comes a moment when we are used to it, when we wait for it, when we sense that we should miss it if it were missing: and now it continues to compel and enchant us relentlessly until we have become its humble and enraptured lovers who desire nothing better from the world than it and only it.'

Friedrich Nietzsche in *Human, all too human*, 1978

1 General introduction

1.1 Challenges in capturing pathophysiology in dementia

Dementia is an overall term for diseases characterized by chronic and progressive impairments of core cognitive function and/or behaviour that have a have a significant impact of daily life functioning. 46.8 million people live with dementia worldwide in 2020 and we estimate that one new case is detected every 3.2 seconds. Ageing is the most robust risk factor for dementia with 90% of dementia presenting after 65 years old. The mean age of the population is increasing every year and the number of people living with these diseases worldwide is expected to reach 75 million by 2030 and 131.5 million by 2050 (Paraskevaidi *et al.*, 2018). The major dementias that pose the global health and social crisis are manifestations of neurodegenerative diseases of later life, characterised by synaptic and neuronal loss. This loss is gradual and anatomically selective and most neurodegenerative diseases are 'proteinopathies' associated with the aggregation and accumulation of misfolded proteins. Clinical diagnosis relies on various tools and measures to detect the presence of neurodegeneration at the earliest stage and provide an early intervention. Yet, a few factors make this diagnosis very challenging and only 20-50% of cases are being accurately diagnosed in primary care in high-income countries. First, the onset of dementia is insidious and can occur very slowly. Unless the patient has an informant who continuously track these changes and find them suspicious, it is very unlikely that the patient will self-present at a cognitive dementia clinic. Secondly, rare neurodegenerative diseases such as primary progressive aphasias are often under-diagnosed or diagnosed vey late in the course of the disease because of the lack of specialized neurologists trained to recognize symptoms as pathological. It is thus difficult to assess the true prevalence of certain diseases like frontotemporal dementia (FTD) which shows a great discrepancy between the prevalence noted in a sample of over 85 years old (3%, Gislason *et al.*, 2003) and prevalence in post-mortem studies (42%, Snowden *et al.*, 2011). In general, clinical presentations dominated by personality change or aphasia are likely to be misdiagnosed as psychiatric illness (~50% of behavioural-variant frontotemporal dementia receive a prior psychiatric diagnosis), a stroke or a functional disease (Sivasathiaseelan *et al.*, 2019*a*). Despite more and more refined consensus diagnostic criteria, dementia and especially rare forms of it (FTD) remains difficult to diagnose because of its fragmentary phenotype and its high anatomical heterogeneity. For instance, one series noted that 41.3% of their 46 patients with primary progressive aphasias did not meet diagnostic criteria for any of the major syndromes (Sajjadi *et al.*, 2012) and the

observational study ran at the Dementia Research Centre comprises between 10 and 20% of ambiguous cases which are unclassifiable according to the current criteria.

The major issue with neurodegenerative diseases is their intrinsic complexity of the processes and brain functions that they target. This intrinsic heterogeneity is compounded by individual variation and epigenetic factors that remain poorly understood. The lack of sensitive and specific standardised tests and measurement tools, especially for detecting and tracking complex changes in social and emotional behaviours, leads to a diagnosis late in the course of the disease, which make it even harder to delineate syndromes due to the incidence of more than one pathology increasing with age (mixed pathology) (Pennington *et al.*, 2020). Phenotypes as disease evolves also tend to converge which greatly complicates the picture. Current diagnostic criteria and tests in fact still reflect downstream effects of diseases rather than the underlying brain processes. More importantly, current drugs aiming to improve and delay the deterioration, such as cholinesterase inhibitors, should be administered at an early, presymptomatic state in order to test their true effectiveness. The recent failures of high-profile clinical trials conducted in patients with mild to moderate Alzheimer's disease may have been because therapy was too late (Yiannopoulou *et al.*, 2019). The lack of effective treatments for neurodegenerative diseases is unfortunately still a reality but the tools aiming at measuring changes and tracking responses to therapy would need to be improved as the current ones are long-latency methods relying on cell death (e.g. structural MRI) or the detection of tissue deposition of a pathogenic protein (e.g. molecular ligand imaging).

More generally, the fundamental issue with the diagnosis of neurodegenerative diseases is that we do not adequately understand how these diseases 'work' at the whole-brain level and how pathogenic proteins are linked to particular phenotypic effects at the macro-level. There is no simple one-to-one correspondence between a single or a combination of pathogenic proteins to a single coherent phenotype (Rohrer *et al.*, 2011); accessing intermediate systems- levels of physiological effects of neurodegenerative diseases may help cross the bridge between molecular and clinical levels. Hence, progress toward earlier and more accurate diagnosis and ultimately disease-modifying therapy is likely to depend on better physiologically informed diseases models and novel diagnostic tools that can capture a physiological 'read-out' of protein expression and its effect of synaptic activity and circuit dysfunction at a mesocortical level.

1.2 Current paradigms of neurodegenerative disease

Defining the correspondence between protein and phenotype more accurately is a fundamental problem that requires the study of how proteins translate into distinctive profiles of damage across brain networks – the 'molecular nexopathy' paradigm (Warren *et al.*, 2013) and how disturbances within large-scale networks contribute to distinct clinical phenotypes - the 'network' paradigm (Raj *et al.*, 2012).

The widespread 'network' paradigm focuses on predicting clinical phenotypes from intrinsic structural and functional large-scale brain networks. It is based on the assumption that distributed brain areas forming brain networks and their synchronized activity over time are responsible for specific cognitive and behavioural features. Investigating cognitive and affective dysfunction in neurological disorders has been coupled to the study of large-scale brain networks with the recent development of sophisticated conceptual and methodological tools. It is well established that neurodegenerative disorders are associated with structural brain abnormalities and for decades, structural brain imaging has been the major imaging technique used to map grey matter atrophy profiles to dementia syndromes. Mapping cognitive processes onto individual brain areas implying that the brain has a highly modular organization is however outdated (Fotopoulou, 2014). Instead, cognitive functions generally arise from the specific temporal pattern of crosstalk between various large-scale neural networks. This would imply that individual brain areas (defined for instance by histological properties: see Brodmann classification) could be involved in very different cognitive functions; particular functions are mediated by the interaction of different areas. Capturing this interaction requires brain imaging connectivity based-techniques. Functional MRI (fMRI) offered the first modality to identify the neural bases of cognitive deficits in relation to specific experimental manipulations. Diffusion tensor imaging (DTI) is another modality providing measures of white-matter pathways linking nodes (brain regions) and edges (functional integration between two regions). In addition to modalities, there are different methodologies for characterizing brain networks. The most widely used methodology is graph-theory which defines brain network by a collection of brain regions (nodes) and functional connections (edges) that link them. Graph-theoretical metrics such as clustering coefficient, path length, centrality and degree offer a new quantitative characterization of neurological disorders. Analysis of resting-state fMRI has led to the identification of three main intrinsic connectivity networks (ICNs): the central executive network (CEN), the default-mode network (DMN) and the salience network (SN) (Seeley *et al.*, 2009). Task-related fMRI, which probes the working brain, has also identified the engagement of the same core networks which suggest that studying the

integrity of these networks and their interactions provide a unique window into brain disorders (see review (Menon, 2011)).

Although describing network damage qualitatively and quantitively helped to uncover core mechanisms of neurodegenerative diseases, it still remains unclear how molecular abnormalities translate to these network abnormalities. I will now briefly describe the 'molecular nexopathy' paradigm and its key features (Warren et al., 2013). The paradigm posits not just that proteinopathies spread via large-scale networks but claims that there are coherent conjunctions between pathogenic protein properties and the characteristics of particular network elements. One conjunction is the intrinsic vulnerability of certain brain networks to abnormal proteins due to epigenetic effects driving local profiles of abnormal protein expression or local expression of neuroprotective factors. A second principle applies information-processing framework and proposed that an initial dysfunction led by a misfolded protein could promote subsequent molecular alterations and destruction of other network elements, which would then change synaptic function and patterns of activity in local circuits. Computational neurobiology is currently looking at this cascade effect by modelling the impact of an insult on information exchange (synaptic transmission) across artificial neural networks.

1.3 Current diagnostic tools

In general, there has been a tremendous effort in developing new biomarkers in the last two decades. Clinical diagnostic criteria are regularly updated and provide international consensus guidelines on how to conduct a clinical investigation. As communication problems and lack of insight are common in certain neurodegenerative diseases, the clinician must interview always the patient's main caregiver. A detailed neurological examination is also required to identify motor neuron deficits that frequently develop during the course of the disease. Neuropsychological assessment is also essential to capture associated cognitive deficits and quantify their evolution over time (decisive in the case of phenocopies). Structural MRI is still the most widely used technique to confirm or infirm the clinician's diagnosis. Where MRI is initially inconclusive to decide on a diagnosis, MRI studies at a yearly interval may document progressive atrophy and corroborate a first clinical impression. Assessment of structural brain images typically requires both an expert radiologist and well experienced dementia clinician which suggests that non-expert clinicians would not necessarily be able to make the diagnosis solely relying on structural imaging results. Group-level patterns of atrophy for rarer forms of dementia is more and more refined but it is still difficult to identify individuals with specific forms of dementia

only using structural T1-weighted imaging because of significant overlap in atrophy maps. One must also keep in mind that grey matter atrophy is a 'normal' ageing process and does not necessarily translate into a clinical phenotype while the reverse situation has also been observed (severe clinical phenotype with little changes in grey matter: phenocopies). Fluorodeoxyglucose-positron emission tomography (FDG-PET) is considered as the second tier of imaging biomarkers when the combination of clinical evaluation and structural imaging fails to secure the diagnosis. FDG-PET provides information on the first stages of glucose metabolism and is a proxy of synaptic activity. The use of FDG-PET which enables visualization of alterations in brain metabolism have proven effective in detecting changes before the onset of symptoms and grey matter atrophy. However, it also produces a substantial number of false positive findings in some psychiatric disorders mimicking certain neurodegenerative diseases, hence future quantitative assessment of metabolic patterns is needed to confirm the diagnostic value of FGD-PET (Elahi and Miller, 2017; Sheikh-Bahaei *et al.*, 2017; Borroni *et al.*, 2018; Baldacci *et al.*, 2020). Metabolic measurement is a poor proxy for synaptic function (and rather reflects glial cell function and their role in inflammation) and seems to reflect a fairly nonspecific neurodegeneration process. In general, altered patterns of atrophy or hypometabolism on structural MRI and FDG-PET, respectively, reflect clinical phenotypes but not pathophysiologies.

Structurally, diffusion tensor imaging (DTI) is an ideal method to assess changes in white-matter structure and provides indirect insights of the brain microstructural characteristics of patients and potentially improves our comprehension of the underlying pathophysiological processes of neurodegeneration (Bozzali and Cherubini, 2007). Imaging techniques assessing connectivity alterations can also reflect pathological processes more closely than structural MRI or FDG-PET. Functional resting-state connectivity patterns measured with fMRI offered valuable insights about brain networks disintegration (Seeley *et al.*, 2009) and resting-state magnetoencephalography (MEG) had recently been used to examine functional connectivity patterns based on neuronal synchrony within each frequency bands in certain dementia syndromes (Ranasinghe *et al.*, 2017). DTI and resting-state techniques have only been investigated at a group level so far and not at a single-patient level which makes their clinical relevance uncertain to date. In order to make these tools clinically relevant, reference data is essential, however the assembly of this data is challenging due to variability across studies (difference between cohorts, scanners, field strengths, choices of DTI metrics, method of analysis, etc) (Elahi and Miller, 2017). Electrophysiological recordings using MEG or EEG have been increasingly used in the last decade and have demonstrated altered spectral patterns and impaired coherence of network dysfunctions underlying specific

cognitive deficits and behavioural changes in major dementia syndromes (Pekkonen, 2000; Hughes *et al.*, 2011; Hughes and Rowe, 2013; Ranasinghe *et al.*, 2016; Horvath *et al.*, 2018, Hughes *et al.*, 2018*a*; Toller *et al.*, 2019). Similarly, recordings of autonomic function are starting to attract attention as a potential biomarkers to aid in the early diagnosis of neurodegenerative diseases and in treatment trials. Such measures provide key insights on changes of neural structures mediating physiological changes including reward pathways, motor systems and the autonomic nervous system (Scheller *et al.*, 2013; Ahmed *et al.*, 2015, Fletcher *et al.*, 2015*c*; Marshall *et al.*, 2017; Ahmed *et al.*, 2018, Marshall *et al.*, 2018*b*, *a*).

Turning now to fluid biomarkers, amyloid peptides and tau levels in cerebrospinal fluid (CSF) is the only validated fluid biomarker so far (with, notably, a specificity of 79% and sensitivity of 89% at differentiating frontotemporal dementia from Alzheimer's disease) (Meeter *et al.*, 2017). Along with brain binding of amyloid and tau-PET ligand capturing tissue deposition *in vivo*, they are consistent surrogates of Alzheimer's disease pathology. Neurofilament proteins (NFL) carries the most promising avenue for dementia monitoring because it showed strong correlation with CSF levels but can also be measurable in blood instead of requiring an invasive lumbar puncture which makes repetitive measurements over time much easier (Skillbäck *et al.*, 2014; Illán-Gala *et al.*, 2020). Thought to reflect axonal damage, we still lack a clear understanding of the role of NFL in disease progression and its interaction with other biomarkers. Blood NFL is probably the most promising tool currently available for a multistep diagnostic approach, especially in selected populations at risk for dementia (Hampel *et al.*, 2018). Key diagnostic priorities hence also include screening genetic mutations with implications for screening of other family members and forming initial target groups for disease-modifying clinical trials (Rohrer *et al.*, 2015).

All these biomarkers face similar challenges: sensitivity and specificity of all these tests decrease significantly with age; there is generally a substantial overlap in atrophy and hypometabolism maps between syndromes with segregated phenotypes; the potential of newer biomarkers has mainly been demonstrated at a group-level and still need to be validated at individual-level which is especially difficult when dealing with rare dementia syndromes as strong discriminative power between patient groups is needed; multicentre standardization of methods and establishment of quality control programmes are still lacking; generally more validation and longitudinal data are needed to determine the role of the newly developed biomarkers. It is especially important to clarify the place of these biomarkers in earlier stages of the disease, since so far, trials of disease-modifying drugs (in Alzheimer's disease only) at a relatively established stage have failed and focus is now shifting towards targeting the disease early, even before symptoms develop (Yiannopoulou *et al.*, 2019).This is

problematic in 'sporadic' disease hence the important of genetic screening and large population screening with optimised tools (minimally invasive, fast, easily repeatable, and costeffective).

Most importantly, most of these biomarkers constitute 'blunt' tools at revealing how pathogenic proteins actually function at the level of the neural circuit and lead to damages at subsequent scales. More information is needed about the sequential order of these damages and associations between biomarkers and their relationship to other age-related brain changes. As I described, novel biomarkers such as the molecular ligand PET scanning capturing deposition of protein tau in vivo, or wet biomarkers looking at CSF and blood assays of tau or NFL may detect and track neuronal dysfunction more closely. Tools derived from functional neuroimaging, autonomic and electrophysiology addressing neural network dysfunction are particularly promising for disentangling complex clinical phenotypes. Although they are difficult to implement for heterogeneous diseases (such as FTD), multimodal biomarkers combining these measures might provide this "read-out" of cellular and synaptic function needed to identify the pathogenic protein before irrecoverable neural damage (Paraskevaidi *et al.*, 2018) and would help in determining if candidate treatments are working. To date, the feasibility of these strategies is ongoing and remain unproven in rarer forms of dementia such as frontotemporal dementia (Sivasathiaseelan *et al.*, 2019*a*).

1.4 Target diseases addressed by this thesis

Despite the diagnostic challenges described above, a majority of neurodegenerative diseases can be assigned to a syndromic group according to detailed diagnostic criteria (Dubois *et al.*, 2007; Gorno-Tempini *et al.*, 2011; Rascovsky and Grossman, 2013). These criteria don't fully account for the clinico-anatomical diversity within each syndrome nor the underlying molecular pathology as I underlined in my previous sections. They are mainly useful for the clinician in establishing certainty around a specific diagnosis and for harmonising clinical cohorts for research purposes (including the experimental work in this thesis). I will focus here on Alzheimer's disease pathology, as the most common form of dementia, and frontotemporal dementia as a model for clinico-anatomical complexity in younger forms of dementia.

1.4.1 Alzheimer's disease

Clinical presentation: Alzheimer's disease (AD) is the most common cause of dementia and typically presents with the gradual onset of episodic memory impairment. AD then progresses to involve other domains of cognition

including language, visuospatial abilities, and executive function. Advancing age is the greatest risk factor for AD. However, AD is also a common cause of dementia among patients younger than 65 years (early-onset AD). Whilst older NINCDS–ADRDA clinical criteria for AD (McKhann *et al.*, 1984) focus on performance on neuropsychological tests of cognition and general function such as the Mini-Mental State Examination (MMSE: (Folstein *et al.*, 1975)), these criteria have been revised for both clinical and research purposes (Dubois *et al.*, 2007, 2014; McKhann *et al.*, 2011), incorporating biomarkers and defining typical and atypical variants. The phenotypic variability of AD pathology includes logopenic-variant primary progressive aphasia attacking language function, posterior cortical atrophy leading to visuo-perceptual and visuospatial impairments, and a frontal variant of AD, characterized by personality change and a dysexecutive syndrome (Warren *et al.*, 2012). Yet, even within the 'typical AD' group, variation in phenotypic profiles is evident (Snowden *et al.*, 2007). Defining more clearly this variability is crucial in linking neuropathology to clinical profiles. The majority of AD cases are sporadic, predominantly occurring late (7^{th} to 9^{th} decade). Familial AD accounts for a very small proportion (1 to 5%) of cases and is caused by mutations in one of three major genes: PSEN1, PSEN2 and APP.

Behavioural symptoms are common in Alzheimer's disease, particularly depression, anxiety, and irritability in early stages, and paranoid delusions and agitation in moderate-to-severe stages. Personality and social behaviour often remain relatively preserved.

Diagnostic tools: Key supporting biomarkers of AD are medial temporal lobe atrophy on structural imaging, an increased ratio of total tau to beta-amyloid1-42 in CSF and temporoparietal hypometabolism and/or brain amyloid deposition indexed by PET imaging. The majority of clinical trials for AD now require biomarker confirmation as inclusion criteria (Cummings, 2019). Currently, a definite diagnosis of AD in an individual presenting with an AD phenotype can only be obtained by genetic confirmation of a known autosomal dominant mutation or histopathological evidence of characteristic protein aggregates in the brain after death.

Pathology: The cardinal pathologies of Alzheimer's disease are amyloid plaques and neurofibrillary tangles and longitudinal studies indicate that these pathologies may accumulate years prior to any cognitive decline. The gradual spread of neurofibrillary tangles (Braak stages: Braak *et al.*, 2006) correlates better with progression of cognitive deficits compared to amyloid (Brier *et al.*, 2016). Tau and beta-amyloid are likely to be synergistically

responsible for the progression of the pathology into dementia though the details of this interplay are still being worked out (Busche and Hyman, 2020).

Neuroanatomy: AD is characterized by grey matter atrophy in posterior medial cortex (precuneus, posterior cingulate and retrosplenial cortex), medial prefrontal cortex, inferior parietal lobe, lateral temporal cortex and hippocampal formation. These regions are core areas of the DMN mapped in healthy subjects with rsfMRI (Greicius *et al.*, 2004).

AD and the neural network paradigm: The DMN participates in episodic memory retrieval, mental state attribution, visual imagery and is generally known for its task-related deactivations. In AD, intrinsic connectivity studies have confirmed a decrease in connectivity between key hubs of the DMN over the disease span indicating that altered activity of the DMN relates to the severity of the disease (Greicius *et al.*, 2004; Sorg *et al.*, 2007; Supekar *et al.*, 2008). The cortical hub of the DMN, the posterior medial cortex, is affected across AD phenotypes in terms of cortical thickness and functional connectivity which might suggest that this region is particularly vulnerable to the underlying AD pathogenic proteins (Almgren *et al.*, 2018). DMN disruptions appear in early phases and has been linked to core memory and visuospatial deficits (Sorg *et al.*, 2007). Moreover, salience network and central executive network intrinsic connectivity have been shown to be upregulated at very early stages of the disease and correlate with behavioural symptoms seen in AD such as anxiety and irritability and with frontal-executive and language scores (Agosta *et al.*, 2012). DTI is another useful to measure connectivity in an indirect way, looking at damage of major white-matter tracks connecting major brain regions. Reduced fractional anisotropy, reflecting damage along axonal bundles preventing the free motion of water molecules, was found in the temporal lobe and the posterior cingulate white matter, which correlated to cognitive measures of delayed recall (Huang and Auchus, 2007), while frontal white matter damage contributed to executive dysfunction (Fellgiebel *et al.*, 2004) and the posterior part of the corpus callosum damage to verbal fluency (Kavcic *et al.*, 2008). The anatomical background and the behavioural and psychiatric symptoms of AD, the most challenging to capture, has not been explored to date.

AD and the nexopathy paradigm: NFT pathology advances from layer II of the entorhinal cortex toward limbic and associated cortices (Braak *et al.*, 2006). Abnormally phosphorylated tau no longer binds to microtubules, leading to misfolding and aggregation, forming 'pretangles' that gradually fill affected neurons. Pretangles transform into

insoluble fibrillary and argyrophilic neuropil threads, and eventually NFTs. Based on mouse models, tau pathology is likely to propagate to surrounding neurons and astrocytes and spread misfolded proteins to downstream synaptically connected areas such as the dentate gyrus, the hippocampus and cingulate cortex (de Calignon *et al.*, 2012). In addition, tau is extensively involved in neuronal signalling pathways, which become affected with disease progression Similarly, toxic oliogomers derived from amyloid precursor protein is also thought to contribute to the disruption of synaptic function (Wirths *et al.*, 2006) and subsequent neural network disintegration. Affected cells survive for years, eventually undergoing premature apoptosis, which results in loss of grey matter and symptomatic progression. Network disintegration along a distributed parieto-temporo-frontal gradient relates to current pathological disease staging (Braak *et al.*, 2006). However, the differentiated pathophysiological roles of the two pathogenic proteins beta amyloid et tau and the factors that modulate the profile of network damage leading to variant AD syndromes remain unclear (Kuo and Rajesh, 2019).

1.4.2 Frontotemporal dementia

FTD is a clinic-anatomically and pathologically diverse group of diseases sharing a propensity to target the frontal and temporal lobes. It accounts for around 40% of cases of young-onset dementia. Onset is most often in the 6th decade but ranges very widely between third and ninth decades. The prevalence in the United Kingdom approaches 15/100,000 in the 45-64 age group which is similar to the prevalence of Alzheimer's disease in the same age group (Ratnavalli *et al.*, 2002). Overall, around 20% of the FTD spectrum is genetically mediated, with autosomal dominant inheritance, and most cases attributable to mutation in the microtubule-associated protein tau (MAPT) and progranulin (GRN) genes or abnormal hexanucleotide repeat expansions on the open reading frame on chromosome 9 (C9orf72). There are three canonical clinical FTD syndromes: behavioural variant FTD (bvFTD), semantic variant primary progressive aphasia (svPPA) and non-fluent variant primary progressive aphasia (nfvPPA). However, this current classification still allows considerable overlap with a general tendency for syndromes to converge at later stages of the disease and merge with the atypical parkinsonism spectrum (progressive supranuclear palsy PSP and cortical basal degeneration CBD) (Pablo-Fernández *et al.*, 2020). A high rate of false-positive diagnosis is commonly reported (Shinagawa *et al.*, 2016) with the existence of numerous FTD 'phenocopies' of undefined basis (Gossink *et al.*, 2016).

FTDs could be regarded as paradigmatic examples of 'molecular nexopathies' due to the strikingly diverse and frequently selective clinical, neuroanatomical and histopathological signatures exhibited by this group of diseases (Warren *et al.*, 2013). The special cases of genetic FTD where the underlying pathology is known can provide in certain cases confirmation of the hypothesized link between a protein and neural circuit characteristics with clear clinicoanatomical patterns (Rohrer *et al.*, 2010*b*, Sivasathiaseelan *et al.*, 2019*a*). However, this mapping remains incomplete, particularly for the more common behavioural variant.

1.4.2.1 Behavioural-variant frontotemporal dementia

Clinical presentation: bvFTD is the most common FTD syndrome (50-60% of cases) (Rohrer *et al.*, 2011)(Rohrer et al., 2011) and the most likely to have a genetic basis (30-50% of cases) (Rohrer *et al.*, 2015). This syndrome is generally led by impaired socio-emotional awareness and reactivity and abnormal interpersonal behaviour, with the current diagnostic criteria (Rascovsky *et al.*, 2011)emphasising features such as social disinhibition, emotional blunting with loss of empathy, apathy, perseveration, stereotyped behaviours, hyperorality, altered eating behaviours (tendency to gluttony and sweet tooth). There is often executive dysfunction with relative sparing of episodic memory and visuospatial functions on neuropsychological assessments. bvFTD remains the most heterogenous FTD syndrome. This may in part reflect the nature of behavioural symptoms, which are typically very difficult to assess and quantify, shift over time and rely on a detailed history from an informant who knows the patient very well. Many patients perform well on neuropsychological testing and if executive dysfunction does appear, this dysfunction is not particularly helpful in discriminating FTD from Alzheimer's disease. 'Phenocopies' are very common where informants testify on drastic changes in behaviour despite lack of neuroimaging or neuropsychological abnormalities (Gossink *et al.*, 2016; Ducharme *et al.*, 2020). Other clinical features not included in the current criteria include impaired social cognition, changes in sense of humour (shift to less complex and callous humour often accompanied by Schadenfreude), altered libido and affection, altered sensitivity to pain, temperature or sound, changes in aesthetic preferences with a preference for more 'abstract' features such as obsessive craving for music and colour (musicophilia and chromophilia) (Eslinger *et al.*, 2011; Ibañez and Manes, 2012; Fletcher *et al.*, 2013; Mendez and Shapira, 2013, Clark *et al.*, 2015*b*, Fletcher *et al.*, 2015*b*, *a*). Patients with C9orf72 mutations are particularly prone to develop psychotic symptoms such as delusions, hallucinations, prominent anxiety underpinned by alterations in self/non-self differentiation. Later in the course

of the disease, language impairments with anomia and semantic deficits frequently emerge signalling convergence with the spectrum of progressive aphasia (especially semantic dementia) (Hardy *et al.*, 2015). Physical examination not infrequently reveals features overlapping other neurodegenerative syndromes such as motor neuron disease or atypical parkinsonism suggesting progressive supranuclear palsy or corticobasal syndrome (Sivasathiaseelan *et al.*, 2019*a*).

Pathology: The underlying pathology of bvFTD is largely split between tau and TDP with a small minority of cases due to FUS and occasionally AD. It is however extremely difficult to predict the pathology of sporadic bvFTD with confidence (Ranasinghe *et al.*, 2016) although certain network signatures can suggest hypothesis about underlying pathologies (see next paragraph on nexopathy) (Rohrer *et al.*, 2011).

Neuroanatomy: Structural MRI shows variable patterns of atrophy in frontal, insular and temporal cortices and subcortical structures (striatum, thalamus and cerebellum). Variability of atrophy can map into clinical subsyndromes of bvFTD, the most common being the right temporal variant associated with focal right temporal lobe atrophy and characteristic clinical features: profound loss of emotional reactivity, prosopagnosia, hypochondriasis, hyper-religiosity, hallucinations and cross-modal sensory experiences (Ulugut Erkoyun *et al.*, 2020). Other proposed neuroanatomical subcategories (frontal predominant, frontotemporal and subcortical) do not reliably predict particular symptoms or molecular aetiologies and have little clinical utility (Ranasinghe *et al.*, 2016).

Diagnostic tools: Atrophy at first consultation is highly variable and a normal MRI scan does not exclude a diagnosis of bvFTD. In this case, serial scanning with registration is helpful to assess any progression. FDG- PET scan may occasionally help with the diagnosis when MRI scans are inconclusive (e.g. in case of 'phenocopies') but has generally a limited role in diagnosis.

bvFTD and the neural network paradigm: Seeley et al. (2009) defined bvFTD as a 'salience network' (SN) disease with atrophy of orbitofrontal cortex, anterior cingulate, anterior insula and presupplementary motor area. bvFTD has reduced SN intrinsic connectivity correlating with apathy and disinhibition but enhanced connectivity in posterior DMN which may correlate with stereotyped, ritualistic and compulsive behaviours. In anterior frontal

and temporal DMN regions, connectivity is reduced, which may account for bvFTD-related deficits in insight and self-projection (Irish *et al.*, 2012).

bvFTD and the nexopathy paradigm: Cortical layers 2 and 3 contain early pathogenic protein aggregates and cell loss in human and animal models of bvFTD (Kersaitis *et al.*, 2004). Moreover, selective loss of layer V projections from Von Economo, fork- and surrounding pyramidal neurons occurs in bvFTD (Kim *et al.*, 2012), with an estimated 70% reduction in cell number post-mortem (Seeley *et al.*, 2006). This layer V atrophy is a hallmark of bvFTD pathology. Certain characteristic network signatures that predict underlying molecular pathology have been observed in genetic forms of bvFTD, MAPT mutations leading to predominant bilateral medial temporal lobe atrophy whereas TDP-43 type A associated with GRN mutations produces strongly asymmetrical hemispheric atrophy extending posteriorly into the parietal lobe (Beck *et al.*, 2008).

1.4.2.2 Semantic-variant primary progressive aphasia

Clinical presentation: Semantic dementia or svPPA begins as difficulty finding words and inability to express thoughts with precision. It is led by an erosion of semantic memory, the memory system responsible for our cumulative knowledge of words, objects (from any modality) and concepts that allows us to attribute meaning to the world (Warrington, 1975; Hodges and Patterson, 2007). The patient's conversation is fluent and well structured, however becomes progressively more circumlocutory and empty as fine-grained content is replaced by generic ciphers ('sparrow' becomes 'bird' and ultimately 'animal' or 'thing') (Chen *et al.*, 2017). Language impairment generally leads the presentation but later in the course, erosion of semantic memory affects other sensory channels with progressive failure to recognise faces, visual objects, sounds, odours and flavours. On a standard neuropsychological examination, anomia is the most marked deficit but praxis, arithmetical, visuospatial and other parieto-occipital cortical functions are generally well preserved (Ding *et al.*, 2020). In contrast to the other FTD syndromes, the neurological examination is usually normal in svPPA.

Behavioural symptoms similar to those seen in bvFTD characteristically develop early in svPPA which makes these two syndromes sometimes difficult to differentiate. Absent or misplaced empathy, social disinhibition and faux pas, a blunter sense of humour and pathological sweet tooth are common features. Certain behavioural features such as exaggerated reactions to pain, rigidity with clock-watching and obsessional interest in numbers, puzzles and music seem particularly prevalent in svPPA (Rosen *et al.*, 2006; Rohrer and Warren, 2010).

Impoverished sense of self may also explain the increased rate of depression and suicidality in this syndrome (Irish and Piolino, 2016).

Pathology: svPPA constitutes the most coherent of all dementia syndromes most cases exhibiting highly uniform and characteristic clinical, neuroanatomical and pathological features. Most cases are sporadic with post-mortem analysis revealing TDP-43 type C pathology.

Neuroanatomy: The MRI signature is focal, asymmetric atrophy principally involving the dominant antero-inferior and mesial temporal lobe including amygdala and anterior hippocampus (Gorno-Tempini *et al.*, 2011). The profile of atrophy shows a clear gradient within the temporal lobe with a 'knife-blade' appearance signifying early destruction of the temporal pole with relative sparing of the superior temporal gyrus and more posterior temporal cortices. Over time, the atrophy spreads to more posterior temporal regions and homologous gyri in the right temporal lobe as well as the bilateral orbitofrontal cortex. This typical atrophy profile is highly consistent across patients (Rohrer *et al.*, 2008).

Diagnostic tools: The atrophy profile is highly consistent across patients which makes MRI a sufficient method to reliably diagnose svPPA. However, like for other neurodegenerative diseases, dynamic markers providing a "read-out" of cellular and synaptic function crucial for detecting the effects of candidate treatments are still missing.

svPPA and the neural network paradigm: svPPA targets an intrinsic temporal pole-subgenual cingulate-ventral striatum-amygdala network with a primary hub in the left temporal pole. This network is often referred to the semantic appraisal network. Functional connectivity and graph theoretic analyses of resting-state fMRI data in svPPA have documented a generalised disruption of the physiological integrity of the semantic appraisal network overall loss of network integrative capacity (Guo *et al.*, 2013; Agosta *et al.*, 2014; Battistella *et al.*, 2019; Benhamou et al., 2020). In contrast to bvFTD, key hubs of the salience network are relatively preserved in svPPA (Seeley *et al.*, 2009; Zhou *et al.*, 2012).

svPPA and the nexopathy paradigm: Contrary to all other syndromes described in this section (and in general most dementia syndromes), svPPA is a highly coherent clinical, anatomical and pathological syndrome. It suggests that the pathogenic protein TDP-43 type C predominantly target clustered (shorter-range) connections with a strong gradient of network damage, which leads to a relatively focal and asymmetrical atrophy profile. A recent

study using dynamic causal modelling for resting-state fMRI data showed a weakening of the normal inhibitory self-coupling of bilateral antero-mesial temporal lobes accompanied with an abnormal excitatory fronto-temporal projection in the dominant hemisphere (Benhamou *et al.*, 2020). These findings suggest the potential detrimental role of TDP-43 type C in the attenuation of tonic inhibitory GABAergic transmission in the semantic appraisal network, normally responsible for sharpening the activation of neural representations (Lambon Ralph *et al.*, 2010; Isaacson and Scanziani, 2011; Jung *et al.*, 2017).

1.4.2.3 Non-fluent variant primary progressive aphasia

Clinical presentation: Patients with nfvPPA present with effortful, hesitant and poorly constructed speech. Speech errors affect individual speech sounds (phonological errors if the syllable is wrongly selected and phonetic errors if articulation is impaired), word or lemma selection (particularly reversal of binary alternatives such as 'yes and 'no') (Sivasathiaseelan *et al.*, 2019*b*) and sentences (grammatical errors mostly affecting syntax and verb usage) (Marshall *et al.*, 2018*c*). 'Speech apraxia' (cortically based dysarthria) often dominates the presentation (Gorno-Tempini *et al.*, 2011). Speech production errors are accompanied by impaired comprehension of more complex sentences reflecting impaired grammar and verbal working memory (Rohrer *et al.*, 2010*b*). Spared naming and single word comprehension are emphasised in the current diagnostic criteria. In general, the clinical spectrum of nfvPPA is diverse with a number of variant sub-syndromes (for instance 'pure' progressive speech apraxia without agrammatism (Josephs *et al.*, 2012)). A degree of executive dysfunction is often observed with initial relative sparing of other cognitive functions. Behavioural symptoms may appear, chiefly apathy or impulsivity (Rohrer and Warren, 2010). A significant proportion of patients with nfvPPA develop symptoms of Parkinsonism (Kremen *et al.*, 2011) that overlap with PSP and CBD. Patients with underlying CBS-PSP pathology tend to have prominent verbal adynamia ('dynamic aphasia') with significant reduced spontaneous speech output disproportionate to the level of motor speech impairment (Magdalinou *et al.*, 2018). Impaired comprehension of more complex sentences is accompanied by deficits at discriminating prosodic contours (Rohrer *et al.*, 2012), understanding foreign accents (Hailstone *et al.*, 2012), degraded speech (Cope *et al.*, 2017; Hardy *et al.*, 2017), and generalised non-verbal auditory deficits in processing rhythm and pitch of brief non-linguistic sequences (Grube *et al.*, 2016), discrimination of timbre (Goll *et al.*, 2010) and recognition of vocal emotions (Rohrer *et al.*, 2012). These studies all suggest that nfvPPA extends beyond neurolinguistic impairments with generalised impairment of auditory

early perceptual analysis, corroborated by a recent finding of impaired peripheral hearing (using pure-tone audiometry) (Hardy *et al.*, 2019).

Pathology: As anticipated from heterogenous clinical spectrum, the underlying proteinopathy is more heterogeneous than the one seen in svPPA. A majority of patients have underlying tau pathology, but a substantial minority represent TDP-43 or Alzheimer pathology (Rohrer *et al.*, 2011; Spinelli *et al.*, 2017). Motor features are indicative of underlying tau pathology (Gorno-Tempini *et al.*, 2011). However, there are still very few reliable predictors of underlying pathology for nfvPPA patients. Around 30% of patients have a family history and mutations in all major genes (GRN, MAPT and C9orf72), with some forms presenting a distinct clinical phenotype (e.g. GRN mutations present with severe agrammatism and semantic impairment without apraxia of speech, (Snowden *et al.*, 2006, Rohrer *et al.*, 2010*b*, *a*).

Neuroanatomy: T1-weighted MRI shows asymmetric atrophy in the inferior frontal gyrus (Broca's area), insular cortex, and anterior superior temporal gyrus in the dominant hemisphere. However, these atrophy profiles vary extensively between individual patients, both in severity and extension along and around the superior temporal gyrus. Associated atrophy of the midbrain and other subcortical regions is also though less consistently observed.

Diagnostic tools: Serial MRI with registration is often helpful to assess progressive regional atrophy. PET or SPECT may have a role when MRI scan is inconclusive.

nfvPPA and the neural network paradigm: The targeted ICN is anchored in the left inferior frontal gyrus and encompass the frontal operculum, the primary and supplementary motor cortices, and the bilateral parietal lobule. This ICN links the language and motor system which together enable speech planning and execution (Damoiseaux *et al.*, 2006; van den Heuvel *et al.*, 2008; Seeley *et al.*, 2009).

nfvPPA and the nexopathy paradigm: As with bvFTD, it is challenging to link clinical phenotype, network signatures and the underlying proteinopathy in nfvPPA. The rare GRN mutation associated with a diagnosis of nfvPPA suggests that TDP-43 type A would preferentially target layer II of the inferior frontal gyrus before spreading following longer-range connections with a strong gradient leading to asymmetrical hemispheric atrophy extending posteriorly into the superior temporal gyrus. A more refined classification of sporadic nfvPPA into

subtypes could help drawing patterns between molecular aetiologies, network breakdown and clinical presentation.

1.5 Predictive coding: a new framework to characterise dementia

The foregoing sections illustrate the considerable heterogeneity and complexity of these representative neurodegenerative diseases in the AD and FTD spectra. I described two key paradigms across the neurodegenerative disease spectrum that attempt to account for the way pathogenic proteins spread in neural circuits and the ways in which macroscopic networks break down to translate into phenotypes. While more evidence is still needed to corroborate the assumptions on which these paradigms rest, we could also choose to adopt an alternative approach which offers the possibility of drawing a more exhaustive protein-network-phenotype map, the grail in the research field of neurodegenerative diseases.

In psychiatry, sophisticated models encapsulating a theoretical, often mechanistic, understanding of clinical phenomena are at the core of a new growing field, computational psychiatry (Friston *et al.*, 2014*b*; Huys *et al.*, 2016). Models, informed by data from multiple sources, can bridge different research modalities and levels of analysis and can be used to infer the likely causes of an observed phenomenon (for instance, what kind of disturbance in the concentration of a certain neurotransmitter can give rise to an observed network disturbance and/or symptom). Computational neurosciences notably make a clear distinction between *normative models*, which describe 'what' the brain is trying to do (for instance, maximising reward; retain representation in working memory) and *process models* which describe the mechanisms i.e. 'how' it is done (reinforcement learning models such as Rescorla-Wagner; cortical gain control via excitatory-inhibitory balance). One particular pairing of normative and process models has gained very wide currency as a plausible unifying description of how the brain normally operates under a range of conditions: the 'what' normative model summarised in a single outcome, minimising 'surprise' or free energy; and the 'how' process model referred to as 'predictive coding'.

The tenet of this thesis is that the clinical variability of proteinopathies could be understood on the basis on this very general normative/process account of brain function. Predictive coding is a physiologically informed systems-level paradigm that could generate 'emergent' properties of diseases by inferring the probability of observations given the underlying causes, and this at different levels of the information processing hierarchy. In that sense, in contrast to discriminative models currently in use in clinical practice which learns the probability of some causes given the data, it could constitute a good candidate for generic paradigms of brain disruptions. I will

now describe in detail what it entails, the evidence for abnormal predictive coding in major dementias and the reasons why I think a re-formulation of cognitive, behavioural and physiological deficits in dementia in terms of predictive coding may be useful if we want to gain a protein-network-phenotype mapping of these diseases.

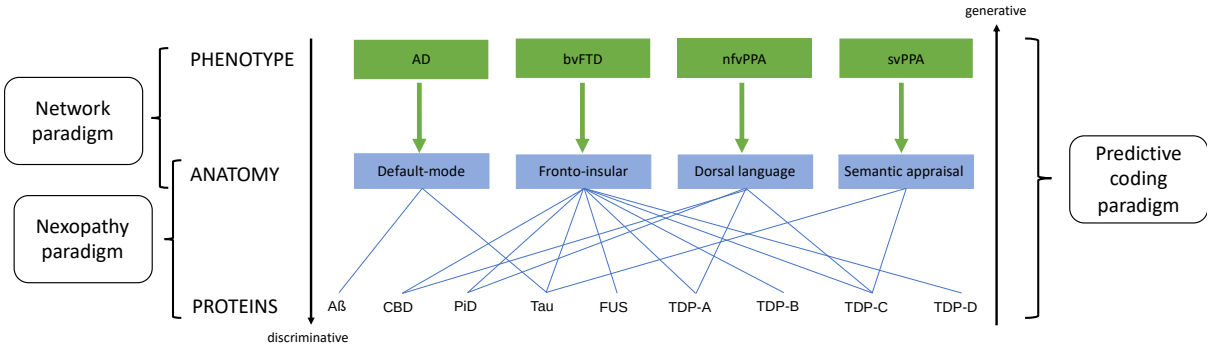

Figure 1.1. The predictive coding paradigm allows the crossing of several scales currently available to describe dementia syndromes.

The network paradigm maps anatomy to clinical syndromes and the nexopathy paradigm maps proteins to large-scale network disruption. The underlying pathology of AD and FTD is very heterogeneous and there is still no universal mapping between phenotypes, network signatures and pathogenic proteins. The predictive coding framework is unique in that it generates 'emergent' properties of diseases from underlying pathological causes (generative: ascending arrow) while the other paradigms infer underlying pathologies from observations (discriminative: descending arrows).

1.5.1 Basic architectures and principles

1.5.1.1 The free-energy principle

The notion that perception is active and relies on predictions about the world at large i.e. probabilistic inference of how reality should look, feel or sound, dates back at least as far as the Helmholtz's theory of perception (1868). Helmholtz popularised the idea that the brain must detect statistical regularities in the environment, learnt from lifelong experience, in order to apply its internal predictions about its sensory inputs. Predictive coding theory, first enunciated in the late 90's (Rao and Ballard, 1999), proposes a mechanistic neural implementation of Helmholtz's theory, constituting a message passing scheme between hierarchical neural circuits (at both a micro and macro level). Top-down predictions and bottom-up prediction errors are integrated to identify the hidden causes of sensory signals. Predictive coding is naturally allied to a very general principle governing living organisms: the free energy principle (Friston, 2005), according to which (Friston, 2005) living organisms resist the tendency to disorder (second law of thermodynamics) and maintain an upper bound on their free energy, information quantity that bounds the evidence for a model of data. Friston and colleagues (Friston and Kiebel, 2009; Friston, 2010; Friston *et al.*, 2010) recognised that together, the free energy principle and its

instantiation via predictive coding constitute a powerful, general theory of brain operation. According to this theory, the brain obeys the free energy principle by comparing incoming sensory data with its internal neural model of the environment and minimising any discrepancy via predictive coding and active inference, manifest in percepts and actions, respectively. I now consider the key features and candidate neural substrates for these operations.

1.5.1.2 Predictive coding mechanisms within a hierarchical cortical network

The neural instantiation of predictive coding theory has at its core the hierarchical functional organisation of cerebral cortex (Mesulam, 1998). Partly based on the hierarchical pattern of maturation during development (Chan *et al.*, 2016), lower levels of this hierarchy are located in primary sensory and motor cortices representing local spatiotemporal properties of sensory inputs and their motor mappings, while higher levels are instantiated in transmodal association areas, coding more complex and distributed spatiotemporal properties such as semantic or object-scene relationships (Himberger *et al.*, 2018; Huntenburg *et al.*, 2018).

Predictive coding could plausibly be enacted via common set of input-output mechanisms applied at each level of this hierarchy. In an iterative way and at each level of the cortical hierarchy, the brain would predict lower-level data by comparing it to higher-level representations or prior beliefs, thereby generating prediction errors. This prediction error is fed forward to the next level which updates the prior belief which is in turn fed back to the previous level to reduce prediction error. This system is highly efficient since the only information that needs to be communicated upward is the prediction error which acts as a proxy for sensory information itself. The minimisation of prediction errors thus involves reciprocal exchange of signals between hierarchical levels: prediction errors ascend the hierarchy to revise expectations, which generate descending predictions that resolve or suppress prediction errors at the level below.

Prediction errors and prior beliefs are probabilistic distributions with a first-order moment (average) and a second-order moment (variance). This second-order moment is termed precision and is fundamental to predictive coding. For instance, regarding prior beliefs, predictions (or expectations) of 'what' is going to happen are different from predictions of 'context'- the confidence placed in those expectations. Prediction errors and prior beliefs are said to be *precision-weighted*. The internal predictive models are directly influenced by the relative precision-weight allocated to bottom-up prediction errors compared to top-down priors. In a novel 'reliable' (relatively predictable) environment, prediction errors are more likely to hold higher precision while, in an 'unreliable' (or less predictable) environment or environment with low sensory information, priors would be

more precision-weighted (Palmer *et al.*, 2019). Precision-weighting is believed to be mediated via neuromodulatory mechanisms (Friston *et al.*, 2012, 2014*b*). Neuromodulation not only elicits plasticity but tunes the balance of top-down versus bottom-up influences. Cortical circuits at each level of the processing hierarchy require three core neural components in order to implement predictive coding: a comparator circuit which calculates the prediction error between bottom-up inputs and descending predictions, a circuit to maintain a stable internal representation giving rise to predictions; and a modulating signal that sets the precision of the prediction error.

Predictive coding hence provides principled constraints on normal cortical structure-function relationships. The dynamic aspect of this theory is crucial as it suggests that the spatial location of a cortical area also determines the time-scale of its engagement i.e. the further it is from primary sensory areas, the more likely it will encode slower contextual changes of the environment in contrast to the fast fluctuations of sensory inputs (Kiebel *et al.*, 2008; Hohwy, 2013). Within this framework, disruptions of the fine dynamic balance between cortical layers associated with neuromodulatory effects and/or destruction of anatomical regions at certain stages of the hierarchy can result in a cascade of domain-general impairments such as over-reliance on priors, over-reliance on sensory input, generalised failure to detect an error in sensory input, generalised failure to update internal models and inability to capture probabilistic structure.

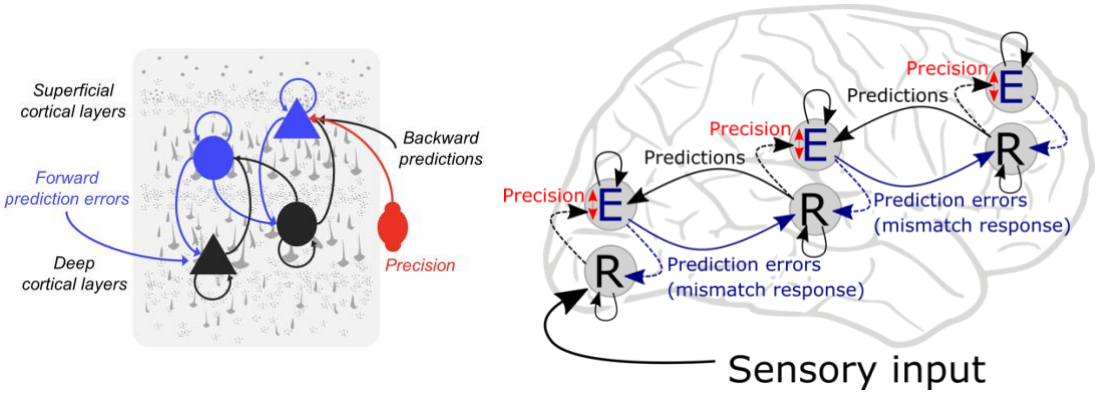

Figure 1.2 Simplified scheme of the predictive coding mechanism within a hierarchical brain organisation

The left panel shows a single cortical layer within the hierarchy: prediction errors from lower levels are passed bottom-up (blue arrows) to the representation units (black nodes) in deep cortical layers to update the predictions and lead to conditional expectations; these expectations are passed to error units in the superficial cortical layers (blue nodes) and compared with backward predictions (black arrows) coming from the deep cortical layers of the higher level in the hierarchy. Triangles represent pyramidal neurons. Circles represent inhibitory interneurons. Precision-weighting (red node) neuromodulated the post-synaptic gain of the error units. The right panel is a simplified scheme of message passing in the hierarchical brain: R units are representation units and E are error units. Adapted from (Stefanics *et al.*, 2014; Kocagoncu *et al.*, 2020)

1.5.1.3 Memory and learning

A key hypothesis of predictive coding is that top-down descending projections carry sensory predictions. To test this hypothesis, one needs to probe the nature of neural prediction itself. Some priors can be hardwired into neural structure (through phylogenetic development) while others emerge from sensory regularities extracted from the environment. Typically, the natural environments contain regularities, from simple repetitive patterns to more complex contingencies. Perceptual inference thus requires a certain level of 'on-line' probabilistic learning which allows the brain to interpret input rapidly and predict upcoming events (Wang *et al.*, 2017). Another type of prediction arises from recall of previous spatio-temporal episodes or object statistics, in other words, episodic or semantic memory. Recall of the past and ongoing predictions would be mediated by the same neural elements i.e. descending GABA-ergic inhibitory interneurons, crucial for sharpening the activation of neural representations and simultaneously, inhibiting ascending prediction errors. Modulatory gain of prediction error units (precision-weighting) would facilitate the reinstantiation of cortical representations during recall of past autobiographical experience or semantic knowledge (Isaacson and Scanziani, 2011; Jung *et al.*, 2017; Barron *et al.*, 2020).

Another hypothesis posited by predictive coding principles states that expectation modulations and minimization of prediction errors are not uniform across the cortex and depend on the hierarchical position of the processing unit (Walsh *et al.*, 2020). Paradigms such as repetition suppression (RS) and expectation suppression (ES) are well adapted to assess this hypothesis since they are based on the same mechanism but at two different levels of the hierarchy: RS is an automatic expression of detection of simple transitional statistics in the environment while ES is the expression of a higher-level sensitivity to complex regularities integrated over a longer period. The recruitment of distributed high-level areas for processing violations of complex regularities versus early sensory cortex for processing simple deviants have now been extensively demonstrated (see review for the auditory modality in Heilbron and Chait, 2017). The mismatch negativity (MMN) paradigm is an effective way to measure the efficiency of the auditory system to extract regularities in a sequence of sounds. MMN refers to the evoked potential measured with electrophysiological modalities in response to a deviation from a learnt pattern. It can be a deviation in frequency, intensity, spatial localization or duration (Näätänen *et al.*, 2007). Fronto-temporal cortical generators contribute to MMN signal, with temporal sources thought to extract sensory patterns and frontal sources associated with the involuntary switch of attention towards the deviant. MMN is

affected in a number of different diseases, suggesting a sensitive but nonspecific marker of disease (Näätänen *et al.*, 2012).

1.5.1.4 The laminar cortical microcircuit

Another key hypothesis to assign predictive coding a substrate in the brain posits that there are two neural subpopulations representing predictions and predictions errors at each level of the cortical processing hierarchy. This hypothesis is in fact grounded in the basic architecture of a neuronal circuit which is reiterated across the brain. The cortical microcircuit has six layers each with specific histomorphological properties and afferent and efferent connections: it is well-established that forward signals are transmitted from superficial to middle and deep layers of the next cortical column (higher-level areas) while backward connections originate from deep layers and terminate in superficial and deep layers of the level below (Markov *et al.*, 2014) (see Figure 1.2). Thanks to high-resolution neuroimaging techniques, it is now possible to exploit this laminar architecture and dissociate predictions from prediction error signals in humans. For instance, Kok et al. (Kok *et al.*, 2016) used 7T fMRI and found increased activation of the deep layers of the primary visual cortex when subjects viewed an illusory triangle (the Kanizsa illusion) which may represent the activity of expectation units suppressing bottom-up information to make the illusion possible. When the illusion was broken into its subcomponents features, the study recorded suppressed activity in middle and superficial layers of V1 which could be interpreted as a dampening of error signals in response to a very predictable stimulus. Laminar segregation is also reflected in neuronal oscillations measurable with electrocorticography, electroencephalography (EEG) or magnetoencephalography (MEG). Evidence from monkey and human studies indicate that the superficial cortical layers show neuronal synchronization predominantly in the gamma frequency bands while deep layers generate oscillations in the alpha or beta bands (Bauer *et al.*, 2014). A few experimental studies have provided evidence that gamma and beta-band activity embodies prediction error and expectation signals (Fujioka *et al.*, 2009; Arnal *et al.*, 2011; Todorovic *et al.*, 2011; Sedley *et al.*, 2016): when a stimulus is expected, beta power gradually builds up and gamma activity is reduced when those expectations are finally realized. On the contrary, when expectations are violated, there is an increase in gamma power and beta oscillations are first reduced before resynchronizing. It is possible to 'exploit' the cortical laminar architecture and its properties in order to dissociate predictions from prediction error signals. One way of doing so is to record neuronal oscillations during rest measurable with electrocorticography, EEG or MEG. The resulting frequency bands of activity can reveal the

directionality of information flows, with high frequency bands reflecting a predominance of bottom-up prediction error information passing and low frequency bands reflecting top-down information flow of predictions (Hillebrand *et al.*, 2012; Bauer *et al.*, 2014). Furthermore, spectral characteristics of resting-state EEG data can be used to infer the neuronal microstructure of the laminar cortex.

1.5.1.5 Active inference and goal-directed behaviours

Minimization of free energy can be achieved by two complementary strategies: changing predictions to match sensations or sampling sensations to match predictions. Predictive coding typically refers to the first strategy while the second strategy is known as active inference. Active inference has opened new avenues for understanding perception and action as tightly bound together: one would need to have expectations about the sensory consequences of moving in order to initiate a movement. In other words, action can be understood as fulfilling prior beliefs about proprioceptive inputs and/or external sensory inputs. Dopamine and acetylcholine are key neuromodulators in this scheme by regulating the precision assigned to proprioceptive/interoceptive priors and external inputs, respectively (Friston *et al.*, 2010).

Active inference can successfully explain motor control (Kilner, 2011) but has also been generalised to goal-directed behaviours. Formulations around goal-directed behaviours are usually united by the normative model of maximising value or expected reward in the future. Value-learning has been translated into free-energy principles by transforming the value of 'loss' or negative value into surprise. Based on reward signals from the environment, reinforcement learning models suggests that an agent assigns value to environmental cues and actions by comparing the received reward or punishment with the expected outcome and uses these values to inform its decisions. Recasting reinforcement learning in terms of active inference, value-functions can be replaced with prior expectations about sensory trajectories and the optimal policy (or sequence of actions) replaced by explorations of specific sensory states to match prior expectations (Friston *et al.*, 2009). The attribution of value or weight to prediction errors – or precision – determines to what extent deviations from expectations should induce new learning. The role of precision is thus conceptually the same as that of the learning rate parameters in reinforcement learning (see Rescorla-Wagner learning in Chapter 6). Dopamine, within the conventional reinforcement learning paradigm, is thought to encode the prediction error on value (or reward prediction error) (Pessiglione *et al.*, 2006; Schultz, 2016). Within the active inference paradigm, dopamine codes the precision of proprioceptive sensory inputs. Goal-directed behaviours are thus a direct manifestation of

predictive processes where high precision-weighted predictions carry greater motivational salience and exert greater control over actions (Friston *et al.*, 2014*a*).

1.5.2 Evidence of aberrant predictive coding in neurodegenerative diseases

In this section, I will re-assess the main deficits seen in typical AD and canonical FTD syndromes following the predictive coding framework. I will categorise deficits in terms of perception, probabilistic learning, and goal-directed behaviours. I will also describe the spectral neurophysiological signatures of AD and FTD and what these potentially entail in terms of predictive coding.

1.5.2.1 Alzheimer's disease

AD pathology equally affects the visual and auditory systems and multiple studies have focused on disruptions of visual perception in AD. For the purpose of this thesis, I will only report auditory examples of aberrant predictive coding in AD.

Perception

A number of studies have now demonstrated an early and specific impairment of AD patients in segregating, tracking and grouping auditory objects (Goll *et al.*, 2012, Golden *et al.*, 2015*a*). Auditory scene analysis is a classic example of the necessity to deploy top-down expectations to identify discrete sources in a chaotic and muffled stream of sounds, especially in a noisy environment (e.g. cocktail party effect) (Bregman and McAdams, 1994; Griffiths and Warren, 2002; Pressnitzer *et al.*, 2011). Context-based predictions aid the segregation of auditory input into its constituent sources over time and space. This function is known to depend on temporo-parietal areas within the DMN, regions heavily atrophied in AD.

Probabilistic learning

AD patients consistently demonstrate reduced auditory MMN amplitude and longer peak latencies to pitch deviants only at long inter-stimulus intervals (>3sec), suggesting that the sensory memory trace decays faster in AD but that probabilistic learning of patterns may be preserved (Pekkonen *et al.*, 1994; Pekkonen, 2000). A normal performance on the weather prediction task further confirms a relatively preserved ability to extract statistical regularities from the environment in AD (Klimkowicz-Mrowiec *et al.*, 2008).

Goal-directed behaviours

Apathy is an important behavioural change in behaviour in AD (Landes *et al.*, 2001). Apathy is defined as a disorder of motivation and has three main presentations: diminished goal-directed behaviour, goal-directed

cognitive activity or 'blunted' emotional responses. In predictive coding terms, apathy signifies a diminished precision of predictions at higher processing levels i.e. a low certainty in mapping action to outcome (Hezemans *et al.*, 2020). As a consequence, there is bias towards sensory evidence which overrides the weak predictions, resulting in an absence of action initiation. Altered trafficking of noradrenaline in AD is thought to account for such altered precision weighting (Ruthirakuhan *et al.*, 2018).

Laminar microcircuits disruptions

Resting-state EEG and MEG studies showed that AD patients had diminished gamma oscillations in medial temporal areas (Ranasinghe *et al.*, 2016; Sami *et al.*, 2018) which suggests a vulnerability of superficial cortical layers to amyloid beta and tau pathogenic proteins in entorhinal cortex and hippocampus, potentially underpinning a diminished precision of prediction errors and over-reliance on prior expectations.

1.5.2.2 bvFTD

Perception

Aberrant perceptual inference in bvFTD has been reported in relation to somatosensory and interoceptive processing with reduced sensitivity to pain and temperature (Fletcher *et al.*, 2015*b*) and deficient processing of interoceptive signals such as heartbeat (Guo *et al.*, 2016). This evidence suggests that central interoceptive (autonomic) control is deficient in bvFTD and provides a candidate generic mechanism for socio-emotional deficits within the 'embodied cognition framework'. Low resting skin conductance in bvFTD has thus been linked to emotional blunting (Joshi *et al.*, 2014), impaired blood pressure reactivity correlated with reduced emotional ratings of disgust (Eckart *et al.*, 2012) and reduced cardiac responses to facial emotions has been directly linked to impaired emotion identification (Marshall *et al.*, 2018*a*). A predictive coding account of this impaired 'embodied cognition' in bvFTD would posit decreased precision of interoceptive prediction errors (corresponding to the difference between interoceptive afferent data and the generative model of the state of the body). Strategies deployed to minimise this prediction error are potentially three-fold: an action, a revision of the model or a recruitment of central autonomic network to induce autonomic efferent changes and maintain physiological homeostasis. Because of this constant bidirectional information exchange between central and peripheral states, a diminished prediction error accompanied by central autonomic dysfunction would interrupt a cascade of feedback loops, ultimately leading to blunted physiological and higher-level cognitive reactivity to salient signals, with social and emotional connotations. Within that framework, interoceptive malfunction in

bvFTD overlaps with emotional processing, motivation, reward processing and affective mental state inference (García-Cordero *et al.*, 2016).

Over-reliance on external contextual information has also been described for bvFTD patients in the context of facial emotion identification (Kumfor *et al.*, 2018, p. 20). Similarly, bvFTD patients perform better at detecting humour in familiar compared to novel scenarios depicted in visual cartoons (Clark *et al.*, 2015*b*). Although further studies need to corroborate these results, they suggest an aberrantly heightened precision ascribed to sensory inputs relative to the precision ascribed to prior expectations.

Probabilistic learning

bvFTD patients exhibit a global reduction of MMN signals to all types of auditory deviants (pitch, duration, location, intensity, gap) (Hughes and Rowe, 2013). Rather than reflecting a dysfunction of early preattentional processing, this reduction was associated with changes in higher-level network connectivity: left frontotemporal coherence was reduced in the lower-frequency bands and fronto-frontal coherence was reduced in the gamma frequency band. Left frontotemporal coherence disruption may reflect a failure to establish a predictive model in response to standard tones while frontal intra-hemispheric coherence disruption might reflect reduced prediction error processing in the prefrontal cortex, putatively related to the pathological insult targeting the superficial cortical layers (Mann and Snowden, 2017). bvFTD patients' performance at a flanker paradigm, which measures the ability to detect targets in the presence of distractors, was significantly reduced, suggesting a failure of predictive models to lower prediction errors induced by distractors (Krueger *et al.*, 2009). On the weather prediction task, bvFTD patients performed poorly during the acquisition of probabilistic learning rules (Dalton *et al.*, 2012) but their performance gradually improved as the task progressed suggesting a delay in forming predictive models compared to healthy controls. Poor performance correlated with atrophy of the dorsal striatum.

Goal-directed behaviours

Apathy and impulsivity or disinhibition are both used as criteria for the diagnosis of bvFTD (Lansdall *et al.*, 2017). In predictive coding terms, both behaviours could arise from impaired precision of internal predictions generated at higher processing levels. However, in the case of apathy, precision of predictions is decreased while in the case of disinhibition, it is increased. A predictive coding framework can therefore reconcile two distinct behavioural manifestations via a common mechanism. This mechanism is presumably instantiated in specific network activity and microcircuit properties: Hughes et al. (2018) provided a comprehensive account of

disinhibition in bvFTD, describing how layer-specific pathology in superficial prefrontal layers disrupts the cross-frequency coupling between frontal cortical regions, attenuates the beta desynchronization preceding movement execution and consequently impairs movement control during a go-no go task.

For more complex decisions involving valuation of reward or punishment during classic gambling tasks, risk-taking is increased in bvFTD reflecting an abnormal processing of prediction error, possibly due to atrophy and dysfunction of dopaminergic structures (Rahman *et al.*, 1999, 2006; Torralva *et al.*, 2007; Chiong *et al.*, 2014). Diffusion drift models are commonly used to analyse response times during impulsive and risky decision-making (Tajima *et al.*, 2016). Applied to patients with prefrontal and orbitofrontal cortex lesions, the model revealed response bias towards the decision boundary, i.e. a high confidence in their prior to perform an action (Peters and D'Esposito, 2020). Although this study needs to be replicated in patients with bvFTD, it suggests that computational modelling might constitute a useful tool to verify hypotheses about precision of priors.

Laminar microcircuit disruptions

A mouse model of bvFTD showed a specific loss of alpha power at both parietal and prefrontal recording sites (Koss *et al.*, 2016). Resting-state electrophysiological recordings in humans have replicated these results and showed that bvFTD patients had a reduction of slow oscillatory bands (theta to beta) over the frontal cortex (Sami *et al.*, 2018). Interpreting the distribution of rhythms across cortical layers, both studies suggest that the pathological insult targeting the superficial cortical layers in bvFTD is responsible for a failure to update predictions in frontal areas, reflected in a reduction in slower oscillations.

1.5.2.3 svPPA

Perception

Erosion of predictive models for semantic information is the current dominant pathophysiological account of svPPA pathology (Lambon Ralph *et al.*, 2010; Chen *et al.*, 2017). Semantic processing requires top-down signalling from 'semantic' areas, conveying prior knowledge; and from frontal areas, providing contextual information (Lyu *et al.*, 2019). In accordance with the highly consistent atrophy profile in the semantic appraisal network displayed by svPPA patients, top-down semantic control, necessary to disambiguate meaningful objects in noisy environments (Cumming *et al.*, 2006) or to differentiate concepts from the same semantic category (Chen *et al.*, 2017), is significantly degraded. Weakness of semantic priors manifesting as a significantly reduced N400 electrophysiological signal was evident when patients with svPPA were required to disambiguate semantically related words (Hurley *et al.*, 2012). Aberrant perceptual inference in svPPA generally resembles the bvFTD

syndrome, with similarly reduced interoceptive prediction errors (and aberrant responses to aversive stimuli, pain and temperature (Hoefer *et al.*, 2008, Fletcher *et al.*, 2015*b*)) promoting deficits of emotion processing and social cognition. Interoceptive accuracy during a heartbeat counting task was shown to be specifically reduced in svPPA patients and correlated with reduced daily-life sensitivity to the emotions of others (Marshall *et al.*, 2017).

Probabilistic learning

Experimental paradigms looking at comprehension of degraded speech offer an ideal framework to study predictive processing as it depends heavily on an efficient computation of the probability of various possible incoming messaged according to context (Sohoglu and Davis, 2016). Hardy et al. (2017) showed that patients with svPPA have impaired ability to extract statistical regularities from incoming speech signals, despite an intact capacity for processing bottom-up information (spectrotemporal analysis of speech). In particular, svPPA patients were impaired at differentiating between sequences of high and low entropy (or uncertainty, see section 1.5), correlating with atrophy in a distributed fronto-cingulo-striatal network. In another study, processing of semantic and emotional congruency in auditory scenes was impaired in svPPA patients and correlated with atrophy of temporal and insular cortices and striatum (Clark *et al.*, 2017).

Goal-directed behaviours

Behavioural rigidity with clock-watching and obsessional interest in numbers and music are often prominent in svPPA. To the extent to which semantic predictive models extract and represent stable, organising features of the world, the loss of such models might make the world generally less predictable and more surprising for patients with svPPA. Increased engagement in activities involving mathematics and music, highly predictable domains bound with implicit rules less dependent on semantic knowledge, may therefore be partly compensatory (Marshall *et al.*, 2018*c*). Conversely, weak top-down predictions, dominated by bottom-up sensory input, would give rise to stereotyped repetitive behaviour that would tend to make the input more predictable. This behavioural strategy is commonly observed in svPPA patients, along with social withdrawal and inability to predict other people's intentions. There may be a pathophysiological analogy here with autism, which has now benefited from several decades of predictive coding formulation (Lawson *et al.*, 2014; Gonzalez-Gadea *et al.*, 2015), notably giving rise to new hypothesis about dysfunctional GABA and acetylcholine neuromodulation. Disinhibition is another key behavioural feature of the svPPA phenotype and was recently linked to attenuated inhibitory self-coupling within anterior temporal regions, supposedly explained by abnormal tonic inhibitory GABAergic transmission in temporal lobe superficial cortical laminae (Benhamou *et al.*, 2020).

Laminar microcircuit disruptions

Resting-state electrophysiological profiling in svPPA patients has revealed reduced synchronization of alpha and beta frequencies within the left temporo-parietal junction and reduced alpha power in bilateral temporal poles (Ranasinghe *et al.*, 2017). This observation confirms the disruption of top-down flow of information associated with low-frequency bands, suggesting a disruption deep cortical layers. To date, a number of studies have showed that TDP-43 type C predominantly target superficial layer II (Mackenzie *et al.*, 2011; Tan *et al.*, 2013; Mann and Snowden, 2017). Further studies need to clarify this apparent paradox.

1.5.2.4 nfvPPA

Perception

Doubly hit in low-level sensory areas and in high-order areas in inferior frontal gyrus, nfvPPA patients frequently have impaired spectrotemporal analysis of speech and other complex sounds with accompanying hearing loss (Goll *et al.*, 2010; Rohrer *et al.*, 2012; Grube *et al.*, 2016; Hardy *et al.*, 2017, 2019). This suggests a potential distortion of bottom-up prediction errors. Deficits extend to impaired perception of unfamiliar accents, emotional and linguistic prosody and reduced modulation of social signals such as laughter (Rohrer *et al.*, 2009, 2012; Hailstone *et al.*, 2012; Pressman *et al.*, 2017). This suggests a reduced flexibility of predictive models to minimise prediction errors.

Probabilistic learning

This second hypothesis of reduced flexibility of predictive models in nfvPPA has been tested in a MEG experiment using a degraded speech paradigm (Cope *et al.*, 2017). By manipulating top-down (written text) and bottom-up information (degraded spoken words), these authors showed that the atrophy level of frontal cortical regions predicted the delayed neural resolution of predictions at the level of the temporal lobe. Using Bayesian modelling, they demonstrated that prior knowledge of expected speech content is applied in an inflexible way by nfvPPA patients. In consequence, patients rated graded-difficulty vocoded spoken words as being similarly difficult and engaged frontal regions uniformly across stimuli, lacking the normal difficulty-related modulation of neural activity. This study was the first to demonstrate a link between inferior frontal atrophy and overly precise top-down predictions. Inflexible priors about linear word ordering within sequences may also underpin the agrammatism typically observed in nfvPPA.

nfvPPA patients have also demonstrated impaired categorisation of sound sequences with high and low entropy (Hardy *et al.*, 2017). However, these deficits are likely to reflect impairment at processing early

spectrotemporal features rather than reflecting an inability to form on-line short-term priors for novel non-verbal sound sequences.

Goal-directed behaviours

Similarly to bvFTD patients, apathy and impulsivity are observed in nfvPPA patients (albeit developing later in the illness) and may reflect an aberrant precision allocation to internal predictions linked to actions.

Laminar microcircuit disruptions

nfvPPA patients revealed a reduction in slow rhythms in centroparietal regions (Sami et al., 2018) and displayed hyposynchrony of alpha and beta frequencies in the left inferior frontal region (Ranasinghe et al., 2017), suggesting circuit dysfunction in the deep cortical layers of medial parietal and inferior frontal regions.

1.6 The case of music

In this section, I will first explain why music is relevant to predictive cognition and will review the experimental evidence for predictive coding principles at work in music processing in healthy populations. In a second part, I will describe the reasons why music is particularly well suited as a tool to probe neurodegenerative disease pathophysiology and will review the available evidence for the way AD and canonical syndromes of FTD impact the musical brain.

1.6.1 Relevance to predictive coding

As a paradigm for addressing predictive cognition, music is particularly promising. Music is ubiquitous in daily life and constitutes a model 'environment' that is bound by a finite set of implicit 'rules'. Even musically untrained listeners internalise these automatically through lifelong exposure to the dominant musical culture and accordingly acquire strong and reliable psychological expectations about musical patterns and events (Koelsch *et al.*, 2000). Moreover, 'surprise' of various kinds is easily engendered in music by violating these rules. The inherently rule-based nature of music and the role of expectation and surprise in achieving many of its psychological and physiological effects (Blood and Zatorre, 2001; Huron, 2006) together suggest that the neural processing of music might follow the principles of predictive coding. Listening to music (like other complex cognitive functions) presents the brain with a challenging computational problem of information processing, comprising a number of component operations (Koelsch, 2011). Contemporary cognitive models of music processing have characterised these operations and their interactions in some detail (Peretz, 1990, 2006; Peretz and Coltheart, 2003; Patel, 2008; Koelsch, 2011, Clark *et al.*, 2015*a*). Basic information theory concepts as

described by Shannon (Shannon, 1948) have been introduced in musical psychology research and have allowed a new taxonomy of psychological effects of music in terms of entropy which quantifies the listener's degree of uncertainty about the prevailing musical environment, and information-content which represents the degree of unexpectedness (or 'surprise') associated with a particular musical event (Pearce, 2005; Pearce *et al.*, 2010).

Manipulating surprise, defined in predicting coding terms as the prediction error, is a relatively simple way to study the strategies employed by the human brain to minimize the free energy of its interoceptive and exteroceptive states. The auditory modality is ideal for assessing surprise, in this sense: sounds unfold over time and therefore always entail holding information online to compare incoming data with what has gone before. However, most research on auditory surprise has employed very simple and repetitive stimuli and little is known about prediction in more natural auditory environments. The main issue in using naturalistic stimuli is the inherent difficulty controlling for parameters that might influence the measured variables of interest. For instance, a study looking at how one resolves violations of expectations listening to speech might be contaminated with factors such as the semantic associations one makes when hearing a word; additionally, there is generally a large repertoire of plausible candidate words when building a sentence.

Music on the other hand does not necessarily carry extrinsic semantic associations and is intrinsically much simpler to manipulate. The structure of music is, however, governed by combinatorial rules that determine shorter- and longer-range transition probabilities between notes and intervals. These 'rules' are internalised by listeners automatically through lifelong exposure to the dominant musical culture and bear some formal similarities to syntax in human languages. These rules can be thought as regularities which constrain how tones, intervals, chords and durations of tones are arranged to form meaningful melodies, rhythmical phrases and harmonic progressions (Huron, 2006). Rohrmeier and Koelsch (Koelsch *et al.*, 2013; Rohrmeier *et al.*, 2015) described musical structural 'syntactic' relations (such as harmonic progressions and the nesting of melodic and rhythmic motifs) over different timescales using hierarchical models of information processing analogous to those use in human language processing but also intrinsic to music. There are multiple ways of building expectations within these syntactical models of music and this special modality has already been proposed as an ideal probe of information flow within a neural processing hierarchy (Michael and Wolf, 2014; Koelsch *et al.*, 2019): it is built from acoustic regularities and establishes strong perceptual predictions based on 'rules' internalised from past experience, but at the same time, it often violates or defers expectations to achieve its most salient effects ('chills' are a case in point: (Huron, 2006)).

1.6.2 Behavioural and physiological responses to violations of musical expectations in healthy populations

1.6.2.1 Pitch and harmony perceptual expectations

Pitch is a fundamental building block of musical patterns. The relationships between the pitch values of individual notes convey musical structure as intervals (pitch change between successive notes), melody (the contour of 'up' and 'down' pitch shifts in a note sequence) and key (the harmonic rules that determine how notes are grouped into chords and scales). Pitch is a percept that is actively 'constructed' by auditory cortex from incoming sensory data. This is illustrated by the phenomenon of the 'missing fundamental', whereby the pitch of a harmonic series is perceived by normal listeners even though the corresponding fundamental frequency is physically absent (Zatorre, 1988). Building expectations about these 'constructed' percepts require the knowledge (implicit for untrained listeners) of musical syntax. Syntax refers to the rules underlying the organization of sounds into musical sequences. Various paradigms have been used to test the presence of such internalized predictive models during music perception. The first one is the classic implicit priming paradigm involving the manipulation of 'prime' context and a 'target' by changing their congruity to determine how this influences performance on an irrelevant task. Based on the robust phenomenon of facilitation for more versus less expected targets (measured in terms of reaction time or performance accuracy), this musical priming paradigm has demonstrated that listeners possess knowledge of musical syntax even without any formal musical training (Bharucha and Stoeckig, 1986; Bigand and Parncutt, 1999; Tillmann *et al.*, 2006; Omigie *et al.*, 2013).

Another classic paradigm to test the generation of musical expectations during music listening is the MMN paradigm. Unexpected tones in highly familiar or novel melodies consistently elicit a P300 and a frontal negative evoked-response potential (ERP) emerging 100ms after onset of deviants (N1) (Paller *et al.*, 1992; Besson and Faïta, 1995; Miranda and Ullman, 2007; Koelsch and Jentschke, 2010). More recent studies have used computational modelling of information-theoretic properties of music to produce continuous estimates of auditory expectations in unfamiliar melodies (Pearce, 2005; Pearce *et al.*, 2010). Without introducing highly unexpected events, they replicated the previous observation of an N1 signature of subtle changes in auditory surprise: N1 increased with higher levels of estimated surprise (Omigie *et al.*, 2013, 2019; Quiroga-Martinez *et al.*, 2020). In the most recent study, Quiroga et al. (2020) proposed that N1 is in fact restricted to tonotopic predictions about lower-level acoustic features of sounds (spectral content) such as pitch interval size, while

another later positive ERP, the P300, would reflect higher-level predictions requiring the encoding of patterns spanning longer temporal scales. Source reconstruction has also suggested hierarchical auditory processing with MMN generated in more anterior parts of the right primary auditory cortex whereas N1 and P300 generators are located more widely among frontal and parietal cortices.

Another ERP signature of violations of musical expectations is the so-called early right anterior negativity or ERAN elicited by irregular chords in a harmonic chord progression (Koelsch *et al.*, 2001; Koelsch and Jentschke, 2010). This has attracted considerable attention among music neuroscientists: the ERAN seems to be music-specific, it is present even when no task is required from the listener and its amplitude does not change when individuals are being told that a deviant will occur. For these reasons, it is often referred to the 'music-syntactic MMN'.

The functional neuroanatomy of pitch processing has been extensively studied in the healthy brain (Janata *et al.*, 2002; Patterson *et al.*, 2002; Koelsch, 2005), delineating a peri-Sylvian network in which elementary pitch percepts are achieved in lateral Heschl's gyrus and pitch patterns of increasing complexity are analysed hierarchically in posterior and anterior superior temporal and inferior frontal cortices. Seger et al. suggested a dissociation between the posterior and anterior STG with the former engaged in more basic pitch processing and the latter, along with the IFG and the basal ganglia, recruited for higher-order harmonic processing (Seger *et al.*, 2013). Again, fMRI correlates of deviance detection in musical contexts include the bilateral superior temporal gyrus, the right inferior frontal gyrus and the right inferior parietal lobule (Koelsch, 2005; Tillmann *et al.*, 2006; Royal *et al.*, 2016; Cheung *et al.*, 2018). In particular, the right inferior frontal gyrus is commonly considered the key structure for processing musical syntax, mirroring the left inferior frontal gyrus typically reported for processing grammatical syntax in language (Maess *et al.*, 2001; Cheung *et al.*, 2018).

1.6.2.2 Precision modulation of expectations

Computational modelling of information-theoretic properties of music have also allowed the investigation of precision modulation of musical expectations, varying uncertainty levels of the musical 'environment' and observe the effect on perceptual and neural processes. Two behavioural studies have shown that unexpected tones are rated as more salient in contexts with low compared to high uncertainty (Hansen and Pearce, 2014; Hansen *et al.*, 2016) and one study addresses this question at the neural level using MEG (Quiroga-Martinez *et al.*, 2019): using a multi-feature paradigm (pitch, slide, intensity and timbre deviants) and manipulating the predictability (or entropy) of melodies consisting in non-repetitive 32-tone patterns, they found

a strong reduction in MMN amplitudes in response to pitch deviants in highly uncertain (high entropy) melodies compared to predictable (low entropy) melodies. Accuracy and confidence measures in a subsequent behavioural experiment were also reduced for the detection of deviants in high-entropy melodies. Interestingly, this result has been replicated using autonomic recordings of pupil dilatation (Bianco *et al.*, 2020) with a larger pupil dilatation response to pitch deviants in unfamiliar melodies in low than high entropy contexts. Processing of statistical structure in melodies also occurs at the subcortical level: a recent study showed modulation of activity in dorsal and ventral striatum by the uncertainty level of harmonic progressions (Cheung *et al.*, 2019). The same study revealed activity in the amygdala, the hippocampus and auditory cortex in response to increasing surprise level of unexpected chords, replicating a previous study which found an increased BOLD activity in bilateral amygdala in response to irregular chords (Koelsch *et al.*, 2008*a*). These results emphasize the role of limbic and striatal circuits in processing surprise or uncertainty in music and suggest that violations of musical expectations are directly linked with emotion and reward processing.

1.6.2.3 Semantic memory for music

Musical pitch expectations also derive from representations of musical objects instantiated at higher levels of the musical processing hierarchy (Koelsch *et al.*, 2013). Musical object representations require semantic processing in which musical pitch patterns become associated with stored knowledge about the objects of experience. Music is one of the sensory categories processed by the semantic memory system, which mediates the storage and mobilisation of an encyclopaedic lexicon of verbal and nonverbal concepts, derived from the individual's accumulated experience of the world. As a classical tenet of neuropsychology, semantic memory dissociates both from perceptual mechanisms and from other memory systems (in particular, episodic memory). This tenet has been found to apply to music, with well attested cases of selective sparing or impairment of musical semantic memory (musical 'associative agnosia') following focal brain damage (Eustache *et al.*, 1990; Wilson *et al.*, 1995; Peretz, 1996; Schuppert *et al.*, 2000; Finke *et al.*, 2012). Musical semantic memory is engaged during recognition of familiar melodies, musical instruments and (in those with musical training) musical symbols and notation systems, as well as explicit knowledge of the 'rules' that govern musical compositions.

Functional neuroimaging studies of musical semantic memory in the healthy brain have delineated an extensive cerebral network including anterior temporal, insular, inferior and dorsomedial prefrontal cortices (Platel *et al.*, 2003, Groussard *et al.*, 2010*b*, *a*; Herholz *et al.*, 2012; Sikka *et al.*, 2015; Freitas *et al.*, 2018).

1.6.2.4 Emotion and reward processing

The capacity of music to generate emotional responses is the key to its appeal for most listeners: considering that abstract tone patterns have no intrinsic biological value, this capacity is indeed remarkable, as illustrated by the intense autonomic arousal that accompanies musical 'chills' or 'shiver' (Blood and Zatorre, 2001). Music carries substantial reward potential for many people, and this motivates behaviours such as music seeking and repeated exposures to particular music.

Musical pleasure is thought to rely on generation of psychological expectations and their subsequent violation or confirmation (Huron, 2006). I described the electrophysiological and anatomical correlates of the violation of musical expectations above. Beyond addressing how the human brain creates expectations, studies have started to look at the emotional impact of such manipulations. Generally, unexpected musical events are rated as unpleasant in unfamiliar complex pieces (Koelsch *et al.*, 2008*b*, *a*; Egermann *et al.*, 2013). More systematic studies manipulating both uncertainty of contexts and 'levels' of surprise using an information-theoretic model of auditory expectation revealed an interesting pattern: listeners consistently prefer music of intermediate predictive complexity (musically surprising events) in low-uncertainty context while the preference shifts towards expected musical outcomes (musically less surprising events) in uncertain contexts (Cheung *et al.*, 2019; Gold *et al.*, 2019). A neuroanatomical correlate of this modulatory effect of musical contextual uncertainty has been identified in nucleus accumbens, a core component of dopaminergic circuitry in the ventral striatum. A widely accepted hypothesis is that dopamine codes the 'reward positive prediction error' ('better than expected' signal) (Schultz, 2016). Studies have shown that dopamine is indeed released when expected events are both heard and anticipated, for familiar but also previously unheard music (Blood and Zatorre, 2001; Salimpoor *et al.*, 2011, 2013, 2015). Cheung et al.'s study suggests that striatal activity may modulate attention deployment toward seeking more information that could potentially resolve uncertainty, in the case of both positive and negative reward prediction errors (better or worse than expected outcomes). This apparent paradox has been termed the 'epistemic value' in the jargon of active inference: both positive and negative prediction errors elicit activity in reward networks because both help improve our learned model of musical syntax (Friston *et al.*, 2015; Koelsch *et al.*, 2019).

The functional neuroanatomy of musical emotion and reward processing has been widely studied in the healthy brain (Blood *et al.*, 1999; Blood and Zatorre, 2001; Menon and Levitin, 2005; Steinbeis *et al.*, 2006; Salimpoor *et al.*, 2013, 2015; Zatorre and Salimpoor, 2013; Koelsch, 2014; Lehne *et al.*, 2014). This work has

demonstrated that the neural substrates of musical emotion are very extensive. These substrates encompass structures that analyse relatively elementary affective attributes (such as roughness and dissonance) or mediate autonomic responses, in medial temporal lobe and insula; higher order areas that evaluate salience and behavioural relevance and the representation of mental states, in medial prefrontal and orbitofrontal cortices; and subcortical (mesolimbic) dopaminergic circuits involved in coding reward value, including nucleus accumbens and ventral striatum. There is an important overlap with the musical semantic memory network, underscoring the role of familiarity in musical preference (Brown *et al.*, 2004; Pereira *et al.*, 2011; Lehne *et al.*, 2014).

In summary, musical emotion and reward processing has emerged as a major theme in contemporary music neuroscience; the recognition that music engages the neural machinery of biological reward processing and social connectome (Laurita and Nathan Spreng, 2017; Alcalá-López *et al.*, 2018) has in turn prompted a reappraisal of the evolutionary 'purpose' of music and its possible role in human social cognition, in particular the signalling of affective mental states (Zatorre and Salimpoor, 2013; Clark *et al.*, 2014). This research notably positions music as a useful probe of 'biologically relevant' goal-directed behaviour and active inference (see section 1.4.1.5) and by extension, the socio-emotional disturbances that characterise psychiatric and neurological disorders (Koelsch, 2014).

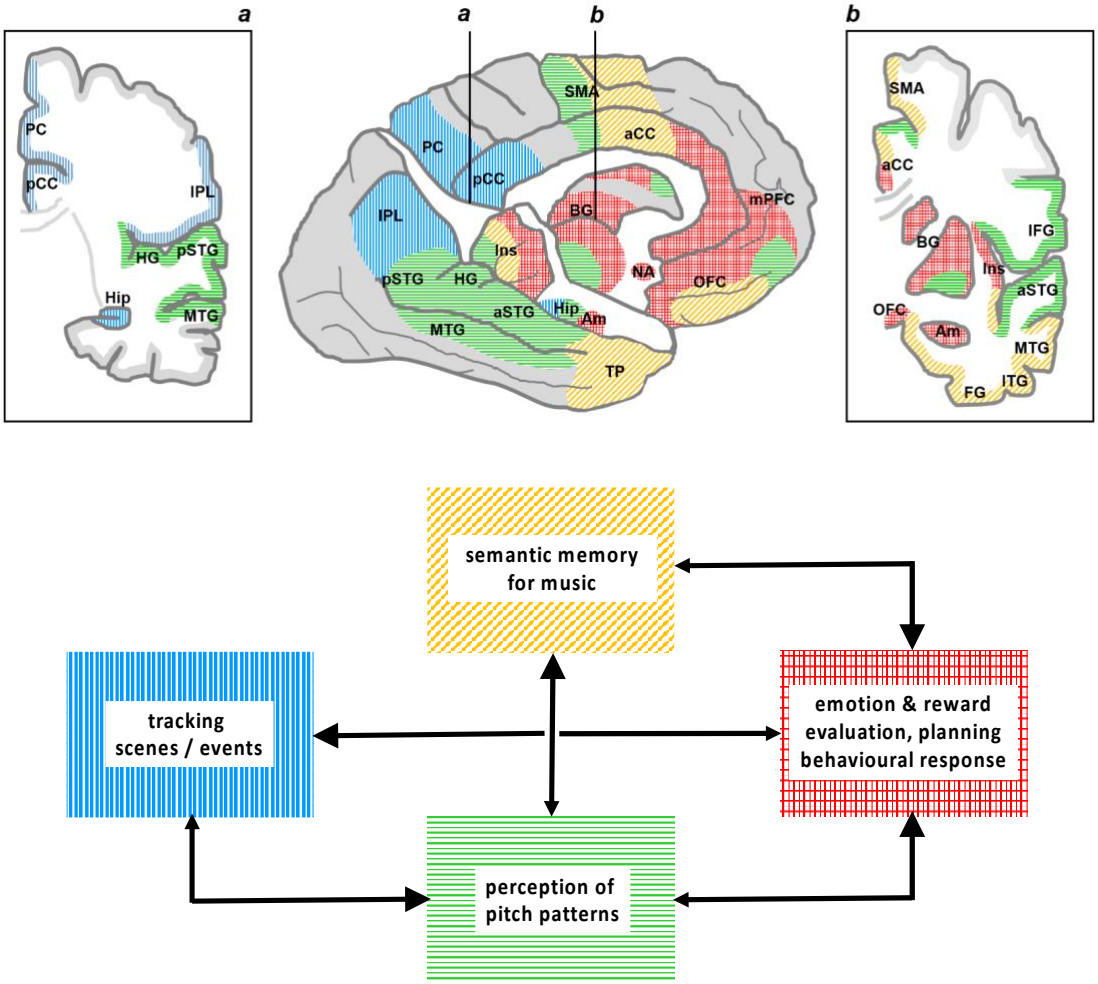

Figure 1.3. The musical brain in healthy populations

The brain cartoon (top centre) shows a right lateral cut-away view of the cerebral hemispheres with the right hemisphere projected forward (right frontal lobe and right anterior superior temporal cortex removed) to reveal the major cortico-subcortical networks implicated in music processing, based on studies of focal brain damage and functional imaging of the healthy brain (see also Table 2). Coronal hemi-sections through the intact (rear) left hemisphere at levels **a** (posterior) and **b** (anterior) are also provided, to orient the projected neural networks three-dimensionally. These brain networks mediate key cognitive operations or processing stages that extract different kinds of information from musical stimuli: the major operations and their interactions are diagrammed below. The shading code indicates the corresponding neural network substrate for each cognitive operation (see text for details); arrows indicate major pathways of information transfer between musical processing stages (as indicated by the relative size and direction of the arrow heads, information exchange at each stage is generally reciprocal, allowing for predictive updating according to musical context but with a predominant flow of information from earlier perceptual stages [left of diagram] to subsequent semantic and evaluative stages [right of diagram] that ultimately mediate behavioural responses). Auditory working memory is not diagrammed here but is likely to interact importantly with each of the processing stages shown. aCC, anterior cingulate cortex; Am, amygdala; aSTG, anterior superior temporal gyrus; BG, basal ganglia; FG, fusiform gyrus; HG, Heschl's gyrus; Hip, hippocampus; Ins, insula; IPL, inferior parietal lobe; IFG, inferior frontal gyrus; ITG, inferior temporal gyrus; mPFC, medial prefrontal cortex; MTG, middle temporal gyrus; NA, nucleus accumbens; OFC, orbitofrontal cortex; PC, precuneus; pCC, posterior cingulate cortex; pSTG, posterior superior temporal gyrus; SMA, supplementary motor area; TP, temporal pole.

1.6.3 Musical disorders in dementia

The apparent power of music to unlock memories and other cognitive capacities in people with dementia, to soothe the agitated and to comfort the bereft have always captured the popular imagination. For neurologists as well as the lay public, the chief motivation for studying music in dementia has traditionally been the prospect of musical therapies. Only recently has it come to be appreciated that music might also serve as a tool to understand the neurobiology of neurodegenerative diseases and in particular, the pathways and mechanisms by which molecular pathologies give rise to complex cognitive and behavioural effects. Music has several properties that makes it a very useful and flexible vehicle for capturing predictive coding mechanisms, as described in the foregoing section, but has also a particular pertinence for studying neurodegenerative diseases: it is highly ecological and very important for people across life stages; it cuts through linguistic barriers and aphasia as it does not rely on verbal or other extra-musical associations; it is relatively easy to manipulate and administer as a neuropsychological tool and usually well tolerated; it has physiological signatures that may allow for disease effects to be captured over a wide range of disease stages (e.g. very early / very advanced) that are challenging to access using conventional cognitive tests; bound by strong but largely implicit rules and frequently admitting unexpected events, it is an ideal model for the much less tractable milieu of expectation and surprise that surrounds the socio-emotional milieu of daily life and offers a way to track socio-emotional processes that are targeted by FTD and AD but are still very difficult to measure using standard tests; based on evidence from functional imaging studies of the healthy musical brain (see foregoing section), it samples the entire processing hierarchy over the whole brain, ranging from early perceptual analysis to the programming of complex behaviours, and is therefore well suited to delineate disease with highly distributed neural network signatures.

The study of music processing in dementia is at a crossroads. Considerable progress has been made in defining a spectrum of disorders and in applying sophisticated (especially, neuroimaging) techniques borrowed from basic neuroscience to elucidate the brain mechanisms by which neurodegenerative pathologies impact musicality. However, we lack validated neuropsychological instruments for quantifying deficits in cognitively impaired listeners from a range of musical backgrounds and the literature is still largely informed by studies in a single disease. To date, appropriately, music psychologists have adopted a largely reductionist approach to the analysis of musical deficits, breaking music into its component cognitive parts to assess how these are affected by disease. I will now summarise the musical deficits associated with AD and FTD syndromes addressed in this

thesis. These deficits relate to the disturbed formation of expectations throughout the cortical hierarchy, from low-level spectrotemporal analysis to the integrity of predictive models at a semantic level. I conclude the overview with a summary of deficits in musical reward and emotional processing. A summary of the general mechanisms by which AD and FTD impact the musical brain is presented in Figure 2.

1.6.3.1 Pitch pattern processing

At the level of pitch pattern decoding, patients with AD syndromes have difficulty detecting deviant notes in a tone sequence that disrupt pitch contour (global) but not pitch interval (local), while patients with nfvPPA have difficulty detecting both interval and contour deviants (Golden *et al.*, 2017). On the contrary, another study by Grube et al., 2016 showed that patients with nfvPPA have more severe difficulty processing pitch changes across tone sequences (global) than between tone pairs (local) (Grube *et al.*, 2016). Less consistent deficits of pitch change detection were documented in AD and FTD syndromes in other studies, probably due to the inconsistent covarying of auditory working memory which highly contributes to the processing of sequential pitch changes (Goll *et al.*, 2010; Omar *et al.*, 2010; Hsieh *et al.*, 2011; Johnson *et al.*, 2011; Campanelli *et al.*, 2016). Deficits of musical pitch sequence contour (melody) processing in AD and nfvPPA resonate with other cognitive features of these syndromes. In AD, there is evidence for impaired processing of global stimulus characteristics in cognitive domains beyond music (Delis *et al.*, 1992; Matsumoto *et al.*, 2000; Slavin *et al.*, 2002), perhaps signifying a more general impairment of sensory feature integration. In particular, impaired processing of melody contour could reflect the difficulty AD patients experience with auditory scene analysis, as these processes engage the posterior temporal-parietal network including precuneus, posterior cingulate, posterior superior temporal and inferior parietal cortices (Zündorf *et al.*, 2013; Ragert *et al.*, 2014) that is primarily targeted by AD pathology. In nfvPPA, impaired processing of musical melody suggests an analogy with the processing of speech prosody, which is likely to present similar neural computational challenges and is likewise impaired in this syndrome (Rohrer *et al.*, 2012). These deficits are predicted by the neuroanatomical signature of nfvPPA syndromes which target anterior peri-sylvian cortices. Patients with AD have been shown to activate posterior superior temporal cortex less strongly than healthy older individuals during the processing of pitch sequences (Golden *et al.*, 2017). However, direct evidence for the neuroanatomical substrates of pitch pattern processing in these diseases remain limited.

Data on the processing of harmonic tonal relationships (keys and scales) in the dementias likewise remain limited. In one study, after adjusting for auditory working memory and elementary pitch discrimination

performance patients with AD and bvFTD had impaired ability to determine whether novel melodies were harmonically resolved or unresolved, whereas patients with nfvPPA and svPPA performed comparably to healthy age-matched individuals (Clark *et al.*, 2018). Using voxel-based morphometry of patients' brain MR images, impaired detection of harmonic structure has been shown to correlate with atrophy of entorhinal, anterior superior temporal and inferior frontal cortices targeted by AD and FTD pathologies.

1.6.3.2 Semantic memory for melodies

An important issue in assessing musical semantic memory in patients with dementia is the frequent presence of word retrieval or verbal semantic deficits, so that naming tasks in general do not reliably index music recognition.

The balance of evidence suggests that melody recognition is relatively preserved in AD, at least in the earlier stages of the illness (Beatty, 1999; Platel *et al.*, 2003; Vanstone and Cuddy, 2010; Hsieh *et al.*, 2011; Johnson *et al.*, 2011; Samson *et al.*, 2012; Kerer *et al.*, 2013; Cuddy *et al.*, 2015; Golden *et al.*, 2017). Most clinical studies have assessed recognition of melodies based on decisions about their familiarity or fidelity (presence of false notes). Whereas patients with bvFTD and nfvPPA may recognise melodies normally, svPPA is usually associated with impaired melody recognition as part of a pervasive disintegration of semantic memory across cognitive domains and modalities (Hsieh *et al.*, 2011; Johnson *et al.*, 2011, Golden *et al.*, 2015*b*, 2017); this deficit is not attributable to conjoint verbal or cross-modal impairments, since it is elicited by within-modality matching tasks (deciding whether two serially presented melodic fragments belong to the same or different pieces (Golden *et al.*, 2015*b*). It is noteworthy, however, that a substantial minority of patients with svPPA show relatively well preserved knowledge of melodies which may dissociate from other aspects of semantic function and is not contingent on prior musical expertise (Hailstone *et al.*, 2009; Omar *et al.*, 2010; Hsieh *et al.*, 2011; Weinstein *et al.*, 2011). A similar isolation of musical semantic competence has been reported after focal brain damage (Finke *et al.*, 2012). However, associative agnosia for melodies has been described in association with a rather wide cerebral distribution of culprit lesions (Clark *et al.*, 2015*a*): neuroanatomical inferences from neurodegenerative syndromes (notably, svPPA) with selective temporal lobe degeneration should therefore be qualified.

Using voxel-based morphometry, melody recognition across FTD and AD syndromes has been correlated with regional grey matter volume in anterior superior temporal and temporal polar cortex, extending into medial temporal lobe, insula and orbitofrontal cortex (Hsieh *et al.*, 2011; Johnson *et al.*, 2011). Within the musical

semantic memory network, the supplementary motor area is likely to mediate affective salience and preparedness to move on listening to familiar music and may play a pivotal role in modulating the effects of neurodegenerative pathologies. It has been proposed that sparing of this region may account for the relative preservation of musical semantic memory in AD (Jacobsen *et al.*, 2015) and it is noteworthy that this area is also relatively spared in svPPA. Functional MRI evidence suggests that patients with AD activate supplementary motor cortex comparably to healthy age-matched individuals in response to familiar melodies (Slattery *et al.*, 2019) and show enhanced activity and connectivity of this region following exposure to favourite music (King *et al.*, 2019). Conversely, reduced activation of inferior frontal cortex in AD during processing of musical familiarity (Slattery *et al.*, 2019) suggests at least partial loss of the functional integrity of the network that may account for musical semantic deficits documented in some previous studies (Groussard *et al.*, 2019).

1.6.3.3 Emotion and reward processing

Although the nature of musical emotion and its similarity to 'animate' emotions remains controversial (Juslin and Laukka, 2003), musical emotion processing has been most widely studied neuropsychologically by labelling or matching of emotions expressed in music to 'universal emotions' of human facial and vocal expressions (usually, happiness, sadness, anger and fear).

Using such procedures, patients with AD have been shown to have retained ability to identify different musical emotions (Drapeau *et al.*, 2009; Omar *et al.*, 2011) and can use mode and tempo cues to classify 'happy' and 'sad' music (Gagnon *et al.*, 2009). This ability may dissociate from recognition of facial expressions (Drapeau *et al.*, 2009). In contrast, recognition of basic emotions from music is impaired in bvFTD and SVPPA, usually (though not invariably) as part of a pervasive difficulty interpreting emotional and other social signals in these syndromes (Omar *et al.*, 2011; Hsieh *et al.*, 2012, Sivasathiaseelan *et al.*, 2019*a*). The rare phenomenon of selective musical anhedonia has been described following focal lesions of amygdala and insula (Griffiths *et al.*, 2004), prime sites of involvement in FTD syndromes. Compared with healthy older controls, patients with bvFTD also have difficulty inferring more complex affective mental states (though not non-mental representations) from music (Downey *et al.*, 2013); again, music here is signalling a core deficit of bvFTD affecting mentalising or 'theory of mind' (Bora *et al.*, 2015). On the other hand, patients with bvFTD can reliably detect dissonance and change in musical (major / minor) mode (Agustus *et al.*, 2015), suggesting that their deficit lies predominantly with higher order 'symbolic' processing of emotions rather than the perception of more elementary affective cues in music.

Assignment of reward value to music has been little addressed in people with dementia. Building on evidence that normal listeners find melodies with a harmonic structure that fulfils expectations subjectively pleasurable or rewarding but unresolved melodies unpleasant (Koelsch *et al.*, 2008*b*; Salimpoor *et al.*, 2015), one study found that patients with bvFTD and svPPA rated the pleasantness of 'unfinished' melodies differently from healthy age-matched individuals, whereas patients with AD and nfvPPA performed comparably to controls (Clark *et al.*, 2018). A further consideration here is that impaired explicit understanding of musical emotions does not preclude a patient continuing to derive pleasure from music (Matthews *et al.*, 2009).

The neuroanatomical evidence in dementia syndromes aligns with the picture drawn in the normal brain (section 1.5.2.4). Music emotion recognition across dementia syndromes has been correlated with grey matter loss in a similar distributed cerebral network including insula, orbitofrontal cortex, anterior cingulate and medial prefrontal and anterior temporal cortices, amygdala and the subcortical mesolimbic system (Omar *et al.*, 2011; Hsieh *et al.*, 2012). More specifically, musical mental state attribution in bvFTD correlated with atrophy of anterior temporal and ventromedial prefrontal cortices (Downey *et al.*, 2013) while processing of musical affective reward value correlated with atrophy of orbitofrontal cortex (Clark *et al.*, 2018), all areas that have been implicated in theory of mind and musical reward processing in the healthy brain (Steinbeis and Koelsch, 2009; Zahn *et al.*, 2009; Lehne *et al.*, 2014; Salimpoor *et al.*, 2015). In a functional MRI study (Agustus *et al.*, 2015), the processing of musical mode variation was associated with reduced activation of brainstem raphe nuclei in bvFTD compared with healthy older controls: these brainstem nuclei are hubs of serotonergic and noradrenergic transmission and regulate emotional arousal.

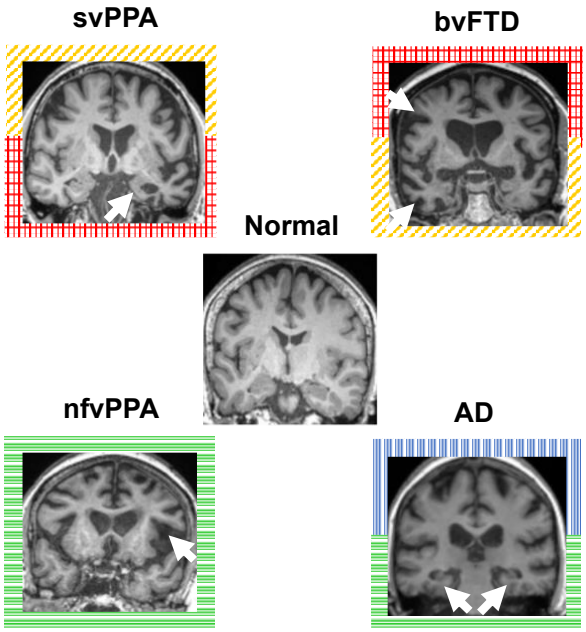

Figure 1.4. Musical disorders in AD and canonical syndromes of FTD

The panels show representative anatomical (T1-weighted) coronal brain magnetic resonance imaging (MRI) sections from patients with selected dementia syndromes and associated profiles of selective cerebral regional atrophy, in comparison to the brain of a healthy 61 year-old individual (Normal, centre). The left hemisphere is presented on the right in all sections; overlaid white arrows indicate the site of characteristic regional atrophy in each dementia syndrome. The frames for each clinical panel are coded following the shading convention corresponding to the cognitive operations principally affected in each syndrome, as delineated in the modular model of music processing represented in Figure 1.3. Represented are typical Alzheimer's disease (AD), with medial temporal and parietal lobe atrophy symmetrically involving both cerebral hemispheres; progressive nonfluent aphasia (nfvPPA), with predominantly left-sided atrophy involving peri-Sylvian cortices; semantic dementia (svPPA), with predominantly left-sided antero-medial temporal lobe atrophy; and behavioural variant frontotemporal dementia (bvFTD), with frontal and temporal lobe atrophy more marked in the right hemisphere.

1.7 Rationale and hypotheses

1.7.1 Motivations for the work in this thesis

The clinical complexity and pathological diversity of neurodegenerative diseases impose immense challenges for diagnosis and the design of rational interventions. To address these challenges, there is a need to identify new paradigms and biomarkers that capture shared path physiological processes and can be applied across a range of diseases. The generic psychophysiological paradigm of predictive coding promises to be of wide and potentially unifying relevance to neurodegenerative pathologies on at least two levels. Clinically, patients with Alzheimer's disease (AD) and major syndromes of frontotemporal dementia (FTD) show impaired ability to encode and decode auditory and other sensory patterns and/or to adapt behaviour to unexpected events; while physiologically, these processes are likely to require integration of information across neural circuits and therefore to be particularly sensitive to the effects of network disintegration wrought by pathogenic protein spread.

However, to date the predictive coding paradigm has been little applied to neurodegenerative disease (Hughes and Rowe, 2013; Shaw et al., 2019; Cope et al., 2017; Kogagoncu et al., 2020).

In the preceding section, I have outlined a taxonomy of music processing disorders in AD and FTD. This taxonomy is hierarchical, tracing the flow of musical information through the brain networks outlined in Figure 1.3 and the effects of neural network damage at each processing stage. However, despite longstanding interest in the musical capacities of patients with dementia, most information to date has been gleaned from studies of single patients or small case series. More importantly, studies have followed a modular organisation, looking at particular musical functions in specific diseases (in fact usually chosen according to the symptoms patients commonly exhibit, leading to potential source of bias). None of the studies reported in the previous section have adopted an information processing approach and looked at disruptions of information flows between these modules. Yet, canonical syndromes of FTD and AD have distinctive profiles of musical perceptual, semantic and affective impairment, reflecting the neural networks targeted by particular proteinopathies (Figures 1.3 and 1.4). These diseases are therefore anticipated to produce separable but overlapping cognitive and physiological profiles of musical information processing. Investigating cognitive expectation in hierarchical models of musical information processing can be of invaluable value for assessing aberrant predictive coding in dementia, and in particular, musical surprise processing, intelligible in terms of the predictive coding paradigm.

For the purposes of this thesis, I therefore elected to use music as a vehicle to assess the integrity of predictive coding mechanisms in AD and FTD. This enterprise requires certain fundamental questions to be addressed in the target diseases:

i) What is the status of musical expectation and deviant ('surprise') processing?

ii) How does this processing reflect the basic informational structure of the musical environment at large?

iii) What is the status of reward prediction error processing and updating via actions, i.e. online learning?

iv) How can this processing best be characterised in computational terms?

These questions will only be resolved through a combination of neuropsychological, physiological and computational techniques that can capture different facets of the predictive coding mechanism as revealed in music. As described earlier, various paradigms have been proposed to verify the predictive coding account of brain operation and include priming paradigms, violation paradigms, congruency and regularity detection task,

perceptual learning task, degraded auditory stimuli comprehension task and reward-based reinforcement learning paradigms. These are generally accompanied by computational modelling based on statistical learning of information and classical learning conditioning. Foremost of these, neuropsychological instruments that can capture musical expectancy and surprise are clearly essential. In addition, recordings of autonomic function and in particular, pupil dilatation robustly signal the violation of expectations and violations of statistical regularities of sensory input in the healthy brain (Liao *et al.*, 2016; Zhao *et al.*, 2018, 2019; Alamia *et al.*, 2019; Zénon, 2019). Pupil dilatation is therefore potentially a proxy for prediction errors and resetting of predictive models (Dayan and Yu, 2006; Zénon, 2019). Recording physiological markers of autonomic arousal is thus highly relevant to investigate musical predictive coding and, particularly in neurodegenerative disease, may signal dissociations between higher-level cognitive processes and activity of responses at the level of the central autonomic control network (Bradley, 2009). Further, to link these processes to neural substrates and to clinical phenomenology will require neuroanatomical and clinical correlation, respectively.

Each chapter of this thesis will report both behavioural and pupillometry signals of musical expectations and its violations (Chapters 3 and 5). It will be accompanied by the use of information-theoretic computational model of auditory expectation to assess key information properties of musical signals (Chapter 4), along with computational model of reinforcement learning (Chapter 6).

1.7.2 Key aims and experimental hypotheses

The overall rationale for this thesis is to explore predictive cognition in AD and FTD syndromes using tailored musical paradigms, with five overarching aims:

1. To define cognitive phenotypes of musical expectation (prediction) and deviant (prediction error) processing in these syndromes
2. To define autonomic physiological (pupillometric) signatures of these processes for each syndrome
3. To characterise these phenotypic signatures in computational terms, motivated by predictive coding and information theory
4. To link these signatures to structural neuroanatomy with the aim of demonstrating specific relationships between psychophysiological profiles and underlying patterns of network degeneration in the target diseases
5. To relate these phenotypes to key cognitive and behavioural symptoms in these diseases

Specific aims and hypotheses for each data chapters are as follows. The rationale for the listed hypotheses here is contained within the relevant chapters.

Chapter 3: Behavioural, autonomic and neuroanatomical correlates of musical surprise processing

Question: What is the status of musical expectation and deviant ('surprise') processing?

In this first experiment, I was interested in drawing profiles of surprise processing in relatively naturalistic environment (music) for each FTD and AD syndromes with the hope it could 'generalise' to more complex socio-emotional profiles observed in these syndromes, yet challenging to characterise. Three types of deviant were embedded in highly familiar melodies and targeted three levels of musical organisation: basic acoustic structure, the general harmonic rules governing musical sequences or musical 'syntax' and the regularities or 'semantics' specifying melodies as individual musical objects (Griffiths and Warren, 2004). These three deviants all constituted violations of semantic memory. However, while acoustic deviants represented violations of timbre, 'semantic' or in-key deviants were memory-only violations and 'syntactic' or out-of-key deviants were both violations of rules (or syntax) and memory (Miranda and Ullman, 2007).

I had three overall goals:

1. Define impairments in behavioural and autonomic reactivity to three types of deviants inserted in familiar melodies across the AD and FTD spectrum.
2. Assess three levels of musical organisation from early perception to syntactic and semantic processing.
3. Delineate structural neuroanatomical correlates of identification and autonomic reactivity to all types of deviants.

Based on previous work addressing more general musical and auditory cognitive and perceptual functions in dementia, my main hypotheses were as follows:

- FTD syndromes are associated with more severe impairments of deviance detection and autonomic reactivity than AD, with the most severe autonomic profile seen in svPPA and bvFTD patients (Johnson et al., 2011; Clark et al., 2018; Fletcher et al., 2015a,b; Hughes and Rowe, 2013).
- nfvPPA patients show a high rate of false-alarm for the detection of all types of deviants (Goll et al., 2010, Hardy et al., 2017a; Cope et al., 2017). .
- Cognitive and autonomic impairments relate to grey matter loss in fronto-temporo-parietal networks delineating hierarchical cortical networks associated with different types of musical information (Benhamou and Warren, 2020).

Chapter 4: Sensitivity to the statistical structure of melodies: link with deviance detection and autonomic reactivity

Question: How does this processing reflect the basic informational structure of the musical environment at large?

The approach used in this first chapter directly derived from 'traditional' psychology considering the brain as having a modular organisation which would differentially process deviants depending on the system they were targeting (e.g. in-key deviants predominantly requiring semantic processing, 'out-of-key' deviants predominantly requiring syntactic processing). I chose to use the same type of carrier, i.e. familiar melodies, for each deviant with the premise of creating a continuous scale of 'surprise' involving a common semantic memory processing unit which corresponds to a high-level system in the cortical hierarchy. This chapter, contrary to chapter 3, exploited the property of these deviants and adopted an information-theoretical approach to study the behavioural and autonomic reactivity to parametric properties of the stimuli in contrast to discrete categories. This approach is more in adequation with the predictive coding theory which considers the brain as a Bayesian machine applying the same computation at each level of the hierarchy with the same goal of minimising surprise, in contrast with the modular segregation of brain regions responsible for specific functions (e.g. semantic function 'reserved' to the temporal pole; syntax processing 'reserved' to the inferior frontal gyrus; etc).

In this chapter, I extracted two main information-theoretic properties of my stimuli (deviants and carriers). My goals were threefold:

1. Investigate the ability of AD and FTD patients to track the statistical structure of a musical environment in terms of information-content (unexpectedness) of deviants and entropy (uncertainty) of melodies
2. Explore the extent to which uncertainty of melodies modulate behavioural and autonomic sensitivity to unexpected musical events
3. Delineate structural neuroanatomical correlates of sensitivity to information-content and entropy across the AD and FTD spectrum

Based on previous work addressing perceptual learning of auditory sequences in healthy and clinical populations (further discussed in the chapter), my hypotheses were as follows:

- There is a modulatory effect of entropy on the level of sensitivity to information-content at both a cognitive and autonomic level in healthy controls (Hansen and Pearce, 2014; Hansen et al., 2016; Garrido et al., 2013; Quiroga-Martinez et al., 2019).
- Sensitivity to information-theoretic parameters of melodies is most severely affected in svPPA patients (Hardy et al., 2017a, b).

- bvFTD patients reveal a dissociation between sensitivity to entropy and sensitivity to information-content based on previous evidence of environmental-dependency in this syndrome (Ghosh and Dutt, 2010; Kumfor et al., 2018).
- Sensitivity to information-theoretic parameters of melodies correlate with limbic and striatal regions (Overath et al., 2007; Grahn & Rowe, 2013; Cheung et al., 2018; Omigie et al., 2019).

Chapter 5: Musical reward processing in frontotemporal dementia: the exploration-exploitation dilemma

Question: What is the status of reward prediction error processing and updating via actions?

In this chapter, I focused on bvFTD patients and looked at the ability of this patient group to deploy strategies and action policies to minimise surprise, a process commonly denoted active inference. I leveraged the property of music to induce expectations in the listener, and 'mimicked' reward when expectations were met or punishment when they violated these expectations using a well-known priming musical paradigm (Tillmann et al., 2006) and consonance/dissonance properties. Incorporating these stimuli in an exploration-exploitation paradigm (three-armed bandit problem), I assessed participants' ability to learn how to navigate in environments with different overall reward exposure and how to choose reward over punishment in each instance. I had four overall aims:

1. Define exploration and exploitation behaviours in musical environments with three levels of reward rate in bvFTD patients and healthy controls.
2. Assess the integrity of valuation processing of individual actions and musical reward prediction error in bvFTD looking at pupil reactivity and reaction times.
3. Relate choice accuracy and valuation metrics to characteristic changes in reward-based goal-directed behaviours seen in bvFTD, i,e. disinhibition, apathy, ritualistic/compulsive behaviour, hyperorality, hypersexuality and depression.
4. Delineate structural neuroanatomical correlates of choice accuracy and valuation of individual actions and musical reward prediction error.

Based on previous work addressing reward-based decision-making in bvFTD and healthy populations, my hypotheses were as follows:

- bvFTD patients display a general impairment in choosing the best option (i.e. exploiting), specifically in environments where less effort is required to obtain a reward (high reward rate environment) (Bertoux et al., 2015; Perry et al., 2015; 2017; Chiong et al., 2014).
- This deficit correlates with behavioural changes linked to impulsivity, disinhibition and stereotypy (Ghosh and Dutt, 2010; Ghosh et al., 2013; Johnen and Bertoux, 2019).

- bvFTD patients have reduced autonomic sensitivity to musical reward prediction error (Joshi et al., 2014; Fletcher et al., 2015b).
- Neuroanatomical correlates of choice accuracy involve regions previously involved in reward processing and exploration-exploitation attention reallocation (Daw et al., 2006; Laureiro-Martínez et al., 2015).

Chapter 6: Computational modelling of learning dynamics in a musical reinforcement learning paradigm

Question: How can prediction error processing and action updating best be characterised in computational terms?

Chapter 6 extends the work presented in Chapter 5 and offers a trial-by-trial analysis of choices instead of measures averaged across the whole experiment. This is done by deriving hidden variables from actions and outcomes using reinforcement-learning computational models. My goals here were as follows:

1. Draw a distinction between the different processes involved in reward-based decision-making, i.e. assigning values to stimuli, mapping values into actions and iteratively updating values depending on the outcome of an action.
2. Define alterations of these processes in bvFTD patients in comparison to healthy controls.
3. Verify a key hypothesis about bvFTD patients and a specific reduction in their sensitivity to aversive events (Perry et al., 2017; Bocchetta et al., 2016).
4. Relate learning dynamics to characteristic changes in goal-directed behaviours seen in bvFTD, i.e. disinhibition, apathy, ritualistic/compulsive behaviour, humour processing, hyperorality, hypersexuality, depression and empathy.

Based on my previous chapter and the literature looking at reward processing in bvFTD patients, my hypotheses were as follows:

- Both representations of musical reward prediction error (reinforcement learning) and representations of action value (action selection) are impaired in bvFTD.
- bvFTD patients show a specific reduction of sensitivity to aversive musical stimuli (Perry and Kramer, 2015; Perry et al., 2017; Bocchetta et al., 2016).
- bvFTD patients have lower learning rate in response to aversive stimuli compared to learning rate in response to pleasant stimuli (Snowden et al., 2001; Rahman et al., 2006; Torralva et al., 2007; Strenziok et al., 2011; Perry et al., 2015).
- Learning dynamics are associated with behavioural changes related to social cognition (Snowden et al., 2001; Perry et al., 2015).
- Neuroanatomical correlates of learning parameters would be found in structures specialized in processing aversive events (dorsal striatum, anterior insula: Palminteri et al., 2012).

2 Methods overview

This chapter provides an overview of the experimental methods common to all chapters in this thesis. Further information about specific experimental procedure will be given in each individual chapter.

2.1 Participants

2.1.1 Participant recruitment and consent

Patients were recruited over a three-year period between January 2018 and March 2020, principally from the specialist Cognitive Disorders Clinic at the National Hospital for Neurology and Neurosurgery, with a minority through direct referral to the research programme by external clinicians. Healthy controls were recruited from a local database of volunteers aged between 50 and 80 so that the healthy cohort matched patient groups as far as possible in terms of age and gender in all studies. A minority of healthy controls were contacted through the University of Third Age (www.u3a.org.uk). All participants gave informed consent for their involvement in the study. Ethical approval was granted by the University College London and National Hospital for Neurology and Neurosurgery Joint Research Ethics Committees in accordance with Declaration of Helsinki guidelines.

2.1.2 Diagnostic groupings

All participants underwent detailed clinical assessment and volumetric T1 MR brain imaging, and fulfilled consensus for Alzheimer's disease (Appendix 1; Dubois *et al.*, 2007), bvFTD (Appendix 2; Rascovsky and Grossman, 2013) or one of the two canonical FTD-related PPA syndromes, nonfluent-aggrammatic (nfv)PPA or semantic variant (sv)PPA (Appendix 3; Gorno-Tempini *et al.*, 2011). AD patients were included if they met the 'Probable AD' criteria (Appendix 1). All AD patients included in the studies reported in this thesis had brain imaging findings, seven (out of nineteen) had abnormal cerebrospinal fluid biomarkers (a total tau:beta-amyloid1-42 ratio >0.8, based on local laboratory reference ranges) and three (out of nineteen) had abnormal amyloid-PET imaging scans compatible with the diagnosis. bvFTD patients were included if they met the level III of diagnosis (Appendix 2: 'probable bvFTD'); bvFTD patients with genetic mutations had 'definite' bvFTD pathology; patients presenting with behavioural features without evidence of relevant brain atrophy were excluded as likely 'phenocopies'. Suspected PPA patients were included only if they had supportive brain imaging findings (Appendix 3: 'Imaging-supported PPA'). Where patients exhibited behavioural and language impairment, a combination of the

'dominant' clinical feature(s) and regional brain atrophy profile were used to assign a relevant grouping of bvFTD, svPPA, or nfvPPA. Applying these criteria, it is anticipated that the majority of the patients here will have underlying AD or FTLD spectrum pathology (Spinelli *et al.*, 2017).

2.2 Clinical and behavioural assessment

2.2.1 Clinical assessment

Each participant met with a clinical neurologist during their research visit, accompanied by an informant to provide reliable collateral information. Demographic details were first collected, comprising age, education level, language and occupation, handedness. Subsequent clinical assessment included a detailed family history and a detailed patient medical history (changes to behaviour, neuropsychiatric symptoms, language, cognition, motor and autonomic symptoms), a neurological examination for amyotrophic and Parkinsonian symptoms and bedside cognitive and linguistic tests including the Mini-Mental State Examination (MMSE) (Folstein *et al.*, 1975) and the Queen Square Screening Test for Cognitive Deficits. All participants gave blood samples for screening of pathogenic genetic mutations causing FTD and AD and underwent lumbar puncture for neurodegeneration markers. A subset of patients also consented have a lumbar puncture in order to detect Alzheimer's disease pathology (Ewers *et al.*, 2015). Each patient's primary caregiver (in most cases, primary caregiver who knew the patient premorbidly) underwent a private session with a clinical neurologist to respond to a set of questions assessing behavioural and neuropsychiatric traits developed by the patient since the onset of the disease on a scale from 0 to 3 (0, absent; 1, mild; 2, moderate; 3, severe).

2.2.2 Informant questionnaires

Each participant's informant was also given a set of questionnaires at the start of the research visit. These questionnaires were developed to distinguish between the behavioural and psychiatric symptoms of Alzheimer's dementia and fronto-temporal dementia; they are widely used in clinical research and were validated in clinical populations. These include the revised Cambridge Behavioural Inventory (CBI) (Wear *et al.*, 2008), the Frontotemporal Dementia Rating Scale (FRS) (Mioshi *et al.*, 2010), the modified Interpersonal Reactivity Index (mIRI) (Davis, 1983) and the Revised Self-Monitoring Scale (RSMS) (Lennox and Wolfe, 1984). Scores obtained using the mIRI were used as correlates in Chapter 6 . The mIRI (see Appendix 7) is a 14-item questionnaire that aims to measure both cognitive and emotional components of empathy (Davis, 1983). Seven items measure cognitive empathy: Perspective Taking (PT) and Fantasy (FS) and seven items measures emotional empathy:

Empathic Concern (EC) and Personal Distress (PD). It uses a 5-point Likert response scale from (1) "Does NOT describe well" to (5) "Describes VERY well" respectively.

2.2.3 Musical background questionnaire

For all studies in this thesis, to provide an index of participants' musical experience (level of formal practice and general exposure to music, patients' caregivers and healthy control participants completed a questionnaire detailing years spent learning or playing an instrument (prior musical expertise, scored on a 4-point scale ranging from 0 (never played an instrument or sang in a choir) to 3 (learned an instrument for >10 years) and hours per week on average currently spent listening to music (Hailstone *et al.*, 2009). The detailed questionnaire is in Appendix 4.

2.2.4 Other questionnaires

For the study in Chapters 5 and 6, patients' caregivers and healthy control participants were also asked to fill an adapted version of the Barcelona Music Reward Questionnaire (BMRQ) (Mas-Herrero *et al.*, 2013) looking at mood regulation, music seeking, sensorimotor and social functions of music (see Appendix 5). Right before the start of the experiment, after the instruction and practice trials, participants also had to fill a mood questionnaire. This questionnaire was adapted from the newly developed Immediate Mood Scaler (Nahum *et al.*, 2017) momentary mood symptoms of anxiety, alertness and depression (see Appendix 6).

2.2.5 General neuropsychological assessment

A comprehensive general neuropsychological assessment by a trained research psychologist was completed with all participants. Standardized tests of general intellectual level and domain-specific cognitive performance were assessed listed in Table 2.1. Test results were used to corroborate clinical and neuroimaging based syndromic categorization. In experiments weighted towards domain-specific performance, where competence in these domains was potentially confounding in the interpretation of experimental task performance (e.g. forward digit span and working memory, or British Picture Vocabulary for semantic knowledge), these test scores were used as covariates during statistical analysis.

Table 2.1. List of tests included in the core psychology battery completed by all participants

Cognitive domains and associated tests	Reference
General Intellect	
WASI Performance IQ	Wechsler (1981)
WASI Verbal IQ	Wechsler (1981)
Episodic Memory	
Recognition Memory Test for Words	Warrington (1984)
Recognition Memory Test for Faces	Warrington (1984)
Camden Paired Associate Learning	Warrington (1996)
Executive Function	
WASI Block design	Wechsler (1997)
WASI Matrices	Wechsler (1997)
Digit Span Forward and Reverse	Wechsler (1987)
Fluency – Letter and category (animals)	In house test
Trails Making Test	Tombaugh (2004)
D-KEFS Colour-Word Inference Test	Delis, Kaplan, and Kramer (2001)
Language Skills	
WASI Vocabulary	Wechsler (1997)
National Adult Reading Test (NART)	Nelson (1982)
British Picture Vocabulary Scale (BPVS)	Dunn and Whetton (1982)
Graded Naming Test	McKenna and Warrington (1980)
Posterior cortical skills	
Graded Difficulty Arithmetic	Jackson and Warrington (1986)
Visual Object and Space Perception Test (VOSP)	Warrington and James (1991)

WASI, Wechsler Abbreviated Scale of Intelligence; D-KEFS, Delis Kaplan Executive System

2.2.6 Assessment of peripheral hearing function

In order to generate a covariate for interpretation of group effects on experimental musical tasks, peripheral hearing function was assessed in each participant for all experiments presented in this thesis. Using an Otovation Roto® audiometer (https:/www.auditdata.com/) with a single TDH-39P 10-ohm Telephonics® earphone (www.telephonics.com) in a quiet room, steady tones of 500, 1000, 2000, 4000 and 6000Hz were presented separately to each of the participant's ears, over ascending intensity levels commencing at 20 dB HL (decibel hearing level). At each frequency, the participant indicated (verbally or by gesture) when they first heard a noise. If the participant was unable to hear the tone, the level was increased in 5 dB increments (maximum 70dB HL). This procedure was repeated three times to establish the mean threshold at that frequency. For each participant a composite score was created by calculating the mean threshold across all frequencies in the best ear.

2.2.7 Assessment of pitch change direction processing

Discrimination of pitch change direction was assessed in each participant at the beginning of each experiment presented in this thesis. I adopted a procedure similar to those originated by Seashore (Seashore, 1919). This task was designed as a control task to determine whether participants had any deficit of elementary pitch change perception relevant to music. Scores on this task indicated a potential confounding factor in assessing task performance and were used as a rudimentary screen for amusia (Stewart *et al.*, 2006) and included as a covariate indexing pitch contour perception, musical working memory (holding pitches and order in memory) and task decision-making (comparator) for interpretation of group effects on experimental musical tasks. Notes were derived from a synthetic piano sound (Musescore®) and presented as pairs, such that each note had a duration of 1s with inter-note gap of 1s. The notes comprising each pair differed in pitch by one to five semitones. Ten trials (pairs) were presented and the direction of the pitch shift between notes in each pair was varied randomly across trials (five ascending, five descending). The task on each trial was to decide if the second note of the pair was 'higher' or 'lower' than the first note. Examples and practice trials were used to familiarise participants with the task requirements.

2.3 Generation and presentation of auditory stimuli

All experimental sound stimuli were created in MATLAB v 7.0/2012a (The Mathworks, Inc.) and Musescore© (www.musescore.org) and stored as wavefiles at a 44100Hz sampling rate. Within any test, sounds were matched for mean intensity (root-mean-square) over trials and all sounds created in MATLAB were windowed with 20ms onset-offset temporal ramps to prevent click artefacts. All sound stimuli were presented in randomised order from a notebook computer running Experiment Builder® (www.sr-research.com/experiment-builder) binaurally via headphones (Audio-Technica®) with an HD Digital 7.1 USB Audio Box at a constant, comfortable listening level (around 70 dB).

2.4 Pupillometry

2.4.1 Acquisition

Pupillometry experiments are presented in chapters 3, 4 and 5. Pupil diameter was measured (sampling rate 500 Hz) from the right pupil using an infra-red camera [Eyelink II; SR Research, Canada] mounted on a headset just below the line of sight. Participants were seated approximately 50 cm from a desktop computer monitor in a dimly and uniformly illuminated quiet room, fixating a small white circle in the centre of the monitor screen. Prior

to data acquisition, a five-dot calibration was conducted to ensure adequate gaze measurements. Participants were asked to keep head movements to a minimum throughout the recording session and to restrict motion artefacts, the participant's head was stabilised using the SR Research Head Support chinrest. For each stimulus trial I first ensured that fixation was stable at less than two arbitrary gaze units away from the central fixation point before triggering the next trial.

2.4.2 Preprocessing

Pupil diameter data were conditioned using previously described procedures (Mathôt *et al.*, 2018). I first excluded all samples beyond three standard deviations of the mean signal for each participant and those with fixations directed at the periphery of the display screen (within 1 cm of the monitor border). Blinks were identified and removed from the signal using a procedure in MATLAB R2016b. Blinks were characterised by a rapid decline towards zero from blink onset, and a rapid rise back to the regular value at blink offset; 100ms of signal was removed before and after the missing data points and missing data were interpolated (four equally spaced time points were used to generate a cubic spline fit to the missing time points between blink onset (t2) and blink offset (t3) of the unsmoothed signal, with t1= t2-t3+t2 and t4= t3-t2+t3 (Mathôt *et al.*, 2018). Data were then band-pass filtered (low cut-off = 1Hz, high cut-off = 1/128 Hz) to remove slow fluctuations and smooth the signal (Kret and Sjak-Shie, 2019). To allow for comparisons across trials and participants, data for each participant were z-scored based on the signal mean and standard deviation computed across that participant's dataset. Epochs with more than 50% missing data were excluded from further analysis. Finally, z-scored epoched data were baseline-corrected on a trial-by-trial basis by subtracting the z-scored baseline window. This normalised pupil diameter was time-domain-averaged across trials for each condition. I then estimated a single, mean time series for each participant group in each condition by averaging across participants. The resulting time-series were plotted in separate figures to illustrate differences between groups or differences between conditions.

2.4.3 Permutation analysis

In this thesis, I used cluster-based permutation tests to detect the temporal extent of an effect of condition or an effect of diagnostic group in my pupillometry data, mentioning the 'approximate' onset times of significant clusters. Cluster-based permutation analysis has been implemented for M/EEG analysis to circumvent the issue of multiple comparisons when dealing with an extremely high number of sensor-time pairs. Family-wise error rate cannot be controlled with the usual parametric statistical methods without dramatically reducing the power and

increasing the rate of false-negative. Cluster-based permutation analysis is a non-parametric method which allows a high power (high type II) and low Type I error rates. It builds on the assumption that effects are clustered along the dimensions of interest (in the case of MEEG: time and space; in the case of pupillometry: time), i.e. a true signal has a temporal extension over the adjacent time-points. Here, I refer to a permutation analysis for one-dimensional data looking at independent samples (contrast between conditions). First, clusters must be identified and this entails: 1) comparing time-samples for each condition by means of t-value; 2) selecting samples that are larger than some pre-specified threshold; 3) clustering the selected samples in connected sets depending on their temporal adjacency; 4) calculating cluster-level statistics summing t-values within each cluster 5) extracting the largest of the cluster statistics. This last result will be the basis for the non-parametric permutation test as it allows p-values to be calculated for all found clusters under the permutation distribution of the maximum cluster-level statistic. The permutation distribution was derived by: 1) pooling all the trials (from the two compared conditions) in a single set 2) randomly partitioning the trials in two subsets 3) calculating the test-statistic on this random partition 4) repeating step 2 and 3 5000 times and constructing a histogram of the test statistics. Finally, I calculated the proportion (called the p-value) of random partitions that resulted in a larger test statistic than the one observed (the largest cluster statistics). If the p-value is smaller than 0.05, one can conclude that the data in the two conditions are significantly different. The advantage of this method is that it does not depend on the probability distribution of the data, nor on the test statistic used and most importantly, it solves the multiple comparison problem. However, there are several potential pitfalls. First, cluster-based permutation tests provide no guarantee that the temporal extent of a cluster is valid because it has not been the subject of an inferential test. While the latency of a cluster will be strongly correlated with the true extent of effect, there is no error rate control on these latencies which renders cluster-based permutation tests unable to provide precise estimates of temporal onset or offset of differences between conditions. In this thesis, I accompanied cluster-based permutation analysis with further statistical inference on the maximum pupil size or area under the curve extracted from a temporal window that spanned the significant clusters previously found.

2.5 Neuroanatomical imaging and voxel-based morphometry

2.5.1 Image acquisition

At each visit, each participant (unless they had a contra-indication for MRI) had a volumetric T1 MR brain image acquired on a 3T Siemens Magnetom Prisma MRI scanner, using a 32-channel head-and-neck receiver array

coil and a T1-weighted sagittal 3D magnetization prepared rapid gradient echo (MPRAGE) sequence (TE = 2.93ms, TI = 850ms, TR = 2000ms), with matrix size 256x256x208 and voxel dimensions 1.1x1.1x1.1mm. Structural scans were used for voxel-based morphometry analysis to assess the relationship between grey matter atrophy and performance on specific experimental tasks.

2.5.2 Image preprocessing

Preprocessing of brain images was performed using the New Segment (Weiskopf et al., 2011) and DARTEL (Ashburner, 2007) toolboxes of SPM12 (www.fil.ion.ucl.ac.uk/spm) under Matlab and following an optimised protocol (Ridgway et al., 2008). Normalisation, segmentation and modulation of grey and white matter images were performed using default parameter settings and grey matter images were smoothed using a 6 mm full width-at-half-maximum Gaussian kernel. A study-specific template mean brain image was created by warping all bias-corrected native space brain images to the final DARTEL template and calculating the average of the warped brain images. Total intracranial volume (TIV) was calculated for each patient by summing grey matter, white matter and cerebrospinal fluid volumes after segmentation of tissue classes (Malone *et al.*, 2015).

2.5.3 Small volume generation

Studies in this thesis focused on specific networks involved in music, syntax and reward processing. Therefore, I used small volume corrections in testing of study-specific a priori hypotheses relating to structural imaging. Volumes were derived from Oxford-Harvard cortical atlas (Desikan et al., 2006) and AAL atlas (Tzourio-Mazoyer et al.). Further details of small volumes appropriate to particular experimental questions are outlined in the relevant chapters.

2.5.4 Voxel-based morphometric analysis

Pre-processed structural images were entered into VBM analyses to assess neuroanatomical associations of experimental parameters of interest in all chapters of this thesis. For chapters 3 and 4, I only included the patient cohorts as there would be a risk of identifying anatomical associations resembling grey matter atrophy maps of each syndrome rather than identifying regional brain volume associated with the experimental parameter of interest. For Chapters 5 and 6, I tested a single syndromic group and chose to include healthy controls in my analysis. While the previous chapters focused on finding differences (or similarities when grouping them all) between syndromic groups (thus testing the specificity of my tests), in these two last chapters, I was interested in detecting the regions, among the ones showing a clear grey-matter volume difference

compared to controls, responsible for a deficit in the experimental measures of interest. For all four chapters, in order to minimise the effect of anatomical heterogeneity between groups and reduce the potential risk of identifying spurious anatomical associations where patients have significant grey matter atrophy relative to healthy controls in regions not necessarily associated with the parameter of interest, I used a full factorial design with diagnostic group as the main factor. This design was based on a general linear model expressed by the equation:

$$y = intercept + \beta x + \varepsilon$$

where y represents a matrix of voxel intensity and β represents each parameter to be estimated, x is a variable of interest or a nuisance covariate and ε is the error (the difference between the observed data and the data predicted by the model). In this thesis, individual voxel grey matter volume was modelled as a function of an experimental test score. I systematically incorporated nuisance covariates of age, TIV and scores at the pitch screen direction task. TIV was used as a proxy for gender as it has been shown that gross morphological differences account for most univariate sex differences in grey matter volume (Sanchis-Segura *et al.*, 2020). Pitch direction discrimination performance score was used here as a proxy for disease severity as it indexed both auditory working memory and decision-making abilities. While there no ideal measure of disease severity across the heterogeneous groupings of AD and FTD, the pitch screen discrimination score is a reasonable measure of nonverbal executive function as it indexes pitch contour perception, musical working memory and task decision-making. Inclusion of such covariate is crucial if one wants to increase the specificity of VBM findings as it reduces the variance of widespread grey matter atrophy attributable to advanced disease stage. To control for multiple comparisons (which reduces the risk of Type I error), I used a FWE correction either across the whole brain or within pre-specified regional volumes of interest. FWE correction is based on the assumption that distribution of statistics in the imaging data follows a smoothly varying random field (due to highly dependent tests: if one voxel is atrophied, it is very likely that the surrounding voxels will be too). The method of random-field theory as originally proposed by Worsley *et al.*, (1992) required the data to have a minimum level of smoothness, which I ensured by using a Gaussian smoothing kernel of 6mm during pre-processing. In general, FWE corrections over the whole brain are particularly stringent and small volume corrections, if defined a priori on neuroanatomical grounds informed by previous literature, is an appropriate way of reducing Type I error while still preserving power to detect real effects.

2.5.5 Presentation of results

Peak (local maxima) coordinates (given in MNI standard space) are reported in tables within each chapter, indicating which loci were significant at the specified threshold of $p<0.05$ after family-wise error (FWE) correction over the whole brain, and which were within prespecified regions of interest (ROIs). The statistical parametric maps that are presented in each chapter are superimposed on the study- specific template mean brain image in MNI space at an uncorrected threshold of $p<0.001$. The uncorrected threshold is mainly adopted for display purposes, but it also provides an indication of the overall distribution of change. Colour bars code T-values for each SPM. The MNI coordinate (mm) of the plane of each section is indicated, and the right hemisphere is shown on the right in coronal sections.

2.6 Statistical analysis

All statistical analysis on behavioural and pupillometry data were performed using Stata14.1®. Brain imaging analyses were ran in SPM12 (http://www.fil.ion.ucl.ac.uk/spm/) in MATLAB R2016b.

2.6.1 Behavioural and pupillometry analysis

For each experimental dataset analysed in this thesis, I typically verified key assumptions about homoscedasticity and normality using Levene's test and Q-Q plot of residuals. In all my experimental chapters, I looked at effects of group, condition and their interaction. I chose a mixed linear model over a repeated measures ANOVA because it makes the analysis less susceptible to outliers by attenuating the impact of participants with missing data. Indeed, it calculates both fixed and random effects while ANOVA only calculates fixed effects (factors assumed to have the same impact on each observation). I systematically used a random intercept of participants which allowed modelling of the difference between the average score for one participant and the average score of their group as a random effect following a normal distribution. Fixed effects included diagnostic group and a range of covariates were detailed in each chapter. When an effect was found, I used post-hoc pairwise comparisons and when appropriate, I corrected for multiple comparison using a Bonferroni adjustment. In case the assumption of normal residuals was violated, I performed a transformation of the original data (log, square root) and if the normality assumption still did not hold, bootstrapping was used to calculate 95% confidence intervals (1000 replications, sampling with replacement).

2.6.2 Signal detection theory

Signal detection theory was adopted by psychologists as a way to understand sensory decision making and assesses the participant's ability to differentiate between a signal and noise. Based on the proportions of hits, misses, false-alarms and correct rejections, summary metric can be generated. In this thesis, I calculated the sensitivity index d-prime (d'):

$$d' = z(Hit) - z(FP)$$

with z corresponding to the inverse of the normal distribution function that transforms the Hit or FP rates into z scores.

3 Behavioural, autonomic and neuroanatomical correlates of musical surprise processing

3.1 Chapter summary

Making predictions about the world and responding appropriately to unexpected events are essential functions of the healthy brain. In neurodegenerative disorders such as frontotemporal dementia and Alzheimer's disease, impaired processing of 'surprise' may underpin a diverse array of symptoms, particularly abnormalities of social and emotional behaviour, but is challenging to characterise. Here I addressed this issue using a musical deviant paradigm. I studied 62 patients (24 female; aged 53-88) representing major syndromes of frontotemporal dementia (behavioural variant, semantic variant primary progressive aphasia, nonfluent-agrammatic variant primary progressive aphasia) and typical amnestic Alzheimer's disease, in relation to 33 healthy controls (18 female; aged 54-78). Participants heard famous melodies containing no deviants or one of three types of deviant note – acoustic (white-noise burst), syntactic (key-violating pitch change) or semantic (key-preserving pitch change). Using a regression model that took elementary perceptual, executive and musical competence into account, I assessed accuracy detecting melodic deviants and simultaneously-recorded pupillary responses to these deviants. Neuroanatomical associations of deviant detection accuracy and pupillary responses were assessed using voxel-based morphometry of patients' brain MR images. Relative to healthy controls, syndromic groups showed differentiated signatures of musical surprise detection and autonomic reactivity. Whereas Alzheimer's disease was associated with normal deviant detection accuracy and pupillary response magnitude, behavioural and semantic variant frontotemporal dementia syndromes were associated with strikingly similar profiles of impaired syntactic and semantic deviant detection and reduced pupillary reactivity, consistent with a deficient predictive model of the sensory environment. On the other hand, nonfluent-agrammatic primary progressive aphasia was associated with impaired auditory deviant detection accuracy ($p<0.05$) due to excessive false-alarms but enhanced pupillary reactivity to deviants, consistent with over-precise sensory predictions. Across the patient cohort, grey matter correlates of acoustic deviant detection were identified in a predominantly temporo-parietal network; correlates of syntactic deviant detection in an anterior fronto-temporo-striatal network; and a common correlate of salience coding in supplementary motor area. Grey matter correlates of autonomic reactivity to acoustic and syntactic deviants were found in the posterior parietal cortex and the anterior cingulate cortex (all $p<0.05$, corrected for multiple comparisons in pre-specified regions of interest).

3.2 Introduction

Predicting the future based on past experience and responding appropriately to unexpected, 'surprising' events are fundamental functions of the healthy brain. These functions are targeted prominently and early in a number of neurodegenerative disorders. Impaired understanding of social norms, 'rules' and boundaries define behavioural variant frontotemporal dementia (bvFTD) (Warren *et al.*, 2013; Johnen and Bertoux, 2019; Sivasathiaseelan *et al.*, 2019), signifying deficient predictive 'modelling' of the social milieu (Ibañez and Manes, 2012) and implicating more fundamental processes such as error detection and monitoring, ambiguity and conflict resolution, probabilistic learning, risk evaluation and decision making (Krueger *et al.*, 2009; Dalton *et al.*, 2012; Gleichgerrcht *et al.*, 2012; Clark *et al.*, 2015, 2017; Chiu *et al.*, 2018; Kumfor *et al.*, 2018; Johnen and Bertoux, 2019). These processes are also affected in other FTD syndromes - semantic variant primary progressive aphasia (svPPA) and nonfluent-agrammatic (nfv)PPA - and Alzheimer's disease (AD) (Chenery *et al.*, 1998; Daffner *et al.*, 1999; Bettcher *et al.*, 2008; Peraita *et al.*, 2008; Rohrer and Warren, 2010; Clark *et al.*, 2015, 2017; Duclos *et al.*, 2018; Kumfor *et al.*, 2018; Lenoble *et al.*, 2018; Fittipaldi *et al.*, 2019; Ho *et al.*, 2019).

A plausible unifying mechanism for this diverse phenotypic spectrum is abnormal predictive coding i.e. an impaired integration of expectation (established by environmental context) with surprise (unexpected events). This mechanism has a neurophysiological signal in altered mismatch negativity (Ito and Kitagawa, 2005; Hughes and Rowe, 2013; Hsiao *et al.*, 2014; Ruzzoli *et al.*, 2016; Jiang *et al.*, 2017; Laptinskaya *et al.*, 2018; Mazaheri *et al.*, 2018) and a neuroanatomical signature in dysfunctional frontotemporal neural circuitry (Hughes and Rowe, 2013; Hughes *et al.*, 2013; Hsiao *et al.*, 2014; Firbank *et al.*, 2016; Josef Golubic *et al.*, 2017; Kobeleva *et al.*, 2017; Shaw *et al.*, 2019). Impaired deviance detection may develop early in the course of neurodegeneration and indexes a core mechanism of the culprit proteinopathy in animal models (Reichelt *et al.*, 2013; Ahnaou *et al.*, 2017; Kim *et al.*, 2020). Taken together, this evidence suggests that neural processes establishing expectations and decoding 'surprise' may underpin diverse pathophysiological and clinical effects of proteinopathies such as FTD and AD. However, these processes remain poorly characterised and difficult to quantify, particularly in the setting of neurodegenerative disease.

A large body of work discussed in detail in chapter 1 has identified music as an ideal model to study predictive coding in dementia. The emerging picture of the musical brain, derived from cognitive and functional neuroimaging studies in both health and disease (Benhamou and Warren, 2020) (see Figure 1.2), provides

candidate neural substrates for predictive coding of musical information. Canonical syndromes of FTD and AD have distinctive profiles of musical perceptual, semantic and affective impairment (Hsieh *et al.*, 2011; Johnson *et al.*, 2011, Golden *et al.*, 2015*b*, 2016*b*; Clark *et al.*, 2018; Benhamou and Warren, 2020), reflecting the neural networks targeted by particular proteinopathies. These diseases are therefore anticipated to produce separable but overlapping cognitive and physiological profiles of musical surprise processing. A predictive coding account of various perceptual and behavioural deficits have already been described (Hughes and Rowe, 2013; Hughes *et al.*, 2013; Cope *et al.*, 2017; Shaw *et al.*, 2019), however, music remains unexplored as a paradigm of predictive coding and 'surprise' processing in neurodegenerative disease.

Here I addressed this issue in a cohort of patients representing all major FTD syndromes - bvFTD, svPPA and nfvPPA – and typical AD, referenced to healthy older individuals. I manipulated musical surprise by inserting notes representing three kinds of deviant 'event' condition into an 'environment' of familiar melodies with variable predictability levels. These deviant conditions targeted three levels of musical organisation: basic acoustic structure, the general harmonic rules governing musical sequences or musical 'syntax' and the regularities or 'semantics' specifying melodies as individual musical objects (Griffiths and Warren, 2004). These three deviants all constituted violations of semantic memory but while acoustic deviants represented violations of timbre, 'semantic' or in-key deviants were memory-only violations and 'syntactic' or out-of-key deviants were both violations of rules (or syntax) and memory (Miranda and Ullman, 2007). I simultaneously assessed participants' ability to detect and their autonomic (pupillary) reactivity to deviant notes. Structural neuroanatomical associations of behavioural and autonomic reactivity to melodic deviants were assessed using voxel-based morphometry (VBM) of patients' brain MR images.

Based on previous work addressing more general musical and auditory cognitive and perceptual functions in dementia (Hsieh *et al.*, 2011; Johnson *et al.*, 2011; Fletcher *et al.*, 2015, Golden *et al.*, 2015*b*, 2016*b*; Clark *et al.*, 2018; Groussard *et al.*, 2019; Slattery *et al.*, 2019), I hypothesised that FTD syndromes would be associated with more severe impairments of musical deviant detection and autonomic reactivity than would AD; and further, that FTD syndromes would be stratified by their relative degree of impairment in cognitive and autonomic reactivity for particular deviant conditions: impaired detection of semantic and syntactic deviants in bvFTD and svPPA (Johnson *et al.*, 2011; Clark *et al.*, 2018) and a generalised impairment of auditory deviant detection in nfvPPA (Goll *et al.*, 2010, Hardy *et al.*, 2017*a*); and relatively more severely impaired autonomic reactivity in svPPA

and bvFTD (Fletcher *et al.*, 2015). Finally, I hypothesised that the cognitive coding of musical surprise in the patient cohort would have separable neuroanatomical correlates depending on the type of deviants within the hierarchical distributed brain networks previously implicated in processing different kinds of musical information (Koelsch *et al.*, 2007; Stewart *et al.*, 2008; Johnson *et al.*, 2011; Sammler *et al.*, 2013; Lehne *et al.*, 2014; Bianco *et al.*, 2016; Cheung *et al.*, 2018; Omigie *et al.*, 2019; Benhamou and Warren, 2020). More specifically, I predicted that common correlates would be found in the cingulo-insular network for the detection of surprise (Critchley et al., 2001; Sander et al., 2005) and in the posterior temporo-parietal network for the analysis of sensory patterns regardless of the type of deviants (Tsai et al., 2018; Zatorre et al., 2010) while more anteroventral regions involved in semantic appraisal and musical syntax processing would be found for the detection of semantic or syntactic deviants (Jacobsen et al., 2015; Maess et al., 2001; Sammler et al., 2012; Lappe et al., 2013a) compared to limbic regions mediating physiological arousal and preparing responses to potentially behaviourally relevant events for the detection of acoustic deviants (Zatorre and Salimpoor, 2013; Koelsch, 2014).

3.3 Materials and methods

3.3.1 Participants

Nineteen patients with typical AD, twenty-one patients with bvFTD, twelve patients with svPPA and twelve patients with nfvPPA were recruited. All patients fulfilled consensus clinical criteria for the relevant syndromic diagnosis (Gorno-Tempini *et al.*, 2011; Rascovsky and Grossman, 2013; Dubois *et al.*, 2014), of mild to moderate severity. Thirty-three healthy older individuals with no history of neurological or psychiatric disorders also participated. None of the participants had a history of clinically significant hearing loss, congenital amusia or pupillary disease. All participants had a comprehensive general neuropsychological assessment.

To provide an index of participants' musical experience, patients' caregivers and healthy control participants completed a musical questionnaire (details in Methods 2.2.3). All participants had audiometric screening of peripheral hearing function (details in Methods 2.2.6) and assessment of their ability to discriminate the direction of pitch changes relevant to melodies (details in Methods 2.2.7). Demographic details (including musical background), clinical and general neuropsychological characteristics of the study cohort are summarised in Table 3.1.

Table 3.1. Demographic, clinical and general neuropsychological characteristics of participant groups

Characteristic	Healthy controls	AD	bvFTD	svPPA	nfvPPA
Demographic and clinical					
No. (male:female)	15:18	9:10	16:5	7:5	8:4
Age (years)	64.8 (5.1)	71.4 (8.6)[a]	65 (5.7)	65.5 (6.0)	70.6 (7.3)
Handedness (R:L)	31:2	17:2	19:2	12:0	12:0
Education (years)	15.9 (2.3)	15.1 (2.9)	14.6 (2.9)	15 (2.6)	13.2 (2.6)
Symptom duration (years)	N/A	6.1 (4.0)	8.5 (4.5)	5.9 (2.2)	3.7 (1.8)[a]
MMSE (/30)	29.4 (0.9)*	21.1 (5.5)	25.9 (3.4)	23 (7.4)	20 (8.4)[a]
Hearing threshold (dB)	27.6 (9.4)	31.6 (6.6)	28.5 (5.6)	25.7 (8.1)	32.8 (7.5)
Genetic mutations	N/A	0	4 *C9orf72*, 5 *MAPT*	0	2 *GRN*
Acetylcholinesterase inhibitor use (n)	N/A	11	0	0	0
Neuropsychological functions					
Episodic memory					
RMT words (/50)	40.9 (6.3)**	31.7 (6.9)	34.3 (7.6)	30.7 (3.4)[b]	35.4 (5.6)
RMT faces (/50)	48 (2.3)**	30.9 (7.5)	38.6 (7.7)	34.8 (6.5)[b]	37.9 (9.5)
Camden PAL (/24)	20.2 (2.0)**	6.8 (5.4)[b]	11.1 (7.2)	9.4 (8.1)	14.4 (5.0)
Executive skills					
WASI Block Design (/71)	51 (12.7)***	15.1 (8.5)[a,c]	31.2 (13.4)	41.1 (17.9)	19.3 (20.4)[a,c]
WASI matrices (/32)	25.5 (5.2)***	13.2 (4.7)[c]	17.3 (7.2)[c]	26.4 (5.0)	16.6 (9.7)[c]
WMS-R digit span forward (max)	7.1 (1.2)***	6.2 (1.2)	6.2 (1.2)	6.5 (1.1)	4.6 (1.3) [a,c,d]
WMS-R digit span reverse (max)	6 (1.1)***	3.8 (1.5)[c]	4.6 (1.5)	5.4 (1.6)	3.4 (0.8)[c]
D-KEFS Stroop colour naming (s)	28.4 (4.8)**	52.5 (14.2)[a]	44.1 (15.9)	43.2 (14.9)	77.7 (14.9)[a,c,d]
D-KEFS Stroop word reading (s)	21.7 (4.5)**	36.4 (16.9)[a,c]	26.2 (6.0)	27.6 (10.2)	68.7 (20.5)[a,c,d]
D-KEFS Stroop interference (s)	56 (15.8)**	126.3 (38.8)[a,c]	78.9 (24.9)	83.3 (26.9)	139.6 (24.3)[a,c]
Trails A (s)	28.5 (10.6)**	85.6 (40.2)[a,b,c]	48 (21.2)	45.4 (18.1)	60.1 (43.2)
Trails B (s)	65.2 (23.7)**	219.5 (83.1)[c]	157.3 (90.4)	134.4 (97)	147.2 (64.7)
Letter fluency (F, 1 min)	17.9 (5.5)**	9.7 (4.3)	10.6 (5.9)	8.1 (4.6)	6.6 (6.3)
Category fluency (animals, 1 min)	25 (4.7)**	10.8 (4.7)	13.5 (6.6)	6.1 (5.6) [a]	10.1 (5.3)
Language skills					
WASI Vocabulary (/80)	71.6 (5.2)**	56.8 (13.1)	47.9 (19.9)	27 (21.4)[a,d]	24 (21.4)[a,d]
Graded Naming Test (/30)	24.9 (3.0)**	14.6 (8.3)	14.8 (9.9)	1.9 (5.3)[a,b,d]	14.9 (7.7)
BPVS (/150)	147.9 (1.2)***	133.4 (24.2)	115.7 (44.9)	64.6 (46.1)[a,d]	105.3 (48.8)
Other skills					
Graded Difficulty Arithmetic (/24)	17 (4.2)**	5.4 (5.8)[c]	8.7 (6.7)	13.4 (5.8)	6.4 (6.7)
VOSP Object Decision (/20)	18.5 (1.7)**	10.6 (5.1)[a]	15.1 (5.2)	11.5 (6.2)	14.3 (6.6)
Musical skills and background					
Pitch direction discrimination (/10)††	9.1 (1.1)	8.6 (1.3)	7.9 (1.5)[c]	9.6 (0.5)	8.3 (2.2)
Recognition of melodies: % correct	0.94 (0.08)	0.93 (0.08)	0.85 (0.16)	0.89 (0.04)	0.84 (0.17)
d-prime	3.25 (0.54)	2.56 (0.60)	2.16 (1.07)	1.95 (1.61)	2.61 (1.10)
Prior musical expertise (/3)†	0.8 (0.9)	0.8 (0.6)	1 (0.8)	0.9 (1.0)	0.5 (0.7)
Current music listening (hrs/ week)	7.1 (7.6)	5.8 (5.7)	7.6 (6.6)	7.7 (10.5)	5.2 (5.5)

Mean (standard deviation) scores are shown unless otherwise indicated; maximum scores are shown after tests (in parentheses). Significant differences ($p < 0.05$) from healthy control values are indicated in bold; *data from 19 healthy controls; **data from 23 healthy controls; ***data from 25 healthy controls; †musical training assessed on a 4-point scale (details in Methods chapter 2); [a]significantly different from bvFTD group; [b]significantly lower than nvfPPA group; [c]significantly lower than svPPA group; [d]significantly lower than AD group.

3.3.2 Experimental design and stimuli

The melodies were chosen based on the results of a survey involving 15 healthy older British individuals who did not form part of the experimental cohort. From an initial set of 150 melodies, 48 highly familiar melodies were selected based on mean familiarity rating >3.5 on a 5-point scale ranging from 1 (completely unfamiliar) to 5 (very familiar). Details of all stimuli are presented in Table 3.2 and stimulus examples enclosed with this thesis. The note sequences corresponding to each melody were synthesised with piano timbre as digital wavefiles using MuseScore®; acoustic deviants were created using the Gaussian white-noise function in Matlab and were fixed for loudness (rms intensity) to the rest of the melody. Stimuli were fixed for overall loudness (rms intensity) and varied in length between three and five bars. A deviant note was always positioned in the second half of the melody, in order to allow initial establishment of the melodic context, and occurred on an on-beat; a pitch deviant always violated the contour of the canonical melody (between three and nine semitones). The melody conditions did not differ significantly in mean length (one-way ANOVA with Bonferroni correction, $F(3,44) = 0.98$, $p=0.41$), pitch range (Kruskal-Wallis non parametric test and post-hoc two-sample Wilcoxon tests with Bonferroni correction, $p>0.05$), tempo (Kruskal-Wallis non parametric test and post-hoc two-sample Wilcoxon tests with Bonferroni correction, $p>0.05$) or familiarity rating (Kruskal-Wallis non parametric test and post-hoc two-sample Wilcoxon tests with Bonferroni correction, $p>0.05$). From these famous melodies, I created four experimental conditions, comprising melodies containing either: no deviant note; a single note that deviated from the canonical melody while preserving its key ('semantic' deviants); a single note that deviated from the canonical melody by violating its key or tonality ('syntactic' deviants); or a single note that deviated in timbre ('acoustic' deviants, formed from white-noise bursts). I chose to have a different melody for each trial in order to avoid any repetition effect and most importantly, avoid a priming effect which would have potentially affected the performance. The final stimulus set comprised 48 trials (12 exemplars of each condition).

Table 3.2. **Characteristics of experimental melody stimuli**

Melody	**Duration** (ms)	**Onset** (ms)	**Key**	**Tempo** (bpm)	**Pitch range**	**Fam**
No deviant						
Colonel Bogey March	8500	6000	Cmaj	120	E4 - E5	5.00
Edelweiss (The Sound of Music)	7478	3000	Cmaj	120	E4 - D5	4.75
Moon River	8407	4498	Cmaj	90	F4 - D5	3.67
Morning (Peer Gynt)	7790	4813	Dmin	120	D4 - D5	4.88
My Way	6911	5681	Fmin	140	C4 - A4	4.70
Peter's Theme (Peter and the Wolf)	8478	5990	Cmaj	120	C4 - E5	5.00
Star Wars Theme	9636	5352	Amin	90	C4 - E5	4.85
Summertime	8088	5990	Emaj	120	E4 - E5	4.63
Swan Lake 'Theme'	8088	5753	Gmin	120	D4 - D5	4.79
Symphony No. 40 (Mozart)	7500	5739	Amin	90	D4 - C5	5.00
William Tell Overture	7253	5805	Gmaj	120	D4 - D5	5.00
You Are My Sunshine	10421	7000	Gmaj	120	D4 - E5	4.92
Semantic deviant						
Auld Lang Syne	8443	6000	Gmaj	120	D4 - E5	5.00
Away In A Manger	7372	4800	Gmaj	100	D4 - E5	4.79
All Things Bright And Beautiful	7444	5000	Cmaj	120	C4 - C5	5.00
Frere Jacques	8392	5000	Gmaj	120	G4 - D5	5.00
God Save The Queen	9403	6500	Gmaj	120	F4 - C5	5.00
Hark! The Herald Angels Sing	8152	6500	Gmaj	120	D4 - D5	5.00
Jerusalem	6980	4888	Gmaj	90	C4 - C5	5.00
Jingle Bells	8465	6000	Gmaj	120	G4 - D5	5.00
Lullaby (Brahms)	6915	4000	Cmaj	120	E4 - D5	4.42
O Come All Ye Faithful	8613	6000	Gmaj	120	D4 - D5	4.83
Que Sera, Sera	8500	6140	Gmaj	90	G4 - E4	4.42
We Wish You A Merry Christmas	6987	4012	Gmaj	120	C4 - C5	5.00
Syntactic deviant						
Deck The Halls	7000	5636	Gmaj	140	G4 - D5	5.00
Do-Re-Mi (The Sound of Music)	6142	3440	Gmaj	140	G4 - C5	5.00
Fly Me To The Moon	7652	5000	Cmaj	120	E4 - C5	3.25
For He's A Jolly Good Fellow	5550	3800	Gmaj	100	D4 - C5	4.79
Für Elise (Beethoven)	7173	3524	Amin	120	E4 - E5	4.96
Hey Jude	9500	5053	Cmaj	90	D4 - C5	4.54
Joy To The World	7790	5231	Cmaj	120	C4 - C5	4.70
La Donna E Mobile (Rigoletto)	8245	5582	Gmaj	140	G4 - D5	4.88
O Little Town Of Bethlehem	10000	6873	Gmaj	90	D4 - D5	4.92
Rudolph The Red-Nosed Reindeer	6655	4300	Cmaj	140	E4 - E5	4.96
Silent Night	6082	4000	Cmaj	120	E4 - B4	4.92
When The Saints Go Marching In	8198	5247	Gmaj	120	G4 - E5	4.83
Acoustic deviant						
Autumn Leaves	9718	4750	Dmin	120	C4 - B4	3.70
Greensleeves	5749	3500	Gmaj	120	D4 - C5	4.85
London Bridge Is Falling Down	10000	6500	Gmaj	120	G4 - D5	4.96
Mary Had A Little Lamb	10000	5000	Gmaj	120	G4 - D5	4.63
Once In Royal David's City	6620	5000	Gmaj	120	C4 - G4	4.96
Singin' In The Rain	7449	6000	Gmaj	120	D4 - D5	4.64
Somewhere Over The Rainbow	7500	4500	Cmaj	90	C4 - C5	4.93
Three Blind Mice	10000	6000	Gmaj	120	G4 - D5	4.85
Tonight (West Side Story)	8000	4125	Cmaj	90	C4 - C5	4.67

Twelve Days Of Christmas	8640	6550	Gmaj	90	D4 - E5	4.89
We Three Kings	5924	4000	Gmaj	120	E4 - B4	4.88
Yesterday	9776	6000	Cmaj	90	C4 - C5	4.54

The table lists each melody from the stimuli set, its key parameters and the condition in which it was used. *values for equivalently positioned standards in the case of melodies with no deviant; ENT, mean melody entropy (see text for details); Fam, familiarity rating; IC, information-content of deviants; Interval, no. of semitones difference between original (standard) and deviant note; NA, not applicable; Onset, time of deviant onset from start of stimulus; Position, position of deviant in melody note sequence (coded as: -2, penultimate on-beat; -3, third from last on-beat; -4, fourth from last on-beat (equally distributed across conditions with four trials at each position); Tempo, beats per minute (bpm; values were set to 90, 120 or 140 bm to reduce overall tempo variability across the stimulus set while also allowing natural tempo variations inherent to the melodies).

3.3.3 Experimental procedure

All participants were first familiarised with the experiment and given several practice trials (using melodies not presented in the main experiment) to ensure they understood and could comply with the procedure. The participant was seated approximately 50 cm from a desktop computer monitor in a dimly and uniformly illuminated, quiet room, fixating a small white circle in the centre of the monitor screen. Each experimental trial comprised an initial brief silent baseline interval (2 s), followed by the melody stimulus and a final silent equilibration interval (varied randomly between 2 and 4 s). Please refer to Methods Section 2.3 for details about generation and presentation of stimuli and Methods Section 2.4 for details about acquisition of pupil data. On completion of the post-stimulus equilibration interval (to avoid any confounding effects of online decision-making or motor processes on pupil dilatation), the task on each trial was to decide whether the melody contained a wrong note; the participant responded verbally or by pointing to the word 'Yes' or 'No' presented on the monitor.

Following the pupillometry session, I conducted a test to assess recognition of the stimulus melodies. Each participant was asked to listen to the famous melodies presented during the pupillometry session in canonical form (from the beginning of the melody to the time of onset of any deviant in the main experiment) alongside 24 unfamiliar (novel) melodies. Unfamiliar melodies were either pseudo-reversed versions of the familiar melodies or tunes composed de novo by an experienced musician (EB); the set of unfamiliar melodies was closely matched to the familiar melody set for loudness, duration, key, pitch range and tempo. The task on each trial was to indicate whether or not the melody was a well-known tune.

All participant responses were stored for offline analysis. No feedback about performance was given during the pupillometry session or the melody recognition test session and no time limits were imposed.

3.3.4 Analysis of behavioural data

Demographic characteristics and neuropsychological data were compared between participant groups using Fisher's exact test for categorical variables, and for continuous variables, either two-sample t-tests or Wilcoxon rank-sum tests where t-test assumptions were violated (for example, due to skewed data distribution). d-prime values were calculated for detection of deviants in each condition. A global test (restricted maximum likelihood mixed-effects model with participant identity as a level variable) was used to test for main effects of diagnostic group and experimental condition (deviant type) and their interaction. Post hoc pairwise group comparisons of predictive margins were performed where main effects were found. To take account of potentially confounding factors, age, gender, pitch direction discrimination performance (indexing pitch contour perception, musical working memory and task decision-making), prior musical expertise score and mean hours of listening to music per week were included as covariates in the regression model. In addition, I used Pearson's correlation tests to separately assess any linear relationship between deviant detection accuracy with age, gender, prior musical expertise and hours of listening, musical familiarity d-prime, peripheral hearing function, pitch contour processing (pitch direction discrimination score) and general disease factors (Mini-Mental State Examination (MMSE) score, symptom duration), across the patient cohort.

A threshold $p<0.05$ was accepted as the criterion of statistical significance for all tests.

3.3.5 Analysis of pupillometric data

Pupil diameter data were conditioned using previously described procedures (Mathôt *et al.*, 2018) (details in Methods section 2.7), normalised to baseline and time-domain-averaged across trials for each condition. To identify time windows with significant discrepancies between deviant and 'standard' time series, paired t-tests were conducted on each pair of conditions (two-tailed; over the entire epoch length), with family-wise error (FWE) control using a non-parametric permutation procedure with 5000 iterations (cluster-defining height threshold $p<0.05$ with FWE-corrected cluster-size threshold $p<0.05$, implemented in the Fieldtrip toolbox (Maris and Oostenveld, 2007).

To assess effects of participant group and experimental conditions on pupillary response, I extracted the maximum of the normalised pupil dilatation response (averaged across trials for each participant) during the two seconds following deviant onset, an interval chosen according to both permutation analysis and previous studies

(Bianco *et al.*, 2020). I also extracted the temporal latency of the maximum pupil size relative to deviant onset (averaged across trials for each participant). I used the same mixed linear model employed for the behavioural data (with the same covariates) to compare pupil response amplitudes and latencies between participant groups and experimental conditions.

3.3.6 Brain MRI acquisition and voxel-based morphometry

For 58 patients (15 AD, 20 bvFTD, 12 svPPA, 11 nfvPPA), T1-weighted volumetric brain MR images were acquired on a Prisma 3T MRI scanner using a 32-channel phased-array head-coil and pre-processed using standard procedures in SPM12 (www.fil.ion.ucl.ac.uk/spm) (Ridgway *et al.*, 2008) (details in Methods Section 2.5).

In a VBM analysis of the combined patient cohort, full factorial linear regression models were used to assess associations between regional grey matter volume (indexed as voxel intensity) separately with detection accuracy (hit rate) for each deviant condition. Age, total intracranial volume and pitch direction score were incorporated as covariates of no interest. Statistical parametric maps of regional grey matter associations were assessed at threshold $p<0.05$ after FWE correction for multiple voxel-wise comparisons within pre-specified anatomical regions of interest (see Figure 3.1). These regions were informed by previous studies of music and musical surprise processing in both the healthy brain and neurodegenerative disease and comprised: a posterior temporo-parietal network involved in sensory pattern analysis (posterior superior temporal gyrus, angular and supramarginal gyri and precuneus: Zatorre *et al.*, 2010; Tsai *et al.*, 2018; Slattery *et al.*, 2019); an anteroventral network involved in semantic appraisal (anterior superior temporal gyrus, middle temporal gyrus, temporal pole and inferior frontal gyrus: Johnsrude *et al.*, 2000; Hsieh *et al.*, 2011; Johnson *et al.*, 2011; Sammler *et al.*, 2013; Agustus *et al.*, 2018; Slattery *et al.*, 2019); a striato-limbic network involved in emotion and reward evaluation (putamen, caudate, nucleus accumbens, hippocampus and amygdala: Zatorre and Salimpoor, 2013; Koelsch, 2014; Lehne *et al.*, 2014; Clark *et al.*, 2018; Cheung *et al.*, 2019; Gold *et al.*, 2019) and a cingulo-insular network involved in salience processing and motor output (anterior insula, anterior cingulate cortex and supplementary motor area: Lima *et al.*, 2016; Freitas *et al.*, 2018).

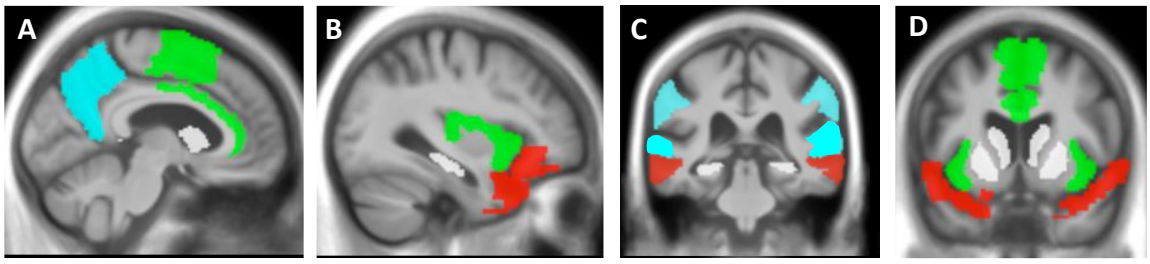

Figure 3.1. Pre-specified anatomical regions of interest for voxel-based morphometric analysis.

Representative sagittal (A, B) and coronal (C, D) sections are shown for the neuroanatomical volumes selected for multiple voxel-wise comparison correction in the region-of-interest analyses based on prior anatomical hypotheses. These regions were customised from the Oxford/Harvard brain maps to fit the group mean template brain image. Regions comprise a posterior temporo-parietal network including posterior temporal gyrus, angular and supramarginal gyri and precuneus (cyan); an anteroventral network including temporal pole, anterior superior and middle temporal gyri and inferior frontal gyrus (red); a cingulo-insular network including anterior cingulate, supplementary motor area and insula (green); and a striato-limbic network including putamen, caudate nucleus, nucleus accumbens, hippocampus and amygdala (white).

3.4 Results

3.4.1 General participant characteristics

Patient groups did not differ significantly from healthy controls in gender distribution, handedness, years in formal education or composite audiometry score (all $p>0.05$; Table 1). Patients with AD were on average significantly older than healthy controls ($p<0.05$). The patient groups did not differ in mean symptom duration but did differ in overall severity of cognitive impairment (MMSE score; Kruskal-Wallis $chi^2 = 102.9$, $p <0.001$). Participant groups did not differ significantly in musical expertise or average time spent listening to music each week. However, the bvFTD group performed significantly worse than both the healthy control and svPPA groups on the pitch direction discrimination test (Kruskal-Wallis non-parametric test and post-hoc two-sample Wilcoxon tests $p <0.001$).

3.4.2 Behavioural data: detection of deviants in melodies

Group data for detection of deviants in melodies are summarised in Table 3.3 and individual data are plotted in Figure 3.1.

There were significant main effects on performance (d-prime) of participant group ($\chi^2(4)=20.4$, $p<0.001$) and deviant condition ($\chi^2(2)=127.36$, $p<0.001$) and a significant interaction between group and condition ($\chi^2(8)=33.3$, $p<0.001$).

Comparing each patient group with the healthy control group, the bvFTD, svPPA and nfvPPA groups were significantly less accurate in detecting semantic deviants (all $p< 0.001$) and syntactic deviants (all $p< 0.005$) and

the nfvPPA group was additionally less accurate in detecting acoustic deviants (p=0.031), reflecting excessive false alarms (Table 2). Comparing between patient groups, the bvFTD and svPPA groups were significantly less accurate than the AD group in detecting syntactic deviants (all p<0.042); while the nfvPPA group was significantly less accurate than the AD group in detecting both syntactic deviants (p=0.013) and semantic deviants (p=0.045).

Comparing experimental conditions within participant groups, all groups were significantly more accurate in detecting syntactic and acoustic deviants than semantic deviants (all p<0.05). The bvFTD and svPPA groups were additionally significantly more accurate in detecting acoustic than syntactic deviants (all p< 0.001).

Overall accuracy of deviant detection across the patient cohort correlated with musical background (r=0.31, p=0.01), pitch direction discrimination score (r=0.39=0, p=0.003), musical expertise score (r=0.31, p=0.012) and musical familiarity d-prime (r=0.53, p<0.001). There was no correlation of deviant detection accuracy with age, gender, symptom duration, MMSE or peripheral hearing score.

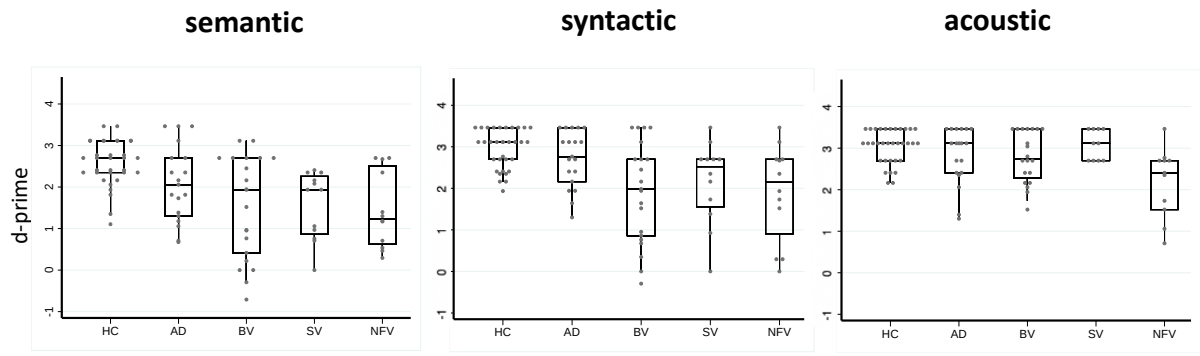

Figure 3.2. Accuracy of detection of different types of deviants in melodies, for all participant groups.

For each panel (deviant condition), detection accuracy (d-prime score) is plotted for individuals within each participant group (see also Table 2). Boxes code the interquartile range and whiskers the overall range of values in each group; the horizontal line in each box represents the median. Values falling outside these ranges are indicated.

Table 3.3. Summary of melodic deviant detection accuracy and pupillary response profiles for participant groups and conditions

Group	Condition	Hit rate*	Detection		Pupil peak response		
			d-prime	IC correlate	Amplitude**	Latency (s)	IC correlate
Controls	No deviant	0.90 (0.10)	NA	rho = 0.41 (0.14)[1]	0.35 (0.22)	NA	rho = 0.56 (0.14)[1]
	Semantic	0.89 (0.10)	2.58 (0.55)		0.53 (0.26)	1.32 (0.32)	
	Syntactic	0.98 (0.05)	2.95 (0.47)		0.61 (0.25)	1.22 (0.39)	
	Acoustic	1 (0)	3.04 (0.41)		0.78 (0.26)	1.18 (0.27)	
AD	No deviant	0.87 (0.16)	NA	rho = 0.10 (0.16)	0.47 (0.25)	NA	rho = 0.53 (0.15)[1]
	Semantic	0.75 (0.26)	2.08 (0.91)		0.53 (0.27)	**1.85 (0.53)[a]**	
	Syntactic	0.94 (0.14)	2.72 (0.68)		0.71 (0.44)	**1.73 (0.52)[a]**	
	Acoustic	0.97 (0.07)	2.82 (0.68)		0.81 (0.46)	1.52 (0.38)	
bvFTD	No deviant	0.85 (0.16)	NA	**rho = -0.16 (0.19)[b]**	0.27 (0.31)	NA	rho = 0.20 (0.15)
	Semantic	**0.62 (0.35)**	**1.52 (1.24)**		0.39 (0.30)	0.98 (0.05)	
	Syntactic	**0.73 (0.35)**	**1.91 (1.21)[c]**		0.42 (0.28)[b,c]	1.25 (0.62)	
	Acoustic	0.99 (0.05)	2.80 (0.62)		0.68 (0.38)	1.28 (0.46)	
svPPA	No deviant	0.89 (0.10)	NA	**rho = -0.43 (0.14)[1b]**	0.29 (0.32)	NA	**r = 0.21 (0.16)**
	Semantic	**0.61 (0.31)**	**1.56 (0.81)**		0.32 (0.26)	1.47 (0.61)	
	Syntactic	**0.77 (0.32)**	**2.16 (0.99)[c]**		**0.36 (0.29)[b,c]**	1.49 (0.50)	
	Acoustic	1 (0)	3.09 (0.36)		0.71 (0.33)	1.15 (0.42)	
nfvPPA	No deviant	**0.74 (0.26)**	NA	rho = 0.39 (0.13)[1]	0.40 (0.31)	NA	r = 0.54 (0.11)[1]
	Semantic	0.71 (0.24)	**1.45 (0.92)[d]**		0.53 (0.48)	1.44 (0.53)	
	Syntactic	0.84 (0.23)	**1.90 (1.16)[d]**		**0.76 (0.44)**	**1.87 (0.46)[a]**	
	Acoustic	0.93 (0.15)	**2.19 (0.83)**		0.90 (0.47)	1.52 (0.48)	

Mean (standard deviation) values are shown; 12 trials were presented in each condition. Significant differences ($p < 0.05$) from healthy control values are indicated in bold. *for no-deviant condition, values refer to correctly-rejected trials (1 – false-alarm rate), thus a reduced hit rate in this condition signifies a raised false alarm rate; **in arbitrary units; [1]significantly different from null hypothesis (no correlation); [a]significantly slower than bvFTD group; [b]significantly lower than nvfPPA group; [c]significantly lower than AD group.

3.4.3 Pupillometric data: autonomic responses to deviants in melodies

Participant groups did not differ significantly in resting baseline pupil size (mean over the two-second silence interval before the start of each stimulus trial) [$\chi 2(4)=6.6$, $p=0.16$] or overall pupil dynamics (mean pupil response across all trials) [$\chi^2(4)=8.2$, $p=0.09$].

Group data for pupillary responses to melody deviants are summarised in Table 3.3; mean time courses of pupillary dilatation responses for each experimental condition are shown in Figure 3.3. There were significant main effects on mean pupillary response magnitude of participant group [$\chi 2(4)=10.3$; $p=0.03$] and deviant condition [$\chi 2(3)=123.18$; $p<0.001$] but no interaction [$\chi 2(12)=13.8$; $p=0.31$]. There was a significant main effect on mean pupillary response latency of group [$\chi 2(4)=28.2$; $p<0.001$] but not condition [$\chi 2(2)=5.60$; $p=0.06$].

Comparing each patient group with the healthy control group, the svPPA group showed a significantly smaller mean pupillary response to syntactic deviants [$z=-2.19$, $p=0.029$] while the nfvPPA group showed a significantly larger pupillary response to syntactic deviants [$z=2.40$, $p=0.016$]; in addition, the nfvPPA group showed a significantly slower pupillary response to syntactic deviants and the AD group showed significantly slower responses to both syntactic and semantic deviants (all $p<0.05$) than did healthy controls. Comparing between patient groups, the AD and nfvPPA groups showed significantly larger mean pupillary responses to syntactic deviants than did the bvFTD and svPPA groups (all $p<0.05$); in addition, the nfvPPA group showed a significantly slower pupillary response to syntactic deviants and the AD group showed a significantly slower response to both syntactic and semantic deviants (all $p<0.05$) than did the bvFTD group. No other significant differences between groups were identified.

Compared with the no-deviant baseline condition, all participant groups showed significant mean pupillary responses to acoustic deviants (all $p<0.001$); the healthy control, AD and nfvPPA groups additionally showed significant pupillary responses to syntactic deviants (all $p<0.001$), while only the healthy control group showed a significant pupillary response to semantic deviants ($p<0.05$). All participant groups showed significantly greater mean pupillary responses to acoustic deviants than semantic deviants (all $p<0.05$), while the healthy control, bvFTD and svPPA groups additionally showed significantly greater pupillary responses to acoustic deviants than syntactic deviants (all $p<0.05$).

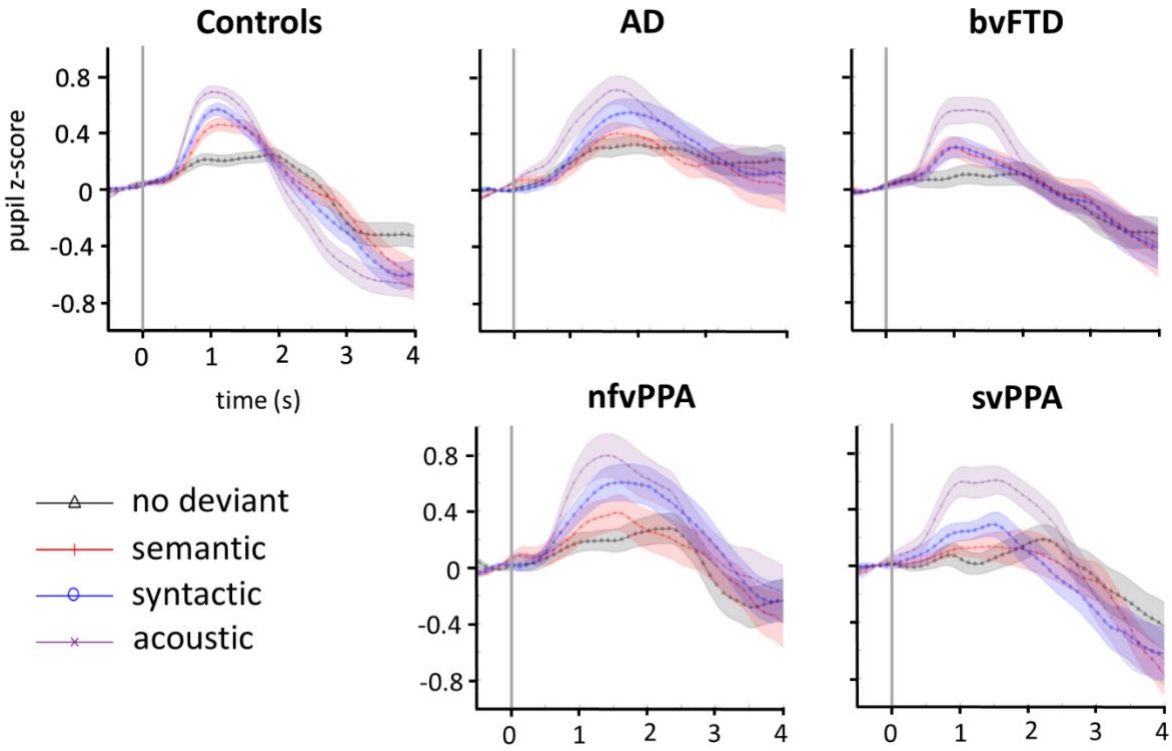

Figure 3.3. Time course of pupil dilatation responses to melodic deviants in each of the experimental conditions, for all participant groups.

Onset of the deviant note is at time 0 (indicated by vertical grey line on each panel). To generate these pupil time series, trial-by-trial pupil time series from individual participants were first filtered, smoothed, converted to z-scores based on the signal mean and standard deviation for that participant's dataset and baseline-corrected by subtracting the pre-deviant baseline; the plots show the mean normalised pupil time series flanked by error envelopes representing the standard deviation of the group pupillary response, for each experimental condition (coded at lower left).

3.4.4 Neuroanatomical associations

Significant grey matter associations of deviant detection accuracy and pupillary responses to deviants for the combined patient cohort are summarised in Table 3.4; statistical parametric maps of these associations are presented in Figure 3.4. All associations here are reported thresholded at $p<0.05$ after FWE correction for multiple voxel-wise comparisons within pre-specified anatomical regions of interest.

Accuracy of syntactic deviant detection correlated with regional grey matter in bilateral supplementary motor area and right pars orbitalis of inferior frontal gyrus, temporal pole and putamen. Accuracy of acoustic deviant detection correlated with regional grey matter in a more postero-ventral, bi-hemispheric network including right precuneus and middle temporal gyrus, hippocampus and amygdala as well as left supplementary motor area. No associations of semantic deviant detection accuracy were identified at the prescribed significance threshold.

Maximum pupillary responses to syntactic deviants and acoustic deviants correlated with regional grey matter in left anterior cingulate cortex and right precuneus. An additional correlate was found in a region spanning left middle temporal gyrus and superior temporal sulcus for the pupillary responses to acoustic deviants. No associations of pupillary responses to semantic deviants were identified at the prescribed significance threshold.

Table 3.4. Neuroanatomical correlates of melodic deviant detection and pupillary responses to deviants in the combined patient cohort

Condition	Region	Side	Cluster (voxels)	Peak (mm)			T score	P_{FWE}
				x	y	z		
Accuracy of detection of deviants								
Acoustic	Precuneus	R	471	9	-46	67	4.94	0.022
		L	451	-10	-50	57	4.48	0.028
	Hippocampus	L	94	-14	-40	4	4.66	0.032
	Middle temporal gyrus	R	1489	64	-40	-14	4.59	0.022
	Supplementary motor area	L	75	-5	2	62	4.46	0.031
	Amygdala	L	124	-27	-6	-12	4.19	0.039
Syntactic	Supplementary motor area	R	982	4	-2	50	5.13	0.004
		L	1352	-4	-16	51	4.92	0.005
	Inferior frontal gyrus: pars orbitalis	R	488	50	38	-8	4.79	0.014
	Putamen	R	121	22	20	-6	4.61	0.006
	Temporal pole	R	1807	46	10	-20	4.51	0.015
Pupillary response to deviants								
Acoustic	Anterior cingulate cortex	L	50	-2	40	16	5.02	0.004
	Precuneus	R	117	22	-56	16	5.00	0.006
	Middle temporal gyrus	L	52	-69	-26	-14	4.59	0.024
Syntactic	Anterior cingulate cortex	L	332	-9	39	6	4.53	0.014
	Precuneus	R	204	4	-48	66	4.51	0.020

The table presents the results of the voxel-based morphometry analysis. Shown are the locations of regional grey matter positively associated with accuracy of detection for different types of deviants in familiar melodies, over the combined patient cohort (see also text and Figure 3.4). P values were all significant ($p<0.05$) after family-wise error (FWE) correction for multiple voxel-wise comparisons within pre-specified anatomical regions of interest (see text and Figure 3.1).

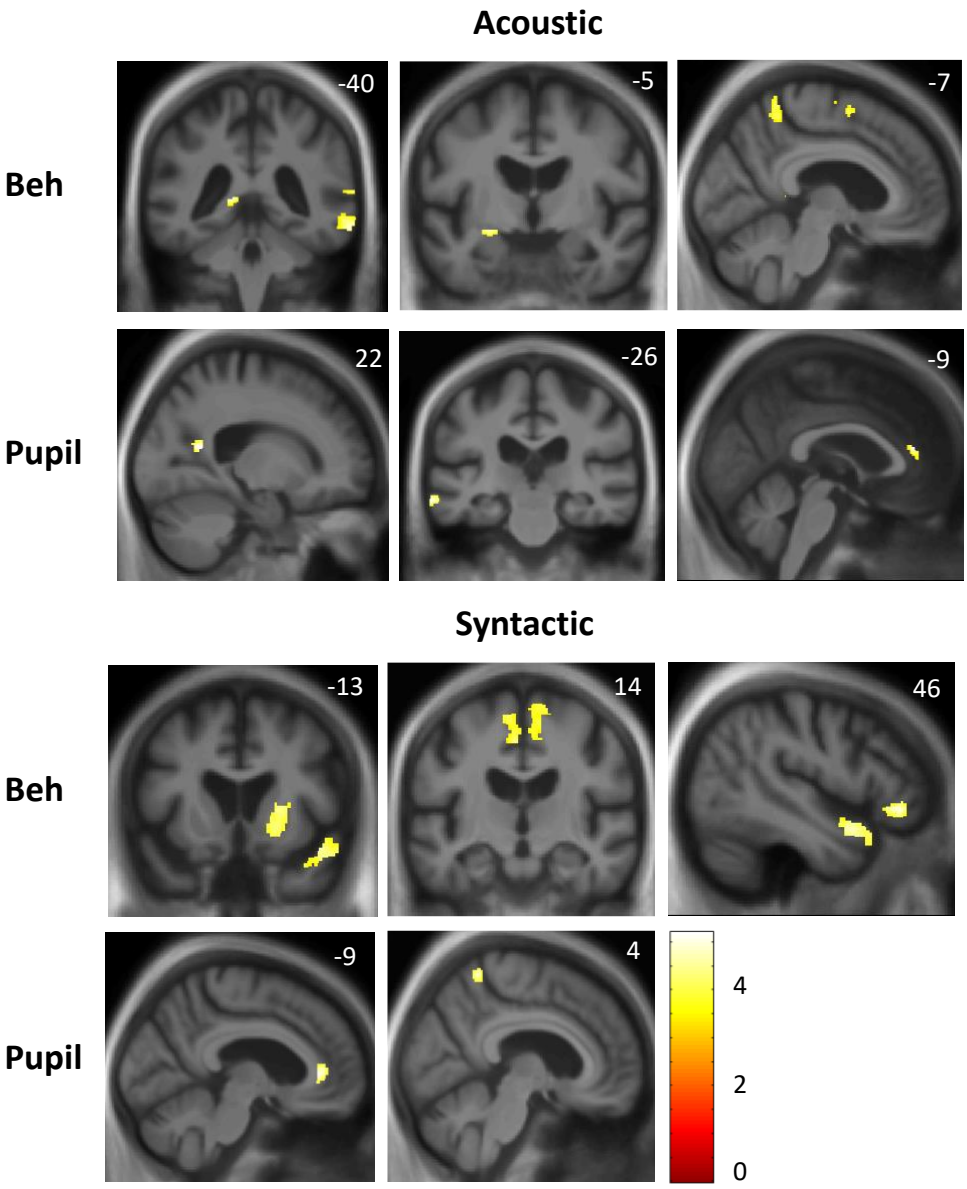

Figure 3.4. Neuroanatomical correlates of accurate detection of melodic deviants and pupillary responses to deviants in the combined patient cohort.

Statistical parametric maps (SPMs) show regional grey matter volume positively associated with acoustic) and syntactic deviant detection accuracy in familiar melodies, based on voxel-based morphometry of patients' brain MR images. SPMs are thresholded for display purposes at $p < 0.001$ uncorrected over the whole brain, however, local maxima of areas shown were each significant at $p < 0.05$ after family-wise error correction for multiple voxel-wise comparisons within pre-specified anatomical regions of interest; the MNI coordinate (mm) of the plane of each section is indicated.

3.5 Discussion

Here I have shown using the paradigm of music that canonical syndromes of FTD and AD have differentiated behavioural and autonomic responses to surprising events. Consistent with previous evidence (Miranda and Ullman, 2007; Tillmann and Bigand, 2010; Guo and Koelsch, 2016, Zénon, 2019*a*), healthy older controls here showed a graded response profile with more accurate detection and greater physiological reactivity to 'surprising' deviations in fundamental acoustic structure and generic syntactic musical rules than to deviations in the semantic structure of specific musical objects (melodies). Whereas the AD group detected musical deviants normally, the bvFTD and svPPA groups showed strikingly similar profiles of impaired syntactic and semantic deviant detection relative both to healthy controls and other syndromic groups; while the nfvPPA group showed a generalised deficit of auditory deviant detection accuracy. All disease groups showed impaired autonomic reactivity to syntactic deviants, however this was more marked in bvFTD and svPPA than other syndromic groups. These syndromic signatures were evident after taking elementary pitch pattern perception and musical experience into account. Across the patient cohort, detection of musical and acoustic deviants and autonomic reactivity to deviants had separable neuroanatomical substrates in cortico-subcortical networks previously implicated in the perceptual, semantic and hedonic analysis of music.

Behaviourally, impaired detection of musical 'rule' violations in bvFTD and svPPA accords with previous evidence that these syndromes impair psychological expectations in melodies (Clark *et al.*, 2018) (Johnson *et al.*, 2011, Golden *et al.*, 2016*b*), auditory scenes (Clark *et al.*, 2017) and other complex sensory signals (Krueger *et al.*, 2009; Dalton *et al.*, 2012; Gleichgerrcht *et al.*, 2012; Clark *et al.*, 2015; Chiu *et al.*, 2018; Kumfor *et al.*, 2018; Johnen and Bertoux, 2019). Such deficits are in turn likely to underpin the difficulties these patients experience in interpreting the often ambiguous or conflictual emotional and social signals of other people and in regulating their own socio-emotional behaviours (Koenig *et al.*, 2006; Downey *et al.*, 2015; Clark and Warren, 2016; Perry *et al.*, 2017; Van den Stock *et al.*, 2017; Sivasathiaseelan *et al.*, 2019). In predictive coding terms, such phenomena might reflect impaired matching of incoming signals to stored neural 'templates' (predictions established through past experience), inefficient updating of those predictions and/or degraded templates per se. While any of these may operate in bvFTD and svPPA, the correlation here between detection accuracy and melody recognition (familiarity d-prime) underlines how an 'incorrect model' of the current sensory environment precludes detection of incongruent events. In bvFTD and svPPA, environmental deviations are essentially rendered 'unsurprising',

while false alarm rates (most strikingly, in svPPA) are correspondingly low (Table 2): this pattern would follow if stored melody templates are degraded to the extent that most incoming facsimiles of the template (including aberrant ones) achieve a 'match'.

My finding of a generalised failure of musical and acoustic deviant detection in nfvPPA builds on emerging evidence for disordered auditory processing in this syndrome (Goll *et al.*, 2010; Rohrer *et al.*, 2012; Grube *et al.*, 2016, Hardy *et al.*, 2017*a*, 2019). In contrast to other dementia syndromes (and mirroring the profile in svPPA), nfvPPA was associated with an abnormally high false-alarm rate (Table 2), indicating that these patients tended to over-interpret variations from musical canonicity in melodies without deviant notes (for example, timbral or key changes associated with transcribing the melodies) as errors. In predictive coding terms, when listening to music or (as has been previously shown) degraded speech (Cope *et al.*, 2017), they tend to make predictions about incoming auditory data that are inflexible or 'over-precise' (overestimating the reliability of prior knowledge) while still retaining sensitivity to sensory surprise value (illustrated here by normal deviant detection hit rates for melodies; Table 2). In patients' daily lives, reduced predictive flexibility under dynamic listening conditions may contribute to impaired hearing even in quiet environments, impaired perception of less familiar accents and emotional prosody and reduced modulation of social signals such as conversational laughter (Hailstone *et al.*, 2012; Rohrer *et al.*, 2012; Pressman *et al.*, 2017; Hardy *et al.*, 2019).

The reduced pupillary response to syntactic deviants in the svPPA and bvFTD groups here extends the evidence for central autonomic dysregulation in these syndromes (Femminella *et al.*, 2014; Joshi *et al.*, 2014, 2017; Fletcher *et al.*, 2015; Ahmed *et al.*, 2018; Marshall *et al.*, 2018, 2019). While abnormalities of autonomic effector control have also been demonstrated in AD and nfvPPA (Fletcher *et al.*, 2015; Marshall *et al.*, 2019), the picture in these syndromes is complex: here, the magnitude of the peak pupillary response to musical deviants was normal in AD and enhanced in nfvPPA. As a marker of physiological arousal, peak pupillary response magnitude constitutes a proxy for sensory salience (Liao *et al.*, 2016; Wang *et al.*, 2017, Zénon, 2019*a*). The syndromic pupillary response profiles here, taken together with the behavioural data on detection accuracy, suggest that musical deviants were less surprising (less salient) to patients with bvFTD and svPPA (which are associated with degraded stored predictions about the musical environment) but normally surprising to patients with AD and relatively *more* surprising to patients with nfvPPA. A mutual interplay between prediction formation

and salience coding, and between cognitive and autonomic mechanisms, is essential to our normal experience of musical events (Salimpoor *et al.*, 2015; Cheung *et al.*, 2019; Koelsch *et al.*, 2019).

Across the patient cohort, changes in pupillary response latency were dissociated from the magnitude and not linked to the accuracy of deviant detection. Slower pupillary responses in the AD and nfvPPA groups might potentially reflect a modulatory effect of neurotransmitter deficits. However, in AD, the balance of cholinergic and noradrenergic effects on pupillary response shows a complex and variable dependence on disease stage, medication and behavioural context (Chougule *et al.*, 2019), while involvement of cholinergic pathways in nfvPPA does not translate simply to changes in cholinergic activity (Schaeverbeke *et al.*, 2017). Both AD and nfvPPA frequently involve dorsal brainstem structures (including locus coeruleus and Edinger-Westphal nucleus) that mediate pupillary latency effects (Samuels and Szabadi, 2008).

Neuroanatomically, cognitive detection and autonomic signalling of musical surprise in the combined patient cohort were linked to distributed cortico-subcortical networks. Cognitive reactivity to acoustic deviants correlated with grey matter in a predominantly temporo-parietal distribution, overlapping the so-called 'default-mode' network that governs the interface between self and environment. Postero-medial cortex (including precuneus) and its hippocampal outflow play a key role in auditory scene analysis, both in the healthy brain and in neurodegenerative disease (Goll *et al.*, 2012, Golden *et al.*, 2015*a*). Noise bursts interrupting a melody potentially signal a fundamental change in the prevailing auditory environment, engaging neural mechanisms that decode the significance of environmental fluctuations in relation to the internal milieu and the neural record of continuous auditory experience. Connected brain regions mediate the preparation of responses to such salient, potentially behaviourally relevant events: semantic control processes that integrate incongruous sensory information with stored conceptual representations are mediated via middle temporal gurus (Hickok and Poeppel, 2007; Davey *et al.*, 2016; Kocagoncu *et al.*, 2017) while physiological arousal is mediated via limbic structures, including amygdala (Critchley *et al.*, 2001; Sander *et al.*, 2003).

On the other hand, detection of syntactic deviants had neuroanatomical correlates in a right-lateralized anterior fronto-temporo-striatal network. The inferior frontal gyrus (pars orbitalis) is commonly reported in the context of MMN oddball paradigm (Molholm et al., 2005; Opitz et al., 2002) with a right-lateralization for violations of musical expectations (Sammler et al., 2012; Maess et al., 2001; Levitin & Menon, 2005). The temporal polar cortex, the canonical 'hub' of the semantic memory system, is directly connected to the inferior

frontal cortex via the uncinate fasciculus. Together, both regions evaluate incoming musical patterns against stored templates and rules acquired implicitly through the individual's cumulative past experience of music (Griffiths and Warren, 2004; Warrier and Zatorre, 2004, Lappe *et al.*, 2013*a*) and are essential for processing harmony and syntax (Johnsrude, Penhune & Zatorre, 2000; Patterson, Uppenkamp, Johnsrude, & Griffiths, 2002; Koelsch et al., 2014; Clark et al., 2018; Koelsch and Siebel, 2005; Sammler *et al.*, 2013; Bianco *et al.*, 2016; Cheung *et al.*, 2018; Omigie *et al.*, 2019) and for recognition of melodies (Groussard *et al.*, 2010; Johnson *et al.*, 2011; Herholz *et al.*, 2012; Jacobsen *et al.*, 2015; Sikka *et al.*, 2015; Freitas *et al.*, 2018; Slattery *et al.*, 2019). The involvement of the putamen suggests that detection of syntactic deviants might have been facilitated by a coding of musical expectations in a probabilistic manner as the dorsal striatum is commonly implicated in tracking statistical structure of sensory signals (Overath et al., 2007; Grahn & Rowe, 2013; Nastatse et al., 2015; Hardy et al., 2017; 2018; Cheung *et al.*, 2019; Omigie *et al.*, 2019). I will develop this question in more details in the next chapter.

A common correlate of syntactic and acoustic surprise processing at a cognitive level was identified in supplementary motor cortex. This is a core effector region for predicting actions and preparing behavioural responses to salient and arousing events, in music, vocalisations and other cognitive domains (Warren *et al.*, 2006; Jacobsen *et al.*, 2015; Sammler *et al.*, 2015; Lima *et al.*, 2016; Gordon *et al.*, 2018; Slattery *et al.*, 2019). Its involvement here might plausibly signal preparedness to react to incongruence in familiar melodies.

At an autonomic level, common correlates of syntactic and acoustic surprise processing were identified in the anterior cingulate cortex and the precuneus. This posteromedial portion of the parietal lobe is involved in episodic memory retrieval and self-processing operations as part of the default-mode network (Platel *et al.*, 2003; Cavanna and Trimble, 2006; Sestieri *et al.*, 2011); its involvement here in both cognitive and autonomic signalling of musical surprise might have been primed by the use of highly familiar melodies. The anterior cingulate cortex is a key hub of the salience network and has repetitively been shown to predict task-evoked changes in sympathetically mediated autonomic activity. It is proposed to be responsible for the integration of bodily state with behavioural engagement (Matthews *et al.*, 2004; Critchley *et al.*, 2011) and thus constitutes an important region of the central autonomic control network. The conjoint involvement of the salience network and the default-mode network for autonomic processing of changes in acoustic fluctuations in relation to contextual milieu corroborates several studies looking at impairments of auditory scene analysis in neurodegenerative

diseases targeting these networks which suggested that segregating auditory sources necessitates the engagement of a generic interface between external sensory events and the internal monitoring of those events over time (Goll *et al.*, 2012, Golden *et al.*, 2015*a*; Hardy *et al.*, 2020). Lastly, the neural correlate found in a region spanning middle temporal gyrus and superior temporal sulcus adds to the previous finding of semantic control processes for integrating salient sensory information with stored 'auditory objects' of melodies with a specific role of posterior superior temporal sulcus in transiently representing relevant sound features that provide the basis for identifying newly acquired sound categories (in this case, white-noise) (Limb, 2006; Liebenthal *et al.*, 2010).

As a naturalistic stimulus that is familiar and meaningful to many people, bound by strong but largely implicit rules and admitting the unexpected frequently and often fruitfully, music is an ideal model for the much less tractable milieu of expectation and surprise that surrounds our emotional and social lives. As a predictive coding paradigm, music is generally characterised by fine-grained, non-disruptive fluctuations that more closely mimic everyday sensory environments than the highly disruptive stimuli conventionally used to assess the psychophysics of deviance processing (Quiroga-Martinez *et al.*, 2020). It remains to demonstrate that deficits in detecting musical highly surprising events relate to a more generalised impairment in tracking the probabilistic information of a musical environment. The work I present in Chapter 4 attempts to do just this, employing an unsupervised machine learning model of auditory expectancy to quantify key information-theoretic properties of my stimuli and relate them to the measured behavioural and autonomic reactivity described in this chapter.

4 Sensitivity to the statistical structure of melodies: link with behavioural and autonomic reactivity to deviants

4.1 Chapter summary

The previous chapter demonstrated differentiated behavioural and autonomic profiles in response to surprising events in a musical environment. The current chapter investigated the ability of patients to track the probabilistic structure of a musical environment. More specifically, it sought to examine if they signalled this knowledge at an autonomic level, if they were able to use it to guide their conscious detection of surprising events and finally, if the uncertainty of the environment exerted any modulation on their probabilistic sensitivity to surprise. Using the Information Dynamics of Music computational model (Pearce, 2010), I calculated deviant surprise value (information-content) and carrier melody predictability (entropy) and related these to accuracy detecting melodic deviants and simultaneously-recorded pupillary responses. In healthy controls, both detection accuracy and autonomic reactivity to musical events correlated with the information-theoretic quantity of surprise (IC) in deviant musical events but were differentially modulated by the uncertainty (ENT) of the musical environment, with stronger associations for more predictable musical environments. The AD group had a similar profile at the autonomic level, showing a linear association of deviant IC with pupillary responses, enhanced in more predictable environments . The nfvPPA group, on the other hand, while showing retained cognitive and autonomic sensitivity to deviant IC, had differentiated modulation of environmental uncertainty. The svPPA group showed the most severe profile with a generalised loss of sensitivity to both surprise and uncertainty, at both a cognitive and autonomic level. Finally, the bvFTD group showed the most complex profile with a generalised loss of sensitivity to both surprise and uncertainty at the cognitive level but a retained sensitivity to surprise at an autonomic level when controlling for uncertainty level of the musical environment. Across the patient cohort, the partial correlations between deviant detection accuracy or pupillary responses and IC, covarying for uncertainty level, had separable neuroanatomical substrates in cortico-subcortical networks including the dorsal and ventral striatum, previously implicated in tracking probabilistic information in musical sequences.

4.2 Introduction

The formation of musical expectations has been the focus of many decades of research in music cognition and led to the notion that listeners internalize patterns of occurrence of musical events and ultimately acquire an implicit knowledge of musical structure (Huron, 2006). This concept has been very influential and has notably inspired a computational model of musical expectations. Based on information theory and statistical learning, this model is especially powerful in the way that, contrary to previous models (Narmour, 1990; Schellenberg, 1997), it incorporates both a long and short-term model. While the long-term model, trained on a large corpus of melodies, represents expectations learnt over a lifetime of exposure to music, the short-term model simulates local influences on expectations formed dynamically as a specific piece of music unfolds. This model has successfully predicted listeners' subjective expectations (Pearce *et al.*, 2010; Egermann *et al.*, 2013; Sauvé *et al.*, 2018) but also electrophysiological and autonomic measures of expectations (Carrus *et al.*, 2013; Omigie *et al.*, 2013, 2019; Quiroga-Martinez *et al.*, 2019; Bianco *et al.*, 2020). This model yields two key information theoretic parameters: surprise, expressed in terms of information-content which represents bits of information based on the probability of occurrence of a particular event; and level of uncertainty, expressed in terms of entropy which is typically high when events have equal probability to occur and low when events with high probability of occurrence are mixed with events with low probability of occurrence.

Uncertainty and surprise are in fact two key components of the predictive coding model instantiated in a hierarchical cortical organisation with surprise representing the prediction error and uncertainty the precision allocated to sensory input (see Chapter 1 for definitions). There is currently an increasing interest and effort toward understanding the interaction of these two variables in predicting pleasure and rewarding effect of music (Gold et al., 2020; Cheung et al., 2019) and at a more fundamental level, in predicting subjective experience of musical surprise and electrophysiological or autonomic signals of auditory expectations. Perceptually, unexpected tones have been shown to be experienced as more salient when they occur in contexts with low as compared to high uncertainty (Hansen and Pearce, 2014; Hansen *et al.*, 2016). At a neurophysiological level, responses to auditory surprise (ERAN, MMN) were larger when unexpected tones were embedded in context with low compared to high uncertainty levels (Garrido *et al.*, 2013; Quiroga-Martinez *et al.*, 2019). At an autonomic level, Bianco *et al.* (2020) demonstrated the same contextual modulation of uncertainty on pupillary responses to unexpectedness of deviants with, again, a greater pupillary response to pitch deviants in melodic context with

low rather high uncertainty. In mechanistic terms, what these studies demonstrate is that the human brain infers the precision or reliability of sensory inputs such that, in case of surprise, the ascending prediction error is heightened and more likely to lead to model updating. On the contrary, unreliable inputs (low precision) are down-weighted and lead to reduced prediction errors in response to unexpected changes that are less likely to ascend the cortical processing hierarchy and modify the predictive model.

As reviewed in Chapter 1, impairments at any level of the distributed hierarchical process are likely to result in a cascade of errors that manifests as cognitive dysfunction, notably in the language and speech domains, ranging from segregating sources during auditory scene analysis (Bendixen, 2014) to production of intelligible speech and understanding of non-native accents. These disorders rapidly extend to more complex social and emotional behaviours such as disinhibition, apathy or loss of empathy (Dalley *et al.*, 2011; Lansdall *et al.*, 2017; Johnen and Bertoux, 2019). Such formulations of cognitive and behavioural deficits associated with neurodegenerative diseases are becoming more and more common (Cope *et al.*, 2017, Hardy *et al.*, 2017*a*; O'Callaghan and Hornberger, 2017; Kocagoncu *et al.*, 2020). However, a systematic investigation of the effect of proteinopathies on the ability to track surprise and uncertainty levels of musical information, serving here as a tractable model system for more complex everyday behaviours, is still missing. This chapter looked at the differences in behavioural and autonomic reactivity to surprise and uncertainty of music in neurodegenerative diseases and offered a first pilot study before its extension to neurofunctional investigation which would describe the disruptions of information flow at the mesoscale and large-scale network levels and their link to complex social and emotional behaviours.

In this chapter, I used the same stimuli as outlined in Chapter 3 and estimated the entropy or uncertainty of the musical environment and the information content of musical events. I then assessed, for each diagnostic group, how the entropy of the melody and the information-content of deviant 'surprising' events related to behavioural and physiological responses. Structural neuroanatomical associations of the strength of coupling between behavioural and autonomic measures with information-theoretic parameters were assessed using voxel-based morphometry (VBM) of patients' brain MR images.

Based on the aforementioned studies (Quiroga-Martinez *et al.*, 2019; Slattery *et al.*, 2019; Bianco *et al.*, 2020), I hypothesized a modulatory effect of the environmental entropy on the ability to track information-content of musical events, at both a cognitive and autonomic level. I predicted that sensitivity to information-

theoretic parameters of melodies would be relatively more severely affected in FTD than in AD (Dalton *et al.*, 2012; Hughes and Rowe, 2013, Hardy *et al.*, 2017*a*, *b*). More specifically, based on previous evidence of increased environmental dependency in patients with frontal lobe lesions, I expected bvFTD patients to display a dissociated profile with retained sensitivity to environmental entropy but reduced sensitivity to deviant information-content (Ghosh and Dutt, 2010; Kumfor *et al.*, 2018). Finally, I hypothesised that the cognitive and autonomic coding of musical information-content in the patient cohort would have neuroanatomical correlates within the hierarchical distributed brain networks previously implicated in the probabilistic coding of auditory signals, i.e. in the anterior cingulate cortex and insula, the limbic regions and the nucleus accumbens (Overath et al., 2007; Grahn & Rowe, 2013; Cheung *et al.*, 2018; Omigie *et al.*, 2019).

4.3 Material and methods

4.3.1 Participants

The participant cohort was the same as described in Chapter 3. Please refer to Table 3.1 for demographic, clinical and general neuropsychological characteristics of participant groups.

4.3.2 Experimental design and stimuli

Please refer to Chapter 3 for the experimental design and synthesis of stimuli.

4.3.3 Experimental procedure

Please refer to Chapter 3 for details about the procedure.

4.3.4 Information-theoretic modelling

4.3.4.1 Description

Pearce et al. (Pearce, 2005) built IDyOM based on music informatics, statistical language modelling and data compression techniques. IDyOM provides reliable computational measures of musical pitch unexpectedness or 'surprise' (as represented by information-content) and uncertainty (as represented by entropy) for Western listeners (Pearce *et al.*, 2010; Omigie *et al.*, 2012; Pearce and Wiggins, 2012; Egermann *et al.*, 2013; Hansen and Pearce, 2014; Sauvé *et al.*, 2018). IDyOM has also successfully predicted several electrophysiological measures of expectation violation (Carrus *et al.*, 2013; Omigie *et al.*, 2013; Quiroga-Martinez *et al.*, 2019) and even psychophysiological and subjective emotional responses (Egermann *et al.*, 2013; Sauvé *et al.*, 2018).

To index musical expectations, IDyOM models both dynamic local learning of repeated patterns within stimuli (short-term or 'online' listening) and stylistic or rule-based learning through lifelong exposure to a large corpus of musical sequences (long-term listening). Information-content and entropy can be computed using different musical features (or viewpoints) as inputs to IDyOM: one could model the probability of the next pitch value, registral direction, time, inter-onset interval ratio, etc., and one could model these different 'viewpoints' independently or simultaneously. Based on empirical findings concerning the integration of pitch information in melodies from pitch intervals and scale degrees (Pearce and Müllensiefen, 2017), here I chose two viewpoints as inputs to IDyOM based on previous work studying cognitive and neurophysiological effects of predictability and uncertainty in monophonic melodies (Quiroga-Martinez et al., 2019; Omigie et al., 2012; Omigie et al., 2019; Gold et al., 2019; Cheung et al., 2019): 'cpitch' (representing chromatic notes counted up and down from the middle pitch number, C=60) and 'cpintfref cpint' (representing chromatic pitch interval combined with scale degree – the chromatic interval from tonic, where 0 = tonic, 4 median, 7 dominant, etc.).

As a proxy for long-term listening (participants' life-long exposure to Western tonal music), the model was trained on a large, representative sample of Western tonal music. I trained IDyOM on a corpus of 449 Western tonal melodies, comprising 43 American tunes, 71 English tunes, 150 German folk songs from the Essen folk collection (Schaffrath, 1992), and 185 chorale melodies harmonized by Bach as in other applications of IDyOM (Omigie *et al.*, 2012; Egermann *et al.*, 2013; Hansen and Pearce, 2014; Quiroga-Martinez *et al.*, 2019). This corpus constituted the 'training set' which allowed IDyOM to learn the statistical structure of Western tonal melodies, via variable-order Markov modelling (Pearce, 2005), This training on general musical structures mimics the listener's life-long exposure to music; the trained 'long-term' model, therefore, represents 'musical syntax', the 'rules' about tonal music that listeners automatically internalise through their accumulated past experience of music. When listening to individual pieces of music, listeners continuously update their expectations about how the piece will subsequently unfold; these expectations depend not only on the long-term context established by past musical experience but the short-term context established by that particular piece. As a proxy for such short-term (online) listening, I used a second, 'short-term' model which dynamically learned the statistical structure of each stimulus used in my experiment. The short-term and long-term models both produce distributions characterising each note in information-theoretic terms as the melody unfolds.

In combining the short-term and long-term models, the distributions of note characteristics generated by each model were weighted according to probability distribution, such that the less probable model is discounted relative to the more probable model. The weighted combined model outputs two key information theoretic parameters: the information-content (IC) or actual degree of unexpectedness of the pitch of each note and the entropy of each note (ENT), or the prior uncertainty about its pitch based on the variability of previously experienced notes. In mathematical terms, IC (typically denoted h) corresponds to the base-2 negative log probability of that note 'event', which is inversely proportional to the probability of an event x_i

$$h(x_i|c) = -log_2\big(p(x_i|c)\big)$$

with c referring to the preceding context (MacKay, 2003) while ENT (typically denoted H) is the sum of the expected value of the IC across all possible continuations:

$$H(c) = \sum_{i \in A} p(x_i|c) \times h(x_i|c)$$

maximal when all potential events xi are equally probable, with $p(x_i|c) = \frac{1}{n}$ where n equals the number of notes. In psychological terms, IC is a "backward-looking" metric reflecting the amount of information processing required given the past melody context (the degree of unexpectedness or surprise associated with an event, such as a musical note, for the listener); while entropy is a "forward-looking" metric reflecting the predictability of an upcoming note (the listener's degree of uncertainty about the event).

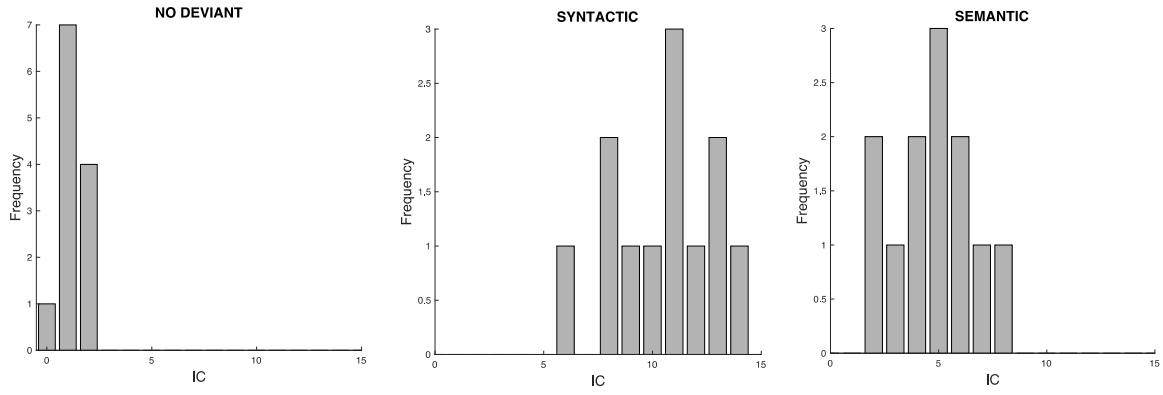

Figure 4.1. Information-content distributions for the deviant (or 'deviant-like' in the no-deviant condition) in each stimulus condition

Table 4.1. **Information-theoretic characteristics of experimental melody stimuli**

Melody	ENT	Deviant characteristics		
		Interval	Position*	IC*
No deviant				
Colonel Bogey March	2.72	NA	-2	1.81
Edelweiss (The Sound of Music)	3.39	NA	-4	1.57
Moon River	3.15	NA	-3	1.10
Morning (Peer Gynt)	2.65	NA	-4	0.59
My Way	2.43	NA	-2	0.74
Peter's Theme (Peter and the Wolf)	2.63	NA	-3	2.41
Star Wars Theme	2.16	NA	-4	0.39
Summertime	3.09	NA	-3	0.75
Swan Lake 'Theme'	2.78	NA	-3	1.83
Symphony No. 40 (Mozart)	2.30	NA	-2	0.61
William Tell Overture	2.04	NA	-2	1.38
You Are My Sunshine	2.57	NA	-4	0.65
Semantic deviants				
Auld Lang Syne	2.66	8	-2	5.55
Away In A Manger	2.79	4	-3	3.24
All Things Bright And Beautiful	2.76	6	-3	6.18
Frere Jacques	2.98	3	-4	2.40
God Save The Queen	2.59	5	-3	8.06
Hark! The Herald Angels Sing	2.54	5	-2	4.60
Jerusalem	2.98	7	-2	5.09
Jingle Bells	2.39	3	-2	3.51
Lullaby (Brahms)	2.92	3	-4	4.25
O Come All Ye Faithful	2.89	3	-3	2.19
Que Sera, Sera	2.66	9	-4	7.19
We Wish You A Merry Christmas	2.81	3	-4	5.12
Syntactic deviants				
Deck The Halls	2.76	4	-2	9.36
Do-Re-Mi (The Sound of Music)	3.19	4	-3	6.09
Fly Me To The Moon	2.82	6	-3	10.74
For He's A Jolly Good Fellow	2.65	6	-2	7.82
Für Elise (Beethoven)	2.80	4	-4	8.12
Hey Jude	3.38	6	-4	13.21
Joy To The World	2.83	5	-3	12.61
La Donna E Mobile (Rigoletto)	2.72	4	-4	11.13
O Little Town Of Bethlehem	2.69	4	-3	14.04
Rudolph The Red-Nosed Reindeer	2.94	8	-2	11.82
Silent Night	3.20	3	-2	11.03
When The Saints Go Marching In	2.56	4	-4	10.25

*values for equivalently positioned standards in the case of melodies with no deviant; ENT, mean melody entropy (see text for details); IC, information-content of deviants; Interval, no. of semitones difference between original (standard) and deviant note; NA, not applicable.

4.3.4.2 Analysis of behavioural and autonomic data

For each melody containing a pitch deviant (or, for melodies without deviants, equivalently positioned 'standard' notes), I calculated the IC of the deviant note and the mean entropy (ENT) of the melody stem (from the first note to the note immediately preceding the deviant note). The deviant conditions described in Chapter

3 (no deviant – syntactic deviants – semantic deviants) did not differ significantly in mean entropy (one-way ANOVA with Bonferroni correction, $F(3,44) = 1.51$, $p=0.22$) of constituent melodies. On the other hand, IC scores for syntactic deviants (mean=10.52 SD=2.26) were significantly greater than IC scores for 'standard' notes (mean=1.15 SD=0.62) ($t=13.35$, $p<0.001$) and IC scores for semantic deviants (mean=4.78 SD=1.75) ($t=6.72$, $p<0.001$). Similarly, IC scores for semantic deviants were significantly greater than IC scores for 'standard' notes ($t=6.55$, $p<0.001$).

I first ran Spearman correlations between ENT and three key parameters: deviant detection accuracy, pupillary responses to deviants and a measure of the 'sustained' pupillary response integrated over the first five seconds of the melody in each participant group. This last variable was derived by calculating the area under the curve (AUC) of the time series spanning the first five seconds of each trial (the minimum interval of time common to all melodies where no deviant occurred) and baseline-corrected over the pre-onset interval [mean pupil size during the 500 ms interval before melody onset]. Note here that ENT was calculated for variable lengths of the melodies from the first note to the note immediately preceding the deviant note and not only for the first five seconds.

IC category level and ENT category level were determined by separating melodies into low IC, high IC, low ENT and high ENT based on the median IC and ENT value for the entire stimulus set. IC values in the low ENT category ranged from 0.38 to 14.1 with a median value of 4.05 while IC values in the high ENT category ranged from 0.75 to 13.2 with a median value of 5.10. There was no significant difference between these two sets ($t=-0.67$, $p = 0.51$). I first calculated non-parametric partial correlations of stimulus IC score with trial-by-trial deviant detection accuracy (hit rate) and pupillary dilatation response over the combined melody set, taking into account the entropy level of melody. I then ran Spearman correlations separately for each melody ENT category (low/high). Finally, I compared correlation strengths between participant groups using one-tailed z-tests, after transforming correlations to Fischer z-scores (Cohen *et al.*, 2013; Sheksin et al., 2004).

4.3.5 Brain image acquisition and analysis

Please refer to Chapter 2 for details about brain image preprocessing and Chapter 3 for details about brain image acquisition.

In the combined patient cohort, I used full factorial linear regression models to assess associations between regional grey matter volume (indexed as voxel intensity) with individual Spearman's correlation values

obtained for each participant when looking at the associations between detection accuracy and deviant IC and between peak pupillary response and deviant IC. Age, total intracranial volume and pitch direction score were incorporated as covariates of no interest. Statistical parametric maps of regional grey matter associations were assessed at threshold p<0.05 after FWE correction for multiple voxel-wise comparisons within an anteroventral network involved in semantic appraisal (anterior superior temporal gyrus, middle temporal gyrus, temporal pole and inferior frontal gyrus: Johnsrude *et al.*, 2000; Hsieh *et al.*, 2011; Johnson *et al.*, 2011; Sammler *et al.*, 2013; Agustus *et al.*, 2018; Slattery *et al.*, 2019), a cingulo-insular network involved in salience processing and motor output (anterior insula, anterior cingulate cortex and supplementary motor area: Lima *et al.*, 2016; Freitas *et al.*, 2018) and a temporo-striato-limbic network involved in detecting statistical regularities in auditory signals (putamen, nucleus accumbens, hippocampus and planum temporale: Overath *et al.*, 2007; Omigie *et al.*, 2013, Hardy *et al.*, 2017*b*, *a*; Cheung *et al.*, 2019).

4.4 Results

4.4.1 Behavioural correlations

4.4.1.1 Sensitivity to environmental uncertainty

No significant correlations were found between accuracy of deviant detection and ENT across the combined stimulus set when looking at separate groups.

4.4.1.2 Sensitivity to deviant unexpectedness

Across the combined stimulus set, IC was positively correlated with accuracy of deviant detection in the healthy control group (rho=0.41, p=0.01) and nfvPPA group (rho=0.40, p=0.02) whereas IC was negatively correlated with accuracy of deviant detection in the svPPA group (rho=-0.43, p=0.008). Correlations were significantly stronger in healthy controls and nfvPPA groups than both the bvFTD and svPPA groups (all p<0.009; see Table 4.2). ENT had minimal impact on the results when performing partial correlation (removing the variance in detection accuracy accounted for by the entropy level) (HC: rho=0.41, p=0.01; nfvPPA: rho=0.36, p=0.03; svPPA: rho=-0.43, p=0.01).

When dividing my stimuli set into low and high ENT melodies, I found that for low ENT (more predictable) melodies, IC was significantly positively correlated with accuracy of deviant detection in the healthy control group (rho=0.52, p=0.03), whereas IC was significantly negatively correlated with accuracy of deviant detection in the

svPPA group (rho=-0.57, p=0.01), driven by a very low false alarm rate in the no-deviant condition (see also Table 2). For high ENT (less predictable) melodies, there were no significant correlations between IC and deviant detection accuracy in any participant group.

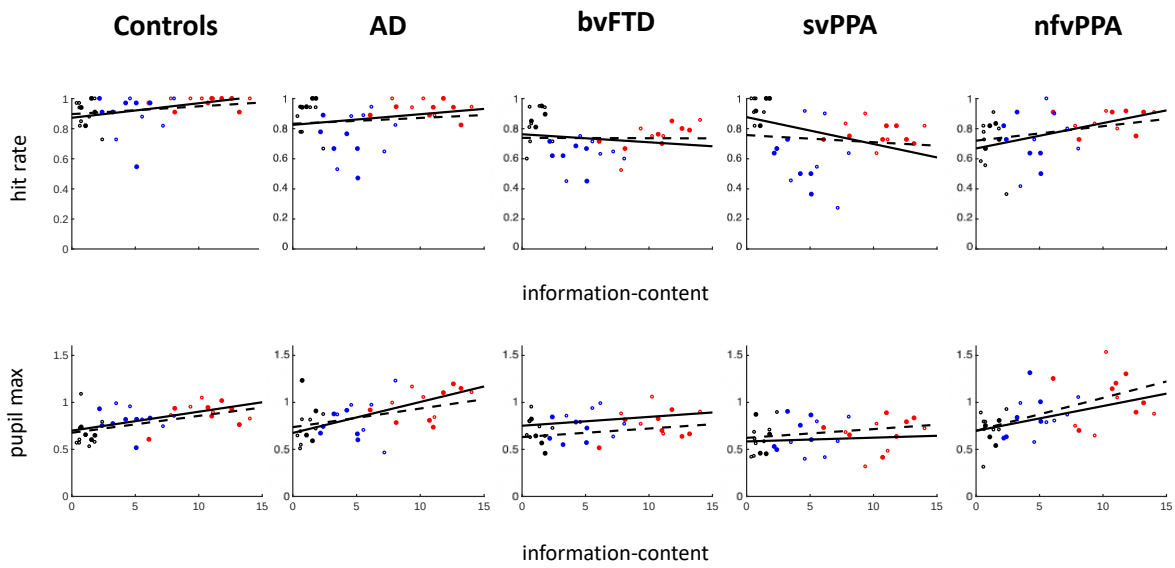

Figure 4.2. Correlations (Spearman's rho) of melodic deviant information-content (IC) with accuracy (hit rate) of deviant detection (top panels) and peak pupillary response (pupil max) to deviants (bottom panels), for each participant group

IC was estimated across the stimulus melody set using the IDyOM model. In each panel, each dot represents one of the 36 stimulus melodies (for the matched no-deviant [black], semantic deviant [blue] and syntactic deviant [red] conditions; see text and Table S1) and fitted lines indicate the predictive linear fit between IC and the participant parameter of interest. Open dots and solid lines code melody stimuli with low entropy; filled dots and dashed lines code melody stimuli with high entropy. Numerical and statistical data on the correlations are in Tables 2 and 3.

Table 4.2. Correlations of detection accuracy with deviant information-content: participant group values and comparisons

Group	Condition	IC correlate	IC partial correlate	Comparisons (IC correlate)			
				AD	bvFTD	svPPA	nfvPPA
Controls	All	**rho = 0.41**	**rho_p = 0.38**	p = 0.09	**p = 0.008**	**p < 0.001**	p = 0.48
	low ENT	**rho = 0.52**		p = 0.18	**p = 0.023**	**p < 0.001**	p = 0.37
	high ENT	rho = 0.27		p = 0.14	p = 0.10	p = 0.06	p = 0.37
AD	All	rho = 0.10	rho_p = 0.07		p = 0.14	**p = 0.01**	p = 0.09
	low ENT	rho = 0.24			p = 0.14	**p = 0.007**	p = 0.28
	high ENT	rho = -0.11			p = 0.42	p = 0.32	p = 0.11
bvFTD	All	rho = -0.16	rho_p = -0.19			p = 0.11	**p = 0.009**
	low ENT	rho = -0.15				p = 0.09	**p = 0.04**
	high ENT	rho = -0.18				p = 0.40	p = 0.075
svPPA	All	**rho = -0.43**	**rho_p = -0.40**				**p < 0.001**
	low ENT	**rho = -0.57**					**p = 0.001**
	high ENT	rho = -0.27					**p = 0.045**

	All	**rho = 0.40**	**rho_p = 0.36**				
nfvPPA	low ENT	rho = 0.43					
	high ENT	rho = 0.33					

The table summarises correlations (Spearman's rho) of melodic deviant information-content (IC) with detection accuracy (hit rate) for each participant group and p-values on pair-wise comparisons of correlation values between groups. Data are shown for the combined stimulus melody set (All), melodies with low entropy (low ENT) and high entropy (high ENT) respectively. Significant correlations and comparisons ($p<0.05$) are indicated in bold.

4.4.2 Autonomic correlations

4.4.2.1 Sensitivity to environmental uncertainty

Across the combined stimulus set, ENT was negatively correlated with pupillary reactivity over the first five seconds of each trial (AUC) in the healthy control group (rho=-0.63, p<0.001), AD group (rho=-0.68, p<0.001), the bvFTD group (rho=-0.75, p<0.001) and the nfvPPA group (rho=-0.44, p=0.008). All correlations were significantly stronger than the svPPA group (all p<0.05) except for the nfvPPA group (p= 0.10).

On the other hand, only the bvFTD group displayed a significant correlation between pupillary responses to deviants and ENT across the combined stimulus set (rho = -0.33, p =0.047).

4.4.2.2 Sensitivity to deviant unexpectedness

Across the combined stimulus set, IC was positively correlated with pupillary dilatation magnitude in the healthy control group (rho=0.56, p<0.001), AD group (rho=0.53, p<0.001) and nfvPPA group (rho=0.54, p<0.001). The correlation was significantly stronger in healthy controls than the svPPA group (p=0.04) and the bvFTD group (p=0.04; see Table 4.3). Using partial correlations removing the variance in pupillary response accounted for by the entropy level, IC was positively correlated with pupillary dilatation magnitude in the healthy control group (rho=0.62, p<0.001), AD group (rho=0.56, p<0.001), the nfvPPA group (rho=0.54, p=0.001) and, this time, also in the bvFTD group (rho = 0.34, p = 0.05). Moreover, the partial correlation between entropy level and pupillary response to deviants (controlling for IC of deviants) was significant in the healthy control group (rho = - 0.34, p = 0.04) and the bvFTD group (rho = - 0.42, p = 0.01).

When dividing my stimulus set into low and high ENT melodies, I found that for low ENT melodies, IC was significantly positively correlated with pupillary dilatation magnitude in the healthy control group (rho=0.58, 0.01) and AD group (rho=0.71, p<0.001). For high ENT melodies, IC was significantly positively correlated with pupillary dilatation magnitude in the healthy control group (rho=0.58, p=0.01) and nfvPPA group (rho=0.63, p=0.01).

Table 4.3. Correlations of maximum pupillary dilatation with deviant information-content: participant group values and comparisons

Group	Condition	IC correlate	IC partial correlate	Comparisons (IC correlate)			
				AD	bvFTD	svPPA	nfvPPA
Controls	All	**rho = 0.56**	**rho_p = 0.62**	p = 0.43	**p = 0.04**	**p = 0.044**	p = 0.45
	low ENT	**rho = 0.58**		p = 0.27	p = 0.13	p = 0.09	p = 0.26
	high ENT	**rho = 0.58**		p = 0.21	p = 0.13	p = 0.11	p = 0.41
AD	All	**rho = 0.53**	**rho_p = 0.54**		p = 0.06	p = 0.06	p = 0.48
	low ENT	**rho = 0.71**			**p = 0.047**	**p = 0.025**	p = 0.10
	high ENT	rho = 0.35			p = 0.37	p = 0.35	p = 0.15
bvFTD	All	rho = 0.20	**rho_p = 0.31**			p = 0.48	p = 0.05
	low ENT	rho = 0.27				p = 0.39	p = 0.34
	high ENT	rho = 0.24				p = 0.48	p = 0.09
svPPA	All	rho = 0.21	rho_p = 0.17				p = 0.06
	low ENT	rho = 0.17					p = 0.24
	high ENT	rho = 0.22					p = 0.08
nfvPPA	All	**rho = 0.54**	**rho_p = 0.53**				
	low ENT	rho = 0.40					
	high ENT	**rho = 0.63**					

The table summarises correlations (Spearman's rho) of melodic deviant information-content (IC) with maximum pupillary dilatation for each participant group and p-values on pair-wise comparisons of correlation values between groups. Data are shown for the combined stimulus melody set (All), melodies with low entropy (low ENT) and high entropy (high ENT) respectively. Significant correlations and comparisons ($p<0.05$) are indicated in bold.

4.4.3 Neuroanatomical associations

Significant grey matter associations of partial strength of coupling between detection accuracy and IC and between maximum pupillary response and IC for the combined patient cohort are summarised in Table 4.4; statistical parametric maps of these associations are presented in Figure 4.3. All associations here are reported thresholded at $p<0.05$ after FWE correction for multiple voxel-wise comparisons within pre-specified anatomical regions of interest.

Partial correlation between detection accuracy and IC of deviants correlated with regional grey matter in an extended bi-hemispheric network comprising bilateral supplementary motor area, superior temporal gyrus, nucleus accumbens and hippocampus; right lateralized temporal pole and putamen and left lateralized inferior frontal gyrus (pars opercularis).

Partial correlation between maximum pupillary response and IC of deviants correlated with regional grey matter in right precuneus. No other significant clusters were found.

Table 4.4. Neuroanatomical correlates of behavioural and autonomic tracking of information-content (controlling for melody entropy) in the combined patient cohort

Region	Side	Cluster (voxels)	Peak (mm)			T score	P_{FWE}
			x	y	z		
Partial correlation between behavioural responses to deviants and IC							
Supplementary motor area	R	660	6	-15	66	5.18	0.003
	L	352	-6	-15	66	4.70	0.010
Nucleus accumbens	R	882	8	6	-2	4.68	0.006
	L	108	-4	10	-3	4.49	0.010
Putamen	R	882	22	18	-6	4.65	0.007
Inferior frontal gyrus: pars opercularis	L	76	-60	6	15	4.60	0.024
Temporal pole	R	1192	46	9	-22	4.54	0.027
Superior temporal gyrus	R	297	56	-16	-6	4.49	0.025
	L	96	-56	-30	2	4.32	0.035
Hippocampus	L	144	-24	-18	-14	4.00	0.038
	R	441	24	-15	-15	3.95	0.044
Partial correlation between pupillary responses to deviants and IC							
Precuneus	R	65	6	-51	69	4.37	0.030

The table presents the results of the voxel-based morphometry analysis. Shown are the locations of regional grey matter positively associated with the individual partial correlations between 1) accuracy of detection and deviant information-content (IC) in familiar melodies 2) maximum pupillary response to deviants and deviant information-content (IC) in familiar melodies, over the combined patient cohort (see also text and Figure 3). Coordinates of local maxima are in standard MNI space. P values were all significant ($p<0.05$) after family-wise error (FWE) correction for multiple voxel-wise comparisons within pre-specified anatomical regions of interest (see text and Figure S1 online).

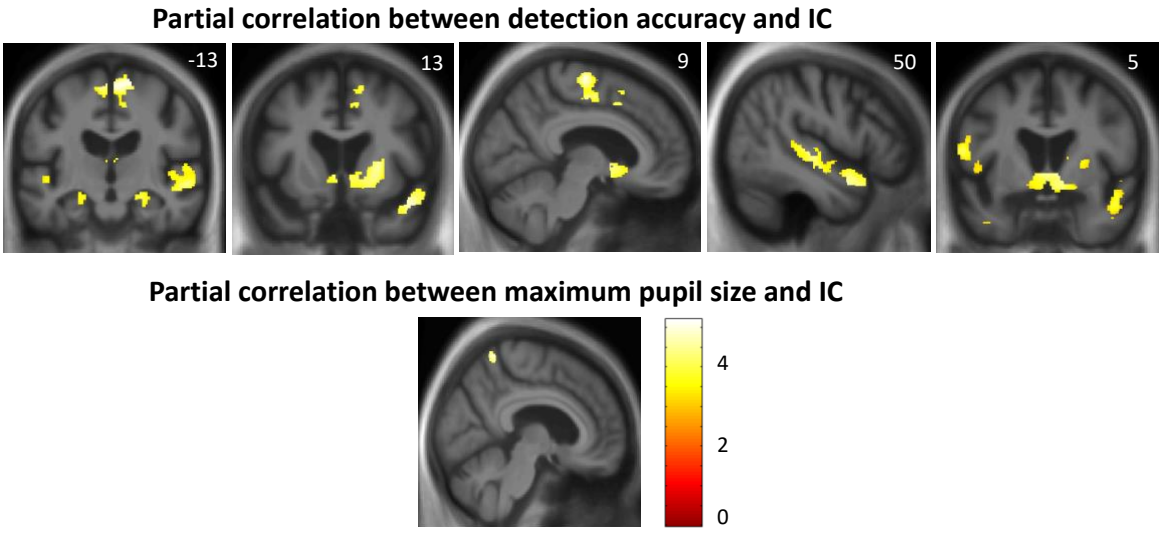

Figure 4.3. Neuroanatomical correlates of accurate detection of melodic deviants and pupillary responses to deviants in the combined patient cohort

Statistical parametric maps (SPMs) show regional grey matter volume positively associated with acoustic) and syntactic deviant detection accuracy in familiar melodies, based on voxel-based morphometry of patients' brain MR images. SPMs are thresholded for display purposes at $p < 0.001$ uncorrected over the whole brain, however, local maxima of areas shown were each significant at $p < 0.05$ after family-wise error correction for multiple voxel-wise comparisons within pre-specified anatomical regions of interest; the MNI coordinate (mm) of the plane of each section is indicated.

4.5 Discussion

Here I have shown that canonical syndromes of FTD and AD have differentiated cognitive and autonomic sensitivity to the surprise level of musical events and uncertainty level of melodies. In healthy controls, both detection accuracy and autonomic reactivity correlated with the information-theoretic quantity of surprise (IC) in deviant musical events but were differentially modulated by the uncertainty (ENT) of the musical environment. In line with previous work (Hansen and Pearce, 2014; Hansen *et al.*, 2016; Bianco *et al.*, 2020), the influence of information-content on cognitive detection accuracy was enhanced in more predictable musical environments, and pupillary responses to deviants displayed a significant partial correlation with environmental uncertainty. The nfvPPA group, on the other hand, while showing retained cognitive and autonomic sensitivity to deviant IC, had differentiated modulation of environmental uncertainty. The AD group showed an association of deviant IC with pupillary responses, enhanced in more predictable environment. All groups, except the svPPA group, showed a negative association between 'integrative' pupil response (in the first five seconds of the melodies) and uncertainty levels. The svPPA group showed generalised loss of sensitivity to both surprise and uncertainty, at both a cognitive and autonomic level. Finally, the bvFTD group showed generalised loss of sensitivity to both surprise and uncertainty at the cognitive level but a retained sensitivity to surprise at an autonomic level after adjusting for uncertainty level of the musical environment. Across the patient cohort, the partial correlations between deviant detection accuracy or pupillary responses and surprise adjusted for uncertainty level had separable neuroanatomical substrates in cortico-subcortical networks previously implicated in tracking probabilistic information in musical sequences.

In the healthy control group, accurate detection of deviants and the amplitude of the pupil response to these deviants were positively correlated to deviant IC. Moreover, this coupling was heightened in more predictable melodies and absent in less predictable melodies. At the autonomic level, there was a significant partial correlation of melody ENT with pupillary responses to deviants, pupillary reactivity increasing with increasing predictability of the environment. Taken together, these results suggest that healthy controls successfully extracted the probabilistic structure from melodies and had stronger predictive models about more predictable melodies compared to less predictable ones, thereby facilitating detection of changes in the environment.

Interestingly, the nfvPPA group retained this sensitivity to information-content of deviants, cognitively and autonomically. The hypothesis of over-precise priors in nfvPPA, described in the previous chapter (Cope *et al.*, 2017) has been fruitful in providing a mechanistic account of impaired understanding of speech in quiet environments, and difficulty understanding sinewave speech, naturalistic foreign accents or emotional prosody. However, nfvPPA pathology, which affects both high levels of the cortical hierarch (IFG) and lower sensory level in the peri-sylvian cortices, may be associated with a 'double-hit' of the information flow system within the hierarchical cortex. In that case, over-precise prior expectations passing down the hierarchy would be compared with down-regulated sensory input, leading to an increased prediction error. The enhancement of pupil reactivity to pitch deviants, described in the previous chapter, already suggested that prediction errors, approximated by pupil response (Liao *et al.*, 2016; Zhao *et al.*, 2019, Zénon, 2019*b*) were abnormally high in nfvPPA patients. This chapter further suggests that prediction errors linearly aligned to the informational value of sensory input and were not affected by up-regulated top-down expectations passing down the hierarchy. Furthermore, these prediction errors, observable at an autonomic level, were efficiently passed through conscious processes driving decision-making related to detection of changes in the environment. Finally, peak pupillary responses tracked deviant surprise value in relatively less (but not more) predictable musical environments, as would be anticipated if pupillary responses in this syndrome tend to signal relatively less salient events linearly but become saturated in more predictable environments (Bianco *et al.*, 2020).

Loss of the normal dependence of deviant detection on IC and lack of any modulatory effect from environmental ENT in svPPA is consistent with previous evidence that svPPA pathology fundamentally impairs analysis of the information content of auditory sequences (Hardy *et al.*, 2017*a*, *b*). The severity of the profile observed in this study might be explained by a general erosion of musical models, as these models have been shown to rely on intact functions of regions involved in general semantic memory, i.e. temporal polar cortex, anterior superior and middle temporal gyri (Hsieh et al., 2011; Johnson et al., 2011). In other domains less reliant on intact semantic memory, svPPA patients showed a significant sensitivity to the contextual intrinsic uncertainty: for example, for speech signals, better comprehension of sinewave transformed spoken numbers than less predictable signals such as geographical place names. This study drew on clinical observations of svPPA patients displaying new interests related to inanimate stimuli bound by very specific rules and thus, more highly predictable (for example, mathematics or music). Hence, the degradation of stored templates in svPPA is likely to

impact processing of surprise and environmental uncertainty in diverse sensory environments, and one would expect exacerbated deficits in less rule-bounded environments (e.g. social interactions). Further studies would need to corroborate this hypothesis.

Similar loss of cognitive sensitivity to information-content of musical events was observed for bvFTD patients, consistent with previous evidence for a general impairment of salience coding (Perry *et al.*, 2017; Clark *et al.*, 2018) corroborated by severe atrophy in the salience network (Zhou et al., 2010; Seeley et al., 2009). Pupillary responses, on the other hand, were efficiently tracking the entropy level of melodies in this syndromic group with a decreasing 'integrative' pupil response to high entropy melodies and an increased 'integrative' pupil response to low entropy melodies. This trend was observable in all other groups with the exception of the svPPA group, and fits into the predictive coding framework if one considers that uncertainty level of melodic sequences directly translates to decreased gain or precision of sensory inputs: i.e., unpredictable melodies are down-weighted while more regular melodies sequences are more informative and up-weighted. This result constitutes the first demonstration of a significant sensitivity of subcortical responses to the statistics of unfolding stimuli, that have already been shown for cortical responses (Barascud et al., 2016; Sohoglu & Chait, 2016), and is consistent with a close linkage between brain systems involved in detecting changes and norepinephrine activity in the locus coeruleus (Joshi *et al.*, 2016; Alamia *et al.*, 2019). Notably it has been proposed that norepinephrine would signal updating of predictive models or interruption of top-down descending projections, promoting more efficient signalling of abrupt contextual change (Zhao et al., 2019).

The bvFTD group was the only patient group to show a direct association between entropy and pupillary responses to musical events with a further preserved sensitivity to information-content after controlling for the effect of entropy on pupil reactivity. In that respect, bvFTD patients seem to retain the ability to use contextual information to influence their response to surprise, exerting a higher precision of sensory input in more predictable environments and generation of larger prediction errors in case of mismatch with their predictive models. However, predictive models are equally likely to be damaged, as seen for svPPA, and corroborated by several studies which provided evidence of generalized failure to establish sensory predictions (Shaw et al., 2019; Hughes et al., 2013, 2018), leading to an imbalance of the precision ascribed to sensory input relative to the precision ascribed to prior expectations. Such a predictive coding formulation might potentially explain the 'environmental dependency syndrome' or utilization behaviour commonly exhibited by bvFTD patients, whereby

they produced inappropriate behaviours 'enslaved to' environmental triggers and contextual information (Burgess et al., 2009; Ghosh et al., 2010; Kumfor et al., 2018). This over-reliance on contextual information has previously been demonstrated in the context of facial emotion recognition (Kumfor et al., 2018) and in empathy tasks (Oliver *et al.*, 2015). Here, I have replicated this result in a more dynamic domain with a quantification of the effect of contextual modulation on change information processing. Finding tests that can assess this behaviour is essential as environmental dependency symptoms, despite being a defining feature of FTD and other frontal lobe lesions, is notoriously difficult to measure (Ghosh and Dutt, 2010; Ghosh *et al.*, 2013). Novel metrics are unique would permit a more accurate diagnosis notably with respect to the numerous phenocopies seen in this syndrome and a better tracking of behavioural changes in this group. While this chapter did not set out to assess environmental dependency behaviours per se, it would be interesting to examine whether my findings are associated with manifestations of these behaviours in a daily basis.

Cognitive sensitivity to information-content of deviants, after adjusting for entropy level of melodies had closely overlapping neuroanatomical correlates within the network engaged by detection of syntactic deviants in the previous chapter, with additional involvement of bilateral superior temporal gyrus, nucleus accumbens and hippocampus. It subsumed a generic fronto-striatal 'prediction network' previously proposed to test sensory hypotheses and minimise prediction error in diverse domains, including music (Siman-Tov *et al.*, 2019). These findings are consistent with a scheme in which the prediction network is hierarchically engaged. According to this scheme, superior temporal gyrus initially represents musical object structure (especially, pitch pattern) and information content (Patterson *et al.*, 2002; Koelsch, 2005, Lappe *et al.*, 2013*b*; Janata, 2015, Golden *et al.*, 2016*a*; Omigie *et al.*, 2019). Temporal polar cortex (the canonical 'hub' of the semantic memory system) and inferior frontal cortex together track and evaluate incoming musical patterns against stored templates and rules acquired implicitly through the individual's cumulative past experience of music (Griffiths and Warren, 2004; Warrier and Zatorre, 2004, Lappe *et al.*, 2013*a*). Both regions are thus essential for processing harmony and syntax (Koelsch and Siebel, 2005; Sammler *et al.*, 2013; Bianco *et al.*, 2016; Cheung *et al.*, 2018; Omigie *et al.*, 2019) and for recognition of melodies (Groussard *et al.*, 2010; Johnson *et al.*, 2011; Herholz *et al.*, 2012; Jacobsen *et al.*, 2015; Sikka *et al.*, 2015; Freitas *et al.*, 2018; Slattery *et al.*, 2019). It is worth highlighting the difference between the IFG substrate associated with syntactic deviant detection in the previous chapter and the IFG substrate associated with tracking of probabilistic information. While the first was found in the pars orbitalis, commonly reported for

subjective experience of expectation violations (Lehne *et al.*, 2014; Mikutta *et al.*, 2015), the second was found in the pars opercularis previously implicated in processing musical syntax and more fine-grained tracking of information (Koelsch and Siebel, 2005; Bianco *et al.*, 2016; Cheung *et al.*, 2018).

The hippocampus has been found to contribute to the discovery of regular patterns in auditory sequences with the joint involvement of sensory auditory cortices and IFG (Barascud et al., 2016). My findings add to the growing evidence for a role of the medial temporal lobe in the rapid detection of regularities (Aly *et al.*, 2013; Yonelinas, 2013) and statistical learning (Turk-Browne *et al.*, 2009; Turk-Browne, 2012; Schapiro *et al.*, 2014). The conjoint involvement of dorsal and ventral striatum here underlines the critical role of striatal dopaminergic circuitry in coding musical expectation and surprise probabilistically (Cheung *et al.*, 2019; Omigie *et al.*, 2019), an operation integral to hedonic valuation of music (Salimpoor *et al.*, 2015; Blood and Zatorre, 2001; Koelsch, 2014). In particular, nucleus accumbens has been shown to track reward prediction errors in music, a prime mover of musical learning and behaviour (Gold *et al.*, 2019). By employing highly familiar melodies, the present study may have primed the engagement of these musical reward circuits.

While MMN-like responses to changes in the environment and pupillary reactivity to these changes have been shown to share a common neural substrate in anterior cingulate cortex (Alamia et al., 2019), the neural substrate of pupillary sensitivity to IC was rather different to the extended network described above. However, the right precuneus, as a major component of the dorsal attention and default-mode networks (Corbetta and Shulman, 2002; Raichle, 2015), has been shown to regulate pupillary dilatation during memory retrieval tasks or insight-based problem solving (Wang and Munoz, 2015; Suzuki *et al.*, 2018).

Here I have demonstrated that musical stimuli, when defined in terms of probabilistic structure characterised with a computational model, are powerful in eliciting a hierarchical neural network underlying predictive processes and reward-based statistical learning. In this way, it offers an ideal model to study how neurodegenerative diseases disrupt processes of probabilistic inference and could be translated to other domains relying on acoustic patterns detection, such as language or emotional vocalizations underpinning social interactions. Limitations of this study include, again, the lack of a formal analysis of how individual familiarity ratings of each melody influenced the statistical tracking of information-content and entropy, considering indeed that the listener's prior expectations will have varied depending on their past exposure to these melodies. Moreover, categorisation of melodies in terms of entropy and information-content levels would have benefitted

from a direct assessment by collecting note unexpectedness ratings and subjective uncertainty ratings within a separate cohort of healthy controls. The findings of striatal substrates suggest a link between reward processing and stimulus information theoretic properties. Future experiments could address this question more directly by capturing listeners' aesthetic experience of music and their ability to track probabilistic information explicitly. This question is likely to have therapeutic implications for patients with dementia, by leveraging their often retained ability to appreciate music and informing intervention to train their sensitivity to fine-grained musical information (Benhamou and Warren, 2020).

5 Musical reward processing in frontotemporal dementia: the exploration-exploitation dilemma

5.1 Chapter summary

In this chapter, I focus on a particular case of prediction error called the reward prediction error. This prediction error is fundamentally different to the prediction errors described in the previous chapters (deviant or high information-content event) because it first requires adequate learning of how to pair a stimulus to a reward or a punishment. In this way, it does not rely on preserved 'templates' of musical lexicon acquired through a lifetime's exposure but instead on a combination of adequate reward processing and decision-making processes. I adapted a classical exploration-exploitation reinforcement learning paradigm in a cohort of 20 bvFTD patients relative to 23 healthy controls. Participants were asked to choose the visual cue associated with the highest probability of obtaining a musical 'reward' compared to cues with higher probabilities of obtaining a musical 'punishment'. Reaction times of cue selection and pupil responses to musical stimuli were also recorded and constituted an implicit measure of individual's valuation of actions and individual's valuation of the outcome of actions, respectively. These valuation systems, along with overall performance, were then correlated with grey matter volume in a voxel-based morphometry analysis. Relative to healthy controls, bvFTD patients were less accurate in choosing the best option. This impairment was accompanied by a decrease in differences between reaction times to visual cues and in pupil reactivity to punishment compared to reward. While environmental reward rate and implicit valuation of musical stimuli (pupil reactivity) had little impact on performance, valuation of cues (reaction times) strongly predicted accuracy of choice. This performance correlated with measures of executive function, cognitive flexibility and with measures of ritualistic and compulsive behavioural changes. Neuroanatomical correlates of choice accuracy and preserved valuation systems emerged along the dorsal and ventral attention networks and in additional regions in anterior insula and parahippocampal gyrus previously implicated in processing aversive information.

5.2 Introduction

The two previous chapters looked at how neurodegenerative disease impacts the ability of the brain to update internal models of the environment when it faces surprising events or/and uncertain environments. The following two chapters will look at the second strategy deployed by the Bayesian brain to minimise prediction errors: actions. I will specifically look at a certain type of prediction error denoted the reward prediction error which represents the difference between an expected reward and the actual outcome. The concept of optimization of one's behaviour, formulated as the maximisation of value or expected reward, has been studied in cognitive psychology through the use of reinforcement learning paradigms (RL). In a RL framework, the agent receives information from the environment (usually termed the *state*) and selects an action to change the environment which in turn, returns a new state. State and actions are continuously given value which we denote the *valuation process.* Reward processing, on the other hand, represents the way the agent uses the reward to update the value functions of states and actions (Hélie *et al.*, 2017). These models have allowed a systematic investigation of the different stages involved during reward-based decision-making and are increasingly used to quantitatively assess impairments of fundamental cognitive functions such as attention, memory, decision-making, and learning and their impact on behaviour in psychiatric and neurological diseases (Maia and Frank, 2011; Deserno *et al.*, 2013; Adams *et al.*, 2016; Chiong *et al.*, 2016; Hélie *et al.*, 2017).

A particular case of reinforcement learning is the multi-armed bandit problem which allows modelling of the classical exploration versus exploitation dilemma. In daily-life scenarios, people are constantly required to choose between repeating an action with a well-known reward value (exploitation) or obtaining more information about the environment by trying an alternative action with an uncertain but potentially higher reward value. Too much exploitation prevents someone from gathering information in an uncertain environment and would induce behavioural inflexibility, habit formation and stereotypy. On the other hand, too much exploration may lead to inefficient decision-making and induce stimulus-bound and utilization behaviours and an increased dependency on contextual changes.

Patients with bvFTD exhibit a diverse panoply of decision-making deficits ranging from overeating to poor financial decisions. The most common behavioural changes reported by caregivers include an increased preference for sweet, carbohydrate rich foods, changes in sex drive, changes in social conduct, apathy, disinhibited behaviour, perseverative and stereotyped behaviour, increase in alcohol consumption, sudden

interest or aversion to music, and changes in humour (see clinical review: Johnen and Bertoux, 2019). Sex, food, social engagement, money, music are considered as primary (essential for survival) or secondary rewards: it is widely recognised that these symptoms are, at least in part, related to defective reward and decision-making processes (i.e. reward-based decision-making). In addition, the reward anatomical circuitry, mainly involving the striatum, the orbitofrontal cortex, the anterior insula and cingulate cortex, is heavily targeted by bvFTD pathology. Yet, only a very few studies have systematically investigated reward-based decision-making in bvFTD (see literature review in Table 5.1) and so far, none has looked at the classical exploration versus exploitation dilemma. This paradigm has notably been used to quantify motivational deficits in psychopathology such as depression and schizophrenia (Barch *et al.*, 2016). Environmental dependency behaviours, stereotypy, ritualistic or compulsive behaviours are examples of behavioural changes related to excessive or reduced exploration or exploitation and all these symptoms have been reported in patients with bvFTD pathology. This is particularly relevant because, unlike other behavioural and neuropsychiatric traits like apathy, lack of empathy and executive dysfunction, motivational symptoms are uniquely related to frontal lesions and could help to distinguish bvFTD from other neurodegenerative diseases (Ghosh *et al.*, 2013; Johnen and Bertoux, 2019).

The capacity of music to create psychological expectancy links it very naturally to reward processing (Li et al., 2015; Tsai & Chen, 2015). Melodies with a harmonic structure that fulfils expectation have repeatedly been shown to induce pleasure while lack of resolution is associated with negative affect (Huron, 2006; Steinbeis *et al.*, 2006; Koelsch *et al.*, 2008; Gingras *et al.*, 2015; Salimpoor *et al.*, 2015; Tsai and Chen, 2015, Gold *et al.*, 2019*b*, *a*). As a complex rewarding stimuli, music entails the potential to influence goal-directed action and one study, by giving participants the opportunity to purchase a piece of music in an auction paradigm, managed to demonstrate the involvement of a complex mesolimbic reward circuitry (comprising nucleus accumbens, ventromedial PFC and limbic regions) during the updating of musical reward value (Salimpoor *et al.*, 2013, p. 201). Thus, the same deep subcortical regions adapted to drive behaviours such as eating and sex are involved when listening to music. Although parallels exist between neural correlates of primary and musical rewards, perceptual and cognitive of music processing are also crucial for listeners' emotional experience. Music unarguably constitutes a unique hedonic stimuli in the way it unites biological and autonomic mechanisms via the neural involvement of several subcortical areas with higher-level socio-emotional mechanisms at the heart of goal-directed behaviours via anterior frontotemporal, temporoparietal and limbic networks (Blood *et al.*, 1999; Blood and Zatorre, 2001; Salimpoor *et al.*, 2009, 2011; Zahn *et al.*, 2009; Brattico *et al.*, 2011; Koelsch, 2014) . Universal, pleasurable for

most listeners, implicitly learned, easily manipulable, and grounded in the dopaminergic system in the striatum and higher-level regions responsible for integrating cognitive processing with autonomic nervous system activity and motor activity, music offers an ideal platform to study how neurodegenerative pathology impacts reward processing and goal-directed behaviours.

Here, I used a three-armed bandit problem where the three arms were associated with a fixed, unknown and independent reward probability distribution. Only presenting two arms at once, I created three environments or states, each related to a different overall reward exposure (high, intermediate or low). Reward (an expected outcome) and its counterpart, punishment (a worse than expected outcome), were induced using a well-known musical priming paradigm, which involved manipulating the congruency between a 'prime context' (in this case three progressing harmonic chords) and a 'target' (the fourth final chord of the harmonic progression). The target was either made expected as a consonant resolution chord or unexpected as a dissonant chord abruptly terminating the harmonic progression. I studied a cohort of bvFTD (n=20) referenced to age-matched healthy older individuals (n=23) and simultaneously assessed participants' ability to choose the best option and their implicit valuation systems related to actions and states (outcomes) using reaction times and pupillometry. I assessed how the environmental reward rate and the ability to update values of actions or musical stimuli predicted choice accuracy. I related the results to specific neuropsychological and neuropsychiatric scores obtained during neuropschological and clinical assessments of the patient cohort. Structural neuroanatomical associations of choice accuracy and implicit sensitivity to reward and punishment were assessed using VBM of patients' and healthy controls' brain images.

Based on previous work addressing reward-based decision-making in bvFTD and healthy populations, I hypothesised that bvFTD patients would be associated with a general impairment in choosing the best option (i.e. exploiting) and that this deficit would be more severe in high reward rate environment compared to low reward rate environment. I also hypothesized that this deficit would correlate with neuropsychological metrics of cognitive flexibility and response inhibition and behavioural changes in stereotypy, compulsion and disinhibition (Ghosh and Dutt, 2010; Ghosh *et al.*, 2013; Johnen and Bertoux, 2019). Moreover, I predicted a reduced autonomic sensitivity to both reward and punishment (Joshi *et al.*, 2014, p. 20, Fletcher *et al.*, 2015*b*). Finally, I hypothesized that choice accuracy and sensitivity to punishment in the participant cohort would correlate with neuroanatomical structures within the reward circuit, the salience network and the postero-dorsal parietal

network described in previous studies investigating exploration-exploitation behaviour (Daw *et al.*, 2006; Laureiro-Martínez *et al.*, 2015).

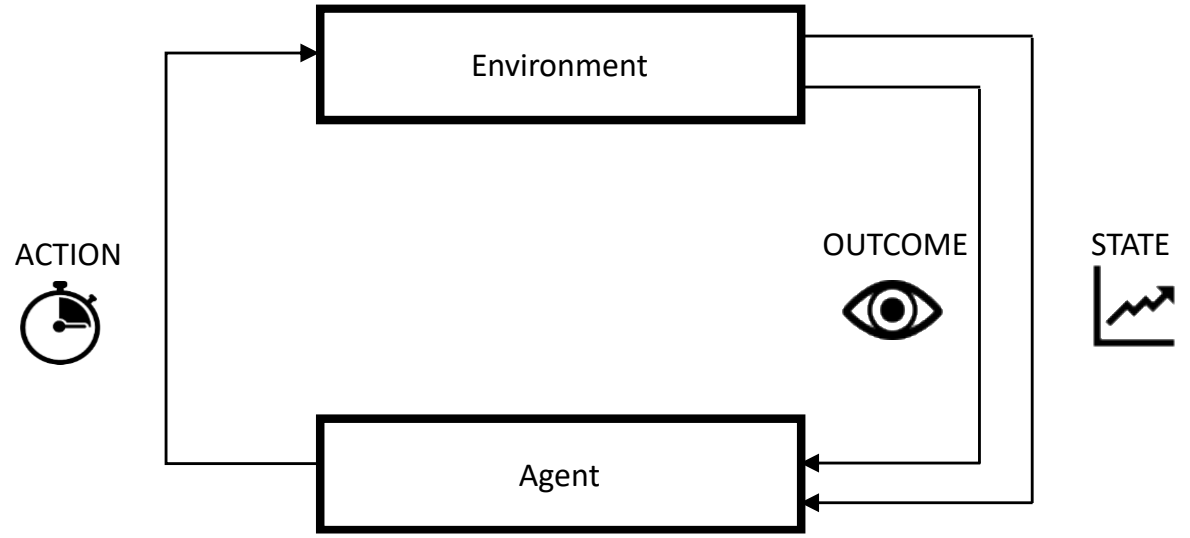

Figure 5.1. Schematic representation of reinforcement learning processes

At each step, an agent interacts with the environment using an action, reaching a new state in the process. The agent receives an outcome (reward or punishment) associated with that action. The aim of the agent is to find the optimal policy. The policy corresponds to the strategy that the agent implements to determines the next action based on the current state. In this study, I looked at several 'fixed' (non-dynamic) proxies for valuation of actions measured with reaction times (clock icon), valuation of outcome using pupillometry (eye icon) and the average accuracy rate of choosing the optimal action. The state here refers to the number of musical rewards accumulated for a specific action.

Table 5.1. Summary of previous literature investigating reward processing and value-based decision-making in bvFTD

Authors	**Design**	**Participants**	**Type of reward/punishment**	**Key findings**
Bertoux et al., 2014	Reward-related decision-making: Allais paradox (anticipation of regret)	n=14 bvFTD n=13 AD n=12 HC	Secondary reward (money)	Significant decrease of Allaisian behaviour (impaired regret processing) for bvFTD patients compared to AD and HC.
Bertoux et al, 2015	Delay-discounted paradigm (small immediate vs delayed larger reward)	n=20 bvFTD n=20 AD n-20 HC	Primary (food) and secondary reward (culture, sport)	bvFTD were more impulsive than AD and HC and were more likely to choose less pleasant but immediate rewards than more pleasant delayed rewards.
Chiong et al., 2014	Exploratory factor analysis	n=100 AD n=50 bvFTD	Secondary reward (money)	bvFTD were more likely to spend excessively with a general decreases in sensitivity to losses- social and affective vulnerability factor was a better predictor of financial errors than cognitive abilities.
Chiong et al., 2016	Loss aversion Delay discounting VBM	n=28 bvFTD n=14 svPPA n=25 AD n=61 HC	Secondary reward (money)	bvFTD were less averse to losses than HC but had preserved delayed discounting of rewards. These metrics did not correlate with any traditional neuropsychological measures and VBM results were null.
Clark et al., 2018	Rule processing: classification of melodies as resolved or unresolved Reward valuation: rating of subjective pleasantness VBM	n=11 bvFTD n=14 PPA n=14 AD n-22 HC	Secondary reward (music)	bvFTD showed impairment of both rule processing and reward valuation compared to controls. Reward valuation impairment correlated with GM in IFG (pars orbitalis)
Hoefer et al., 2008	Reward-based learning: fear conditioning measured with skin conductance VBM	n=15 FTD n=10 svPPA n=25 AD n=25 HC	Primary punishment (100 dB white noise burst)	FTLD showed impaired acquisition of conditioned responses and reduced SCR to aversive stimulus. SCR responses was correlated with GM in amygdala, ACC, OFC and insula.
Perry et al., 2014	VBM analysis of abnormal reward-seeking behaviours	n=103 bvFTD	Primary rewards (food, drugs, sex)	Higher reward-seeking of primary reward correlated with GM loss in right putamen, globus pallidus, insula and thalamus.
Perry et al., 2015	Reward-related decision-making: Monetary Incentive Delay task	n=14 bvFTD n=11 AD n=40 HC	Secondary re: social (emotional faces) and monetary (win or loss)	bvFTD had faster reaction times to monetary win than monetary loss but faster reaction times for social loss than social win greater motivation to gain money than avoid losing it
Perry et al., 2017	Reward-related decision-making and effort task VBM	n=25 bvFTD n=21 HC	Primary: olfactory stimuli	bvFTD had higher subjective pleasantness ratings and autonomic reactivity to unpleasant odours compared to controls: both metrics correlated with bilateral insula, amygdala and frontal pole atrophy.

				bvFTD were less successful at avoiding unpleasant smell but similar reward-seeking performance.
Rahman et al., 1999	Reward-related decision-making: Iowa Gambling Task	n=8 bvFTD n=8 HC	Secondary reward (money)	bvFTD showed genuine risk-taking behaviour with increased deliberation times. This behaviour was not related to impulsive behaviour.
Rahman et al., 2006	Reward-related decision-making: Cambridge Gamble Task Double-blind placebo-controlled procedure to look at the effect of methylphenidate	n=8 bvFTD	Secondary reward (points)	There was no effect of Methylphenidate (psychostimulant acting on NA and DA) on average deliberation time or choice but an effect on betting behaviour with significantly reduced risk-taking.
Strenziok et al., 2011	Reward-related decision-making: Balloon Analog Risk Task VBM	n=27 bvFTD n=19 HC	Secondary reward (money)	bvFTD showed decreased risk-taking behaviour in order to obtain an immediate reward from the previous trial. Impaired performance was related to atrophy in the right lateral OFC
Torralva et al., 2007	Reward-related decision-making: Iowa gambling tasks (IGT) in relation to tests of theory-of-mind (ToM)	n=20 bvFTD n=10 HC	Secondary reward (money)	IGT performance suggests a higher risk-taking behaviour. They were impaired at both IGT and ToM tasks compared to controls but performance measures were not correlated.
Whitwell et al., 2007	VBM analysis of abnormal eating behaviour	n=16 FTLD n=9 HC	Primary reward (food)	Sweet tooth was associated with GM loss in bilateral posterolateral OFC and right anterior insula. Hyperphagia was associated with GM loss in bilateral anterolateral OFC.
Wong et al., 2018	Value-directed word-list learning task	n=10 AD n=21 bvFTD n=22 HC	Secondary reward (points)	Both patient groups showed poorer learning. bvFTD patients showed value-directed enhancement of recognition memory for the points but not for the words.
Woolley et al., 2007	VBM analysis of abnormal eating behaviour	n=32 FTLD n=18 HC	Primary reward (food)	Binge-eating patients had higher GM loss in the right ventral insula, striatum and OFC.

5.3 Materials and methods

5.3.1 Participants

Twenty patients with bvFTD fulfilling consensus clinical criteria for bvFTD of mild to moderate severity were recruited; all had brain MRI images consistent with the diagnosis and none had evidence of significant cerebrovascular burden. No participant had a history of clinically significant hearing loss, congenital amusia or pupillary disease. Genetic screening of the patient cohort revealed pathogenic mutations in 12 cases (five *C9orf72*, four *MAPT*, three *GRN*). Twenty-three healthy older individuals with no history of neurological or psychiatric illness also participated.

Prior to the experimental session, patients' caregivers and healthy control participants completed a questionnaire detailing their prior and current musical experience, an adapted version of the Barcelona Music Reward Questionnaire (BMRQ) and an adapted mood questionnaire from the Immediate Mood Scaler (details in Methods chapter 2). All participants had audiometric screening of peripheral hearing function and an elementary pitch discrimination screening test (details in Methods chapter 2).

5.3.2 Experimental stimuli

Musical stimuli were adapted from a musical priming paradigm (Tillmann *et al.*, 2006, 2008) and based on four chords. In each stimulus, the three first chords were the prime and the fourth chord was the target. Thirty different chord progressions respecting the rules of harmony in Western music were created; across the stimulus set were equally represented four major (G, E, C, A) and two minor (E, C) keys. From this set I created two categories of musical stimulus: 'expected reward', comprising chord progressions with consonant target chords that resolved the progression (using a perfect or imperfect cadence); and 'unexpected punishment', comprising chord progressions in which the target chord was dissonant (-2 semitones for the bass note, -1 semitone for the fifth or -1 semitone for the octave). The distribution of priming chords was identical in each stimulus category. The perceptual effects of the two categories and their physiological effects on pupil reactivity were confirmed in an initial pilot study of eight healthy young individuals (see Appendix 9). Stimuli were synthetized with organ timbre as digital wavefiles using MuseScore® and were fixed for loudness (rms intensity). Each sound trial was 5 seconds long. A total of 60 stimuli (30 expected reward, 30 unexpected punishment) were administered in the experiment (examples of stimuli are enclosed with this thesis).

5.3.3 Experimental design and procedure

Participants were seated in a dimly and uniformly illuminated, quiet room, approximately 50 cm from a desktop computer monitor displaying symbols representing different arms of the bandit; pupil diameter was continuously measured (details in Methods chapter 2). Participants learned how they should choose between the symbols (bandit arms), according to the following instruction (given prior to the start of the experiment and repeated at two occasions during the experiment, after 20 and 40 trials): 'In this study, you will use buttons on the screen to play different musical clips. Some will be nice, some not so nice, depending on which buttons you press. The same button may play different music clips on different presses. Your goal is to try to work out which buttons to press so that, by the end of the study, you hear as much nice music as you can'. Six practice trials were presented at the start of the experiment to familiarise participants with the procedure.

The experimental design followed typical multi-armed bandit paradigms where participants have to associate a visual cue to a certain probability of obtaining a reward. Here, visual cues were three abstract icons derived from the Agathodaimon alphabet. Symbol identities and relative screen positions were fixed throughout the experiment. The reward probabilities corresponding to each symbol were counterbalanced between participants. Each symbol (arm) had three different associated probabilities of playing an 'expected reward' target chord: 90%, 50% or 10% (or the reciprocal probability of playing an 'unexpected punishment', 10%, 50% or 90% respectively). These contingencies were fixed over the course of the experiment. In order to generate environments with different reward rate (Gershman, 2015), only one pair of symbols were randomly presented on each trial and the two stimuli were displayed on the screen, leaving the third position blank. The participant chose one of the two symbols using an external mouse. Only the chosen symbol remained on the screen while the corresponding musical clip was played (after an interval of 1000ms), followed by an equilibration interval (2000ms). Participants were shown each pair of stimuli 20 times, yielding a total of 60 choices. These three pairs corresponded to three conditions: high reward rate, intermediate reward rate and low reward rate. The experimental procedure is presented in Figure 5.1.

All participant responses were stored for offline analysis. No feedback about performance was given during the experimental session and no time limits were imposed.

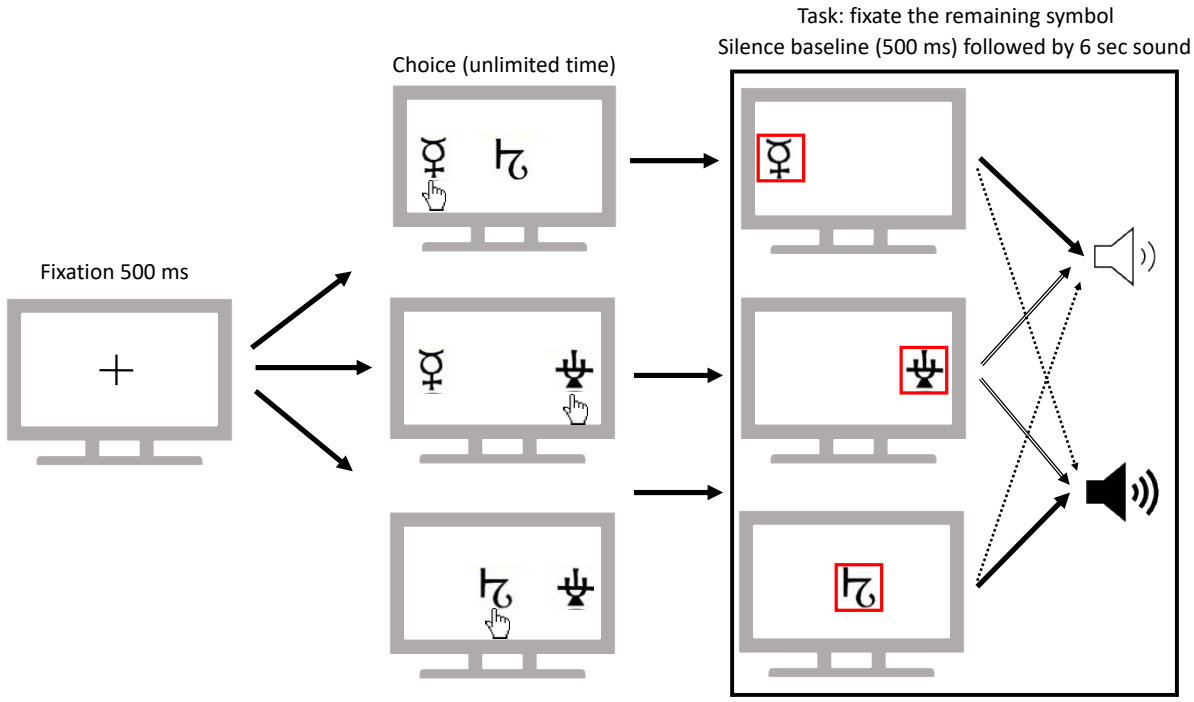

Figure 5.2. Successive screens of the behavioural task displayed during the three versions of a trial

Trials were presented in randomised order. Symbols' locations and their associated reward probabilities were fixed throughout the experiment. Participants selected between two responses using an external mouse corresponding to the two symbols displayed on screen, and subsequently listened to the outcome of their choice indicated with a red square. Chord progressions ending with a consonant chord are coded with a white sound icon and the ones ending with a dissonant chord with a black sound icon. Arrows pointing to sounds correspond to occurrence probabilities of chord progressions associated with each symbol: thick line: 90% - dotted line: 10% - doubled line: 50%.

5.3.4 Analysis of behavioural data

All behavioural data were analysed using Stata14.1®. Clinical and general neuropsychological data were analysed in accordance with the principles outlined in Section 2.9.1.

Three experimental conditions were analysed corresponding to three different reward rates imposed by the presented pair of symbols. During high-reward rate condition, the two options (90% and 50% arms) delivered rewards with probabilities greater than 0.5. During low-reward rate condition, the two options (50% and 10% arms) delivered rewards with probabilities lower than 0.5. During intermediate-reward rate (highly 'polarised'), condition, the two options (90% and 10% arms) delivered rewards with probabilities greater and lower than 0.5 respectively. The percentage of 'correct' choices – i.e., choosing the arm with the highest probability of reward - was calculated for each condition.

Reaction times were also calculated from the onset time of the first display screen to the participant's choice (Figure 5.1). Three reaction times corresponding to the three possible choices (90%, 50% or 10% arms) were measured.

Restricted maximum likelihood mixed effects models, with participant identity as a random effect, was used to analyse performance scores. Joint Wald tests of the relevant coefficients were used to examine the main effects of diagnostic group and experimental condition (reward rate) and their interaction on the response variables. Post hoc pairwise group comparisons with Bonferroni correction were performed where main effects were found. To take account of potentially confounding factors affecting performance, gender, pitch direction discrimination scores (as a surrogate for both musical ability and executive function) and musical reward score (obtained with the BMRQ questionnaire) were included as nuisance covariates in each model. Further, to control for individual differences in implicit ratings of reward and punishment chords, I included two additional covariates in the model assessing performance: average differences in reaction time between choosing the 90% and choosing the 10% arms ($RT_{pun\text{-}rew}$); and average differences in maximum pupillary response (see next section) to punishment relative to reward target chords ($pupil_{pun\text{-}rew}$). In order to estimate the effect of each covariate on the model, I compared the full model with a nested model (where each covariate is dropped in turn) using the likelihood-ratio. To guard against inflated Type I errors, I first establish the overall significance of the full model over the null model (dropping all predictors of interest i.e. diagnostic group, experimental condition and their interaction and the random effect of participant identity).

The same restricted maximum likelihood mixed effects model was used to analyse reaction times and examine difference between groups, conditions and interaction between groups and conditions. However, as this variable was used as a covariate in the main model assessing performance scores, no covariates were included in this analysis.

In addition, in the patient group only, Spearman's correlations were used to separately assess any association of performance scores with age, gender, prior musical expertise, peripheral hearing function, pitch direction discrimination score, auditory working memory (indexed as forward digit span), executive function (WASI Matrices), and scores assessing behavioural changes linked to reward processing, i.e. disinhibition, apathy, ritualistic/compulsive behaviour, hyperorality, hypersexuality and depression. These scores were obtained from ratings on a scale from 0 to 3 (0, absent; 1, mild; 2, moderate; 3, severe) provided by each patient's primary

caregiver during the clinical assessment. I also assessed Spearman's correlations in the patient group between $RT_{pun-rew}$ and psychometric or behavioural scores most susceptible to affect reaction times, i.e. Trail-Making-Test B (assessing executive speed and cognitive flexibility), mood scores obtained with the Immediate Mood Scaler questionnaire, and disinhibition and apathy scores assessed during the clinical assessment.

A threshold $p<0.05$ was accepted as the criterion of statistical significance for all tests.

5.3.5 Analysis of pupillometric data

The pre-processing pipeline is described in chapter 2. Pupil diameter data were first conditioned using previously described procedures (Mathôt et al., 2018; Kret and Sjak-Shie, 2019), baseline-corrected over a one-second interval prior to target chord onset and averaged across trials for each condition. We were interested to compare pupillary responses to consonant (expected reward) and dissonant (unexpected punishment) target chords, in each of the experimental conditions. Mean time series for each condition were analysed using Fieldtrip's cluster-based permutation test (Maris and Oostenveld, 2007) with a threshold at 5% to control family-wise error (FWE), in order to identify time windows with significant discrepancies between consonant and dissonant target chords. To assess effects of participant group and experimental conditions on pupillary responses, we extracted the maximum of the normalised (baseline-corrected) pupil dilatation response during an interval following target chord onset [0.5 to 3sec], based on the permutation analysis. I used a mixed linear model to compare pupil response amplitudes between participant groups and experimental conditions (reward and punishment target chords). Similarly to the analysis of reaction times, no covariates were included in this analysis as I wanted to assess 'pure' differences across groups, with a view to using this variable as a covariate in my main model assessing performance scores.

In the patient group only, Spearman's correlations were used to separately assess any association of $pupil_{pun-rew}$ (average difference between pupil response to punishment and pupil response to reward) with factors that could potentially influence influence pupil size (Bianchi et al., 2016; Guillon et al., 2016), i.e. age, gender, reward score obtained with the BMRQ questionnaire and mood scores obtained with the Immediate Mood Scaler questionnaire.

A threshold $p<0.05$ was again accepted as the criterion of statistical significance for all tests.

5.3.6 Brain image acquisition and analysis

For 18 bvFTD patients and 13 healthy control participants, T1-weighted volumetric brain MR images were acquired and preprocessed for entry into a VBM analysis as described in Chapter 2.

In the VBM analysis, full factorial linear regression models were used to assess associations between regional grey matter volume (indexed as voxel intensity) separately with the average percentage of correct choices in the three conditions; the average reaction time differences between choosing the punishment arm (10%) and choosing the reward arm (90%); the average pupil reactivity (measured as area under the curve) to punishment target chords and to reward target chords. Age, total intracranial volume and pitch direction score were incorporated as covariates of no interest. Statistical parametric maps of regional grey matter associations were assessed at threshold $p<0.05$ after FWE correction for multiple voxel-wise comparisons within pre-specified anatomical regions of interest (see Figure 5.3). These regions were informed by previous studies of reward processing in musical or non-musical settings, in both the healthy brain and neurodegenerative disease and comprised: a striatal network involved in reward and punishment-based learning (putamen, caudate, nucleus accumbens: Delgado *et al.*, 2000; Menon and Levitin, 2005; Haber and Knutson, 2010; Palminteri *et al.*, 2012; Hauser *et al.*, 2017); a limbic network involved in regulating autonomic responses to emotional stimuli (amygdala, parahippocampal gyrus and hippocampus: Gosselin *et al.*, 2006; Koelsch *et al.*, 2008; Baeken *et al.*, 2014; Koelsch, 2014); a prefrontal cortex network involved in decision-making and guidance of goal-directed behaviour (frontopolar cortex, medial and lateral orbitofrontal cortex, dorsal and ventromedial prefrontal cortex: Duuren *et al.*, 2008; Monosov and Hikosaka, 2012; Chase *et al.*, 2015); a parietal network involved in attentional control, in valuation of musical stimuli outcomes and reward expectation under uncertainty (angular and supramarginal gyri and precuneus: Wright *et al.*, 2012; Kahnt and Tobler, 2013; Li *et al.*, 2015) and a cingulo-insular network involved in reward processing during music listening and during avoidance learning in non-musical settings (anterior insula, anterior cingulate cortex: (Blood and Zatorre, 2001; Palminteri *et al.*, 2012).

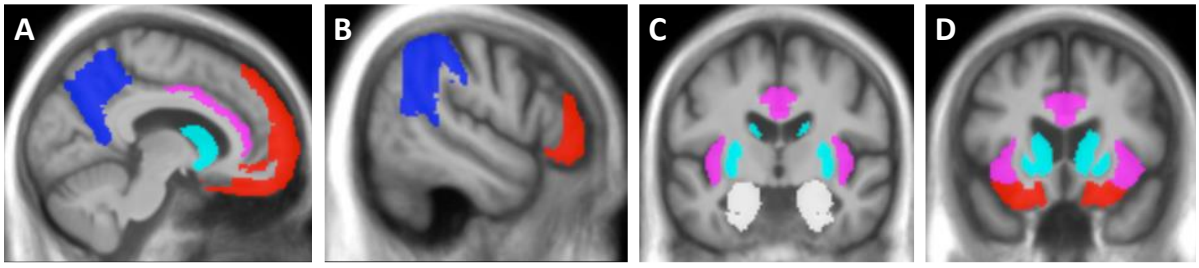

Figure 5.3. Pre-specified anatomical regions of interest for voxel-based morphometric analysis.

Representative sagittal (A, B) and coronal (C, D) sections are shown for the neuroanatomical volumes selected for multiple voxel-wise comparison correction in the region-of-interest analyses based on prior anatomical hypotheses. These regions were customised from the Oxford/Harvard brain maps to fit the group mean template brain image. Regions comprise a posterior temporo-parietal network including angular and supramarginal gyri and precuneus (blue); a prefrontal cortex network including frontopolar cortex, medial and lateral orbitofrontal cortex, dorsal and ventromedial prefrontal cortex (red); a cingulo-insular network including anterior cingulate and insula (purple); a striatal network including putamen, caudate nucleus, nucleus accumbens (cyan); and a limbic network including parahippocampal gyrus, hippocampus and amygdala (white).

5.4 Results

5.4.1 General participant characteristics

Two healthy controls were excluded because of low performance at the pitch direction discrimination task (<60%), resulting in a total number of 23 healthy controls. Results of participant group comparisons are summarised in Table 5.2. bvFTD group did not differ significantly from healthy controls in age, handedness, years in formal education, hearing threshold, musical expertise, average time spent listening to music or BMRQ scores assessing current experienced musical reward (all $p > 0.05$). However, the bvFTD group had an overrepresentation of male participants ($\chi^2 = 6.64$, $p=0.01$) and had lower Mini-Mental State Examination scores (Mann Whitney, $p = 0.004$), as well as pitch direction discrimination (Mann Whitney, $p = 0.02$) and mood scores (Mann Whitney, $p = 0.007$).

Table 5.2. Demographic, clinical and general neuropsychological characteristics of participant groups

Characteristic	Healthy controls	bvFTD
Demographic and clinical		
No. (male:female)	11:12	**16:4**
Age (years)	66.7 (7.0)	66.6 (6.6)
Handedness (R:L)	21:2	18:2
Education (years)	15.6 (3.2) $^{n-7}$	13.7 (2.9)$^{n-1}$
Symptom duration (years)	N/A	9.14 (4.9)$^{n-5}$
MMSE (/30)	29.2 (1.0)$^{n-10}$	**25.4 (3.7)$^{n-4}$**
Hearing threshold (dB)†† (17 controls)	24.8 (5.5)$^{n-9}$	24.5 (6.9)$^{n-4}$
Genetic mutations	N/A	5 C9 /4 MAPT / 3 GRN
Neuropsychological functions *		
Episodic memory		
RMT words (/50) (16 controls)	49.1 (1.1)	**38.6 (8.2) $^{n-6}$**
RMT faces (/50)	41.7 (3.6)	**33.1 (6.9) $^{n-6}$**
Camden PAL (/24) (16 controls)	20.5 (3.2)	**11.5 (7.5) $^{n-9}$**
Executive functions		
WASI Block Design (/71)	50.1 (11.9)	**26.9 (15.9)**
WASI Matrices (/32)	24.6 (4.3)	**15.8 (7.3) $^{n-2}$**
WMS-R digit span forward (max)	6.7 (1.3)	6.1 (1.3)
WMS-R digit span reverse (max)	5.8 (1.2)	**4.3 (1.5) $^{n-1}$**
D-KEFS Stroop colour naming (s)	28.4 (4.6)	**49.7 (19.2) $^{n-1}$**
D-KEFS Stroop word reading (s)	21.8 (5.2)	**28.8 (11.3) $^{n-1}$**
D-KEFS Stroop interference (s)	53.1 (11.9)	**81.6 (35.1)$^{n-1}$**
Trails A (s)	28.1 (10.4)	**58.8 (34.7) $^{n-1}$**
Trails B (s)	64.7 (23.4)	**158.2 (88.9) $^{n-1}$**
Language skills		
Letter fluency (F, 1 min)	16.5 (6.0)	**9.5 (6.1) $^{n-1}$**
Category fluency (animals, 1 min)	24.9 (4.8)	**11.6 (6.5) $^{n-1}$**
WASI Vocabulary (/80)	70.3 (5.9)	**44.7 (20.9) $^{n-4}$**
Graded Naming Test (/30)	25.1 (2.6)	**14.6 (13.1) $^{n-4}$**
BPVS (/150)	147 (2.1)	**118.2 (41.1) $^{n-3}$**
Other skills		
Graded Difficulty Arithmetic (/24)	16.9 (5.0)	**10.3 (7.3) $^{n-5}$**
VOSP Object Decision (/20)	18.6 (1.9)	**14.3 (4.8) $^{n-3}$**
Musical skills, background and reward responses		
Pitch direction discrimination (/10)	9.1 (1.1) $^{n-2}$	**8.1 (1.5)**
Prior musical expertise (/3)	0.8 (1.0)	0.9 (0.9)
Current music listening (hrs/ week)	6.5 (6.0)	8.3 (6.8)
BMRQ (/32)	25.4 (3.8) $^{n-1}$	24.8 (4.3) $^{n-1}$
Mood scale		
Mood score (/20)	16.7 (4.1)$^{n-1}$	**14.8 (3.0) $^{n-2}$**

Mean (standard deviation) scores are shown unless otherwise indicated; maximum scores are shown after tests (in parentheses). Significant differences ($p < 0.05$) from healthy control values are indicated in bold; reduced number of participants are indicated with n: total number of participants in the bvFTD group; * data from 16 healthy controls.

5.4.2 Implicit valuation of choice and outcome

5.4.2.1 Implicit valuation of choice: reaction times

Group data for reaction times for all three conditions are presented in Table 5.3 and individual data are plotted in Figure 5.4.

There were significant main effects of group ($\chi^2(1) = 8.9$, $p = 0.003$) and condition ($\chi^2(2) = 22.22$, $p < 0.001$) but no significant interaction between group and conditions ($\chi^2(2) = 3.27$, $p = 0.19$). The bvFTD group was significantly slower than healthy controls for choosing the 90% arm ($z=2.07$, $p=0.038$), No significant difference between groups was detected for the arm 50% ($z=1.71$, $p=0.087$) or the arm 10% ($z=0.73$, $p=0.46$). Within-group comparisons between conditions showed that both healthy controls and patients were slower for choosing the 10% arm compared to the time they spent choosing the 90% arm (HC: $z=4.77$, $p<0.001$; bvFTD: $z=2.41$, $p=0.47$). Healthy controls were additionally slower for choosing the 50% arm ($z=3.00$, $p =0.008$) compared to the time they spent choosing the 90% arm. No other differences between conditions were detected for the bvFTD group.

$RT_{pun-rew}$ denote the difference (at a participant level) between averaged reaction times to the 10% arm and averaged reaction times to the 90% arm chord. This metric is considered as a proxy for the implicit valuation of choice or action associated with each arm. In the bvFTD group, $RT_{pun-rew}$ negatively correlated with apathy level ($rho = -0.54$, $p =0.013$). No correlations were found between $RT_{pun-rew}$, scores at the Trail-Making-Test B (time spend executing the task), mood scores or disinhibition levels.

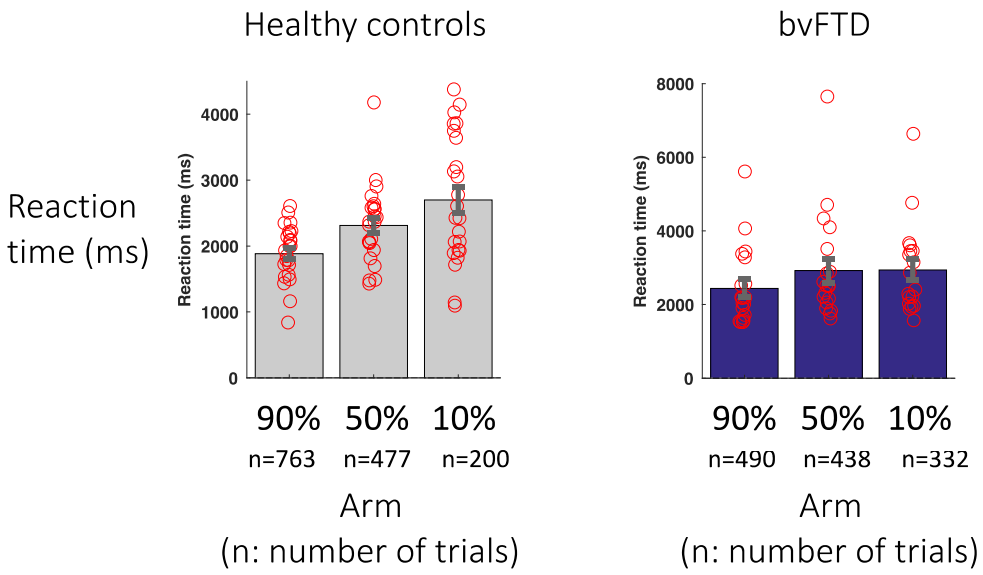

Figure 5.4. Reaction times for participant groups for choosing the 90%, 50% or the 10% arm.

For each participant group, the histograms show mean reaction times for each arm associated with a 90%, 50% or 10% probability of playing an 'expected reward' target chord; red circles are individual data; error bars indicate standard error of the mean. The number of button presses are indicated for each arm.

5.4.2.2 Implicit valuation of outcome: pupil responses to reward and punishment

The healthy control and bvFTD groups did not differ significantly in baseline pupil size (1 sec m before onset of target chord) ($t = -1.38$, $p=0.18$).

Mean times courses of pupillary responses to the target reward chord and the punishment target chord for both participant groups are shown in Figure 5.5.

Permutation analysis showed a significant increase in pupil response to punishment chord compared to reward chord for both healthy controls and bvFTD patients. However, while the divergence occurred 1.2 sec after the target chord onset for healthy controls and lasted for 2.2 sec, the divergence occurred much later for bvFTD patients, 2.1 sec after the target chord onset and lasted only for 0.2 sec. As described in chapter 2, cluster-based permutation tests are unable to provide precise estimates of temporal onset and must be accompanied by further statistical analysis. I thus ran a linear mixed model on the maximum pupil response during the interval [0.5-3sec] after the onset of the target chord. Summary maximum pupillary responses are presented in Table 5.3. There was an effect of type of target chord ($\chi^2(1) = 18.19$, $p < 0.001$) and an interaction of group with type of target chord ($\chi^2(1) = 5.59$, $p = 0.018$) but no overall effect of group ($\chi^2(1) = 3.11$, $p = 0.077$). Within-group comparisons showed that healthy controls had a significantly larger pupil size for the 'punishment' chord compared to the 'reward'

chord (z=4.93, p<0.001) and this difference was significantly larger than the one observed in the bvFTD group (z=2.36, p=0.018). No difference in pupil reactivity to punishment compared to reward chord was identified in the bvFTD group (z=1.28, p=0.19).

$Pupil_{pun\text{-}rew}$ denote the difference (at a participant level) between averaged maximum pupil response to the punishment chord and averaged maximum pupil response to the reward chord. This metric is considered as a proxy for implicit valuation of outcome and is included as a covariate in the linear mixed model looking at choice accuracy.

No significant correlations between $pupil_{pun\text{-}rew}$ and age, gender, reward or mood scores were found in the bvFTD group.

Table 5.3. Summary of reaction times and pupil response profiles for participant groups and conditions

Group	Reward probability or target chord	Reaction time (s)	Maximum pupil response (AU) to target chord
Healthy controls	90% (reward)	1.87 (4.20)	0.43 (0.46)
	50%	2.30 (0.60)	
	10% (punishment)	2.71 (0.97)	0.70 (0.37)
bvFTD	90% (reward)	**2.44 (1.04)**	0.31 (0.43)
	50%	**2.92 (1.41)**	
	10% (punishment)	2.94 (1.22)	0.38 (0.41)

The table shows mean (standard deviation) raw reaction times (average time taken to choose a particular arm) and maximum pupil amplitude in each experimental condition for the healthy control and behavioural variant frontotemporal dementia (bvFTD) groups. Significant differences ($p < 0.05$) from healthy control values are indicated in bold. AU: arbitrary units.

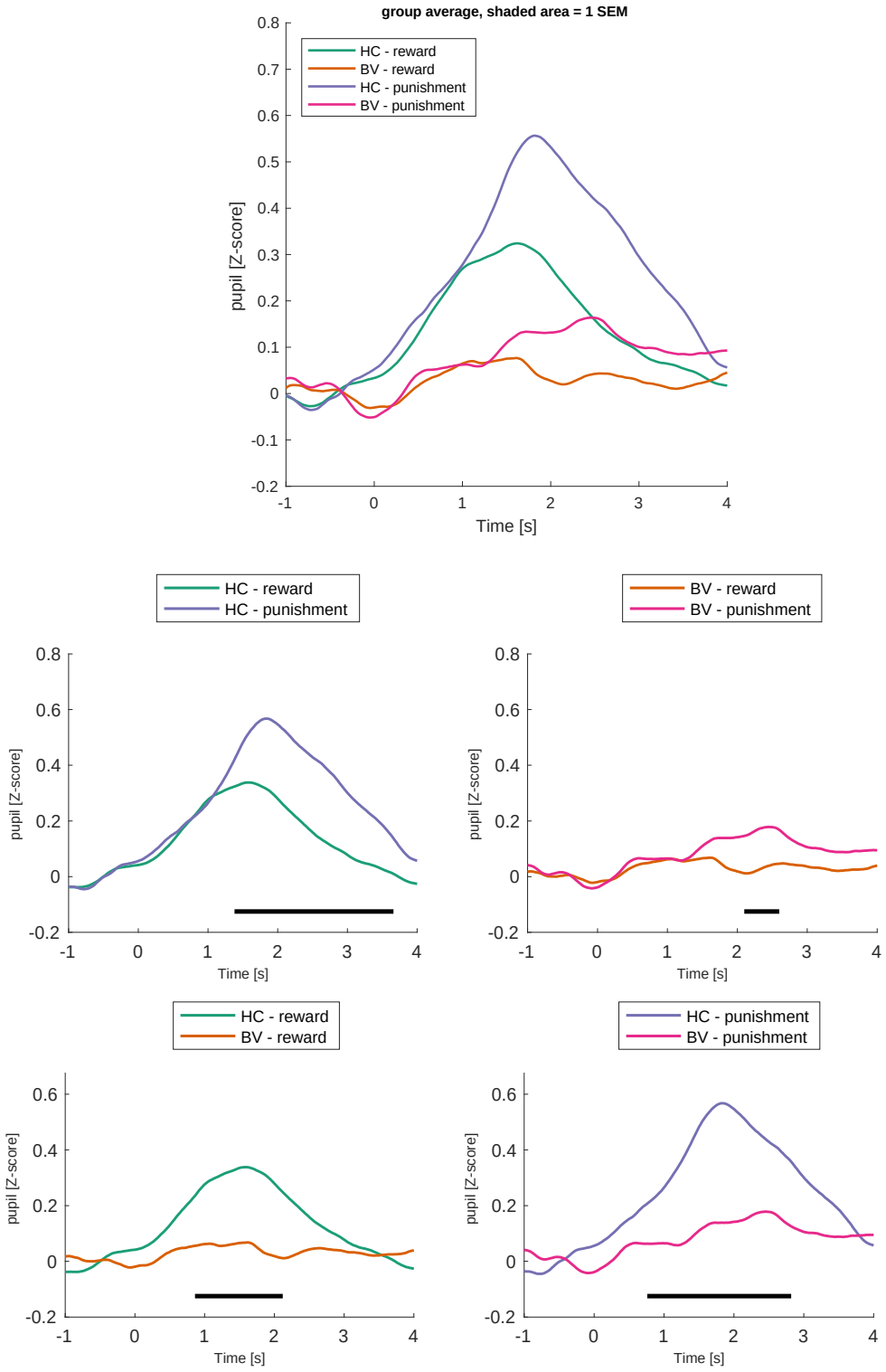

Figure 5.5. Time course of pupil dilatation responses to target chord categories (reward or punishment) for healthy controls and bvFTD patients

Shaded regions around the curves represent standard error in the mean (SEM) estimated with bootstrap resampling (1000 iterations; with replacement). Black horizontal lines represent the time range where timeseries revealed a significant difference after permutation analysis. HC: healthy controls; BV: bvFTD patients.

5.4.3 Choice accuracy

Group data for choice accuracy for all three conditions are presented in Table 5.5; individual data are plotted in Figure 5.6.

When looking at the choice accuracy averaged across conditions taking gender, pitch discrimination score, reaction times, and pupillary reactivity to punishment, bvFTD patients had a significantly lower choice accuracy than healthy controls (t=-3.10, p=0.004).

There were significant main effects of group ($\chi^2(1) = 8.68$, p = 0.003) and condition ($\chi^2(2) = 6.20$, p = 0.04) but no significant interaction between group and condition ($\chi^2(2) = 0.26$, p = 0.88). bvFTD patients were significantly less accurate than healthy controls in choosing the 90% arm in the intermediate reward rate condition (z=-2.42, p=0.016) and in choosing the 50% arm in the low reward rate condition (z=-2.14, p=0.032). Within-group comparisons didn't reveal any significant results when applying Bonferroni correction for multiple comparisons.

After establishing the overall significance of the full model over the null model (likelihood-ration test: ($\chi^2(2) = 10.4$, p = 0.005), the significance of fixed effects included in the mixed model using the likelihood-ratio test (Table 5.4) was tested against reduced models where each effect was dropped. This analysis showed that performance scores were predicted by not only the diagnostic group and the experimental condition (reward rate) but also by the implicit valuation of choice measured with $RT_{pun\text{-}rew}$ and the musical reward score obtained with the BMRQ questionnaire.

In the bvFTD group, the performance score averaged across conditions negatively correlated with scores on the Trail-Making-Test B (time spend executing the task) (rho = -0.60, p =0.02) and BMRQ scores (rho = -0.52, p =0.02) and positively correlated with the performance on WASI Matrices (rho = 0.60, p =0.008). No significant correlations were found for the performance score averaged across conditions and behavioural or psychiatric symptoms. When looking at correlations of separate scores for each condition, significant correlations with WASI matrices were only found for the intermediate reward rate condition (rho = -0.50, p =0.03) and correlations with Trail-Making-Test B scores were only found for the low reward rate condition (rho = -0.53, p =0.04). Moreover, correlations with performance score for the low reward rate condition negatively correlated with the level of ritualistic and compulsive behavioural changes reported by the caregiver (rho =-0.51, p =0.03). No correlations

(of averaged performance or separate performance) were found with age, gender, musical expertise, mood scores, pitch discrimination score, hearing threshold or symptom duration.

Table 5.4. Effect of different fixed-effect predictors on the likelihood of the linear mixed effect model

Fixed-Effect Predictor	Deviance	p
Gender	2.31	0.31
Pitch screen discrimination score	5.60	0.061
BMRQ score	5.97	0.050
Implicit valuation of choice ($RT_{pun-rew}$)	11.11	0.004
Implicit valuation of outcome ($pupil_{pun-rew}$)	-2.49	1.0

Deviance here refers to twice the difference in log-likelihood between the full model and a restricted model with the effect omitted. Significance of individual fixed effects was determined using the likelihood-ratio test after a full-null model comparison.

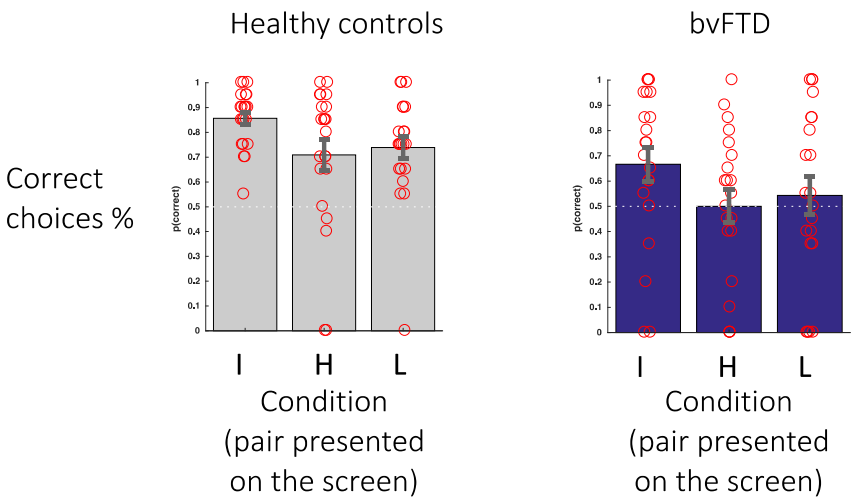

Figure 5.6. Histograms showing mean choice accuracy (%) for participant groups and experimental conditions

Red circles are individual data; error bars indicate standard error of the mean. I: intermediate reward rate; H: high reward rate; L: low reward rate.

Table 5.5. Summary of choice accuracy for participant groups and conditions

Group	Condition	Accuracy (%)	Between-groups	Between conditions	
			bvFTD	High reward rate	Low reward rate
Healthy controls	Intermediate reward rate	0.86 (0.11)	**-0.27 [-0.47 -0.07] p = 0.007**	**-0.18 [-0.36 0.00] p = 0.050**	-0.18 [-0.36 0.001] p = 0.052
	High reward rate	0.71 (0.28)	**-0.26 [-0.45 -0.06] p= 0.011**		0.00 [-0.18 0.02] p = 1.0
	Low reward rate	0.75 (0.21)	-0.17 [-0.37 0.02] p = 0.087		
bvFTD	Intermediate reward rate	0.67 (0.31)		-0.16 [-0.36 0.03] p = 0.147	-0.08 [-0.28 0.012] p = 1.0
	High reward rate	0.49 (0.30)			0.08 [-0.11 0.29] p = 0.93
	Low reward rate	0.55 (0.35)			

The table shows mean (standard deviation) accuracy rate for each experimental condition for the healthy control and behavioural variant frontotemporal dementia (bvFTD) groups. Significant differences ($p<0.05$) are indicated in bold.

5.4.4 Neuroanatomical associations

Significant grey matter associations of choice accuracy and implicit ratings of reward and punishment chords are summarised in Table 5.6; statistical parametric maps of these associations are presented in Figure 5.7. All associations here are reported thresholded at $p<0.05$ after FWE correction for multiple voxel-wise comparisons within pre-specified anatomical regions of interest.

Choice accuracy correlated with regional grey matter in an extended biliateral network comprising the right precuneus and parahippocampal gyrus and the left medial orbitofrontal cortex and supramarginal gyrus.

$RT_{pun-rew}$ correlated with regional grey matter in the right precuneus and anterior insula. $Pupil_{pun-rew}$ correlated with regional grey matter in the right supramarginal gyrus.

Table 5.6. Neuroanatomical correlates of choice accuracy and valuation of choice ($RT_{pun-rew}$) and outcome ($Pupil_{pun-rew}$)

Condition	Region	Side	Cluster (voxels)	Peak (mm)			T score	P_{FWE}
				x	y	z		
Choice accuracy								
Intermediate reward	Precuneus	R	487	16	-64	38	5.53	0.009
	Frontopolar cortex	L	54	-15	32	-27	5.04	0.017
	Parahippocampal gyrus	R	51	24	-42	-4	5.03	0.006
	Supramarginal gyrus	L	955	-63	-48	26	4.76	0.026
Valuation of choice and outcome								
$RT_{pun-rew}$	Precuneus	R	298	22	-60	8	5.96	0.005
	Anterior insula	R	61	34	-24	9	5.69	0.004
$Pupil_{pun-rew}$	Supramarginal gyrus	R	353	58	-33	36	5.54	0.010

The table presents the results of the voxel-based morphometry analysis. Shown are the locations of regional grey matter positively associated with choice accuracy and with the valuation of choice and outcome measured with reaction times and pupillometry respectively. Coordinates of local maxima are in standard MNI space. P values were all significant ($p<0.05$) after family-wise error (FWE) correction for multiple voxel-wise comparisons within pre-specified anatomical regions of interest. $RT_{pun-rew}$: difference in reaction times to the 90% arm compared to the 10% arm; $Pupil_{pun-rew}$: difference in maximum pupil response to punishment chord compared to reward chord.

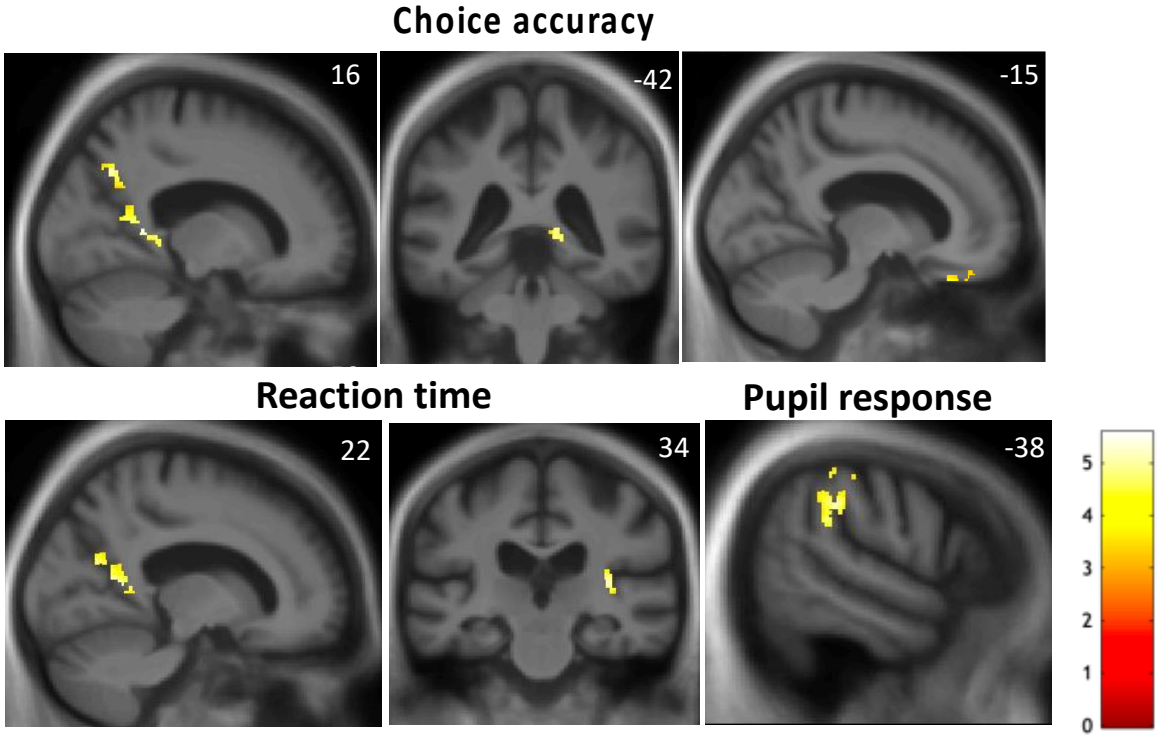

Figure 5.7. Neuroanatomical correlates of choice accuracy and valuation of choices and outcome (measured with reaction times and pupillometry)

Statistical parametric maps (SPMs) show regional grey matter volume positively associated with choice accuracy, $RT_{pun-rew}$ (the difference in reaction times to the 90% arm compared to the 10% arm) and $pupil_{pun-rew}$ (difference in maximum pupil response to punishment chord compared to reward chord) based on voxel-based morphometry of participant' brain MR images. SPMs are thresholded for display purposes at $p < 0.001$ uncorrected over the whole brain, however, local maxima of areas shown were each significant at $p < 0.05$ after family-wise error correction for multiple voxel-wise comparisons within pre-specified anatomical regions of interest; the MNI coordinate (mm) of the plane of each section is indicated.

5.5 Discussion

Here I have shown, using a classical exploration-exploitation paradigm with musical stimuli, that bvFTD patients were less accurate at exploiting or choosing the best option than healthy controls and that this impairment did not depend on the environmental reward rate. The exploration-exploitation profiles in healthy controls and bvFTD patients were predicted by the implicit valuation of actions, an indirect measure of motivated action, but not by the implicit valuation of action's outcome (musical stimuli), an indirect measure of the sensitivity to punishment and reward. Moreover, both measures of motivated action and sensitivity to punishment were reduced in bvFTD compared to healthy controls. Choice accuracy in the bvFTD cohort correlated with psychometric measures of cognitive flexibility and ritualistic and compulsive behavioural changes. Finally, each processing stage involved in this paradigm (see Figure 5.1) had separable but partly overlapping neuroanatomical correlates comprising dorsal and ventral attention networks previously implicated in exploration-exploitation decision-making processes and additional regions involved in processing of aversive information (Daw *et al.*, 2006; Hoefer *et al.*, 2008; Palminteri *et al.*, 2012; Laureiro-Martínez *et al.*, 2015; Perry *et al.*, 2015; Pessiglione and Delgado, 2015; Murty *et al.*, 2016).

In line with my two previous chapters and with a substantial number of other studies, autonomic sensitivity to reward versus punishment, triggered via congruent or incongruent chord target relative to a musical prime, was significantly reduced in bvFTD compared to controls and extends the evidence for central autonomic dysregulation in these syndromes (Femminella *et al.*, 2014; Joshi *et al.*, 2014, Fletcher *et al.*, 2015*b*; Joshi *et al.*, 2017; Ahmed *et al.*, 2018, Marshall *et al.*, 2018*b*, 2019). This result also replicates previous studies of reward processing which have shown a reduced sensitivity to different types of aversive stimuli: their behavioural responses to pain and temperature were blunted in this syndrome (Fletcher et al., 2015), their behavioural, physiological, and self-reported experiential responses to a disgust-eliciting movie were all reduced compared to controls (Eckart et al., 2012), their physiological response to aversive unexpected white noise bursts during a fear-conditioning task was blunted (Hoefer et al., 2008). At a socio-emotional level, bvFTD patients generally have difficulty recognising negative emotions (Goodkind et al., 2015) and they are generally less prone to detect negative valence signals in social contexts (Grossman et al., 2010). Deficiency in autonomic reactivity has raised important questions about the extent to which interoceptive function is responsible for emotional processing, theory-of-mind ability and reward processing (Fletcher *et al.*, 2015*b*, Marshall *et al.*, 2018*b*, *a*). Indeed, the

'embodied mind' theory juxtaposed with the active inference suggests that both intact somatosensory signals and correct interpretation of bodily states are required to form an accurate representation of the future action via internal motor simulations. While my paradigm did not allow me to disentangle raw autonomic reactivity from interpretation of this internal signal, it is nevertheless interesting to note that pupil response, used here as a surrogate for the individual's valuation of outcome (see Figure 5.1) did not significantly predict performance in choosing the best option. On the other hand, Perry *et al.* (2017) showed that impaired choice performance could principally been explained by a lower autonomic reactivity (skin conductance) during anticipation of punishment (in this case, an aversive smell). These alternative results could be explained by the use of a different autonomic modality and the analysis of a different time window (anticipation vs consumption).

On the contrary, performance score was predicted by reaction times, used here as an indirect measure of individual's valuation of choice (see Figure 5.1). Healthy controls were significantly slower at choosing the arm with the highest punishment probability than the two other arms with higher reward probability. This result confirms the evidence of a close coupling of reward with 'go' (or invigoration) and punishment with 'no-go' (inhibition) as is also seen during instrumental conditioning paradigms (McNaughton, 1982). Moreover, the study by Guitart-Masip *et al.* (2011) which orthogonalized subjective valence of outcome (or sensitivity to outcome) and go/no-go actions showed that action dominates sensitivity to outcome via the dopaminergic system in the substantia nigra and the ventral tegmental area and the release of dopamine. The typical impaired performance at the go-no go task for patients with bvFTD (Slachevsky *et al.*, 2004; Hughes *et al.*, 2015) could thus be related to the atrophy of dopaminergic structures (mainly in mesolimbic forebrain) and/or abnormal deployment of dopamine through dysfunction of the relevant circuitry (Rowe *et al.*, 2008; Cools and D'Esposito, 2011; Murley and Rowe, 2018). In active inference terms, dopamine has been re-formulated as a key modulator of the precision assigned to higher-order states, such as action states, in opposition to the precision allocated to sensory input. Apathy, a common behavioural change in FTD, has been linked to deficits in the precision of the action-outcome mapping, i.e. in the precision of predicting how action can change the current sensory state (Hezemans *et al.*, 2020). Reduced reaction time differentiation of punishment and reward correlated with levels of apathy in bvFTD which supports the hypothesis of a reduced allocation of precision to action value, possibly due to an abnormal dopaminergic system. It is important to note that changes in other neurotransmitter systems, notably GABA, also commonly observed in bvFTD (Murley *et al.*, 2020; Murley and Rowe, 2018), are also responsible for changes in

precision-weighting (Moran *et al.*, 2013) and contribute to apathy even in the case of relatively normal dopaminergic function.

This study did not reveal any significant effect of environment reward rate on the ability to choose the right option. Based on Gershman, 2015 who proposed that learning is more efficient when the average reward rate is low than when the average reward rate is high, I expected a similar asymmetry in performance between the low and high reward rate conditions, and more specifically, a better performance in low reward rate conditions. This result would have confirmed the loss-aversion bias, a widespread theory in decision-making which postulates that humans (but also other animal species) are more strongly motivated to avoid potential losses than to achieve potential gains (Kahneman and Tversky, 1979). This would be the result of a valuation bias that overweighs losses relative to gains or, as an alternative view, to a response bias to avoid choices involving potential loss or punishment (Tversky and Simonson, 1993). Under this theory, a larger discrepancy between values in outcome or choices would be more easily achieved in a low reward rate environment while the two alternative choices in a high reward rate environment would carry a similar weight and halt the decision-making process. The absence of environment reward rate modulation on performance may also signal a fundamental difference between musical and other types of outcomes: music is quite asymmetric in its hedonic charge and, unlike musical reward that can sometimes simulate strong biological rewards, the extent to which music can mimic biological or monetary punishment is questionable. Although not significantly different to the other two conditions, it is important to highlight the performance level of bvFTD patients in environments with high reward rate which was below chance level. This 'random' decision-making process, when faced with options with similar reward values, reinforces the evidence of a generalized impairment in cognitive flexibility and response inhibition in bvFTD syndrome (Libon *et al.*, 2007; Hornberger *et al.*, 2008; Ramanan *et al.*, 2017). It may also imply a reverse valuation occurring for certain bvFTD patients showing a systematic choice for the 'punishment' arm, resembling other 'bifurcations' of auditory or more biological hedonic behaviours seen in this syndrome (Fletcher *et al.*, 2015*a*).

Choice accuracy rate, sensitivity to punishment measured with pupillometry and differential reaction times to action cues correlated with an extended grey matter network which overlapped in the right precuneus and the bilateral supramarginal gyrus. The supramarginal gyrus (SMG), according to the theory of attention developed by (Corbetta and Shulman, 2002), would be responsible for the reorientation of attention when unexpected stimuli are detected. Contrary to the salience network, the SMG would solely be activated in response

to relevant stimuli rather than salient stimuli (that could be contextually irrelevant and source of distraction), i.e. related to goals or expectations driven by contextual cues. In particular, it would allow the dorsal attention network encompassing superior posterior parietal cortex and dorsal frontal cortex to switch to another state more appropriate for the new environmental situation (Corbetta and Shulman, 2002; Laureiro-Martínez *et al.*, 2015). In addition, the ventral attention network would also be closely synchronised with the locus-coeruleus norepinephrine system, itself directly correlated with pupillary responses (Aston-Jones and Cohen, 2005; Corbetta *et al.*, 2008; Joshi *et al.*, 2016). Indeed, the SMG was found as a functional neural correlate of the pupillary reactivity to aversive stimuli (mild electric shock) during a fear-conditioning paradigm with simultaneous fMRI and pupillometry (Leuchs *et al.*, 2017).

Another key region of the attentional network is the frontopolar cortex which was found to correlate with a better choice accuracy in the intermediate reward rate environment. Exerting a top-down control over attention, this region, similarly to the SMG would bias attention in favour of 'higher-level' goals in the case of unsatisfactory results and constrain the decision to the relevant options. Such top-down attentional control is crucial to switch from an explorative to an exploitative behaviour or vice versa (Daw *et al.*, 2006; Laureiro-Martínez *et al.*, 2015) since it requires inhibition of the current choice to search and select alternative choices, i.e. a certain cognitive flexibility that ultimately leads to a refined selection and an optimised behaviour during exploitation. Beyond the ventral attentional system, the medial temporal lobe is also crucial in reorienting attention due to its central role in encoding surprising events. The parahippocampal gyrus, also found to correlate with higher performance at choosing the best option, would facilitate the encoding of information associated with punishments (Murty *et al.*, 2012, 2016; Schwarze *et al.*, 2012; Bauch *et al.*, 2014), disambiguate surprising stimuli as threats and trigger a new motivational state: avoidance. It is interesting to note that these neuroanatomical correlates were only found for the intermediate reward condition where exploitative behaviour (highest choice accuracy rate) was observed in both groups. In this condition, unlike in the other two conditions where performance was extremely variable, top-down control over attention coupled with valuation of punishment as threat led to efficient avoidance behaviour.

Another key region involved in processing aversive event was the anterior insula which was found to correlate with choice valuation (reaction times). The anterior insula, along with the amygdala and the dorsomedial PFC, is part of the 'aversive network', as proposed by Pessiglione and Delgado (2015). Some consensus has emerged about some specific neural representation of net value (reward vs punishment) with common findings

in fMRI studies showing a negative correlation with net value with anterior insula (and sometimes amygdala) (reviewed in Bartra *et al.*, 2013) and lesion-studies demonstrating that patients with glioma affecting the anterior insula were impaired in punishment-based learning but not reward-based learning (Palminteri *et al.*, 2012). VBM studies have additionally associated this region with the ability to distinguish the valence of pleasant or unpleasant stimuli, from smell (Perry *et al.*, 2017) to noise (Hoefer *et al.*, 2008) to taste (Small, 2010). This suggests a role for this area in processing aversive information and may be related to its role in passing interoceptive signals to the striatum and anterior cingulate cortex to generate an appropriate behavioural response.

The clinical implications of my study are promising. When correlating choice accuracy scores to psychometric scores, a strong correlation was observed with metrics specifically related to executive function (WASI matrices) and cognitive flexibility (Trail-Making-Test B which requires the participant to constantly re-evaluate the instructions and switch between two tasks). In addition, a significant correlation was found between decreased performance at making the right choice and reported score of heightened compulsive and ritualistic behaviours often manifesting as hoarding, collecting, sorting, inflexible grooming or walking routines, and strict timekeeping. This last result is particularly interesting since it draws for the first time a direct link between cognitive deficits linked to cognitive flexibility and a major behavioural change associated with bvFTD pathology. Behavioural disturbances reported by caregivers include disinhibition, compulsive behaviour, stereotypical behaviour, perseveration, and environmental-dependency symptoms such as imitation or utilization behaviour (Johnen 2019). These behaviours could all represent different facets of the same problem related to decision-making. Yet, studies investigating behaviour alterations in bvFTD have mainly focused on cognitive or social functioning deficits and there is a lack of a paradigm unifying the bewildering array of behavioural difficulties that bvFTD patients exhibit. Experimental paradigms systematically testing decision-making in an environment mimicking the real-world (i.e. comprising reward and punishment) could provide a new model for understanding these symptoms.

In this study, I have shown that a classical multi-armed bandit problem, designed to test the ability to switch from exploration to exploitative behaviours, could be used to detect very specific cognitive and behavioural disturbances linked to cognitive flexibility. Moreover, I related these deficits to a particular network of regions involved in attentional control and encoding of aversive information. Lastly, I showed that the difficulty bvFTD patients encountered switching from an explorative to an exploitative behaviour was more likely to be the result of a deficit in evaluating choice options than a deficit in evaluating punishing stimuli.

One obvious limitation of this study is the lack of subjective ratings of the musical stimuli. As my previous chapters showed at multiple occasions, autonomic blunting can be associated with preserved cognitive valuation and vice-versa. Thus, in principle, pupil reactivity to reward and punishment cannot fully account for the 'value' assigned to reward and punishment. It is yet important to note that in the decision-making field, value to reward and punishment is most commonly measured with the functional activity of specific brain networks (Pessiglione and Delgado, 2015) which also differs from a direct account of subjective valence. Another potentially complicating factor in my study is altered decoding of music as a perceptual and affective signal in patients with bvFTD. Another limitation of my study is the reliance upon bvFTD 'normal' processing of music. Changes in sound processing including musicophilia, music aversion or general misophonia are often reported by caregivers (Fletcher *et al.*, 2015). Although I did not collect reports of these behaviours here, I attempted to capture altered engagement with music with the BMRQ questionnaire. Finally, this study only looked at averaged data across trials and participants, and while I have extrapolated information about distinct stages involved in reward-based decision-making, the study design did not enable the direct estimation of evolution or learning parameters per se. A trial-by-trial analysis would certainly be more adapted to respond to specific questions about dynamic encoding of information and dynamic action selection. Computational modelling enables such a trial-by-trial estimation and the next chapter will describe the implementation of two of these models.

6 Computational modelling of learning dynamics in a musical reinforcement-learning paradigm

6.1 Chapter summary

In this chapter, I used two computational models to draw inferences on the way bvFTD pathology disrupts mechanisms of learning, decision-making and reward processing. The first model demonstrated both a reduced sensitivity to reward and punishment and a higher stochasticity in the conversion of action values into action probabilities. Reduced sensitivity to outcome in the low reward environment correlated with grey matter atrophy in the left supramarginal gyrus and the left putamen, necessary for both an efficient allocation of attention when unexpected stimuli are detected and the deployment of an avoidance behaviour during action selection. While this first model allowed me to investigate the stages of reward processing affected by bvFTD pathology, the second model directly addressed the question of a potential asymmetrical learning rate for reward and punishment. It showed that bvFTD patients had a significantly lower learning rate in response to punishment compared to healthy controls but a preserved learning rate in response to reward. Differential learning rates in the low reward environment correlated with grey matter atrophy in the left supramarginal gyrus and the right angular gyrus. Finally, the sensitivity to outcome extracted from the first model and the negative learning rate extracted from the second model correlated with behavioural changes observed in bvFTD related to empathy and theory-of-mind. This chapter shows the utility of assessing learning dynamics with the help of computational models for identifying the abnormal aspect of reward-based goal-directed behaviours in bvFTD. In particular, it suggests that the use of music within a reinforcement learning setting could provide a powerful paradigm to identify impairments of social cognition in bvFTD.

6.2 Introduction

In the previous chapter, I used classic statistical methods and investigated how variables averaged across the whole experiment differed between bvFTD patients and healthy controls. I derived indirect measures of different mechanisms involved during reward-based decision-making, by using pupil responses as a surrogate of the valuation of outcome and reaction times as a surrogate of the valuation of choices. There are however alternative methods for investigating these stages of reward processing, which make use of computational modelling drawing on classic mathematical models designed to theorise learning in animals and human beings.

The previous chapter posed many unresolved questions. For instance, does blunted autonomic reactivity to reward and punishment necessarily induce an inability to compute a reward prediction error? Indeed, as I demonstrated in the previous chapters, pathology can provoke a dissociation between cognitive and autonomic reactivity to the same stimulus which, in this study, leaves open the question of how autonomic function relates to the internal state of choosing an action based on how much 'surprise' the previous action generated. Similarly, does a lack of differentiation in response times to different cues indicate that the agent didn't learn the value of the available choices or does it reflect an inability to deploy motivation or effort to initiate an action? Indeed, this cost-benefit computation is usually separated from the action-value representation in the traditional formulation of goal-directed behaviour and has even been shown to recruit different neural structures (Klein-Flügge *et al.*, 2016; Hauser *et al.*, 2017; Pessiglione *et al.*, 2018).

A way to draw a clear distinction between the different processes involved in reward-based decision-making is to derive hidden variables from observable measures, i.e. from actions and outcomes (Figure 6.1). One mathematical formulation which allows such a derivation is based on a Markov decision processes which assumes the person (or agent) exists in a series of 'states' where they can exert actions. These actions may lead to reward or punishment, but at each iteration, an action necessarily engenders a change of state. The goal of an agent is to iteratively improve the state she is in by tracking the net reward value of an action. This mapping from states to actions is known as a policy. The agent, in orders to maximise rewards, must find the optimal policy. This type of reinforcement learning algorithm has been shown to act as an excellent model of human behaviour, at both a behavioural and neural level (O'Doherty *et al.*, 2003; Pessiglione *et al.*, 2006; Schultz, 2016).

While it is been widely used to explain behavioural disturbances in Huntington's disease (HD) and Parkinson's disease (PD) (Pessiglione *et al.*, 2006; Bódi *et al.*, 2009; Palminteri *et al.*, 2009; Rutledge *et al.*, 2009; Voon *et al.*, 2011; McCoy *et al.*, 2019), no studies have investigated mechanisms underlying reinforcement learning in bvFTD patients. In particular, behavioural changes such as apathy, compulsive behaviour, novelty-seeking behaviour and perseveration have been the focus of attention in HD and PD, establishing a direct link between dopaminergic depletion in the basal ganglia and certain stages of learning and decision-making. Indeed, pathologies of striatum and its dopaminergic innervation have served as a valuable lesion model on which to elaborate theoretical accounts of human reinforcement learning (Frank, 2006). In bvFTD, low levels of dopamine have been found in the putaman, caudate and substantia nigra (Nagaoka *et al.*, 1995; Rinne *et al.*, 2002). Degeneration of dopaminergic tracts, in addition to extrapyramidal motor features, has been thought to

contribute to behavioural symptoms such as aggression, agitation and psychosis often seen in bvFTD, especially when caused by genetic mutations (Engelborghs *et al.*, 2008), and dopaminergic medication has been shown to reduce risk-taking behaviour (Rahman *et al.*, 2006) and irritability (Moretti *et al.*, 2003). However, serotonin dysfunction in bvFTD makes a significantly larger contribution to the behavioural and cognitive symptoms (Huey *et al.*, 2006; Hughes *et al.*, 2015) including aggressivity, impulsivity, increased appetite and depression. Controlled assessments have shown that serotonin reuptake inhibitor medication reduces disinhibition, irritability, depression (Herrmann *et al.*, 2012) and inappropriate sexual behaviour (Anneser *et al.*, 2007). Serotonin, as opposed to dopamine, is considered as the transporter regulating the 'highest brain functions' related to cognitive control, learning, emotion regulation and social cognition (Canli and Lesch, 2007). Computational models have represented the differential roles of dopamine and serotonin in the basal ganglia within the framework of reinforcement learning and proposed that dopamine responds to appetitive stimuli while serotonin responds to aversive stimuli (Daw *et al.*, 2002; Dayan and Huys, 2008; Balasubramani *et al.*, 2014) (although the theory of serotonin acting as an aversive counterpart to dopamine has since raised some challenges yet to be confirmed (Dayan and Huys, 2015). Although bvFTD constitute a more complex model than PD or HD due to the dysfunction of numerous interacting neurotransmitters, the need to find a theoretical framework capable of bridging neurotransmitter systems, grey matter destruction, and behavioural disturbances, is pressing.

In this study, I addressed this gap in the literature and explore the relationship between grey matter atrophy and key 'hidden' parameters involved during reward-based decision-making. I used two reinforcement learning models to estimate the trial-by-trial variation of different parameters driving 'state evolution' and 'policy' in healthy controls and bvFTD patients. My first model drew on the previous chapter and attempted to make a clear distinction between reinforcement learning stages (reward prediction error (RPE) representation and action value representation) and action selection. My second model drew on current hypotheses about the effect of bvFTD pathology on sensitivity to punishment and avoidance behaviour (Rahman *et al.*, 1999; Torralva *et al.*, 2007; Perry *et al.*, 2017) and notably, the role of the habenula in encoding punishment (Hikosaka *et al.*, 2008; Hikosaka, 2010; Lawson *et al.*, 2014), as a primary region targeted by bvFTD pathology (Bocchetta *et al.*, 2016). I fitted model parameters to each participant's behavioural data, accommodating trial-by-trial fluctuations in response to feedback given (reward or punishment) based on that participant's choices, and determined which of these parameter values better accounted for variation in behavioural performance between the bvFTD and healthy control groups. I correlated these parameters to specific neuropsychological and neuropsychiatric scores

obtained during neuropsychological and clinical assessments of patients. Structural neuroanatomical associations of the model parameters were assessed using VBM on participants' brain MR images.

Based on my previous chapter and the literature looking at reward processing in bvFTD patients, I hypothesized that both reinforcement learning (internal representations) and action selection (mapping representations to actions) would be impaired in bvFTD with a specific reduction in the sensitivity to punishment (Perry and Kramer, 2015; Perry *et al.*, 2017). I also expected a lower learning rate in response to punishment compared to the learning rate in response to reward as suggested by increased risk-taking behaviours in this syndrome (Snowden *et al.*, 2001; Rahman *et al.*, 2006; Torralva *et al.*, 2007; Strenziok *et al.*, 2011; Perry *et al.*, 2015; see Table 5.1). I hypothesized that both sensitivity to punishment and negative learning rate would be associated with behavioural changes related to disinhibition and social conduct (Snowden *et al.*, 2001; Perry *et al.*, 2015, p. 20). Finally, I hypothesized that the fitted learning parameters would correlate with neuroanatomical structures specialized in processing aversive events (dorsal striatum, anterior insula: Palminteri *et al.*, 2012)Palminteri et al., 2012) and in attention reorientation (ventral and dorsal parietal regions: Corbetta and Shulman, 2002).

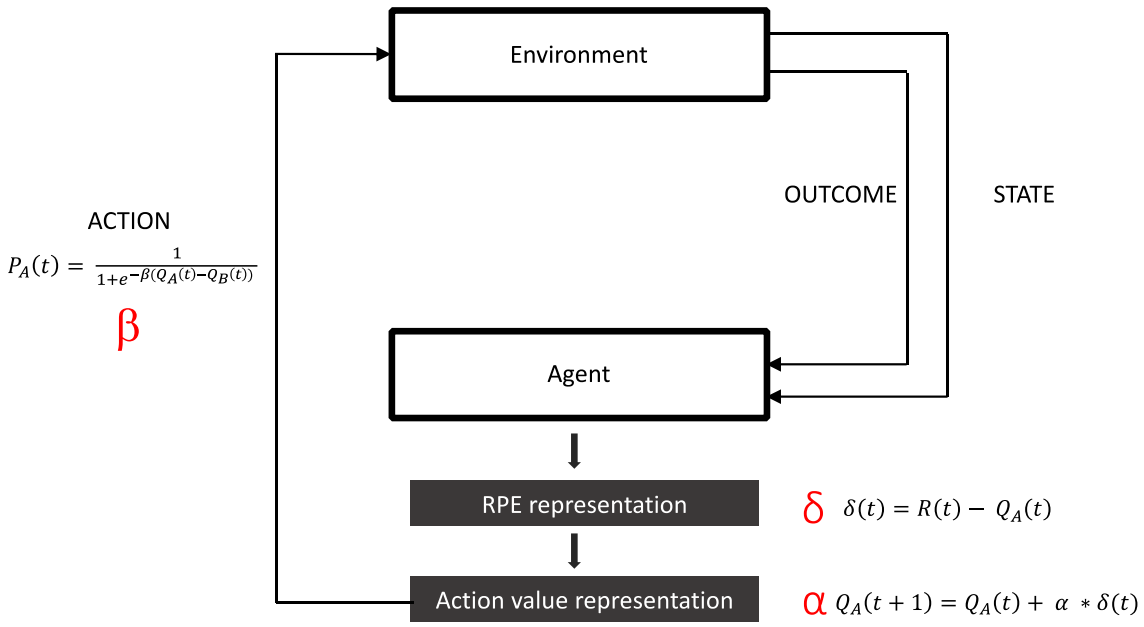

Figure 6.1. Computational process during reinforcement learning

The equations refer to the evolution functions of the Q-learning model and the observation softmax function chosen here to model learning and action selection (see main text). δ is the reward prediction error (RPE), α the learning rate and β the inverse temperature. These parameters can then be fitted to individual participants' trial-by-trial data in order to disentangle participant's performance on different 'hidden' stages of learning, decision-making and reward processing.

6.3 Material and methods

6.3.1 Participants

The participant cohort was the same as described in Chapter 5. Please refer to Table 5.1 for demographic, clinical and general neuropsychological characteristics of participant groups.

6.3.2 Experimental design and stimuli

Please refer to Chapter 5 for the experimental design and synthesis of stimuli.

6.3.3 Experimental procedure

Please refer to Chapter 5 for details about the procedure.

6.3.4 Computational modelling: reinforcement learning paradigm

The reinforcement learning (RL) framework has been widely applied in learning and decision-making studies, in healthy and in clinical populations. It describes how an agent uses feedback from the external environment to inform future actions based on the assignment of internal values to previous actions. Typically, an agent's action that leads to positive feedback is reinforced and likely to be repeated while an action that leads to negative feedback will decrease the likelihood of a similar action in the future. Classic experimental RL paradigms, by mimicking the uncertain environment we live in, generate probabilistic relations between choice options and feedback. In my design, the action-feedback association had three probability distributions with an average reward rate of 90%, 50% and 10% (see previous chapter for description of the experimental paradigm). RL models typically consist of two components: the internal learning and evaluation process and a function translating these internal evaluations into actions. The most widely used evaluation model is the Q-learning model and the most popular action-selection function is the softmax choice rule.

6.3.4.1 The evolution equation: Q-learning model

The Q-learning model is derived from the Rescorla-Wagner rule and quantifies the extent to which an outcome drives the updating of values. In other words, it assumes that the evaluation of a choice option is modified according to the difference between the expected outcome and the actual outcome, called the prediction error. For each pair of cues (the Agathodaimon symbols in our paradigm), the model estimates the value of the two options, Q_A and Q_B. After each trial t, the value of the chosen cue is updated according to the rule:

$$Q_A(t+1) = Q_A(t) + \alpha * \delta(t)$$

δ refers to the prediction error and is formulated as follows:

$$\delta(t) = R(t) - Q_A(t)$$

with R(t) corresponding to the outcome of choosing A (+1 if the outcome is a reward and -1 if it is a punishment) at trial t and α referring to the learning rate. α, in simple terms, quantifies the extent to which the prediction error influences the value update: the higher α is, the stronger the weighting of the prediction error for the value update. In general, it is a surrogate for the speed of learning. However, it also depicts the carry over outcome weight (the cumulative weight of each trial's outcome). A high learning rate thus leads to quicker value updating but oversensitivity to the most recent outcomes, whereas when the learning rate is low, both recent and past outcomes contribute to the value update (Zhang *et al.*, 2020). R(t) can either be fixed or free. Where it is a free parameter, it is termed the reinforcement learning magnitude and its variation reflects how sensitive an agent is to the outcome.

6.3.4.2 The observation equation: softmax choice rule

After values are updated with the prediction error, the next step is to use these values to inform the choice on the next trial. This value-choice mapping (from internal states to actions) is described by the Softmax choice rule (Sutton and Barto, 2018):

$$P_A(t) = \frac{e^{Q_A(t)/\beta}}{e^{Q_A(t)/\beta} + e^{Q_B(t)/\beta}}$$

In other words, it converts action values Q_A and Q_B into action probabilities P_A and P_B: the higher the value of A, the more likely A will be chosen. The softmax function is more commonly simplified as a logistic curve (sigmoid function):

$$P_A(t) = \frac{1}{1 + e^{-\beta(Q_A(t) - Q_B(t))}}$$

with the input as the value difference Q_A - Q_B and the output as the probability P_A. β is the slope of the sigmoid curve which measures choice consistency. β is thus denoted the inverse temperature parameter (term directly extracted from thermodynamics referring to stochasticity of systems). When β is small, the curve is shallow which denotes more random choices while when it is large, the curve is steep and represents more consistent choices.

6.3.4.3 Parameter estimation

The evolution and observation functions together constitute the generative model (a model of the conditional probability of the observed data given certain parameters values). The next step is to invert this model in order to 'fit' the model to the observed data. In other words, we need to determine the values of the free parameters that make the model behave as similarly to the real participant as possible. There are multiple ways to do so and I present below two approaches that I chose for my two models. The first one is the simplest approach and is useful to understand how different parameters interact, while the other one greatly speeds up model fitting and better translates the complexity of the environment.

6.3.4.3.1 Grid search

The aim of the grid search is to find the optimal values that maximise the probability of the observed data given the generative model: p(data|model). This quantity is known as the likelihood of the data and is defined as follows: p(data|model) = $P_{A, t1} * P_{A, t12} * P_{A, t3}$ ..... $P_{A, tn}$ with n the number of trials. These probabilities can be predicted using the evolution and observation functions. To do a grid search of the parameter space, one must first define a range of parameter values for each parameter, and compute for values within this range the probability of the observed responses $P_{A, t1}$, $P_{A, t2}$ etc. Then one must check which set of values explains the data best by finding the maximum of the marginal likelihood (likelihood when one parameter is kept free and the two others constant). The range of parameter values were set as follows: [0:40:1] for α, [0:50:25] for β and [0:50:2] for R based on usual practice (Wilson and Collins, n.d.; Palminteri *et al.*, 2012; Zhang *et al.*, 2020). The grid search approach is conceptually simple and easy to implement. However, since the likelihood of the data needs to be calculated for each single value within this range, the computational cost of the grid search is high. The variational Bayesian approach is one of the multiple ways to constrain parameters and reduce the risk of computational explosion.

6.3.4.3.2 Variational Bayesian approach

The generative model in the variational Bayesian approach is different from the one used in the grid search in the following ways (Daunizeau *et al.*, 2014):

1) it incorporates a state and measurement noise in the evolution and observation functions
2) the statistical behaviour of the initial conditions, the free parameters and the state/measurement noise are approximated by Gaussian prior densities

3) Gamma priors are used on the precision of the state and measurement noise

In simple terms, the generative model used here, despite having the same evolution and observation functions as for the grid search, now describes a stochastic nonlinear state-space model (as a set of input, output and state variables related by differential equations) with the inclusion of priors on state and observation noise distributions. The inversion of this model requires the use of variational approach to deal with nonlinearities: it rests on maximising a free-energy lower bound of the model evidence by minimising the Kullback-Leibler divergence between the approximate posterior density (under Laplace approximation) and the exact posterior density for a particular parameter p(parameter|y, m) with y the observations and m the generative model. The main advantage of this approach is that it is much less computationally costly. More importantly, by including a stochastic term in the model, it takes into account unknown parameters that might have influenced the participants' behaviour. In translating the complexity of the environment, it has generally better performance than more deterministic models

6.3.4.4 Model validation

In order to examine how well the model predicted the data, one must run model validation. There are multiple ways to do so. In this chapter, I chose to compute the coefficient of determination which corresponds to the fraction of explained variance and is formulated as follows: R^2 = max (0, 1 – SS2_err / SS2_tot) with SS2_err corresponding to the sum of squares of errors (the residual sum of squares):

$$SS2_{err} = \sum_{k=0}^{n} (y_k - \widehat{y_k})^2$$

and SS2_tot the explained sum of squares:

$$SS2_{tot} = \sum_{k=0}^{n} (y_k - \bar{y})^2$$

with y_k the observed values, $\widehat{y_k}$ the predicted values of y, $\overline{y_k}$ the average value of y and n the number of trials. In the case of stationary data, y_k would be approaching the average value $\bar{y}$ which would lead to an increased SS2_err / SS2_tot ratio. $SS2_{err}$ is, in this case, a more appropriate measure of model goodness-of-fit as it quantifies the discrepancy between observed and predicted data. In this chapter, I thus report both the R^2 and $SS2_{err}$ averaged across each participant group.

6.3.5 Analysis of fitted parameters

6.3.5.1 Model 1

The first model I applied to the data is a complementary analysis to the analysis described in Chapter 5. The previous chapter showed to what extent the implicit rating of reward and punishment drove the overall choice accuracy at participant level. As explained in the introduction, the RL model quantifies how this sensitivity drives the updating of values of cues at both participant and trial level. Furthermore, extending the first analysis, it also quantifies how much an agent is able to make use of the prediction error to drive learning (informed by the learning rate α) and to translate it into actions (informed by the observation parameter β). I ran this model three times for each participant, corresponding to the three reward rates (high, intermediate and low) conditions (see section 5.4 on experimental procedure). This first model had three free parameters: the learning rate α, the reinforcement learning magnitude R and the inverse temperature β. I used the grid search approach to invert the generative model.

A t-test was first used to assess any difference between the two participants groups in the fitted free parameters averaged across the three conditions. A restricted maximum likelihood mixed effects model, with participant identity as a random effect, was then used to investigate between-group and within-group comparisons. Joint Wald tests of the relevant coefficients were used to examine the main effects of diagnostic group and experimental condition (reward rate) and their interaction on the response variables. Post hoc pairwise group comparisons with Bonferroni correction were performed where main effects were found. To take account of potentially confounding factors affecting learning parameters, age, gender, pitch discrimination, musical expertise and BMRQ scores were included as nuisance covariates.

In addition, Spearman's rho was used to separately assess any correlation of performance scores and free parameter estimates with age, gender, prior musical expertise, peripheral hearing function, pitch direction discrimination score, auditory working memory (indexed as reverse digit span), executive function (WASI Matrices*),* and duration of symptoms. In addition, in the patient group only, Spearman's correlations were used to separately assess any association with scores assessing behavioural changes linked to reward processing, i.e. disinhibition, apathy, ritualistic/compulsive behaviour, humour processing, hyperorality, hypersexuality, and depression. This time, I also looked at correlations with empathy scores derived from ratings provided by each patient's primary caregiver during the clinical assessment and from the validated modified Interpersonal

Reactivity Index (mIRI) (Davis, 1983) questionnaire. Indeed, there is a growing evidence of a direct link between classic learning signals and empathy-related brain responses (Zaki, 2014; Hein *et al.*, 2016; Lockwood *et al.*, 2016). Moreover, if we consider music as 'mimicking' social signals (a well-known 'anthropologic' theory of music (Clark et al., 2014)), in this experiment, the ability to make associations between musical reward and punishment to visual cues could be seen as proxies for deriving social cues from non-verbal cues (Lima et al., 2016), a prerequisite for empathy.

Finally, in order to draw a link with the previous chapter, I looked at correlations between fitted parameters and the implicit valuation of choices ($RT_{pun-rew}$) and implicit valuation of outcome ($pupil_{pun-rew}$).

A threshold $p<0.05$ was accepted as the criterion of statistical significance for all tests.

6.3.5.2 Model 2

The second model leveraged my main hypothesis on bvFTD patients: i.e., impaired learning from aversive events. The asymmetric Q-learning model implemented by the VBA toolbox (Daunizeau *et al.*, 2014) captures the possibility of some asymmetry in the behavioural response to reward and punishment due to different learning rates α_{pos} and α_{neg}. I ran this model three times for each participant, , corresponding to the three environmental conditions (see section 5.4 on experimental procedure).

This second model had three different free parameters: a positive learning rate α_{pos}, a negative learning rate α_{neg} and the inverse temperature β. I used a variational Bayesian approach to invert the generative model.

A t-test was first used to assess any difference between the two participants groups in the fitted free parameters averaged across the three conditions. A restricted maximum likelihood mixed effects model, with participant identity as a random effect, combined positive and negative learning rates obtained for each experimental condition. Joint Wald tests of the relevant coefficients were used to examine the main effects of diagnostic group and experimental condition (reward rate and type of learning rate) and their interaction on the response variables. Post hoc pairwise group comparisons with Bonferroni correction were performed where main effects were found.

Spearman correlation analysis was also conducted to assess any associations with the same range of neuropsychometric and neurobehavioural or psychiatric symptoms described for Model 1. Finally, I also looked at correlations between fitted parameters from Model 1 and fitted parameters from Model 2.

6.3.6 Neuroanatomical associations

For 18 bvFTD patients and 13 healthy control participants, T1-weighted volumetric brain MR images were acquired and preprocessed for entry into a VBM analysis as described in Chapter 2.

In the VBM analysis, full factorial linear regression models were used to assess associations between regional grey matter volume (indexed as voxel intensity) separately with the free parameters from each model in the three conditions, i.e. reinforcement learning magnitude, inverse temperature and overall learning rate from Model 1 and the difference between positive learning rate and negative learning rate from Model 2. Age, total intracranial volume and pitch direction score were incorporated as covariates of no interest. Statistical parametric maps of regional grey matter associations were assessed at threshold $p<0.05$ after FWE correction for multiple voxel-wise comparisons within the pre-specified anatomical regions of interest described in Chapter 5.

6.4 Results

6.4.1 Model 1

6.4.1.1 Model validation

Goodness-of-fit parameters for each condition and each diagnostic group are displayed in Table 6.1. There was no significant difference in coefficient of determination nor in residual sum of squares between diagnostic groups (R^2: high reward rate: t = 0.11, p = 0.91; intermediate reward rate: t = -0.15, p = 0.88; low reward rate: t = -0.21, p = 0.83) (SS2_err: high reward rate: t = -0.09 , p = 0.93; intermediate reward rate: t = 0.14, p = 0.89; low reward rate: t = -0.25, p = 0.80).

6.4.1.2 Evolution parameters

Group data for evolution parameters for all three conditions are presented in Table 6.1; predicted and observed learning curves are plotted in Figure 6.2.

When looking at the evolution fitted parameters averaged across conditions, bvFTD patients had a significantly lower reinforcement learning magnitude compared to healthy controls ($t=-6.16$, $p<0.001$) while the difference in learning rate between diagnostic groups was non-significant ($t=0.11$, $p=0.91$).

In the combined mixed model assessing the reinforcement learning magnitude parameter, there were strong significant effects of group ($\chi^2(1) = 39.15$, $p < 0.001$), condition ($\chi^2(2) = 39.78$, $p < 0.001$) and the interaction between group and condition ($\chi^2(2) = 21.87$, $p < 0.001$). The bvFTD group had a significantly lower

reinforcement magnitude in both high (z=-3.30, p=0.001) and low reward rate environments (z=-7.54, p<0.001) compared to controls. No such difference was seen in the intermediate reward rate condition (z=-1.71, p=0.09). Furthermore, within-group comparisons between conditions showed that healthy controls had a higher reinforcement magnitude in the low reward rate environment compared to both the intermediate reward rate environment (z=5.61, p<0.001) and the high reward rate environment (z=6.99, p<0.001). On the contrary, bvFTD patients had a higher reinforcement magnitude in the intermediate reward rate environment compared to the high reward rate environment (z=2.90, p=0.011).

The mixed model applied to learning rates was not significant ($\chi^2(9) = 13.5$, p =0.14). No further investigations were conducted.

For the bvFTD patient group, the reinforcement magnitude averaged across conditions positively correlated with mIRI scores (rho=0.64, p=0.007), a surrogate for empathy and theory-of-mind abilities. No other significant correlations were found between the evolution parameters averaged across conditions and demographic parameters, symptom duration, psychometric measures of executive function or auditory working memory, musical expertise, peripheral hearing function, pitch direction discrimination score or other neurobehavioural or psychiatric symptoms related to reward processing.

Significant correlations were found between the reinforcement learning magnitude parameter and $pupil_{pun\text{-}rew}$ (rho = 0.37, p = 0.01) and $RT_{pun\text{-}rew}$ (rho = 0.31, p = 0.04) but none with learning rates and $pupil_{pun\text{-}rew}$ or $RT_{pun\text{-}rew}$.

6.4.1.3 Observation parameter

When looking at the observation fitted parameters averaged across conditions, there was a main effect of diagnostic group (t=-3.43, p=0.001). In the combined mixed model, there was a main effect of group ($\chi^2(1) = 10.24$, p = 0.001) but no effect of conditions ($\chi^2(2) = 4.91$, p = 0.08) nor an interaction between group and conditions ($\chi^2(2) = 0.21$, p = 0.90). The bvFTD group had a significantly lower inverse temperature than the healthy control group in both high (z=-1.97, p=0.049) and low reward rate environments (z=-2.40, p=0.02). No such difference was seen in the intermediate reward rate condition (z=-1.83, p=0.07).

No significant correlations were found between the fitted observation parameter averaged across conditions in bvFTD patients and demographic parameters, psychometric scores, neurobehavioural or psychiatric symptoms. However, significant correlations were found between the inverse temperature and $RT_{pun-rew}$ (rho = 0.36, p = 0.02).

Table 6.1. Summary of Model 1 parameters for participant groups and conditions

Group	Condition	Goodness-of-fit		Fitted parameters		
		R^2	SS2_err	Learning rate	Inverse temperature	Reinforcement magnitude
Healthy controls	Intermediate reward rate	0.14 (0.22)	3.20 (3.14)	0.40 (0.17)	12.17 (3.65)	0.47 (0.15)
	High reward rate	0.13 (0.23)	4.17 (3.14)	0.40 (0.16)	10.51 (5.63)	0.40 (0.23)
	Low reward rate	0.05 (0.11)	3.93 (2.93)	0.39 (0.20)	11.60 (4.60)	0.88 (0.37)
bvFTD	Intermediate reward rate	0.15 (0.23)	3.06 (3.22)	0.29 (0.13)	10.60 (6.02)	0.40 (0.25)
	High reward rate	0.12 (0.24)	4.25 (2.97)	0.46 (0.19)	**6.20 (5.20)**	**0.12 (0.10)**
	Low reward rate	0.06 (0.11)	4.06 (1.59)	0.41 (0.19)	**7.59 (5.39)**	**0.27 (0.21)**

The table shows mean (standard deviation) goodness-of-fit parameters and learning fitted parameters obtained with Model 1. Values in bold indicate significant difference with the healthy control group ($p<0.05$). R^2: coefficient of determination; SS2_err: residual sum of squares between observed and predicted values.

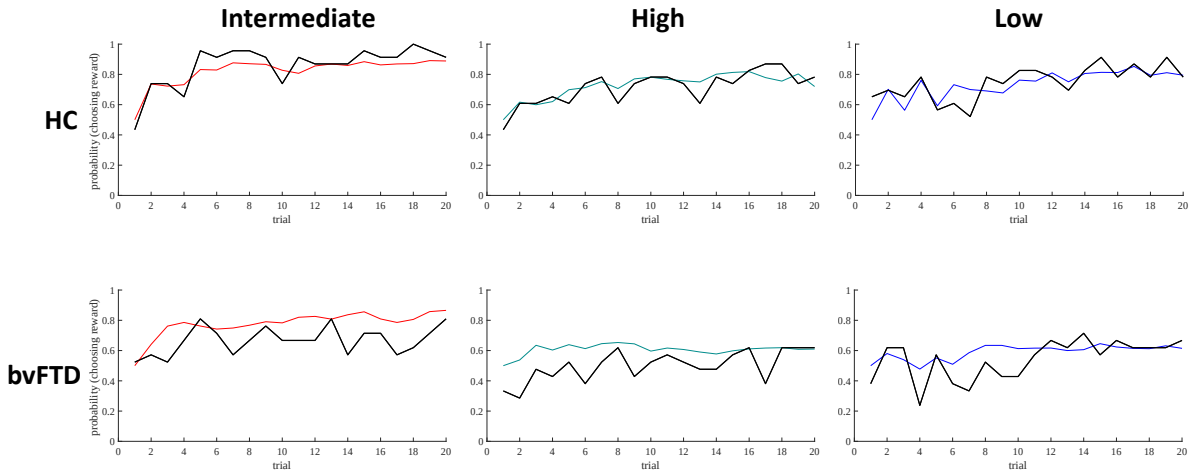

Figure 6.2. Observed and fitted learning curves with Model 1 for each diagnostic group and each reward rate condition

The black curve indicates the observed performance at choosing the best option for each trial (averaged across participants). The coloured curve (flanked by error envelopes representing the standard deviation of the group performance) is the modelled probability of choosing the best option for each trial (averaged across participants). Intermediate: intermediate reward rate condition (90% vs 10%); High: high reward rate condition(90% vs 50%); Low: low reward rate condition (50% vs 10%).

6.4.1.4 Neuroanatomical associations

Significant grey matter associations of fitted parameters with Model 1 are summarised in Table 6.2; statistical parametric maps of these associations are presented in Figure 6.3. All associations here are reported thresholded at p<0.05 after FWE correction for multiple voxel-wise comparisons within pre-specified anatomical regions of interest.

In the combined participant cohort, reinforcement learning magnitude in the low reward rate correlated with regional grey matter in the left supramarginal gyrus and dorsal striatum (putamen). No other correlations survived FWE corrections at the prescribed threshold in the two other conditions.

Table 6.2. Neuroanatomical correlates of the fitted reinforcement magnitude parameter obtained with Model 1 in the combined participant cohort

Condition	Region	Side	Cluster (voxels)	Peak (mm)			T score	P_{FWE}
				x	y	z		
Reinforcement magnitude								
Low reward rate	Supramarginal gyrus	L	145	-58	-46	45	5.27	0.009
	Putamen	L	71	-30	-12	0	4.61	0.015

The table presents the results of the voxel-based morphometry analysis. Shown are the locations of regional grey matter positively associated with higher reinforcement magnitude. Coordinates of local maxima are in standard MNI space. P values were all significant (p<0.05) after family-wise error (FWE) correction for multiple voxel-wise comparisons within pre-specified anatomical regions of interest.

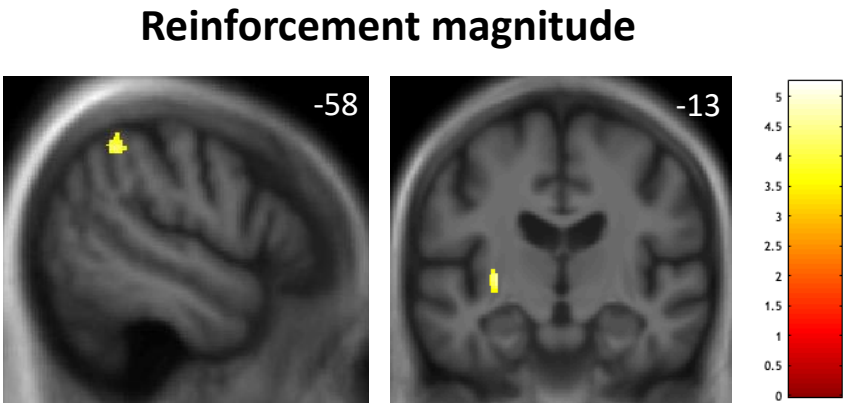

Figure 6.3. Neuroanatomical correlates of the fitted reinforcement learning magnitude parameter

Statistical parametric maps (SPMs) show regional grey matter volume positively associated with reinforcement magnitude parameter in the combined study cohort, based on voxel-based morphometry of participants' brain MR images. SPMs are thresholded for display purposes at p < 0.001 uncorrected over the whole brain, however, local maxima of areas shown were each significant at p < 0.05 after family-wise error correction for multiple voxel-wise comparisons within pre-specified anatomical regions of interest (see chapter 5); the MNI coordinate (mm) of the plane of each section is indicated.

6.4.2 Model 2

6.4.2.1 Model validation

Goodness-of-fit parameters for each condition and each diagnostic group are displayed in Table 6.3. There was no significant difference in coefficient of determination nor in residual sum of squares between diagnostic groups (R^2: high reward rate: t = -1.66 , p = 0.10; intermediate reward rate: t = -2.37, p = 0.07; low reward rate: t = -1.55 , p = 0.13) (SS2_err: high reward rate: t = 0.47, p = 0.64; intermediate reward rate: t = 1.52, p = 0.14; low reward rate: : t = 0.85 , p = 0.40).

6.4.2.2 Evolution parameters

Group data for evolution parameters for all three conditions are presented in Table 6.3; predicted and observed learning curves are plotted in Figure 6.4.

When looking at the evolution fitted parameters averaged across conditions, bvFTD patients had a significantly lower negative learning rate compared to healthy controls (t=-2.06, p=0.041) while the difference between diagnostic groups for the positive learning rate was non-significant (t=0.75, p=0.46).

In the combined mixed linear model, there was a strong significant effect of condition ($\chi^2(5) = 27.1$, $p < 0.001$) but no effect of group ($\chi^2(1) = 2.19$, $p = 0.14$) nor interaction between group and condition ($\chi^2(5) = 4.11$, $p = 0.43$). Within-group comparisons between conditions showed that healthy controls had a significantly lower negative learning rate compared to the positive learning rate in the low reward rate environment (z=-2.87, p=0.024). On the other hand, the bvFTD group had a significantly lower negative than positive learning rate in the high reward rate environment (z=-3.53, p<0.001).

For the bvFTD patient group, the negative learning rate averaged across conditions positively correlated with mIRI scores (rho=0.56, p=0.03), a surrogate for empathy and theory-of-mind abilities. On the other hand, the positive learning rate averaged across conditions positively correlated with a reported loss of empathy (rho = 0.61, p=0.007), altered sense of humour (rho=0.62, p=0.006) and hypersexuality (rho = 0.50, p =0.03). No other significant correlations were found between negative or positive learning rates and demographic measures, psychometric scores, musical abilities, symptom duration or measures of other behavioural and psychiatric symptoms related to reward processing. No significant correlation was found between negative or positive learning rates and $pupil_{pun\text{-}rew}$ or $RT_{pun\text{-}rew}$ found in the previous chapter.

6.4.2.3 Observation parameter

When looking at the observation fitted parameters averaged across conditions there wasn't any effect of diagnostic group (t=-0.32, p=0.19). Moreover, the mixed model applied to this fitted parameter was not significant ($\chi^2(9) = 15.32$, p =0.08). No further investigations were conducted.

Table 6.3. Summary of Model 2 parameters for participant groups and conditions

Group	Condition	Goodness-of-fit		Fitted parameters		
		R^2	SS2_err	Positive learning rate	Negative learning rate	Inverse temperature
Healthy controls	Intermediate reward rate	0.22 (0.24)	1.75 (1.31)	0.49 (0.12)	0.47 (0.13)	5.05 (2.70)
	High reward rate	0.17 (0.24)	2.21 (1.80)	0.43 (0.17)	0.40 (0.17)	6.08 (3.83)
	Low reward rate	0.11 (0.14)	2.82 (1.67)	0.53 (0.11)	0.38 (0.19)	5.53 (3.85)
bvFTD	Intermediate reward rate	0.08 (0.14)	2.57 (2.17)	0.44 (0.13)	0.38 (0.15)	5.33 (5.06)
	High reward rate	0.07 (0.15)	2.50 (2.19)	0.47 (0.15)	0.30 (0.25)	7. 48 (5.75)
	Low reward rate	0.05 (0.12)	3.29 (1.97)	0.49 (0.14)	0.37 (0.19)	4.27 (4.01)

The table shows mean (standard deviation) goodness-of-fit parameters and learning fitted parameters obtained with Model 2. Values in bold indicate significant difference with the healthy control group (p<0.05). R^2: coefficient of determination; SS2_err: residual sum of squares between observed and predicted values.

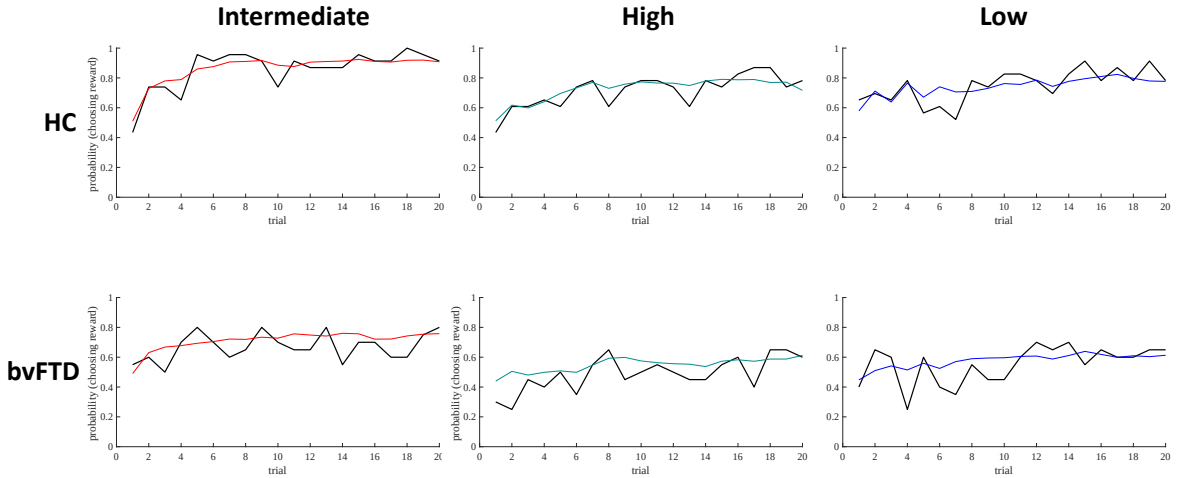

Figure 6.4. Observed and fitted learning curves with Model 2 for each diagnostic group and each reward rate condition

The black curve indicates the observed performance at choosing the best option for each trial (averaged across participants). The coloured curve (flanked by error envelopes representing the standard deviation of the group performance) is the modelled probability of choosing the best option for each trial (averaged across participants). Intermediate: intermediate reward rate condition (90% vs 10%); High: high reward rate condition(90% vs 50%); Low: low reward rate condition (50% vs 10%).

6.4.2.4 Neuroanatomical associations

Significant grey matter associations of fitted parameters with Model 2 are summarised in Table 6.4; statistical parametric maps of these associations are presented in Figure 6.5. All associations here are reported thresholded at p<0.05 after FWE correction for multiple voxel-wise comparisons within pre-specified anatomical regions of interest.

In the combined participant cohort, the difference between the positive and the negative learning rate in the low reward rate correlated with regional grey matter in the left supramarginal gyrus and the right angular gyrus. No other correlations survived FWE corrections at the prescribed threshold in the two other conditions.

Table 6.4. Neuroanatomical correlates of the differential value comparing positive and negative learning rates in the combined participant cohort

Condition	Region	Side	Cluster (voxels)	Peak (mm)			T score	P_{FWE}
				x	y	z		
[Positive learning rate – negative learning rate]								
Low reward rate	Supramarginal gyrus	L	69	-46	-42	26	5.32	0.012
	Angular gyrus	R	25	42	-60	39	5.14	0.021

The table presents the results of the voxel-based morphometry analysis. Shown are the locations of regional grey matter positively associated with a larger difference between the positive learning rate and the negative learning rate in the low reward rate environment. Coordinates of local maxima are in standard MNI space. P values were all significant (p<0.05) after family-wise error (FWE) correction for multiple voxel-wise comparisons within pre-specified anatomical regions of interest.

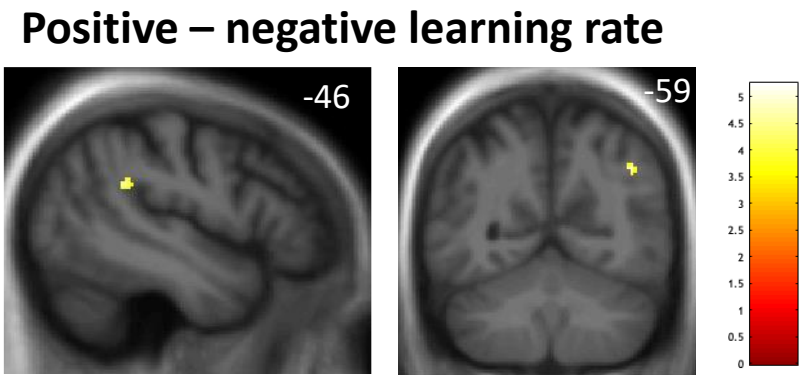

Figure 6.5. Neuroanatomical correlates of the fitted reinforcement magnitude parameter

Statistical parametric maps (SPMs) show regional grey matter volume positively associated with reinforcement magnitude parameter , based on voxel-based morphometry of participants' brain MR images. SPMs are thresholded for display purposes at p < 0.001 uncorrected over the whole brain, however, local maxima of areas shown were each significant at p < 0.05 after family-wise error correction for multiple voxel-wise comparisons within pre-specified anatomical regions of interest (see chapter 5); the MNI coordinate (mm) of the plane of each section is indicated.

6.4.3 Comparisons of Model 1 and Model 2

While Model 1 showed a significantly lower observation parameter in bvFTD patients compared to healthy controls, no significant different was found for the observation parameter in Model 2.

The Model 2 negative learning rate averaged across conditions was positively correlated to the Model 1 reinforcement learning magnitude averaged across conditions (rho=0.57, p=0.008), the Model 1 learning rate averaged across conditions (rho=0.53, p=0.01) and the Model 1 inverse temperature (rho=0.66 p=0.001). No significant correlations were found between Model 1 parameters and the Model 2 positive learning rate.

6.5 Discussion

In this chapter, I used two computational models to investigate how different the hidden stages of learning and action selection were between healthy controls and bvFTD patients during a musical reward-based decision-making paradigm. Results are summarised in Figure 6.6. The two models were designed to investigate different questions: while the first model attempted to distinguish at which stages of reward-based decision-making breakdown occurred, the second model drew on the hypothesis of a specific impairment of bvFTD patients in learning from aversive events. The first model demonstrated both a reduced sensitivity to reward and punishment and a higher stochasticity in the conversion of action values into action probabilities in patients with bvFTD. Reduced sensitivity to outcome in the low reward environment correlated with grey matter atrophy in the left supramarginal gyrus and the left putamen, necessary for both an efficient allocation of attention when unexpected stimuli are detected and the deployment of an avoidance behaviour during action selection. While this first model allowed me to investigate the stages of reward processing potentially affected by bvFTD pathology, the second model directly addressed the question of the asymmetrical learning rate for positive and negative outcomes. It showed that bvFTD patients had a significantly lower learning rate in response to punishment (negative learning rate) compared to healthy controls but a preserved learning rate in response to reward (positive learning rate). The negative learning rate correlated with all three evolution and observation parameters obtained with the first model. Differential learning rates in the low reward environment correlated with grey matter atrophy in the left supramarginal gyrus and the right angular gyrus. Finally, sensitivity to outcome and negative learning rates correlated with key behavioural changes observed in bvFTD related to empathy and theory-of-mind while positive learning rates correlated with positive symptoms related to social conduct.

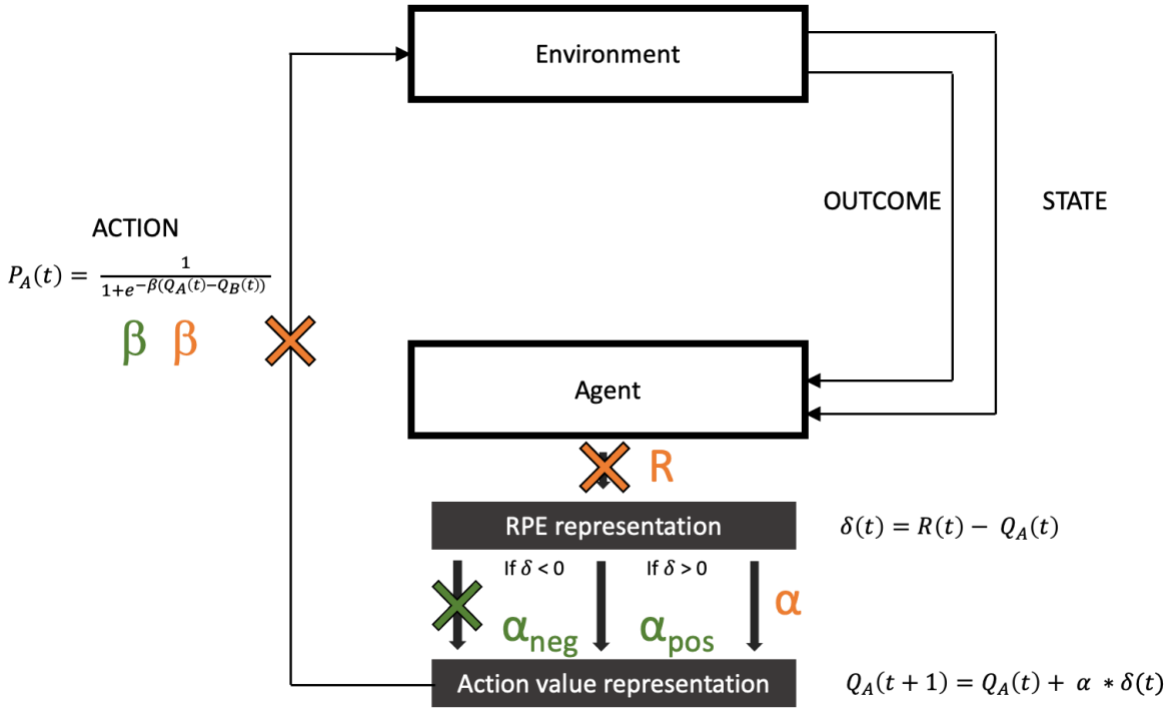

Figure 6.6. Updating of Figure 6.1 including findings from Models 1 and 2

The equations refer to the evolution functions of the Q-learning model and the observation softmax function chosen here to model learning and action selection (see main text). δ is the reward prediction error (RPE), R is the reinforcement learning magnitude, α the learning rate, α_{pos} and α_{neg} the positive and negative learning rates respectively, and β the inverse temperature. Orange symbols refer to parameters included in Model 1 while green symbols are parameters included in Model 2. Significant differences in parameters between healthy controls and bvFTD patients are highlighted with crosses.

In healthy controls, a higher reinforcement learning magnitude was found in the low reward environment compared to environments with higher reward rates. The reinforcement learning magnitude measures how much impact the outcome of an action, independently of its valence (reward or punishment), has on the RPE which itself drives learning through the updating of action values (see Figure 6.5). The higher this impact, the higher the difference between the actual outcome and the expected outcome, i.e. the higher the RPE. In the majority of RL models, the absolute value of RPE is commonly used as a proxy for the agent's surprise (Pulcu, 2019). Similarly, Model 2 revealed a higher learning rate to positive reward prediction error (RPE) than to negative RPE in the low reward environment. These results suggest that learning occurred more efficiently in environments with low reward rate and corroborate the well-known 'loss aversion' theory which posits that punishment more strongly influences motivated action and faster learning than reward does (Kahneman and Tversky, 1979; Baumeister *et al.*, 2001). Furthermore, healthy controls displayed an optimal adaptation to noisy environments, i.e. in low and high reward rate environments which included comparable reward probabilities and thus increased expected level of uncertainty (90% vs 50% or 50% vs 10%). As proposed by recent theories of affective bias (Browning *et*

al., 2015; Pulcu and Browning, 2017; Pulcu, 2019), optimal learning in noisy environments (with higher expected levels of uncertainty) relies on the ability of the learner to discount high RPE (or high levels of surprise) as these wouldn't be informative of the future state of the environment. Learning rates were stable across all conditions which suggests that healthy controls were able to weight the high RPEs induced by low and high reward rate conditions down.

On the contrary, bvFTD patients displayed less consistent learning than healthy controls. Reinforcement learning magnitudes (or sensitivity to outcome) were significantly lower than healthy controls in the 'noisy' environments. However, they showed a retained sensitivity to outcome in the intermediate reward rate environment, which corresponded to the situation where one cue had a high probability of delivering reward and the other had a high probability of delivering punishment, i.e. the 'polarised' condition with the lowest uncertainty level. This suggests that bvFTD patients are more likely to react to reward or punishment in a structured and binarized environment and tend to discard 'salient' cues in noisier environments inducing dysfunctional learning. This over-reliance on environmental noise (or uncertainty) in bvFTD patients is reminiscent of my results described in Chapter 3 and 4 which demonstrated that patients with bvFTD have a significant impairment in detecting unexpected events at both a cognitive and an autonomic level but a retained sensitivity to the environment's entropy level (uncertainty).

Complementing Model 1, the computational model 2 looked at the bias in learning rates for positive or negative prediction errors. According to the Rescorla-Wagner rule, the action values are updated after each trial depending on the RPE, i.e. the difference between the actual reward and the expected reward. Differential learning rates with two learning rates depending on the sign of the RPE were introduced after studies showed that positive and negative feedback were processed by separate neural structures (Frank *et al.*, 2007) Such asymmetric RL models have notably been used to explain risk-seeking/aversion behaviours (Niv *et al.*, 2012): risk aversion would be related to larger learning rate in response to negative RPE than for positive RPE while the opposite would predict risk-taking behaviours. Increased risk-taking behaviours is commonly observed in bvFTD: patients typically overspend (Chiong *et al.*, 2014), make risky monetary gambles and seek monetary gain more than avoid monetary loss (Rahman *et al.*, 1999; Torralva *et al.*, 2007). The question whether bvFTD pathology leads to an aberrant seeking of reward or a loss of sensitivity to punishment is still open. Perry et al., (2017) systematically investigated this question using olfactory stimuli and showed that bvFTD patients were less successful at avoiding unpleasant smells than obtaining pleasant smells because their prior experience and

anticipation of aversive smells was not sufficiently 'punishing' to motivate the extra effort required (pressing a button as quickly as possible). This selective deficit for processing negative stimuli is underpinned by the selective atrophy pattern seen in bvFTD, which targets reward circuitry and in particular a region specialised in the processing of aversive information called the habenula (Ullsperger and Cramon, 2003; Hikosaka, 2010; Lawson *et al.*, 2014). In one large FTD cohort, the habenula showed the largest reduction in volume compared with controls among all the cortical and subcortical regions involved in reward processing (Bocchetta *et al.*, 2016). Here, I substantiated these observations by showing a significantly lower learning rate in response to punishment in the bvFTD group compared to controls while the learning rate in response to reward was the same in both groups. Moreover, while healthy controls learned more rapidly from reward than from punishment in the low reward rate environment, bvFTD patients learned better from reward than from punishment in the high reward rate environment. This last result adds to the evidence of an inefficient optimisation of behaviour in the case of noisy environments described in the previous paragraph: the RPEs associated with punishment in the high reward rate environment, the largest because of the relative 'scarcity' of punishment in this condition, failed to update action values and ultimately failed to guide an optimised behaviour in patients with bvFTD.

Both the reinforcement magnitude parameter (averaged across conditions and in the low reward rate condition) and the negative learning rate (averaged across conditions and in the low reward rate condition) were shown to correlate with a combined score assessing perspective-taking (the ability to adopt the psychological view of others) and empathic concern (feelings of sympathy and concern for unfortunate others) (Davis, 1983). These free parameters did not correlate with any other psychometric measures of executive function, musical expertise, working memory or other behavioural and neuropsychiatric traits related to reward processing. Interestingly, the positive learning rate averaged across conditions only correlated with the so-called positive symptoms which, contrary to negative symptoms related to lack of empathy or social withdrawal, induce the emergence of additional behaviours, in this case, altered sense of humour and hypersexuality.

In my attempt to draw a parallel with my previous chapter and classic methods of trial summary statistics, I found an association between the reinforcement magnitude parameter and both the implicit valuation of outcomes measured with pupillometry and the implicit valuation of choices measured with response times. On the other hand, the inverse temperature (a measure of choice consistency) was only associated with the implicit valuation of choices measured with response times which confirms that this observation parameter is related to a specific stage of reward-based decision making, i.e. the mapping of values into actions. These results legitimise

the use of response times and pupillometry as relatively sensitive measures of different processes involved during reward-based decision-making. The comparison between Model 1 and Model 2 showed that the negative learning rate of model 2 is a mixed measure of all three fitted parameters found in Model 1 comprising sensitivity, learning rate and inverse temperature, suggesting that a redundancy and overlap between all three altered distinct processes identified with the first model could in fact be summarised with the alteration of a single process, i.e. learning from aversive events. The common practice in computational modelling is to pit models against one another to decide on the 'winning model', balancing each model's goodness-of-fit and its generalizability to new datasets (Zhang *et al.*, 2020). Further analysis needs to be conducted in order to identify the model which best explains bvFTD patients' data.

From Model 1, reinforcement magnitude in the low reward rate environment correlated with grey matter correlates in the left supramarginal gyrus and the left putamen. From Model 2, the same left supramarginal gryus (SMG) with the additional right angular gyrus were found as neuroanatomical correlates of a larger differential value between positive and negative learning rates in the low reward rate environment.

As discussed in the previous chapter, the SMG has been shown to be involved in attention control (Corbetta and Shulman, 2002). We can argue that this control was especially important in the low reward rate condition where punishment outcome was common and where an efficient attention reorientation was required to constrain the decision to an optimised 'compromise'. SMG is involved in a wide range of sensory-motor processes notably required for 'enactment' which refers to the facilitating effect of encoding by performing actions (Russ *et al.*, 2003) and more generally involved in action execution, simulation, and observation (Grèzes and Decety, 2001). The right angular gyrus is consistently considered as the key hub of the classic 'theory-of-mind' (ToM) network comprising the middle temporal gyrus, the precuneus and the medial prefrontal cortex (Schurz et al., 2014). The SMG has in fact also been proposed to be involved in theory-of-mind processing. Wiesmann et al. (2020) recently showed that implicit (non-verbal) ToM performance was associated with increase in cortical thickness and surface areas in the SMG and the more dorsal portion of the precuneus, which dissociated from the explicit (verbal) ToM network found in the angular gyrus. While the latter region is part of the default mode network commonly recruited for episodic and semantic memory, the SMG is associated with sensory, motor and body representations. Unlike verbal ToM function, implicit ToM is independent of other cognitive function such as language, executive function, working memory or general intelligence and appears much earlier during child development than explicit ToM reasoning. Similar dissociated networks between explicit and implicit ToM

networks were found in a series of other studies which concluded that the SMG was especially important for overcoming egocentric biases when judging other's emotional states and generally, for developing a social modulation of encoded information (Silani *et al.*, 2013; Schurz *et al.*, 2014, 2015; Kanske *et al.*, 2016).

The putamen is an integral part of the reward circuit, along with the OFC, the insula, the ACC, the caudate and the ventral striatum. The putamen is specifically involved in adjusting the balance between exploration and exploitation (Palminteri *et al.*, 2012) due to its role in inhibiting the selection of the worst option and facilitating the selection of alternative options. The input connections from dorsal prefrontal structures, involved in inhibitory and executive processes (Draganski *et al.*, 2008), endorse this interpretation of a dorsal striatum specialised for coding RPE for aversive outcomes (Delgado *et al.*, 2008). The finding of the putamen correlate in the low reward rate condition where cues predict relatively high probabilities of punishment, confirms the role of this structure in aversive learning underpinning avoidance (Delgado *et al.*, 2008, 2009; Palminteri *et al.*, 2012).

Although this experiment was not designed to test decision processes in a social context per se, the specificity of my results in linking social cognition and corresponding neuroanatomical substrates with learning dynamics builds on previous evidence of musical environments as an ideal model for exploring complex interpersonal and affective behaviours in daily life. In fact, one of the theories surrounding the biological role of music in human evolution proposes that music is a 'rehearsing platform' to learn how to transform emotional mental states into social signals (Clark *et al.*, 2015) and a few studies have related deficit in attribution of mental states to music with other social cognition deficits (Downey *et al.*, 2013) or correlated musicality with social competence and emotional awareness (Lima *et al.*, 2016). RL paradigms in general constitute a powerful tool to investigate learning and decision-making in social contexts as they mimic the uncertainty and ambiguity levels of daily life social cues and the dynamic nature of socio-emotional interactions. This study confirms the utility of combining music and RL paradigms for a systematic investigation of the complex socio-emotional disturbances displayed by patients with bvFTD. Longitudinal studies will be needed to test the sensitivity and specificity of this test in detecting behavioural changes early in the course of the disease.

The detection and characterisation of behavioural alterations in bvFTD still rely on a combination of clinical assessments, questionnaires filled by primary caregivers and a battery of tests investigating cognitive functions. This chapter has demonstrated that reward-based decision-making provides an additional model for understanding these symptoms, which has never been explored in the past. Moreover, computational modelling offers another layer of understanding by revealing the hidden stages involved in such dynamic and complex tasks.

7 General discussion

7.1 Summary of findings:

The central goal of this thesis was to characterise neurodegenerative diseases within the normative models of predictive coding and active inference. Under the free-energy principle, perceptual deficits and impaired goal-directed behaviour can be brought together and interpreted as generalised disorders of predictive processing.

The first major aim of this thesis was to characterise the deficits of musical deviant processing in AD and canonical syndromes of FTD at a cognitive and autonomic level, and to relate these to underlying neuroanatomical changes.

In chapter 3, I used a musical deviant paradigm and manipulated deviant note surprise such that I could assess three levels of the hierarchical organisation of the musical brain: lower-level acoustic, syntactic and semantic processing of musical patterns and 'objects'. AD patients had normal cognitive and autonomic reactivity to deviants. bvFTD and svPPA patients demonstrated impaired cognitive and autonomic reactivity to pitch deviants but preserved reactivity to acoustic deviants, consistent with a deficient predictive model of musical syntax or semantic information. nfvPPA patients demonstrated an excessive rate of false-alarms with erroneous rejection of canonical structures accompanied by an enhanced pupillary reactivity to deviants, suggesting over-precise musical sensory predictions. In a combined VBM analysis of the syndromic groups, performance for the detection of acoustic deviants correlated with a bilateral temporo-parietal network while performance for the detection of pitch deviants correlated with a right-lateralised anterior fronto-temporal network extending into dorsal striatum. This last result suggested that efficient processing of musical pitch deviants requires the comparison of incoming musical patterns against syntactic expectations in the inferior frontal gyrus and semantic expectations in the temporal polar cortex, and further, that this cross-talk might be facilitated by probabilistic coding of incoming musical information in the dorsal striatum.

In chapter 4, I interpreted the results found in chapter 3 in terms of information-theoretic measures of surprise and uncertainty in my stimulus melody set. AD and nfvPPA patients retained cognitive and autonomic sensitivity to the probabilistic structure of the melody with a positive association between autonomic reactivity to deviants and information-content (surprise level) of deviants. This association was differentially modulated by the entropy (uncertainty level) of the musical environment, with a general enhancement in more predictable environment. bvFTD patients showed a deficit in tracking the information-content of deviants but retained

sensitivity to the entropy of the environment, suggesting an imbalance in the precision assigned to sensory input compared to the precision assigned to predictive models. Finally, svPPA patients displayed a generalised loss of sensitivity to both surprise and uncertainty. Partial correlations between deviant detection accuracy and information-content of deviants, when taking entropy levels into account, were associated with grey matter volume in a putative, extended hierarchical 'prediction network'. Within this network, lower regions in bilateral superior temporal gyrus encode pitch patterns, bilateral dorsal and ventral striatum regions along with bilateral hippocampus track the probabilistic structure of musical stimuli, and higher-level regions in right temporal polar cortex and left inferior frontal gyrus generate predictive models.

Together, chapters 3 and 4 identify cognitive deficits of musical surprise processing and for probabilistic tracking of changes in the environment, suggesting a new formulation of the mechanisms whereby FTD and AD pathologies disrupt the integration of predictive errors with prior predictions. Figure 7.1 provides a visual summary of FTD and AD cognitive, autonomic and information theoretic profiles.

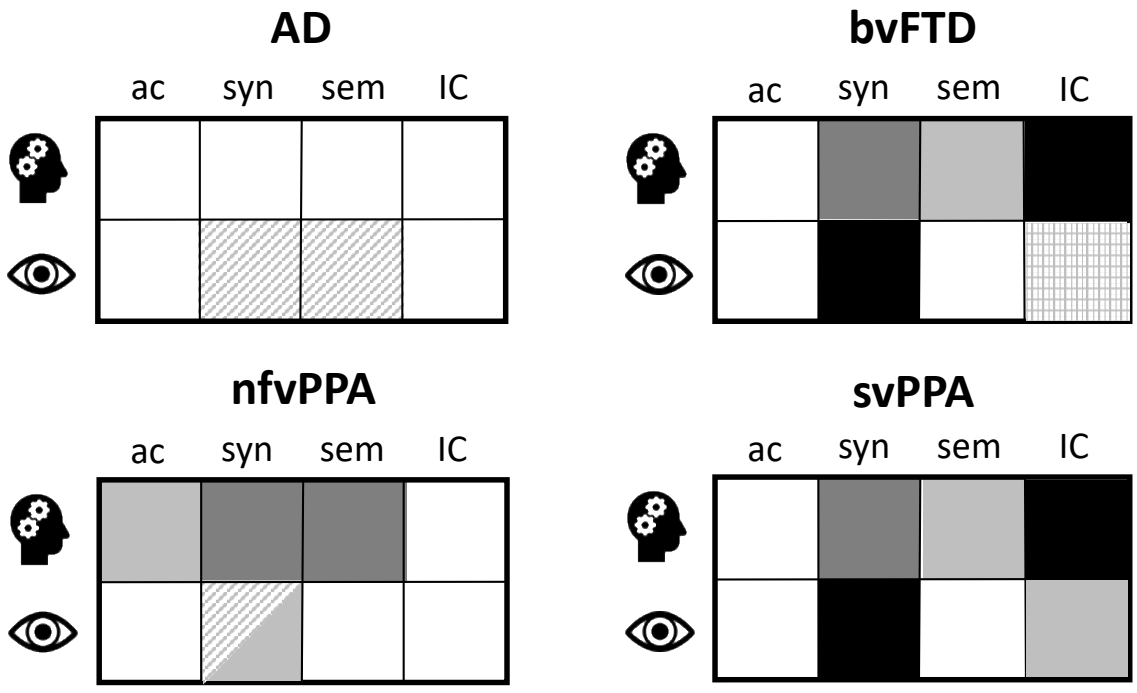

Figure 7.1. Summary profiles of cognitive and autonomic responses to melodic deviants in canonical dementia syndromes, referenced to healthy older individuals

In each panel, rows code accuracy of deviant detection (head icon) and peak pupillary response magnitude and/or latency (eye icon); and columns code different kinds of deviant notes – acoustic (**ac**), syntactic (**syn**) and semantic (**sem**) - and correlation with deviant information-content (**IC**), in famous melodies that were assessed in the experimental conditions here. White cells indicate no significant difference with respect to healthy controls; light grey cells code a significant abnormality compared to healthy controls; dark grey cells code a significant deficit relative to the Alzheimer's disease group; black cells code a significant difference relative to other FTD syndromic groups; diagonal-hatching codes a pupil latency (rather than response magnitude) effect; and cross-hatching codes a deficit when modulatory effect of entropy is not taken into account.

The second major aim of this thesis was to assess the status of reward prediction error processing and updating via actions in bvFTD using a musical reinforcement learning paradigm, and to relate this to underlying neuroanatomical changes.

Chapter 5 investigated the way perception and action are intertwined in bvFTD patients, i.e. how perceptual processing of prediction error is translated into an action directed to minimise prediction errors. Using a classical exploration-exploitation paradigm, I measured the 'efficiency' of actions and weighted this performance in the light of implicit measures of valuation of actions via reaction times and valuation of the outcome of actions via pupillometry. Actions were less accurate (i.e. lower probability of choosing the best option) for bvFTD patients than for healthy controls and were predicted by the implicit valuation of available choices rather than valuation of musical stimuli per se. Neuroanatomical correlates of choice accuracy within the participant cohort emerged along the dorsal and ventral attention networks known to facilitate task switching from exploration to exploitation and in the parahippocampal gyrus previously implicated in processing aversive stimuli. Additionally, accuracy of actions correlated with daily-life measures of ritualistic and compulsive behaviours.

Chapter 6 moved beyond the characterisation of fixed deficits to address dynamic learning with a trial-by-trial estimation of perceptual processing and action selection. Using two computational models of reinforcement learning, I first identified the specific stages of reward processing affected by bvFTD and then addressed the hypothesis of a specific impairment in learning from negative reward prediction errors compared to positive prediction errors. bvFTD patients showed reduced sensitivity to the outcome of actions and a deficit in the conversion of internal action values into observed actions, which correlated with grey matter volume in left supramarginal gyrus and dorsal striatum. They also demonstrated a lower learning rate in response to unexpected aversive stimuli which correlated with grey matter atrophy in left supramarginal gyrus and right temporo-parietal junction. Both reduced sensitivity to outcome and negative learning rates correlated with daily-life measures of social cognition related to empathy and theory-of-mind abilities.

Together, chapters 5 and 6 endorse the utility of the musical reward-based decision-making paradigm for capturing a general mechanism of abnormal reinforcement learning in bvFTD – and suggests a resonance with clinical symptoms in this syndrome.

7.2 The reformulation of cognitive and autonomic musical phenotypes as predictive coding signatures

My findings can be reformulated in terms of predictive coding. Specific deficits were associated with each syndrome: AD was associated with a normal integration of top-down expectations with bottom-up prediction errors; nfvPPA, with over-precise top-down predictions and down-regulated sensory input; svPPA, with a severe deficit integrating prediction errors with prior predictions reflecting a generalised erosion of their music predictive models; and bvFTD, with damaged predictive models and an over-reliance on contextual information. Neuroanatomical correlates were identified within a distributed fronto-temporo-parieto-subcortical network closely overlapping networks implicated in music processing (see Figure 7.1). bvFTD was associated with a generalised loss of sensitivity to reward-based decision outcomes and in particular, a deficit in learning how to minimise negative reward prediction error (i.e. unexpected aversive outcomes). Neuroanatomical correlates were found in a parieto-striatal network implicated in attention orientation and processing of aversive stimuli.

7.2.1 AD as a disorder of inefficient autonomic coding

Chapter 3 and 4 revealed a retained ability of AD patients to detect musical deviants at all levels of the processing hierarchy. They also displayed a normal sensitivity to information-content of deviants and entropy of melodies. The only significant difference compared to healthy controls was a longer latency of autonomic (pupillary) reactivity to syntactic and semantic deviants, which might reflect a modulatory effect of neurotransmitter deficits such as acetylcholine or noradrenaline and/or dysfunction of locus coeruleus, known to be targeted by AD pathology early in the course of the disease (Zarow *et al.*, 2003).

Involvement of the precuneus, targeted by AD pathology as a core component of the 'default mode network', correlated with reduced autonomic signalling of noise bursts in melodies across the patient cohort. No other regions of the default-mode network were involved in the detection of surprise and the tracking of probabilistic structure of melodies. This result suggests that AD patients possess a certain degree of vulnerability for the efficient autonomic encoding of prediction errors.

These findings are consistent with previous studies of pitch error detection involving well-known melodies (Hsieh *et al.*, 2011; Johnson *et al.*, 2011; Golden *et al.*, 2017). Less consistent findings were found for the detection of pitch contour deviants in tone sequences and unfamiliar melodies (Golden *et al.*, 2017), reflecting impaired

processing of global (contrary to local) characteristics in domains beyond music. The use of famous melodies in my paradigm might explain the preserved capacity to detect deviants. AD patients have indeed shown a heightened engagement of musical processing mechanisms during the recall of familiar melodies, notably the temporo-parietal default mode networks (Slattery *et al.*, 2019). My findings in chapter 4 go further and suggest that mechanisms involved in recognition of melodies might facilitate the recruitment of fronto-temporo-striatal regions responsible for the coding of musical expectation and surprise probabilistically. Preserved hedonic valuation of music in AD (Drapeau *et al.*, 2009) could well be related to the normal engagement of this circuitry.

7.2.2 svPPA as a disorder of impaired inference on higher order statistics of music

In svPPA, chapters 3 and 4 showed a generalized impairment of surprise detection and statistical tracking of musical information at both a cognitive and autonomic levels. While svPPA patients presented the same profile found for bvFTD patients in chapter 3, making them difficult to segregate in terms of predictive processes, chapter 4 showed that svPPA group displayed a unique deficit in processing uncertainty of contextual information. In that way, svPPA group differs from bvFTD group. This deficit might reflect impaired matching of incoming signals to a degraded model of musical syntax required to generate prior predictions or inefficient updating of these predictions or indeed, both mechanisms conjointly. The correlation observed between detection accuracy and melody recognition favours the first hypothesis and underlines how an 'incorrect model' of the current sensory environment precludes detection of incongruent events. Moreover, neuroanatomical correlates of surprise detection and statistical processing were found in core regions mediating general semantic memory, i.e. temporal polar cortex, anterior superior and middle temporal gyri. These regions have top-down inhibitory projections that sharpen neural circuit activities related to sensory object representations, attenuated in svPPA (Chiou and Lambon Ralph, 2016; Benhamou *et al.*, 2020). svPPA pathology, characterised by severe atrophy of the semantic appraisal network, can be interpreted as a disease of degraded predictive models. This is consistent with a plethora of evidence showing that svPPA degrades object concept representations across modalities (Pobric *et al.*, 2007; Goll *et al.*, 2012; Chen *et al.*, 2017). According to predictive coding theory, a diminished precision of predictions leads reciprocally to a higher precision being allocated to sensory inputs and deficient minimization of up-regulated prediction errors. Crucial to this formulation is the allocation of precision to all types of sensory stimuli, independently of their intrinsic information load. In other words, an inability to contextualize sensory information with an efficient mapping of incoming stimuli to semantic representations renders sensory prediction

errors overly precise and context insensitive. In the context of my study, deviant and standard tones were not discriminated by this mechanism. Chapter 4 further supports this hypothesis by revealing a general inability to track information-content values of tones and the overall predictability value of melodies (as a sum of information-content values). These findings are in line with recent work showing an impaired ability to differentiate between auditory sequences of high and low entropy (Hardy *et al.*, 2017*a*, *b*). It remains to be demonstrated whether this generic mechanism is translated to other sensory modalities than the auditory one however this would be a strong hypothesis on the evidence of the work I present here.

7.2.3 nfvPPA as a disorder of over-precise predictive models

nfvPPA patients, contrary to all other syndromic groups, showed a relatively preserved accurcay in detecting deviants at all levels of the processing hierarchy, but an abnormally high rate of false-alarms. In other words, nfvPPA patients tended to over-interpret variations from musical canonicity in melodies without deviant notes (perhaps, for example, timbral or key changes associated with transcribing the melodies) as errors. This result aligns with other deficits in this syndrome, including impaired hearing even in quiet environments, impaired understanding of less familiar accents and emotional prosody and reduced modulation of social signals such as conversational laughter (Hailstone *et al.*, 2012; Rohrer *et al.*, 2012; Pressman *et al.*, 2017; Hardy *et al.*, 2019). In predictive coding terms, these observations have been interpreted (Cope *et al.*, 2017) as over-precise or inflexible priors, and related to atrophy in inferior frontal gyrus providing a syntactic model of dynamic stimuli such as speech and music. However, nfvPPA pathology also targets lower-regions of the cortical hierarchy surrounding the Sylvian fissure, notably the insula and the superior temporal gyrus. Structural and functional disturbances in these regions have been repeatedly related to deficient early perceptual analysis of incoming auditory signals in nfvPPA (Goll *et al.*, 2010; Rohrer *et al.*, 2012; Grube *et al.*, 2016, Hardy *et al.*, 2017*a*, 2019). Down-regulated sensory input compared to over-precise priors is likely to lead to heightened prediction errors, at least at the lower levels of the hierarchy. The heightened pupil reactivity to syntactic deviants reported in chapter 3 and increased autonomic sensitivity to sensory surprise value and entropy of melodies reported in chapter 4 further support this hypothesis (as pupil dilatation is increasingly recognised as a proxy for prediction error (Liao *et al.*, 2016; Zhao *et al.*, 2019; Zénon, 2019)). The accurate sensitivity to information-content of deviants at a cognitive level further suggests that these prediction errors, observable at an autonomic level, were efficiently parsed through conscious processes driving decision-making related to detection of changes in the environment.

7.2.4 bvFTD as an 'environmental-dependency syndrome'

Chapter 3 reveals a profile in bvFTD similar to that in svPPA, i.e. an impaired detection of pitch deviants and blunted pupil reactivity to pitch deviants. These results are in line with previous evidence of a failure to form sensory predictions in bvFTD (Hughes and Rowe, 2013; Shaw *et al.*, 2019), accompanied by a generalised impairment of salience coding (Perry *et al.*, 2017; Clark *et al.*, 2018) and corroborated by preeminent atrophy of the salience network (Seeley *et al.*, 2009; Zhou *et al.*, 2010). However, chapter 4 reveals that bvFTD patients retain their autonomic sensitivity to the entropy of melody: they displayed a reduced sustained pupillary response to high entropy melodies and an increased sustained pupillary response to low entropy melodies. Moreover, they showed a positive partial correlation between pupil reactivity to deviants and information-content to deviants when taking into account the entropy of melody which suggested that contextual information (entropy) was an important factor facilitating their autonomic sensitivity to surprising events.

The failure to establish accurate sensory predictions coupled with a retained sensitivity to contextual information generates an intriguing association between autonomic reactivity to unexpected events and autonomic reactivity to predictability of the environment, dissociated in the case of high entropy environments. This could reflect a potential compensatory mechanism for the generalised difficulty of bvFTD patients in processing salient events with an optimisation of cognitive demands and maximisation of salience sensitivity in 'relevant' environments only. It also offers a potential mechanistic explanation for the 'environmental dependency syndrome' or utilization behaviour commonly exhibited by bvFTD patients, whereby they produce inappropriate behaviours 'enslaved to' environmental triggers (Ghosh and Dutt, 2010; Ghosh *et al.*, 2013; Kumfor *et al.*, 2018). According to this account, bvFTD patients would show an automatic reliance of the external context which is no longer modulated by other sources of information (i.e. in my study, deviant notes).This breakdown is particularly evident when processing of these sources of information is itself impaired (i.e. in my study, salience processing).

The first cognitive account made by Shallice et al. (1989) proposed a theory of cognitive of action with several levels of control including 'actions schemas': a set of representations of action sequences triggered by specific environmental stimuli. Frith et al., developed this model further by proposing an 'inverse' model which provides the motor commands associated to a desired state and a forward model which predicts the sensory consequences of this action (Frith *et al.*, 2000) (this theory directly influenced the active inference paradigm,

developed a few years later). These authors proposed that patients with utilization behaviour can no longer link their intentions to their actions.

Chapters 5 and 6, which looked at actions and their consequences within a reinforcement learning paradigm, provided further evidence and a candidate explanation for an environmental dependency syndrome in bvFTD. The findings from these experiments suggest that the disconnection between action and intention results from reduced sensitivity to the consequence of an action coupled with a higher stochasticity in the conversion of action values into action probabilities. However, these deficits were importantly governed by the level of environmental uncertainty: bvFTD patients displayed normal learning dynamics in a structured and binarized environment while they showed exacerbated deficits in noisier environments. Deficits in choosing the best action in noisy environments correlated with measures of ritualistic and compulsive behavioural changes, potential 'compensatory strategies' deployed by patients to reduce the environmental uncertainty. Social interactions could be regarded as the archetype for noisy and uncertain environments. Behavioural strategies to reduce this uncertainty encompass social withdrawal or disengagement with other people's state of mind; and indeed, the abnormally reduced learning dynamics found in chapter 6 correlated with behavioural changes related to empathy and theory-of-mind.

In summary, Chapters 3, 4 and 5 show that bvFTD patients retain a degree of sensitivity to environmental uncertainty by reducing the gain on prediction errors in uncertain environments and increasing this gain in more predictable environments. In line with this formulation, the capacity of these patients to learn to associate an action to its consequences over time was higher in predictable environments compared to more uncertain environments. This 'enslavement' to contextual information might potentially account for certain aberrant behaviours deployed by bvFTD patients in uncertain environments such as the implementation of strict rituals in daily-life activities or reduced engagement with others' states of mind, manifesting as emotional blunting.

7.3 Neurobiological and clinical implications

7.3.1 Neurobiological relevance

Figure 7.2. summarises the neuroanatomical correlates of the behavioural and autonomic findings obtained with my experimental paradigms. The neuroanatomical substrates are very extensive, spanning the entire cortical hierarchy. This reflects both the nature of the musical stimuli used throughout this thesis, well known to recruit a gamut of cognitive processes ranging from early perceptual analysis to the programming of complex behaviours

and the highly distributed atrophy profiles across the combined disease spectrum studied in this thesis. Furthermore, my experimental paradigms were designed to exploit the wide ranging nature of music processing. By directly manipulating the extent to which sensory input differs from predictions, these paradigms allow a systematic investigation of how the brain (or the embodied brain, in the case of action) minimises surprise.

The findings of this thesis build on previous studies showing aberrant processing of unexpected events in auditory sequences, impaired autonomic reactivity, reduced efficiency of contextual processing and altered extraction of statistical structure in the target diseases. This work goes further in several important ways. First, I have systematically studied patients from across the FTD spectrum and compared both to patients with AD and healthy older controls, allowing links to be drawn between behavioural and physiological changes and patterns of large-scale network destruction. Throughout, I have used musical stimuli which potently engage social and emotion processing mechanisms by engaging core components of the human social brain connectome (Alcalá-López *et al.*, 2018): it therefore offers a unique but generic mechanistic model for deconstructing the diverse and complex socio-emotional symptoms exhibited by people with FTD, which are presently extremely challenging to detect and track over the course of the disease. Finally, the diverse experimental modalities I have used here (behaviour, caregiver ratings, pupil reactivity, structural MRI) coupled with computational models of information processing and reinforcement learning, expose the links between observable and hidden processes of predictive cognition in AD and FTD.

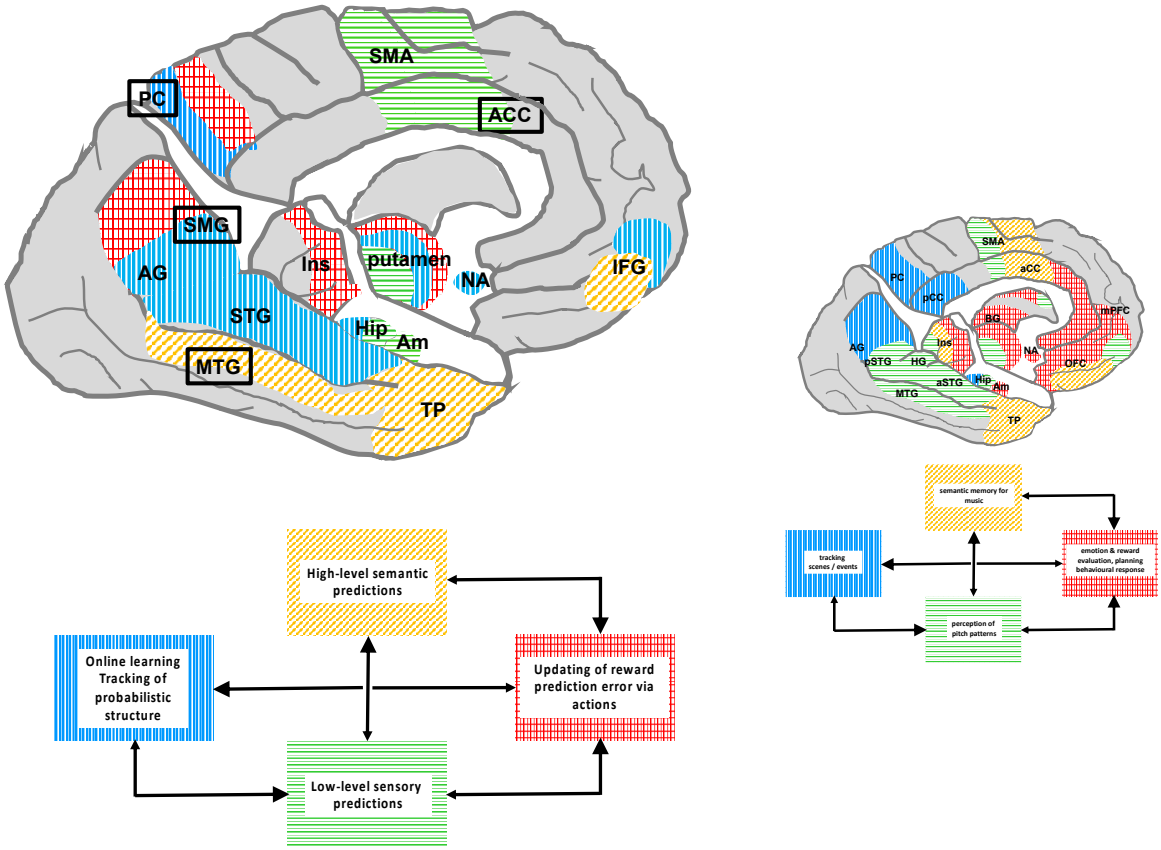

Figure 7.2. 'Updating' of Figure 1.3 based on my findings

This figure shows all neuroanatomical regions found in this thesis and reframing the key processing stages that extract different kinds of information from musical stimuli in terms of predictive coding, i.e. the minimization of prediction errors throughout the cortical hierarchy, the formation of predictions at different levels of the cortical hierarchy, the tracking of statistical dependencies and regularities, the processing of reward prediction error and updating via actions underpinning goal-directed behaviours. The shading code indicates the corresponding neural network substrate for each predictive coding operations. Regions enclosed by oblongs correspond to the regions found to correlate with higher autonomic reactivity.
For easier comparisons, Figure 1.3 is reproduced in smaller dimensions on the right - the initial shading code corresponded to the following cognitive operations: perception of pitch patterns (green); tracking scenes/events (blue); emotion and reward evaluation, planning behavioural response (red); semantic memory for music (yellow). ACC, anterior cingulate cortex; AG, angular gyrus; Am, amygdala; STG, superior temporal gyrus; Hip, hippocampus; Ins, insula; IFG, inferior frontal gyrus; MTG, middle temporal gyrus; NA, nucleus accumbens; PC, precuneus; SMA, supplementary motor area; SMG, supramarginal gyrus; TP, temporal pole.

7.3.2 Syndromic stratification and disease tracking

As described in chapter 1, neurodegenerative diseases are extremely heterogeneous in terms of clinical presentation, anatomy and underlying pathology and the same clinical phenotype can generally be produced by different pathogenic proteins. Stratification of proteinopathies is crucial as potential disease-modifying drug therapies emerge. By relating core deficits of surprise minimization to each of the three FTD syndromes and AD and, where possible, to relate these signatures to underlying neuroanatomy, I hope that the research presented in this thesis will form the basis for the identification of brain mechanisms supporting prediction error

minimization and ultimately stratify the underlying neural architectures at the level of the cortical microcircuit that underpin specific proteinopathies. My work has shown that it is indeed possible to stratify clinical syndromic groups using a set of musical stimuli and tailored paradigms (see Figures 7.1 and 7.3). Beyond facilitating diagnosis, the modalities used here, in particular physiological metrics which constitute a non-invasive method to quantify arousing responses to unexpected events, could constitute potential biomarkers. Indeed, the significant difference between syndromic groups for pupil dilatation and correlations of pupillary reactivity with specific underlying neuroanatomy suggest that there may be an additional role for physiological biomarkers in clinical stratification. Technical advances such as eye-tracking device integrated on reading glasses or integrated in a computer camera offer the further possibility to bring these tools into the home and record physiological reactivity during daily-life activities.

Finally, the use of music has substantial advantages over tests relying on language. Based on my experience as an experimenter and assistant clinical psychologist delivering psychometry tests, I could notice a drastic difference in engagement, interest, stress levels and ability to focus attention between my music paradigms and classical IQ tests. On another level, current and planned clinical trials demand large, multicentre collaborations: a non-linguistic modality such as music could allow a better homogeneity of results by transcending the issues associated with different languages in different countries.

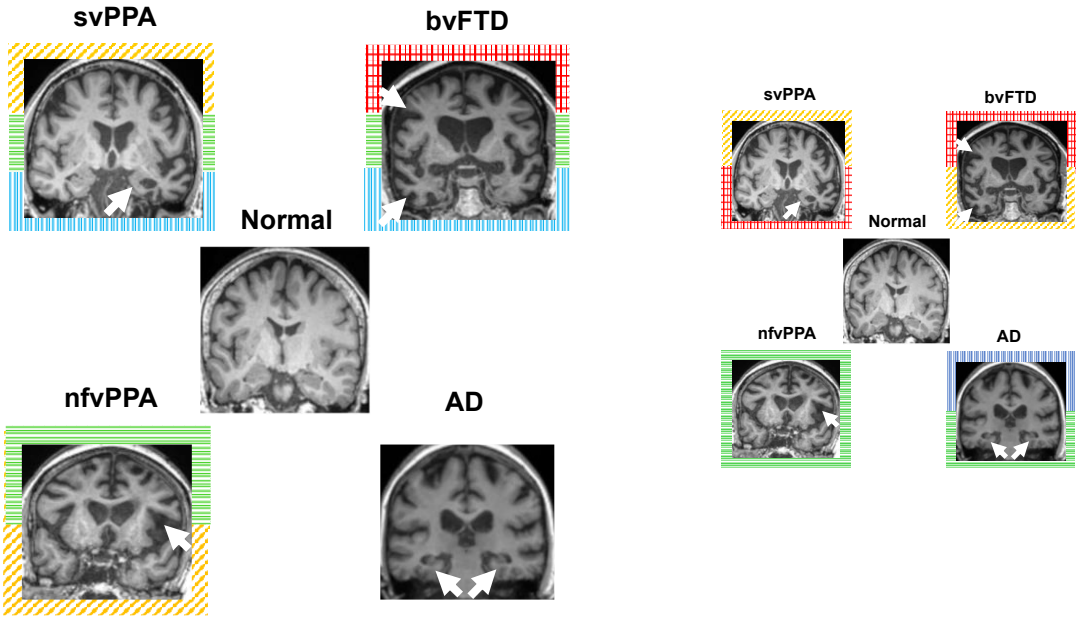

Figure 7.3. 'Updating' of Figure 1.4 based on my findings

The frames for each clinical panel are coded following the shading convention corresponding to the cognitive operations principally affected in each syndrome, as delineated in the model of music processing represented in Figure 7.2. Figure 1.4 is reproduced in smaller dimensions to facilitate comparisons.

7.3.3 Clinical translation

From a clinical perspective, my findings provide a prima face case for developing tools based on music processing to understand the difficulties experienced by patients with dementia in complex and unpredictable 'real world' environments.

The dissociation found for the bvFTD group between detection of unexpected deviants and sensitivity to environmental predictability suggests that bvFTD patients are more likely to extract useful information if the environment does not 'exceed' a certain level of uncertainty. This was further confirmed with the observation that they make better decisions in polarised and predictable environments during reinforcement learning. These results have particular significance for clinical counselling and potentially, also for quantifying environmental dependency in the laboratory setting; it is essential to inform clinicians, experimenters and most importantly, caregivers, of the particular challenge bvFTD patients face when presented with uncertain environments, and explain what behaviours it might trigger. Chapters 5 and 6 notably linked this deficit to ritualistic, compulsive behaviours and reduced empathy levels. Understanding the process underpinning such dysregulations might prepare the patient and their family for the potential evolution of these behavioural changes and further help to guide the development and evaluation of specific interventions, both behavioural and pharmacological. In general, this thesis has demonstrated the power and clinical relevance of using computational models combined with behavioural and physiological experimental data to offer a first glimpse of a computational basis for the bewildering array of behavioural difficulties that FTD patients exhibit. In particular, musical reward-based decision-making could be a unifying paradigm for capturing such changes, especially altered socio-emotional awareness and behaviour: some of the most challenging environments for choosing a course of action are socio-emotional, requiring rapid and implicit decision making. Identifying these changes not only has implications for disease diagnosis and stratification but also the potential for pharmacological treatments via specific neuromodulators such as dopamine or serotonin. This has previously been attempted using methylphenidate (psychostimulant acting on NA and DA) to reduce risk-taking behaviours (Rahman *et al.*, 2006) and citalopram (serotonin reuptake inhibitor) to improve disinhibition in bvFTD (Hughes *et al.*, 2015). If complex behavioural symptoms can be deconstructed into subcomponent stages of decision-making and reward processing, these could become more amenable both to development of biomarkers, as endpoints for trials and in tailoring and personalising treatments.

The hypothesis of 'inflexible priors' in nfvPPA supported by my findings in chapter 3 constitutes a candidate mechanism for understanding peculiar clinical observations such as the difficulty of nfvPPA patients of hearing speech in quiet environments (Cope *et al.*, 2017) or very low performance on pure-tone audiometry tests (Hardy *et al.*, 2019). The work presented in chapter 4 further suggests that nfvPPA patients retain an accurate sensitivity to sensory surprise value and entropy of melodies. This ability to extract regularities from the environment would need to be further explored with future cognitive rehabilitation strategies. Cognitive therapies in the context of PPA typically focus on higher-level linguistic processes. If the residual capacity for statistical learning of musical structures demonstrated here can be harnessed and transferred to improved perceptual learning in linguistic domains, this could be the basis for a new type of cognitive therapy, for instance building training exercises on sound sequence with a 'staircase' of statistical complexity, starting with tone sequences and building up to music and finally speech.

7.4 Limitations

The experiments described in this thesis share several general limitations that could infirm future work. Limitations specific to each chapter are presented separately in discussions.

The syndromic group sample sizes here were relatively small. This is an inherent problem when working with rare neurodegenerative syndromes, recruited via a single study centre. This is likely to have inflated both type I and type II error rates, so all findings here should be interpreted with caution. This thesis provides a further illustration of the necessity to develop multi-centre collaboration.

The syndromic groups were also defined a priori and grouped following clinical criteria for canonical FTD and typical AD which raises doubt on the actual potential of the measures used here to assist in the diagnosis of syndromes. An exciting extension of this thesis would be to run clustering analysis or machine learning Bayes analysis to determine if a certain combination of metrics can predict the membership of a certain syndromic group defined a priori, or even define novel subcategories of patients within the wider FTD or AD group. This is an area of research increasingly popular in areas of medicine where biomarkers that objectively indicate disease state are still lacking with highly complex biology underlying variable clinical presentations. Machine learning techniques provide exciting data-driven tools to reduce heterogeneity by defining new disease subtypes. To date, these have been chiefly used in psychiatric illness and only sparingly in neurodegenerative diseases. Studies have focused on automatic speech analysis in mild cognitive impairment and AD (König *et al.*, 2015), neuroimaging

(Avants *et al.*, 2010; Brier *et al.*, 2016), neuropsychometric data (Ingram *et al.*, 2020) and clinical data (Khanna *et al.*, 2018). The most recent study applied an unsupervised clustering algorithm to post-mortem histopathological data which revealed six new disease clusters (Cornblath *et al.*, 2020), which could explain more variance in cognitive phenotypes than the currently canonical diagnostic categories. Machine learning tools are likely to pave the way to a new era of research in neurodegenerative diseases, again relying on multi-centre collaboration as the very principle of artificial intelligence relies on large datasets.

Another potential limitation of the work in this thesis is that my experiments were all cross-sectional. Collecting longitudinal data would be needed to assess the potential of my tests in detecting and tracking syndrome severity, evolution and convergence across diseases stages. It would also be needed to exploit the potential of physiological biomarkers to track disease over a wider range of severities than conventional tests, both in patients who can no longer perform 'pencil and paper' tests and in pre-symptomatic patients before changes become apparent on conventional tests. Studying genetic cohorts (see GENFi initative (Rohrer *et al.*, 2015)) including at-risk individuals is crucial if one wants to adequately evaluate candidate biomarkers.

More fundamentally concerning the key assumptions of this thesis, there are important caveats about the predictive coding theory itself. As demonstrated throughout my thesis, it is indeed a promising heuristic for parsimoniously characterising a range of deficits in different neurodegenerative diseases. However, simply describing data in the terminology of predictive coding is not sufficient and should be testable at the neurophysiological level. MEG and laminar fMRI are two modalities that allow the investigation of the activity of neuronal populations and indirect reconstruction of the effect of pathogenic proteins on the laminar microcircuit (see next section for details). Yet, there is still a gap between the theoretical formalism of predictive coding and concrete neural mechanisms and discussions about the optimal experimental paradigms to verify its key hypotheses are still ongoing. Among other difficulties, researchers still face issues with disentangling predictive coding mechanisms and neural adaptation, characterising the nature of neural predictions themselves (some arguing that they are hardwired into neural structure through phylogenetic development and some positing that they emerge from persistent regularities extracted from the environment) or disentangling the activity of the two distinct neural subpopulations representing predictions and predictions errors at each level of the cortical processing hierarchy (Heilbron and Chait, 2017; Walsh *et al.*, 2020).

Questions have also been raised regarding the validity of predictive coding and free-energy principles for characterising music processing. An apparent paradox confronting the core principle of 'minimisation of surprise'

for maintaining homeostasis is the apparently universal tendency of humans to seek music featuring a substantial number of expectations' violations (Salimpoor *et al.*, 2015). For instance, a recent study indicated listeners (including musically untrained listeners) have a consistent preference for music with intermediate levels of entropy and information-content, demonstrating the so-called U-shaped "Wundt" effect for music (Gold *et al.*, 2019). Koelsch et al. (2019) recently attempted to resolve this paradox and proposed that music in fact provides an opportunity to continuously resolve uncertainty (or expected surprise), resembling the epistemic foraging seen in exploratory behaviour (Friston *et al.*, 2015). Yet, there are ongoing outstanding questions about the neural mechanisms of this epistemic value of music processing, e.g. is this resolution of uncertainty instantiated in the brain's reward network?; if music listening is indeed an active 'mental action' inferring and minimising surprise, what is the exact role of autonomic/motor networks in this process and how do these networks interact with the typical perceptual networks involved during music listening to generate new predictions and resolve uncertainty (Zatorre and Salimpoor, 2013)?

Although music is a promising model for mimicking dynamic and complex social interactions, achieving salient effects and driving motivational goal-directed behaviours, it is necessarily reductionist and cannot fully capture the complexity of real-world situations. In chapters 5 and 6, I directly correlated measures of behavioural changes with my experimental measures, which offered compelling evidence for the use of such musical paradigm to probe certain daily life socio-emotional symptoms. My first two chapters lack this systematic correlational analysis. More studies are needed to corroborate the hypothesis that music is a good probe for detecting subtle changes in cognition and behaviour in neurodegenerative diseases. In particular, this work should motivate detailed correlative studies to explore the relations between musical predictive coding measures and the repertoire of daily life behaviours and between test scores and daily-life functions or disability measures. This is required to substantiate the claim to real-world relevance and modelling of socio-emotional situations involving other people.

Available standardised tools to assess musical functions, particularly in musically untrained listeners are few and not adapted for clinical use (Peretz *et al.*, 2003; Campanelli *et al.*, 2016). In order to account for the large variability in musical skills, exposure and preferences at large in the general population, I designed a bespoke method for my experiments, using a pitch discrimination task and several questionnaires to assess musical competence. However, this protocol awaits validation. Validated and standardised musical tests would also

reduce the current requirement for a certain level of musical knowledge on the part of the examiner to deliver the tests and interpret results.

7.5 Future directions

The predictive coding framework allows neurocognitive deficits to be conceptualised as mechanistic disruptions of the fine balance of information flow within and between cortical circuits. This thesis has largely focused on interpreting behavioural and autonomic changes as disruptions within hierarchical predictions. In particular, it showed that the same 'superficial' profile of deficits could arise from different disruptions in the network (see svPPA and bvFTD in Chapters 3 and 4). Yet, this leaves unmet the key challenge in the field of neurodegenerative diseases of finding physiological biomarkers that can reflect more closely the spread of pathogenic proteins in cortical microcircuits. The work of this thesis is a necessary first step toward this goal. However, dynamic neuroanatomical tools are required to advance this enterprise. Electrophysiology is the ideal modality to derive the firing patterns of neuronal populations arising from a certain source and how these interact with firing patterns from another source. The 'additive' nature of extracellular signals - which are the sum of a range of sources from synaptic transmembrane currents to ionic fluxes - can only be deconstructed using sophisticated signal processing tools and computational models (Buzsáki *et al.*, 2012). EEG and MEG signals have notably been exploited for predictive coding studies, both by virtue of their exquisite temporal resolution (which can track neuronal activity directly, without the latency imposed by the haemodynamic function in functional MRI) and their stratification of frequency band (oscillatory) activity arising from different components of the cortical microcircuit. Hence, alpha oscillations (8-13 Hz) are related to the precision of priors, beta (13-30 Hz) to the update of prediction errors and gamma (30-45Hz) to the transduction of sensory data into prediction errors (Sedley *et al.*, 2016). In particular, MEG is a particularly attractive proposition. MEG offers clear advantages over EEG including higher spatial resolution (±5 mm), less artefact interference, and a shorter set-up time without

electrodes.

Hypotheses for a MEG study looking at syntactic deviants in familiar and unfamiliar melodies in healthy older controls and primary progressive aphasias (svPPA and nfvPPA)

Considering my key experimental findings in the context of a MEG paradigm, I would expect to see M1 (the MEG equivalent of the early negativity N1) to be correlated with information-content of syntactic deviants in nfvPPA patients and healthy controls (Koelsch and Jentschke, 2010; Omigie *et al.*, 2019; Quiroga-Martinez *et al.*, 2020). N400 amplitude, the evoked potential for semantic deviations, would be significantly reduced for expectancy violations in familiar melodies in svPPA patients compared to nfvPPA patients and healthy controls (Paller *et al.*, 1992; Maess *et al.*, 2001; Miranda and Ullman, 2007; Steinbeis and Koelsch, 2008; Koelsch, 2011; Carrus *et al.*, 2013). Regarding induced responses, which reflect binding or feature integration over larger neuronal populations, I would anticipate an increase in beta power for familiar tunes during the early presentation of the melody before the onset of the deviant (Chang *et al.*, 2018; Little *et al.*, 2019; Palmer *et al.*, 2019). This beta power would reflect the precision assigned to the predictions and would correlate to the subject-specific familiarity ratings of each melody. svPPA patients, based on significantly reduced precision of priors about familiar melodies, would display a reduced induced beta power during presentation of familiar melodies. The 'stop' signal fed back by frontal regions to superior temporal regions (indicating that no further processing is necessary in the case of standard notes) would be reflected in a desynchronization of alpha/beta power (Chang *et al.*, 2018). Alpha/beta desynchronization would be delayed or absent in nfvPPA patients, due to the up-regulated precision of predictions in this syndrome.

In the case of decision-making paradigms, hierarchical Bayesian learning models have been extremely useful to estimate individual beliefs about the environment's level of uncertainty (Mathys *et al.*, 2011). People's intentions are hidden from observers and have to be inferred from their actions, hence the use of computational models. Bayesian models in particular allow estimation of the dynamic fluctuations in uncertainty experienced by each individual based on the predictions of future aversive or reward states. These models have notably been used to test the hypothesis of hierarchically structure recursive thinking during social interactions to infer the volatile intentions of others (Diaconescu *et al.*, 2014) or to understand how subjective and autonomic metrics of stress relate to uncertainty level and predict learning performance (de Berker *et al.*, 2016). Adapting reinforcement learning paradigms to neurodegenerative clinical populations and using adequate Bayesian models

could offer a promising framework to understand if the estimation of uncertainty differs depending on the pathology, and if so, how this estimated uncertainty impacts performance for choosing an optimal course of action and more generally, alters goal-directed behaviours. There is a growing need to combine behavioural experiments with computational models to derive neurocomputational accounts of socio-emotional disturbances and delineate which 'hidden' computations engaged during social interactions are actually targeted by the pathology, with significant implications for the design of new therapeutic strategies (Huys *et al.*, 2016; Teufel and Fletcher, 2016; Pessiglione *et al.*, 2018; Nair *et al.*, 2020).

Finally, my stimulus set strictly controlled a number of spectrotemporal and information-theoretic properties, yet this is a pale simulation of the rich experience of real-world music listening. Future work could manipulate additional musical characteristics such as polyphony, timbre or use personally relevant and engaging playlists and couple this experience with wearable technology in real-world settings.

For those living with dementia as well as clinicians, the ultimate purpose of understanding music processing in these diseases is to design effective music-based interventions that can improve patients' quality of life, adjustment to their illness and perhaps cognitive function. For the first time, a rational approach to this challenge seems to be at hand, due in no small measure to the discovery that the musical brain can be remarkably resilient as well as vulnerable to the effects of neurodegenerative pathologies. The finding that musical semantic memory and emotional reactivity are relatively spared in AD, for example, gives a neurobiological impetus to the use of personalised playlists of favourite music to improve wellbeing (Garrido *et al.*, 2018, 2019; Groussard *et al.*, 2019). The use of rhythm cues to improve motor function in Parkinson's disease is another instance of a neurophysiological principle harnessed for therapeutic ends (Nombela *et al.*, 2013; Volpe *et al.*, 2013; Bella *et al.*, 2015; Hove and Keller, 2015; Dauvergne *et al.*, 2018; Murgia *et al.*, 2018). Studies that directly examine the interaction of music with brain functional organisation are potentially a powerful endorsement for the use of musical interventions and behavioural responses as a 'proxy' for neural effects (Trost *et al.*, 2018; King *et al.*, 2019). It is clear that to be effective, music therapies cannot be 'one-size-fits-all': rather, they should be customised, both to the particular illness and to the individual patient, taking account of psychosocial milieu, mood and disease stage (Garrido *et al.*, 2018). In FTD, for example, musical playlists are unlikely to benefit a person who has profound music aversion but may provide very useful behavioural regulation in someone else with musicophilia (Raglio *et al.*, 2012). All in all, this is an exciting era for musical brain research in dementia, with grounds for optimism that the ancient hope of using music as medicine may finally be realised.

References

Adams RA, Huys QJM, Roiser JP. Computational Psychiatry: towards a mathematically informed understanding of mental illness. J Neurol Neurosurg Psychiatry 2016; 87: 53–63.

Agustus JL, Golden HL, Callaghan MF, Bond RL, Benhamou E, Hailstone JC, et al. Melody Processing Characterizes Functional Neuroanatomy in the Aging Brain [Internet]. Front Neurosci 2018; 12[cited 2019 Apr 30] Available from: https://www.frontiersin.org/articles/10.3389/fnins.2018.00815/full

Ahmed RM, Ke YD, Vucic S, Ittner LM, Seeley W, Hodges JR, et al. Physiological changes in neurodegeneration — mechanistic insights and clinical utility. Nature Reviews Neurology 2018; 14: 259–71.

Ahnaou A, Moechars D, Raeymaekers L, Biermans R, Manyakov NV, Bottelbergs A, et al. Emergence of early alterations in network oscillations and functional connectivity in a tau seeding mouse model of Alzheimer's disease pathology [Internet]. Sci Rep 2017; 7[cited 2020 Apr 28] Available from: https://www.ncbi.nlm.nih.gov/pmc/articles/PMC5660172/

Alamia A, VanRullen R, Pasqualotto E, Mouraux A, Zenon A. Pupil-Linked Arousal Responds to Unconscious Surprisal. J Neurosci 2019; 39: 5369–76.

Aly M, Ranganath C, Yonelinas AP. Detecting changes in scenes: the hippocampus is critical for strength-based perception. Neuron 2013; 78: 1127–37.

Anneser JMH, Jox RJ, Borasio GD. Inappropriate sexual behaviour in a case of ALS and FTD: successful treatment with sertraline. Amyotroph Lateral Scler 2007; 8: 189–90.

Aston-Jones G, Cohen JD. An integrative theory of locus coeruleus-norepinephrine function: adaptive gain and optimal performance. Annu Rev Neurosci 2005; 28: 403–50.

Baeken C, Marinazzo D, Schuerbeek PV, Wu G-R, Mey JD, Luypaert R, et al. Left and Right Amygdala - Mediofrontal Cortical Functional Connectivity Is Differentially Modulated by Harm Avoidance. PLOS ONE 2014; 9: e95740.

Balasubramani PP, Chakravarthy VS, Ravindran B, Moustafa AA. An extended reinforcement learning model of basal ganglia to understand the contributions of serotonin and dopamine in risk-based decision making, reward prediction, and punishment learning [Internet]. Front Comput Neurosci 2014; 8[cited 2020 Oct 28] Available from: https://www.frontiersin.org/articles/10.3389/fncom.2014.00047/full#B17

Barch DM, Pagliaccio D, Luking K. Mechanisms Underlying Motivational Deficits in Psychopathology: Similarities and Differences in Depression and Schizophrenia. Curr Top Behav Neurosci 2016; 27: 411–49.

Bartra O, McGuire JT, Kable JW. The valuation system: a coordinate-based meta-analysis of BOLD fMRI experiments examining neural correlates of subjective value. Neuroimage 2013; 76: 412–27.

Bauch EM, Rausch VH, Bunzeck N. Pain anticipation recruits the mesolimbic system and differentially modulates subsequent recognition memory. Human Brain Mapping 2014; 35: 4594–606.

Baumeister RF, Bratslavsky E, Finkenauer C, Vohs KD. Bad is Stronger than Good: [Internet]. Review of General Psychology 2001[cited 2020 Nov 27] Available from: https://journals.sagepub.com/doi/10.1037/1089-2680.5.4.323

Bendixen A. Predictability effects in auditory scene analysis: a review [Internet]. Front Neurosci 2014; 8[cited 2020 Nov 16] Available from: https://www.frontiersin.org/articles/10.3389/fnins.2014.00060/full

Benhamou E, Warren JD. Chapter 4 - Disorders of music processing in dementia. In: Cuddy LL, Belleville S, Moussard A, editor(s). Music and the Aging Brain. Academic Press; 2020. p. 107–49

Bettcher BM, Giovannetti T, Macmullen L, Libon DJ. Error detection and correction patterns in dementia: a breakdown of error monitoring processes and their neuropsychological correlates. J Int Neuropsychol Soc 2008; 14: 199–208.

Bianco R, Novembre G, Keller PE, Kim S-G, Scharf F, Friederici AD, et al. Neural networks for harmonic structure in music perception and action. Neuroimage 2016; 142: 454–64.

Bianco R, Ptasczynski LE, Omigie D. Pupil responses to pitch deviants reflect predictability of melodic sequences. Brain Cogn 2020; 138: 103621.

Blood AJ, Zatorre RJ, Bermudez P, Evans AC. Emotional responses to pleasant and unpleasant music correlate with activity in paralimbic brain regions. Nat Neurosci 1999; 2: 382–7.

Blood AJ, Zatorre RJ. Intensely pleasurable responses to music correlate with activity in brain regions implicated in reward and emotion. PNAS 2001; 98: 11818–23.

Bocchetta M, Gordon E, Marshall CR, Slattery CF, Cardoso MJ, Cash DM, et al. The habenula: an under-recognised area of importance in frontotemporal dementia? J Neurol Neurosurg Psychiatry 2016; 87: 910–2.

Bódi N, Kéri S, Nagy H, Moustafa A, Myers CE, Daw N, et al. Reward-learning and the novelty-seeking personality: a between- and within-subjects study of the effects of dopamine agonists on young Parkinson's patients. Brain 2009; 132: 2385–95.

Brattico E, Alluri V, Bogert B, Jacobsen T, Vartiainen N, Nieminen SK, et al. A Functional MRI Study of Happy and Sad Emotions in Music with and without Lyrics [Internet]. Front Psychol 2011; 2[cited 2020 Nov 25] Available from: https://www.frontiersin.org/articles/10.3389/fpsyg.2011.00308/full

Browning M, Behrens TE, Jocham G, O'Reilly JX, Bishop SJ. Anxious individuals have difficulty learning the causal statistics of aversive environments. Nat Neurosci 2015; 18: 590–6.

Canli T, Lesch K-P. Long story short: the serotonin transporter in emotion regulation and social cognition. Nat Neurosci 2007; 10: 1103–9.

Carrus E, Pearce MT, Bhattacharya J. Melodic pitch expectation interacts with neural responses to syntactic but not semantic violations. Cortex 2013; 49: 2186–200.

Cavanna AE, Trimble MR. The precuneus: a review of its functional anatomy and behavioural correlates. Brain 2006; 129: 564–83.

Cazé RD, van der Meer MAA. Adaptive properties of differential learning rates for positive and negative outcomes. Biol Cybern 2013; 107: 711–9.

Chase HW, Kumar P, Eickhoff SB, Dombrovski AY. Reinforcement learning models and their neural correlates: An activation likelihood estimation meta-analysis. Cogn Affect Behav Neurosci 2015; 15: 435–59.

Chenery HJ, Ingram JC, Murdoch BE. The resolution of lexical ambiguity with reference to context in dementia of the Alzheimer's type. Int J Lang Commun Disord 1998; 33: 393–412.

Cheung VKM, Harrison PMC, Meyer L, Pearce MT, Haynes J-D, Koelsch S. Uncertainty and Surprise Jointly Predict Musical Pleasure and Amygdala, Hippocampus, and Auditory Cortex Activity. Current Biology 2019; 29: 4084-4092.e4.

Cheung VKM, Meyer L, Friederici AD, Koelsch S. The right inferior frontal gyrus processes nested non-local dependencies in music. Scientific Reports 2018; 8: 1–12.

Chiong W, Hsu M, Wudka D, Miller BL, Rosen HJ. Financial errors in dementia: Testing a neuroeconomic conceptual framework. Neurocase 2014; 20: 389–96.

Chiong W, Wood KA, Beagle AJ, Hsu M, Kayser AS, Miller BL, et al. Neuroeconomic dissociation of semantic dementia and behavioural variant frontotemporal dementia. Brain 2016; 139: 578–87.

Chiu I, Piguet O, Diehl-Schmid J, Riedl L, Beck J, Leyhe T, et al. Facial Emotion Recognition Performance Differentiates Between Behavioral Variant Frontotemporal Dementia and Major Depressive Disorder. J Clin Psychiatry 2018; 79

Chougule PS, Najjar RP, Finkelstein MT, Kandiah N, Milea D. Light-Induced Pupillary Responses in Alzheimer's Disease. Front Neurol 2019; 10: 360.

Clark CN, Downey LE, Warren JD. Brain disorders and the biological role of music. Soc Cogn Affect Neurosci 2015; 10: 444–52.

Clark CN, Golden HL, McCallion O, Nicholas JM, Cohen MH, Slattery CF, et al. Music models aberrant rule decoding and reward valuation in dementia. Soc Cogn Affect Neurosci 2018; 13: 192–202.

Clark CN, Nicholas JM, Agustus JL, Hardy CJD, Russell LL, Brotherhood EV, et al. Auditory conflict and congruence in frontotemporal dementia. Neuropsychologia 2017; 104: 144–56.

Clark CN, Nicholas JM, Henley SMD, Downey LE, Woollacott IO, Golden HL, et al. Humour processing in frontotemporal lobar degeneration: A behavioural and neuroanatomical analysis. Cortex 2015; 69: 47–59.

Clark CN, Warren JD. Emotional caricatures in frontotemporal dementia. Cortex 2016; 76: 134–6.

Cohen J, Cohen P, West SG, Aiken LS. Applied Multiple Regression/Correlation Analysis for the Behavioral Sciences. Routledge; 2013

Cools R, D'Esposito M. Inverted-U-shaped dopamine actions on human working memory and cognitive control. Biol Psychiatry 2011; 69: e113-125.

Cope TE, Sohoglu E, Sedley W, Patterson K, Jones PS, Wiggins J, et al. Evidence for causal top-down frontal contributions to predictive processes in speech perception. Nat Commun 2017; 8: 2154.

Corbetta M, Patel G, Shulman GL. The Reorienting System of the Human Brain: From Environment to Theory of Mind. Neuron 2008; 58: 306–24.

Corbetta M, Shulman GL. Control of goal-directed and stimulus-driven attention in the brain. Nat Rev Neurosci 2002; 3: 201–15.

Critchley HD, Mathias CJ, Dolan RJ. Neural Activity in the Human Brain Relating to Uncertainty and Arousal during Anticipation. Neuron 2001; 29: 537–45.

Critchley HD, Nagai Y, Gray MA, Mathias CJ. Dissecting axes of autonomic control in humans: Insights from neuroimaging. Autonomic Neuroscience 2011; 161: 34–42.

Daffner KR, Mesulam MM, Cohen LG, Scinto LF. Mechanisms underlying diminished novelty-seeking behavior in patients with probable Alzheimer's disease. Neuropsychiatry Neuropsychol Behav Neurol 1999; 12: 58–66.

Dalley JW, Everitt BJ, Robbins TW. Impulsivity, Compulsivity, and Top-Down Cognitive Control. Neuron 2011; 69: 680–94.

Dalton MA, Weickert TW, Hodges JR, Piguet O, Hornberger M. Impaired acquisition rates of probabilistic associative learning in frontotemporal dementia is associated with fronto-striatal atrophy. Neuroimage Clin 2012; 2: 56–62.

Daunizeau J, Adam V, Rigoux L. VBA: A Probabilistic Treatment of Nonlinear Models for Neurobiological and Behavioural Data [Internet]. PLoS Comput Biol 2014; 10[cited 2020 Oct 16] Available from: https://www.ncbi.nlm.nih.gov/pmc/articles/PMC3900378/

Davey J, Thompson HE, Hallam G, Karapanagiotidis T, Murphy C, De Caso I, et al. Exploring the role of the posterior middle temporal gyrus in semantic cognition: Integration of anterior temporal lobe with executive processes. NeuroImage 2016; 137: 165–77.

Davis MH. Measuring individual differences in empathy: Evidence for a multidimensional approach. Journal of Personality and Social Psychology 1983; 44: 113–26.

Daw ND, Kakade S, Dayan P. Opponent interactions between serotonin and dopamine. Neural Netw 2002; 15: 603–16.

Daw ND, O'Doherty JP, Dayan P, Seymour B, Dolan RJ. Cortical substrates for exploratory decisions in humans. Nature 2006; 441: 876–9.

Dayan P, Huys Q. Serotonin's many meanings elude simple theories. Elife 2015; 4

Dayan P, Huys QJM. Serotonin, Inhibition, and Negative Mood. PLOS Computational Biology 2008; 4: e4.

Delgado MR, Jou RL, Ledoux JE, Phelps EA. Avoiding negative outcomes: tracking the mechanisms of avoidance learning in humans during fear conditioning. Front Behav Neurosci 2009; 3: 33.

Delgado MR, Li J, Schiller D, Phelps EA. The role of the striatum in aversive learning and aversive prediction errors. Philos Trans R Soc Lond B Biol Sci 2008; 363: 3787–800.

Delgado MR, Nystrom LE, Fissell C, Noll DC, Fiez JA. Tracking the Hemodynamic Responses to Reward and Punishment in the Striatum. Journal of Neurophysiology 2000; 84: 3072–7.

Deserno L, Boehme R, Heinz A, Schlagenhauf F. Reinforcement Learning and Dopamine in Schizophrenia: Dimensions of Symptoms or Specific Features of a Disease Group? [Internet]. Front Psychiatry 2013; 4[cited 2018 Jul 9] Available from: https://www.ncbi.nlm.nih.gov/pmc/articles/PMC3870301/

Downey LE, Blezat A, Nicholas J, Omar R, Golden HL, Mahoney CJ, et al. Mentalising music in frontotemporal dementia. Cortex 2013; 49: 1844–55.

Downey LE, Mahoney CJ, Buckley AH, Golden HL, Henley SM, Schmitz N, et al. White matter tract signatures of impaired social cognition in frontotemporal lobar degeneration. Neuroimage Clin 2015; 8: 640–51.

Draganski B, Kherif F, Klöppel S, Cook PA, Alexander DC, Parker GJM, et al. Evidence for segregated and integrative connectivity patterns in the human Basal Ganglia. J Neurosci 2008; 28: 7143–52.

Dubois B, Feldman HH, Jacova C, Hampel H, Molinuevo JL, Blennow K, et al. Advancing research diagnostic criteria for Alzheimer's disease: the IWG-2 criteria. Lancet Neurol 2014; 13: 614–29.

Duclos H, Bejanin A, Eustache F, Desgranges B, Laisney M. Role of context in affective theory of mind in Alzheimer's disease. Neuropsychologia 2018; 119: 363–72.

Duuren E van, Lankelma J, Pennartz CMA. Population Coding of Reward Magnitude in the Orbitofrontal Cortex of the Rat. J Neurosci 2008; 28: 8590–603.

Egermann H, Pearce MT, Wiggins GA, McAdams S. Probabilistic models of expectation violation predict psychophysiological emotional responses to live concert music. Cogn Affect Behav Neurosci 2013; 13: 533–53.

Engelborghs S, Vloeberghs E, Le Bastard N, Van Buggenhout M, Mariën P, Somers N, et al. The dopaminergic neurotransmitter system is associated with aggression and agitation in frontotemporal dementia. Neurochemistry International 2008; 52: 1052–60.

Femminella GD, Rengo G, Komici K, Iacotucci P, Petraglia L, Pagano G, et al. Autonomic dysfunction in Alzheimer's disease: tools for assessment and review of the literature. J Alzheimers Dis 2014; 42: 369–77.

Firbank M, Kobeleva X, Cherry G, Killen A, Gallagher P, Burn DJ, et al. Neural correlates of attention-executive dysfunction in lewy body dementia and Alzheimer's disease. Hum Brain Mapp 2016; 37: 1254–70.

Fittipaldi S, Ibanez A, Baez S, Manes F, Sedeno L, Garcia AM. More than words: Social cognition across variants of primary progressive aphasia. Neurosci Biobehav Rev 2019; 100: 263–84.

Fletcher PD, Downey LE, Golden HL, Clark CN, Slattery CF, Paterson RW, et al. Auditory hedonic phenotypes in dementia: A behavioural and neuroanatomical analysis. Cortex 2015; 67: 95–105.

Fletcher PD, Nicholas JM, Shakespeare TJ, Downey LE, Golden HL, Agustus JL, et al. Physiological phenotyping of dementias using emotional sounds. Alzheimer's & Dementia: Diagnosis, Assessment & Disease Monitoring 2015; 1: 170–8.

Frank MJ, Moustafa AA, Haughey HM, Curran T, Hutchison KE. Genetic triple dissociation reveals multiple roles for dopamine in reinforcement learning. PNAS 2007; 104: 16311–6.

Frank MJ. Hold your horses: a dynamic computational role for the subthalamic nucleus in decision making. Neural Netw 2006; 19: 1120–36.

Freitas C, Manzato E, Burini A, Taylor MJ, Lerch JP, Anagnostou E. Neural Correlates of Familiarity in Music Listening: A Systematic Review and a Neuroimaging Meta-Analysis. Front Neurosci 2018; 12: 686.

Garrido MI, Sahani M, Dolan RJ. Outlier responses reflect sensitivity to statistical structure in the human brain. PLoS Comput Biol 2013; 9: e1002999.

Ghosh A, Dutt A, Bhargava P, Snowden J. Environmental dependency behaviours in frontotemporal dementia: have we been underrating them? J Neurol 2013; 260: 861–8.

Ghosh A, Dutt A. Utilisation behaviour in frontotemporal dementia. J Neurol Neurosurg Psychiatry 2010; 81: 154–6.

Gingras B, Marin MM, Puig-Waldmüller E, Fitch WT. The Eye is Listening: Music-Induced Arousal and Individual Differences Predict Pupillary Responses [Internet]. Front Hum Neurosci 2015; 9[cited 2017 Jan 11] Available from: http://journal.frontiersin.org/article/10.3389/fnhum.2015.00619/abstract

Gleichgerrcht E, Torralva T, Roca M, Szenkman D, Ibanez A, Richly P, et al. Decision making cognition in primary progressive aphasia. Behav Neurol 2012; 25: 45–52.

Gold BP, Mas-Herrero E, Zeighami Y, Benovoy M, Dagher A, Zatorre RJ. Musical reward prediction errors engage the nucleus accumbens and motivate learning. Proc Natl Acad Sci U S A 2019; 116: 3310–5.

Gold BP, Pearce MT, Mas-Herrero E, Dagher A, Zatorre RJ. Predictability and Uncertainty in the Pleasure of Music: A Reward for Learning? J Neurosci 2019; 39: 9397–409.

Golden HL, Agustus JL, Goll JC, Downey LE, Mummery CJ, Schott JM, et al. Functional neuroanatomy of auditory scene analysis in Alzheimer's disease. Neuroimage Clin 2015; 7: 699–708.

Golden HL, Clark CN, Nicholas JM, Cohen MH, Slattery CF, Paterson RW, et al. Music Perception in Dementia. Journal of Alzheimer's Disease 2016: 1–18.

Golden HL, Downey LE, Fletcher PD, Mahoney CJ, Schott JM, Mummery CJ, et al. Identification of environmental sounds and melodies in syndromes of anterior temporal lobe degeneration. J Neurol Sci 2015; 352: 94–8.

Goll JC, Crutch SJ, Loo JHY, Rohrer JD, Frost C, Bamiou D-E, et al. Non-verbal sound processing in the primary progressive aphasias. Brain 2010; 133: 272–85.

Goll JC, Kim LG, Ridgway GR, Hailstone JC, Lehmann M, Buckley AH, et al. Impairments of auditory scene analysis in Alzheimer's disease. Brain 2012; 135: 190–200.

Gordon CL, Cobb PR, Balasubramaniam R. Recruitment of the motor system during music listening: An ALE meta-analysis of fMRI data. PLoS ONE 2018; 13: e0207213.

Gorno-Tempini ML, Hillis AE, Weintraub S, Kertesz A, Mendez M, Cappa SF, et al. Classification of primary progressive aphasia and its variants. Neurology 2011; 76: 1006–14.

Gosselin N, Samson S, Adolphs R, Noulhiane M, Roy M, Hasboun D, et al. Emotional responses to unpleasant music correlates with damage to the parahippocampal cortex. Brain 2006; 129: 2585–92.

Grèzes J, Decety J. Functional anatomy of execution, mental simulation, observation, and verb generation of actions: a meta-analysis. Hum Brain Mapp 2001; 12: 1–19.

Griffiths TD, Warren JD. What is an auditory object? Nat Rev Neurosci 2004; 5: 887–92.

Groussard M, Chan TG, Coppalle R, Platel H. Preservation of Musical Memory Throughout the Progression of Alzheimer's Disease? Toward a Reconciliation of Theoretical, Clinical, and Neuroimaging Evidence. J Alzheimers Dis 2019; 68: 857–83.

Groussard M, Rauchs G, Landeau B, Viader F, Desgranges B, Eustache F, et al. The neural substrates of musical memory revealed by fMRI and two semantic tasks. Neuroimage 2010; 53: 1301–9.

Grube M, Bruffaerts R, Schaeverbeke J, Neyens V, De Weer A-S, Seghers A, et al. Core auditory processing deficits in primary progressive aphasia. Brain 2016; 139: 1817–29.

Guitart-Masip M, Fuentemilla L, Bach DR, Huys QJM, Dayan P, Dolan RJ, et al. Action Dominates Valence in Anticipatory Representations in the Human Striatum and Dopaminergic Midbrain. J Neurosci 2011; 31: 7867–75.

Guo S, Koelsch S. Effects of veridical expectations on syntax processing in music: Event-related potential evidence. Sci Rep 2016; 6: 19064.

Haber SN, Knutson B. The Reward Circuit: Linking Primate Anatomy and Human Imaging. Neuropsychopharmacology 2010; 35: 4–26.

Hailstone JC, Omar R, Henley SMD, Frost C, Kenward MG, Warren JD. It's not what you play, it's how you play it: Timbre affects perception of emotion in music. The Quarterly Journal of Experimental Psychology 2009; 62: 2141–55.

Hailstone JC, Ridgway GR, Bartlett JW, Goll JC, Crutch SJ, Warren JD. Accent processing in dementia. Neuropsychologia 2012; 50: 2233–44.

Hansen NC, Pearce MT. Predictive uncertainty in auditory sequence processing [Internet]. Front Psychol 2014; 5[cited 2018 Mar 5] Available from: https://www.frontiersin.org/articles/10.3389/fpsyg.2014.01052/full

Hansen NC, Vuust P, Pearce M. 'If You Have to Ask, You'll Never Know': Effects of Specialised Stylistic Expertise on Predictive Processing of Music. PLoS ONE 2016; 11: e0163584.

Hardy CJD, Agustus JL, Marshall CR, Clark CN, Russell LL, Bond RL, et al. Behavioural and neuroanatomical correlates of auditory speech analysis in primary progressive aphasias [Internet]. Alzheimers Res Ther 2017; 9[cited 2018 Feb 12] Available from: https://www.ncbi.nlm.nih.gov/pmc/articles/PMC5531024/

Hardy CJD, Agustus JL, Marshall CR, Clark CN, Russell LL, Brotherhood EV, et al. Functional neuroanatomy of speech signal decoding in primary progressive aphasias. Neurobiol Aging 2017; 56: 190–201.

Hardy CJD, Frost C, Sivasathiaseelan H, Johnson JCS, Agustus JL, Bond RL, et al. Findings of Impaired Hearing in Patients With Nonfluent/Agrammatic Variant Primary Progressive Aphasia [Internet]. JAMA Neurol 2019[cited 2019 Apr 30] Available from: https://jamanetwork.com/journals/jamaneurology/fullarticle/2723501

Hardy CJD, Yong KXX, Goll JC, Crutch SJ, Warren JD. Impairments of auditory scene analysis in posterior cortical atrophy. Brain 2020; 143: 2689–95.

Hauser TU, Eldar E, Dolan RJ. Separate mesocortical and mesolimbic pathways encode effort and reward learning signals. PNAS 2017; 114: E7395–404.

Hein G, Engelmann JB, Vollberg MC, Tobler PN. How learning shapes the empathic brain. Proc Natl Acad Sci U S A 2016; 113: 80–5.

Hélie S, Shamloo F, Novak K, Foti D. The roles of valuation and reward processing in cognitive function and psychiatric disorders. Ann N Y Acad Sci 2017; 1395: 33–48.

Herholz SC, Halpern AR, Zatorre RJ. Neuronal correlates of perception, imagery, and memory for familiar tunes. J Cogn Neurosci 2012; 24: 1382–97.

Herrmann N, Black SE, Chow T, Cappell J, Tang-Wai DF, Lanctôt KL. Serotonergic function and treatment of behavioral and psychological symptoms of frontotemporal dementia. Am J Geriatr Psychiatry 2012; 20: 789–97.

Hezemans FH, Wolpe N, Rowe JB. Apathy is associated with reduced precision of prior beliefs about action outcomes. J Exp Psychol Gen 2020

Hickok G, Poeppel D. The cortical organization of speech processing. Nat Rev Neurosci 2007; 8: 393–402.

Hikosaka O, Sesack SR, Lecourtier L, Shepard PD. Habenula: Crossroad between the Basal Ganglia and the Limbic System. J Neurosci 2008; 28: 11825–9.

Hikosaka O. The habenula: from stress evasion to value-based decision-making. Nat Rev Neurosci 2010; 11: 503–13.

Ho B-L, Lin S-F, Chou P-S, Hsu C-Y, Liou L-M, Lai C-L. Impaired conflict monitoring in cognitive decline. Behav Brain Res 2019; 363: 70–6.

Hoefer M, Allison SC, Schauer GF, Neuhaus JM, Hall J, Dang JN, et al. Fear conditioning in frontotemporal lobar degeneration and Alzheimer's disease. Brain 2008; 131: 1646–57.

Hornberger M, Piguet O, Kipps C, Hodges JR. Executive function in progressive and nonprogressive behavioral variant frontotemporal dementia. Neurology 2008; 71: 1481.

Hsiao F-J, Chen W-T, Wang P-N, Cheng C-H, Lin Y-Y. Temporo-frontal functional connectivity during auditory change detection is altered in Alzheimer's disease. Hum Brain Mapp 2014; 35: 5565–77.

Hsieh S, Hornberger M, Piguet O, Hodges JR. Neural basis of music knowledge: evidence from the dementias. Brain 2011; 134: 2523–34.

Huey ED, Putnam KT, Grafman J. A systematic review of neurotransmitter deficits and treatments in frontotemporal dementia. Neurology 2006; 66: 17–22.

Hughes LE, Ghosh BCP, Rowe JB. Reorganisation of brain networks in frontotemporal dementia and progressive supranuclear palsy. NeuroImage: Clinical 2013; 2: 459–68.

Hughes LE, Rittman T, Regenthal R, Robbins TW, Rowe JB. Improving response inhibition systems in frontotemporal dementia with citalopram. Brain 2015; 138: 1961–75.

Hughes LE, Rowe JB. The impact of neurodegeneration on network connectivity: a study of change detection in frontotemporal dementia. J Cogn Neurosci 2013; 25: 802–13.

Huron DB. Sweet anticipation: music and the psychology of expectation. Cambridge, Mass: MIT Press; 2006

Ibañez A, Manes F. Contextual social cognition and the behavioral variant of frontotemporal dementia. Neurology 2012; 78: 1354–62.

Ito J, Kitagawa J. Error processing in patients with Alzheimer's disease. Pathophysiology 2005; 12: 97–101.

Jacobsen J-H, Stelzer J, Fritz TH, Chételat G, La Joie R, Turner R. Why musical memory can be preserved in advanced Alzheimer's disease. Brain 2015; 138: 2438–50.

Janata P. Neural basis of music perception. Handb Clin Neurol 2015; 129: 187–205.

Jiang S, Yan C, Qiao Z, Yao H, Jiang S, Qiu X, et al. Mismatch negativity as a potential neurobiological marker of early-stage Alzheimer disease and vascular dementia. Neurosci Lett 2017; 647: 26–31.

Johnen A, Bertoux M. Psychological and Cognitive Markers of Behavioral Variant Frontotemporal Dementia-A Clinical Neuropsychologist's View on Diagnostic Criteria and Beyond. Front Neurol 2019; 10: 594.

Johnson JK, Chang C-C, Brambati SM, Migliaccio R, Gorno-Tempini ML, Miller BL, et al. Music Recognition in Frontotemporal Lobar Degeneration and Alzheimer Disease. Cogn Behav Neurol 2011; 24: 74–84.

Johnsrude IS, Penhune VB, Zatorre RJ. Functional specificity in the right human auditory cortex for perceiving pitch direction. Brain 2000; 123 (Pt 1): 155–63.

Josef Golubic S, Aine CJ, Stephen JM, Adair JC, Knoefel JE, Supek S. MEG biomarker of Alzheimer's disease: Absence of a prefrontal generator during auditory sensory gating. Hum Brain Mapp 2017; 38: 5180–94.

Joshi A, Jimenez E, Mendez MF. Pavlov's Orienting Response in Frontotemporal Dementia. J Neuropsychiatry Clin Neurosci 2017; 29: 351–6.

Joshi A, Mendez MF, Kaiser N, Jimenez E, Mather M, Shapira JS. Skin conductance levels may reflect emotional blunting in behavioral variant frontotemporal dementia. J Neuropsychiatry Clin Neurosci 2014; 26: 227–32.

Joshi S, Li Y, Kalwani RM, Gold JI. Relationships between Pupil Diameter and Neuronal Activity in the Locus Coeruleus, Colliculi, and Cingulate Cortex. Neuron 2016; 89: 221–34.

Kahneman D, Tversky A. Prospect Theory: An Analysis of Decision under Risk. Econometrica 1979; 47: 263–91.

Kahnt T, Tobler PN. Salience Signals in the Right Temporoparietal Junction Facilitate Value-Based Decisions. J Neurosci 2013; 33: 863–9.

Kanske P, Böckler A, Trautwein F-M, Parianen Lesemann FH, Singer T. Are strong empathizers better mentalizers? Evidence for independence and interaction between the routes of social cognition. Soc Cogn Affect Neurosci 2016; 11: 1383–92.

Kim B, Shin J, Kim Y, Choi JH. Destruction of ERP responses to deviance in an auditory oddball paradigm in amyloid infusion mice with memory deficits. PLoS ONE 2020; 15: e0230277.

Klein-Flügge MC, Kennerley SW, Friston K, Bestmann S. Neural Signatures of Value Comparison in Human Cingulate Cortex during Decisions Requiring an Effort-Reward Trade-off. J Neurosci 2016; 36: 10002–15.

Kobeleva X, Firbank M, Peraza L, Gallagher P, Thomas A, Burn DJ, et al. Divergent functional connectivity during attentional processing in Lewy body dementia and Alzheimer's disease. Cortex 2017; 92: 8–18.

Kocagoncu E, Clarke A, Devereux BJ, Tyler LK. Decoding the Cortical Dynamics of Sound-Meaning Mapping. J Neurosci 2017; 37: 1312–9.

Kocagoncu E, Klimovich-Gray A, Hughes LE, Rowe JB. Evidence and implications of abnormal predictive coding in dementia [Internet]. arXiv:200606311 [q-bio] 2020[cited 2020 Nov 5] Available from: http://arxiv.org/abs/2006.06311

Koelsch S, Fritz T, Schlaug G. Amygdala activity can be modulated by unexpected chord functions during music listening. Neuroreport 2008; 19: 1815–9.

Koelsch S, Jentschke S, Sammler D, Mietchen D. Untangling syntactic and sensory processing: an ERP study of music perception. Psychophysiology 2007; 44: 476–90.

Koelsch S, Siebel WA. Towards a neural basis of music perception. Trends Cogn Sci (Regul Ed) 2005; 9: 578–84.

Koelsch S, Vuust P, Friston K. Predictive Processes and the Peculiar Case of Music. Trends in Cognitive Sciences 2019; 23: 63–77.

Koelsch S. Brain correlates of music-evoked emotions. Nat Rev Neurosci 2014; 15: 170–80.

Koelsch S. Neural substrates of processing syntax and semantics in music. Current Opinion in Neurobiology 2005; 15: 207–12.

Koenig P, Smith EE, Grossman M. Semantic categorisation of novel objects in frontotemporal dementia. Cogn Neuropsychol 2006; 23: 541–62.

Krueger CE, Bird AC, Growdon ME, Jang JY, Miller BL, Kramer JH. Conflict monitoring in early frontotemporal dementia. Neurology 2009; 73: 349–55.

Kumfor F, Ibañez A, Hutchings R, Hazelton JL, Hodges JR, Piguet O. Beyond the face: how context modulates emotion processing in frontotemporal dementia subtypes. Brain 2018; 141: 1172–85.

Lansdall CJ, Coyle-Gilchrist ITS, Jones PS, Vázquez Rodríguez P, Wilcox A, Wehmann E, et al. Apathy and impulsivity in frontotemporal lobar degeneration syndromes. Brain 2017; 140: 1792–807.

Lappe C, Steinsträter O, Pantev C. A beamformer analysis of MEG data reveals frontal generators of the musically elicited mismatch negativity. PLoS ONE 2013; 8: e61296.

Lappe C, Steinsträter O, Pantev C. A beamformer analysis of MEG data reveals frontal generators of the musically elicited mismatch negativity. PLoS ONE 2013; 8: e61296.

Lappe C, Steinsträter O, Pantev C. Rhythmic and melodic deviations in musical sequences recruit different cortical areas for mismatch detection. Front Hum Neurosci 2013; 7: 260.

Laptinskaya D, Thurm F, Küster OC, Fissler P, Schlee W, Kolassa S, et al. Auditory Memory Decay as Reflected by a New Mismatch Negativity Score Is Associated with Episodic Memory in Older Adults at Risk of Dementia. Front Aging Neurosci 2018; 10: 5.

Laureiro-Martínez D, Brusoni S, Canessa N, Zollo M. Understanding the exploration–exploitation dilemma: An fMRI study of attention control and decision-making performance. Strategic Management Journal 2015; 36: 319–38.

Lawson RP, Seymour B, Loh E, Lutti A, Dolan RJ, Dayan P, et al. The habenula encodes negative motivational value associated with primary punishment in humans. PNAS 2014; 111: 11858–63.

Lehne M, Rohrmeier M, Koelsch S. Tension-related activity in the orbitofrontal cortex and amygdala: an fMRI study with music. Soc Cogn Affect Neurosci 2014; 9: 1515–23.

Lenoble Q, Corveleyn X, Szaffarczyk S, Pasquier F, Boucart M. Attentional capture by incongruent object/background scenes in patients with Alzheimer disease. Cortex 2018; 107: 4–12.

Leuchs L, Schneider M, Czisch M, Spoormaker VI. Neural correlates of pupil dilation during human fear learning. NeuroImage 2017; 147: 186–97.

Li C-W, Chen J-H, Tsai C-G. Listening to music in a risk-reward context: The roles of the temporoparietal junction and the orbitofrontal/insular cortices in reward-anticipation, reward-gain, and reward-loss. Brain Res 2015; 1629: 160–70.

Liao H-I, Yoneya M, Kidani S, Kashino M, Furukawa S. Human Pupillary Dilation Response to Deviant Auditory Stimuli: Effects of Stimulus Properties and Voluntary Attention. Front Neurosci 2016; 10: 43.

Libon DJ, Xie SX, Moore P, Farmer J, Antani S, McCawley G, et al. Patterns of neuropsychological impairment in frontotemporal dementia. Neurology 2007; 68: 369.

Liebenthal E, Desai R, Ellingson MM, Ramachandran B, Desai A, Binder JR. Specialization along the Left Superior Temporal Sulcus for Auditory Categorization. Cereb Cortex 2010; 20: 2958–70.

Lima CF, Brancatisano O, Fancourt A, Müllensiefen D, Scott SK, Warren JD, et al. Impaired socio-emotional processing in a developmental music disorder. Sci Rep 2016; 6: 34911.

Lima CF, Krishnan S, Scott SK. Roles of Supplementary Motor Areas in Auditory Processing and Auditory Imagery. Trends Neurosci 2016; 39: 527–42.

Limb CJ. Structural and functional neural correlates of music perception. The Anatomical Record Part A: Discoveries in Molecular, Cellular, and Evolutionary Biology 2006; 288A: 435–46.

Lockwood PL, Apps MAJ, Valton V, Viding E, Roiser JP. Neurocomputational mechanisms of prosocial learning and links to empathy. PNAS 2016; 113: 9763–8.

MacKay DJC. Information Theory, Inference and Learning Algorithms. Cambridge University Press; 2003

Maia TV, Frank MJ. FROM REINFORCEMENT LEARNING MODELS OF THE BASAL GANGLIA TO THE PATHOPHYSIOLOGY OF PSYCHIATRIC AND NEUROLOGICAL DISORDERS. Nat Neurosci 2011; 14: 154–62.

Maris E, Oostenveld R. Nonparametric statistical testing of EEG- and MEG-data. Journal of Neuroscience Methods 2007; 164: 177–90.

Marshall CR, Hardy CJD, Allen M, Russell LL, Clark CN, Bond RL, et al. Cardiac responses to viewing facial emotion differentiate frontotemporal dementias. Ann Clin Transl Neurol 2018; 5: 687–96.

Marshall CR, Hardy CJD, Russell LL, Bond RL, Sivasathiaseelan H, Greaves C, et al. The functional neuroanatomy of emotion processing in frontotemporal dementias. Brain 2019; 142: 2873–87.

Marshall CR, Hardy CJD, Russell LL, Clark CN, Bond RL, Dick KM, et al. Motor signatures of emotional reactivity in frontotemporal dementia. Scientific Reports 2018; 8: 1030.

Mathôt S, Fabius J, Van Heusden E, Van der Stigchel S. Safe and sensible preprocessing and baseline correction of pupil-size data. Behav Res Methods 2018; 50: 94–106.

Matthews SC, Paulus MP, Simmons AN, Nelesen RA, Dimsdale JE. Functional subdivisions within anterior cingulate cortex and their relationship to autonomic nervous system function. NeuroImage 2004; 22: 1151–6.

Mazaheri A, Segaert K, Olichney J, Yang J-C, Niu Y-Q, Shapiro K, et al. EEG oscillations during word processing predict MCI conversion to Alzheimer's disease. Neuroimage Clin 2018; 17: 188–97.

McCoy B, Jahfari S, Engels G, Knapen T, Theeuwes J. Dopaminergic medication reduces striatal sensitivity to negative outcomes in Parkinson's disease. Brain 2019; 142: 3605–20.

McNaughton N. Gray's Neuropsychology of anxiety: An enquiry into the functions of septohippocampal theories. Behavioral and Brain Sciences 1982; 5: 492–3.

Menon V, Levitin DJ. The rewards of music listening: Response and physiological connectivity of the mesolimbic system. NeuroImage 2005; 28: 175–84.

Mikutta CA, Dürschmid S, Bean N, Lehne M, Lubell J, Altorfer A, et al. Amygdala and orbitofrontal engagement in breach and resolution of expectancy: A case study. Psychomusicology: Music, Mind, and Brain 2015; 25: 357–65.

Miranda RA, Ullman MT. Double dissociation between rules and memory in music: An event-related potential study. Neuroimage 2007; 38: 331–45.

Monosov IE, Hikosaka O. Regionally Distinct Processing of Rewards and Punishments by the Primate Ventromedial Prefrontal Cortex. The Journal of Neuroscience 2012; 32: 10318.

Moran RJ, Campo P, Symmonds M, Stephan KE, Dolan RJ, Friston KJ. Free Energy, Precision and Learning: The Role of Cholinergic Neuromodulation. J Neurosci 2013; 33: 8227–36.

Moretti R, Torre P, Antonello RM, Cazzato G, Griggio S, Bava A. Olanzapine as a treatment of neuropsychiatric disorders of Alzheimer's disease and other dementias: a 24-month follow-up of 68 patients. Am J Alzheimers Dis Other Demen 2003; 18: 205–14.

Murley AG, Rouse MA, Jones PS, Ye R, Hezemans FH, O'Callaghan C, et al. GABA and glutamate deficits from frontotemporal lobar degeneration are associated with disinhibition [Internet]. Brain[cited 2020 Nov 26] Available from: https://academic.oup.com/brain/advance-article/doi/10.1093/brain/awaa305/5952714

Murley AG, Rowe JB. Neurotransmitter deficits from frontotemporal lobar degeneration. Brain 2018; 141: 1263–85.

Murty VP, LaBar KS, Adcock RA. Distinct medial temporal networks encode surprise during motivation by reward versus punishment. Neurobiology of Learning and Memory 2016; 134: 55–64.

Murty VP, LaBar KS, Adcock RA. Threat of Punishment Motivates Memory Encoding via Amygdala, Not Midbrain, Interactions with the Medial Temporal Lobe. J Neurosci 2012; 32: 8969–76.

Nagaoka S, Arai H, Iwamoto N, Ohwada J, Ichimiya Y, Nakamura M, et al. A juvenile case of frontotemporal dementia: neurochemical and neuropathological investigations. Prog Neuropsychopharmacol Biol Psychiatry 1995; 19: 1251–61.

Narmour E. The analysis and cognition of basic melodic structures: The implication-realization model. Chicago, IL, US: University of Chicago Press; 1990

Niv Y, Edlund JA, Dayan P, O'Doherty JP. Neural Prediction Errors Reveal a Risk-Sensitive Reinforcement-Learning Process in the Human Brain. J Neurosci 2012; 32: 551–62.

O'Callaghan C, Hornberger M. Towards a neurocomputational account of social dysfunction in neurodegenerative disease. Brain 2017; 140: e14.

O'Doherty JP, Dayan P, Friston K, Critchley H, Dolan RJ. Temporal Difference Models and Reward-Related Learning in the Human Brain. Neuron 2003; 38: 329–37.

Oliver LD, Mitchell DGV, Dziobek I, MacKinley J, Coleman K, Rankin KP, et al. Parsing cognitive and emotional empathy deficits for negative and positive stimuli in frontotemporal dementia. Neuropsychologia 2015; 67: 14–26.

Omigie D, Pearce M, Lehongre K, Hasboun D, Navarro V, Adam C, et al. Intracranial Recordings and Computational Modeling of Music Reveal the Time Course of Prediction Error Signaling in Frontal and Temporal Cortices. Journal of Cognitive Neuroscience 2019; 31: 855–73.

Omigie D, Pearce MT, Stewart L. Tracking of pitch probabilities in congenital amusia. Neuropsychologia 2012; 50: 1483–93.

Omigie D, Pearce MT, Williamson VJ, Stewart L. Electrophysiological correlates of melodic processing in congenital amusia. Neuropsychologia 2013; 51: 1749–62.

Overath T, Cusack R, Kumar S, Kriegstein K von, Warren JD, Grube M, et al. An Information Theoretic Characterisation of Auditory Encoding. PLOS Biology 2007; 5: e288.

Palminteri S, Justo D, Jauffret C, Pavlicek B, Dauta A, Delmaire C, et al. Critical Roles for Anterior Insula and Dorsal Striatum in Punishment-Based Avoidance Learning. Neuron 2012; 76: 998–1009.

Palminteri S, Lebreton M, Worbe Y, Grabli D, Hartmann A, Pessiglione M. Pharmacological modulation of subliminal learning in Parkinson's and Tourette's syndromes. Proc Natl Acad Sci U S A 2009; 106: 19179–84.

Patterson RD, Uppenkamp S, Johnsrude IS, Griffiths TD. The processing of temporal pitch and melody information in auditory cortex. Neuron 2002; 36: 767–76.

Pearce M, Müllensiefen D. Compression-based Modelling of Musical Similarity Perception. Journal of New Music Research 2017; 46: 135–55.

Pearce MT, Ruiz MH, Kapasi S, Wiggins GA, Bhattacharya J. Unsupervised statistical learning underpins computational, behavioural, and neural manifestations of musical expectation. NeuroImage 2010; 50: 302–13.

Pearce MT, Wiggins GA. Auditory expectation: the information dynamics of music perception and cognition. Top Cogn Sci 2012; 4: 625–52.

Pearce MT. The construction and evaluation of statistical models of melodic structure in music perception and composition [Internet]. 2005[cited 2020 Sep 3] Available from: https://openaccess.city.ac.uk/id/eprint/8459/

Peraita H, Díaz C, Anllo-Vento L. Processing of semantic relations in normal aging and Alzheimer's disease. Arch Clin Neuropsychol 2008; 23: 33–46.

Perry DC, Datta S, Sturm VE, Wood KA, Zakrzewski J, Seeley WW, et al. Reward deficits in behavioural variant frontotemporal dementia include insensitivity to negative stimuli. Brain 2017; 140: 3346–56.

Perry DC, Kramer JH. Reward processing in neurodegenerative disease. Neurocase 2015; 21: 120–33.

Perry DC, Sturm VE, Wood KA, Miller BL, Kramer JH. Divergent processing of monetary and social reward in behavioral variant frontotemporal dementia and Alzheimer's disease. Alzheimer Dis Assoc Disord 2015; 29: 161–4.

Pessiglione M, Delgado MR. The good, the bad and the brain: Neural correlates of appetitive and aversive values underlying decision making. Curr Opin Behav Sci 2015; 5: 78–84.

Pessiglione M, Seymour B, Flandin G, Dolan RJ, Frith CD. Dopamine-dependent prediction errors underpin reward-seeking behaviour in humans. Nature 2006; 442: 1042–5.

Pessiglione M, Vinckier F, Bouret S, Daunizeau J, Le Bouc R. Why not try harder? Computational approach to motivation deficits in neuro-psychiatric diseases. Brain 2018; 141: 629–50.

Platel H, Baron J-C, Desgranges B, Bernard F, Eustache F. Semantic and episodic memory of music are subserved by distinct neural networks. Neuroimage 2003; 20: 244–56.

Pressman PS, Simpson M, Gola K, Shdo SM, Spinelli EG, Miller BL, et al. Observing conversational laughter in frontotemporal dementia. J Neurol Neurosurg Psychiatry 2017; 88: 418–24.

Pulcu E, Browning M. Affective bias as a rational response to the statistics of rewards and punishments. eLife 2017; 6: e27879.

Pulcu E. A nonlinear relationship between prediction errors and learning rates in human reinforcement learning. bioRxiv 2019: 751222.

Quiroga-Martinez DR, Hansen NC, Højlund A, Pearce M, Brattico E, Vuust P. Decomposing neural responses to melodic surprise in musicians and non-musicians: Evidence for a hierarchy of predictions in the auditory system. Neuroimage 2020; 215: 116816.

Quiroga-Martinez DR, Hansen NC, Højlund A, Pearce MT, Brattico E, Vuust P. Reduced prediction error responses in high-as compared to low-uncertainty musical contexts. Cortex 2019; 120: 181–200.

Rahman S, Robbins TW, Hodges JR, Mehta MA, Nestor PJ, Clark L, et al. Methylphenidate ('Ritalin') can ameliorate abnormal risk-taking behavior in the frontal variant of frontotemporal dementia. Neuropsychopharmacology 2006; 31: 651–8.

Rahman S, Sahakian BJ, Hodges JR, Rogers RD, Robbins TW. Specific cognitive deficits in mild frontal variant frontotemporal dementia. Brain 1999; 122 (Pt 8): 1469–93.

Raichle ME. The Brain's Default Mode Network. Annual Review of Neuroscience 2015; 38: 433–47.

Ramanan S, Bertoux M, Flanagan E, Irish M, Piguet O, Hodges JR, et al. Longitudinal Executive Function and Episodic Memory Profiles in Behavioral-Variant Frontotemporal Dementia and Alzheimer's Disease. Journal of the International Neuropsychological Society 2017; 23: 34–43.

Rascovsky K, Grossman M. Clinical diagnostic criteria and classification controversies in frontotemporal lobar degeneration. Int Rev Psychiatry 2013; 25: 145–58.

Reichelt AC, Killcross S, Wilkinson LS, Humby T, Good MA. Transgenic expression of the FTDP-17 tauV337M mutation in brain dissociates components of executive function in mice. Neurobiol Learn Mem 2013; 104: 73–81.

Ridgway GR, Henley SMD, Rohrer JD, Scahill RI, Warren JD, Fox NC. Ten simple rules for reporting voxel-based morphometry studies. Neuroimage 2008; 40: 1429–35.

Rinne JO, Laine M, Kaasinen V, Norvasuo-Heilä MK, Någren K, Helenius H. Striatal dopamine transporter and extrapyramidal symptoms in frontotemporal dementia. Neurology 2002; 58: 1489–93.

Rohrer JD, Sauter D, Scott S, Rossor MN, Warren JD. Receptive prosody in nonfluent primary progressive aphasias. Cortex 2012; 48: 308–16.

Rohrer JD, Warren JD. Phenomenology and anatomy of abnormal behaviours in primary progressive aphasia. J Neurol Sci 2010; 293: 35–8.

Rowe JB, Hughes L, Ghosh BCP, Eckstein D, Williams-Gray CH, Fallon S, et al. Parkinson's disease and dopaminergic therapy--differential effects on movement, reward and cognition. Brain 2008; 131: 2094–105.

Russ MO, Mack W, Grama C-R, Lanfermann H, Knopf M. Enactment effect in memory: evidence concerning the function of the supramarginal gyrus. Exp Brain Res 2003; 149: 497–504.

Rutledge RB, Lazzaro SC, Lau B, Myers CE, Gluck MA, Glimcher PW. Dopaminergic drugs modulate learning rates and perseveration in Parkinson's patients in a dynamic foraging task. J Neurosci 2009; 29: 15104–14.

Ruzzoli M, Pirulli C, Mazza V, Miniussi C, Brignani D. The mismatch negativity as an index of cognitive decline for the early detection of Alzheimer's disease. Sci Rep 2016; 6: 33167.

Salimpoor VN, Benovoy M, Larcher K, Dagher A, Zatorre RJ. Anatomically distinct dopamine release during anticipation and experience of peak emotion to music. Nature Neuroscience 2011; 14: 257.

Salimpoor VN, Benovoy M, Longo G, Cooperstock JR, Zatorre RJ. The Rewarding Aspects of Music Listening Are Related to Degree of Emotional Arousal. PLOS ONE 2009; 4: e7487.

Salimpoor VN, Bosch I van den, Kovacevic N, McIntosh AR, Dagher A, Zatorre RJ. Interactions Between the Nucleus Accumbens and Auditory Cortices Predict Music Reward Value. Science 2013; 340: 216–9.

Salimpoor VN, Zald DH, Zatorre RJ, Dagher A, McIntosh AR. Predictions and the brain: how musical sounds become rewarding. Trends in Cognitive Sciences 2015; 19: 86–91.

Sammler D, Grosbras M-H, Anwander A, Bestelmeyer PEG, Belin P. Dorsal and Ventral Pathways for Prosody. Current Biology 2015; 25: 3079–85.

Sammler D, Koelsch S, Ball T, Brandt A, Grigutsch M, Huppertz H-J, et al. Co-localizing linguistic and musical syntax with intracranial EEG. NeuroImage 2013; 64: 134–46.

Samuels ER, Szabadi E. Functional Neuroanatomy of the Noradrenergic Locus Coeruleus: Its Roles in the Regulation of Arousal and Autonomic Function Part I: Principles of Functional Organisation. Curr Neuropharmacol 2008; 6: 235–53.

Sander D, Grafman J, Zalla T. The human amygdala: an evolved system for relevance detection. Rev Neurosci 2003; 14: 303–16.

Sauvé SA, Sayed A, Dean RT, Pearce MT. Effects of pitch and timing expectancy on musical emotion. Psychomusicology: Music, Mind, and Brain 2018; 28: 17–39.

Schaeverbeke J, Evenepoel C, Bruffaerts R, Van Laere K, Bormans G, Dries E, et al. Cholinergic depletion and basal forebrain volume in primary progressive aphasia. Neuroimage Clin 2017; 13: 271–9.

Schapiro AC, Gregory E, Landau B, McCloskey M, Turk-Browne NB. The necessity of the medial temporal lobe for statistical learning. J Cogn Neurosci 2014; 26: 1736–47.

Schellenberg EG. Simplifying the Implication-Realization Model of Melodic Expectancy. Music Perception: An Interdisciplinary Journal 1997; 14: 295–318.

Schultz W. Dopamine reward prediction error coding. Dialogues Clin Neurosci 2016; 18: 23–32.

Schurz M, Kronbichler M, Weissengruber S, Surtees A, Samson D, Perner J. Clarifying the role of theory of mind areas during visual perspective taking: Issues of spontaneity and domain-specificity. NeuroImage 2015; 117: 386–96.

Schurz M, Radua J, Aichhorn M, Richlan F, Perner J. Fractionating theory of mind: a meta-analysis of functional brain imaging studies. Neurosci Biobehav Rev 2014; 42: 9–34.

Schwarze U, Bingel U, Sommer T. Event-Related Nociceptive Arousal Enhances Memory Consolidation for Neutral Scenes. J Neurosci 2012; 32: 1481–7.

Sestieri C, Corbetta M, Romani GL, Shulman GL. Episodic memory retrieval, parietal cortex, and the default mode network: functional and topographic analyses. J Neurosci 2011; 31: 4407–20.

Shaw AD, Hughes LE, Moran R, Coyle-Gilchrist I, Rittman T, Rowe JB. In Vivo Assay of Cortical Microcircuitry in Frontotemporal Dementia: A Platform for Experimental Medicine Studies. Cereb Cortex 2019

Sikka R, Cuddy LL, Johnsrude IS, Vanstone AD. An fMRI comparison of neural activity associated with recognition of familiar melodies in younger and older adults. Front Neurosci 2015; 9: 356.

Silani G, Lamm C, Ruff CC, Singer T. Right Supramarginal Gyrus Is Crucial to Overcome Emotional Egocentricity Bias in Social Judgments. J Neurosci 2013; 33: 15466–76.

Siman-Tov T, Granot RY, Shany O, Singer N, Hendler T, Gordon CR. Is there a prediction network? Meta-analytic evidence for a cortical-subcortical network likely subserving prediction. Neuroscience & Biobehavioral Reviews 2019; 105: 262–75.

Sivasathiaseelan H, Marshall CR, Agustus JL, Benhamou E, Bond RL, Leeuwen JEP van, et al. Frontotemporal Dementia: A Clinical Review. Semin Neurol 2019; 39: 251–63.

Slachevsky A, Villalpando JM, Sarazin M, Hahn-Barma V, Pillon B, Dubois B. Frontal assessment battery and differential diagnosis of frontotemporal dementia and Alzheimer disease. Arch Neurol 2004; 61: 1104–7.

Slattery CF, Agustus JL, Paterson RW, McCallion O, Foulkes AJM, Macpherson K, et al. The functional neuroanatomy of musical memory in Alzheimer's disease. Cortex 2019; 115: 357–70.

Small DM. Taste representation in the human insula. Brain Struct Funct 2010; 214: 551–61.

Snowden JS, Bathgate D, Varma A, Blackshaw A, Gibbons ZC, Neary D. Distinct behavioural profiles in frontotemporal dementia and semantic dementia. J Neurol Neurosurg Psychiatry 2001; 70: 323–32.

Steinbeis N, Koelsch S, Sloboda JA. The Role of Harmonic Expectancy Violations in Musical Emotions: Evidence from Subjective, Physiological, and Neural Responses. Journal of Cognitive Neuroscience 2006; 18: 1380–93.

Stewart L, Overath T, Warren JD, Foxton JM, Griffiths TD. fMRI Evidence for a Cortical Hierarchy of Pitch Pattern Processing. PLOS ONE 2008; 3: e1470.

Strenziok M, Pulaski S, Krueger F, Zamboni G, Clawson D, Grafman J. Regional Brain Atrophy and Impaired Decision Making on the Balloon Analog Risk Task in Behavioral Variant Frontotemporal Dementia: Cognitive and Behavioral Neurology 2011; 24: 59–67.

Sutton RS, Barto AG. Reinforcement Learning: An Introduction. MIT Press; 2018

Suzuki Y, Minami T, Nakauchi S. Association between pupil dilation and implicit processing prior to object recognition via insight [Internet]. Sci Rep 2018; 8[cited 2020 Nov 1] Available from: https://www.ncbi.nlm.nih.gov/pmc/articles/PMC5931995/

Tillmann B, Bigand E. Musical structure processing after repeated listening: Schematic expectations resist veridical expectations: [Internet]. Musicae Scientiae 2010[cited 2020 Sep 1] Available from: https://journals.sagepub.com/doi/10.1177/10298649100140S204

Tillmann B, Janata P, Birk J, Bharucha JJ. Tonal centers and expectancy: facilitation or inhibition of chords at the top of the harmonic hierarchy? J Exp Psychol Hum Percept Perform 2008; 34: 1031–43.

Tillmann B, Koelsch S, Escoffier N, Bigand E, Lalitte P, Friederici AD, et al. Cognitive priming in sung and instrumental music: activation of inferior frontal cortex. Neuroimage 2006; 31: 1771–82.

Torralva T, Kipps CM, Hodges JR, Clark L, Bekinschtein T, Roca M, et al. The relationship between affective decision-making and theory of mind in the frontal variant of fronto-temporal dementia. Neuropsychologia 2007; 45: 342–9.

Tsai C-G, Chen C-P. Musical Tension over Time: Listeners' Physiological Responses to the 'Retransition' in Classical Sonata Form. Journal of New Music Research 2015; 44: 271–86.

Tsai C-G, Chou T-L, Li C-W. Roles of posterior parietal and dorsal premotor cortices in relative pitch processing: Comparing musical intervals to lexical tones. Neuropsychologia 2018; 119: 118–27.

Turk-Browne NB, Scholl BJ, Chun MM, Johnson MK. Neural Evidence of Statistical Learning: Efficient Detection of Visual Regularities Without Awareness. J Cogn Neurosci 2009; 21: 1934–45.

Turk-Browne NB. Statistical learning and its consequences. Nebr Symp Motiv 2012; 59: 117–46.

Tversky A, Simonson I. Context-Dependent Preferences. Management Science 1993; 39: 1179–89.

Ullsperger M, Cramon DY von. Error Monitoring Using External Feedback: Specific Roles of the Habenular Complex, the Reward System, and the Cingulate Motor Area Revealed by Functional Magnetic Resonance Imaging. J Neurosci 2003; 23: 4308–14.

Van den Stock J, Stam D, De Winter F-L, Mantini D, Szmrecsanyi B, Van Laere K, et al. Moral processing deficit in behavioral variant frontotemporal dementia is associated with facial emotion recognition and brain changes in default mode and salience network areas. Brain Behav 2017; 7: e00843.

Voon V, Gao J, Brezing C, Symmonds M, Ekanayake V, Fernandez H, et al. Dopamine agonists and risk: impulse control disorders in Parkinson's; disease. Brain 2011; 134: 1438–46.

Wang C-A, Blohm G, Huang J, Boehnke SE, Munoz DP. Multisensory integration in orienting behavior: Pupil size, microsaccades, and saccades. Biol Psychol 2017; 129: 36–44.

Wang C-A, Munoz DP. A circuit for pupil orienting responses: implications for cognitive modulation of pupil size. Current Opinion in Neurobiology 2015; 33: 134–40.

Warren JD, Rohrer JD, Rossor MN. Frontotemporal dementia [Internet]. BMJ 2013; 347[cited 2017 Nov 30] Available from: https://www.ncbi.nlm.nih.gov/pmc/articles/PMC3735339/

Warren JE, Sauter DA, Eisner F, Wiland J, Dresner MA, Wise RJS, et al. Positive Emotions Preferentially Engage an Auditory–Motor "Mirror" System. J Neurosci 2006; 26: 13067–75.

Warrier CM, Zatorre RJ. Right temporal cortex is critical for utilization of melodic contextual cues in a pitch constancy task. Brain 2004; 127: 1616–25.

Wiesmann CG, Friederici AD, Singer T, Steinbeis N. Two systems for thinking about others' thoughts in the developing brain. PNAS 2020; 117: 6928–35.

Wilson RC, Collins AG. Ten simple rules for the computational modeling of behavioral data [Internet]. eLife; 8[cited 2020 Nov 26] Available from: https://www.ncbi.nlm.nih.gov/pmc/articles/PMC6879303/

Wright ND, Symmonds M, Hodgson K, Fitzgerald THB, Crawford B, Dolan RJ. Approach–Avoidance Processes Contribute to Dissociable Impacts of Risk and Loss on Choice. J Neurosci 2012; 32: 7009–20.

Yonelinas AP. The hippocampus supports high-resolution binding in the service of perception, working memory and long-term memory. Behav Brain Res 2013; 254: 34–44.

Zahn R, Moll J, Paiva M, Garrido G, Krueger F, Huey ED, et al. The neural basis of human social values: evidence from functional MRI. Cereb Cortex 2009; 19: 276–83.

Zaki J. Empathy: A motivated account. Psychological Bulletin 2014; 140: 1608–47.

Zatorre RJ, Halpern AR, Bouffard M. Mental reversal of imagined melodies: a role for the posterior parietal cortex. J Cogn Neurosci 2010; 22: 775–89.

Zatorre RJ, Salimpoor VN. From perception to pleasure: Music and its neural substrates. Proc Natl Acad Sci U S A 2013; 110: 10430–7.

Zénon A. Eye pupil signals information gain [Internet]. Proc Biol Sci 2019; 286[cited 2020 Aug 17] Available from: https://www.ncbi.nlm.nih.gov/pmc/articles/PMC6784722/

Zhang L, Lengersdorff L, Mikus N, Gläscher J, Lamm C. Using reinforcement learning models in social neuroscience: frameworks, pitfalls and suggestions of best practices. Soc Cogn Affect Neurosci 2020; 15: 695–707.

Zhao S, Chait M, Dick F, Dayan P, Furukawa S, Liao H-I. Pupil-linked phasic arousal evoked by violation but not emergence of regularity within rapid sound sequences. Nat Commun 2019; 10: 4030.

Appendix

Appendix 1: Diagnostic criteria for AD

Supplementary Table 1. Revised NINCDS–ADRDA diagnostic criteria for AD (Dubois et al., 2007)

Level of diagnosis	Criteria
I. Probable AD	A plus one or more of the following behavioural/cognitive symptoms (B–E) must be present to meet criteria: A. Presence of an early and significant episodic memory impairment that includes the following features: A.1 Gradual and progressive change in memory function reported by patients or informants over more than 6 months A.2 Objective evidence of significantly impaired episodic memory on testing A.3. The episodic memory impairment can be isolated or associated with other cognitive changes at the onset of AD or as AD advances B. Presence of medial temporal lobe atrophy C. Abnormal cerebrospinal fluid biomarker D. Specific pattern on functional neuroimaging with PET E. Proven AD autosomal dominant mutation within the immediate family
II. Exclusionary Criteria for AD	A. History • Sudden onset • Early occurrence of the following symptoms: gait disturbances, seizures B. Clinical features • Focal neurological features including hemiparesis, sensory loss, visual field deficits • Early extrapyramidal signs C. Other medical disorders severe enough to account for memory and related symptoms • Non-AD dementia • Major depression • Cerebrovascular disease • Toxic and metabolic abnormalities, all of which may require specific investigations • MRI FLAIR or T2 signal abnormalities in the medial temporal lobe that are consistent with infectious or vascular insults
III. Criteria for definite AD	A. Clinical (A) and histopathological post-mortem evidence; criteria must both be present B. Clinical (A) and genetic evidence (mutation on chromosome 1, 14, or 21) of AD; criteria must both be present

Appendix 2: Diagnostic criteria for bvFTD

Supplementary Table 2. Rascovsky diagnostic criteria for bvFTD (Rascovsky and Grossman, 2013)

Level of diagnosis	Criteria
I. Neurodegenerative disease	Shows progressive deterioration of behavior and /or cognition by observation or history (as provided by a knowledgeable informant)
II. Possible bvFTD	Three of the following behavioural/cognitive symptoms (A–F) must be present to meet criteria: A. Early behavioural disinhibition (one of the following must be present): A.1 Socially inappropriate behavior A.2 Loss of manners or decorum A.3 Impulsive, rash or careless actions B. Early apathy or inertia (one of the following must be present): B.1 Apathy B.2 Inertia C. Early loss of sympathy or empathy (one of the following must be present): C.1 Diminished response to other people's needs and feelings C.2 Diminished social interest, interrelatedness or personal warmth D. Early perseverative, stereotyped or compulsive/ritualistic behavior (one of the following must be present): D.1 Simple repetitive movements D.2 Complex, compulsive or ritualistic behaviours D.3 Stereotypy of speech E. Hyperorality and dietary changes (one of the following must be present): E.1 Altered food preferences E.2 Binge eating, increased consumption of alcohol or cigarettes E.3 Oral exploration or consumption of inedible objects F. Neuropsychological profile: executive/generation deficits with relative sparing of memory and visuospatial functions (all of the following must be present): F1. Deficits in executive tasks F2. Relative sparing of episodic memory F3. Relative sparing of visuospatial skills
III. Probable bvFTD	All of the following symptoms (A–C) must be present to meet criteria: A. Meets criteria for possible bvFTD B. Exhibits significant functional decline (by caregiver report or as evidenced by Clinical Dementia Rating Scale or Functional Activities Questionnaire scores) C. Imaging results consistent with bvFTD (one of the following must be present): C.1 Frontal and/or anterior temporal atrophy on MRI or CT C.2 Frontal and/or anterior temporal hypoperfusion or hypometabolism on PET or SPECT
IV. Behavioural variant FTD with definite FTLD pathology	Criterion A and either criterion B or C must be present to meet the criteria: A. Meets criteria for possible or probable bvFTD B. Histopathological evidence of FTLD on biopsy or at post-mortem C. Presence of a known pathogenic mutation
V. Exclusionary criteria for bvFTD	Criteria A and B must be answered negatively for any bvFTD diagnosis. Criterion C can be positive for possible bvFTD but must be negative for probable bvFTD: A. Pattern of deficits is better accounted for by other non-degenerative nervous system or medical disorders B. Behavioural disturbance is better accounted for by a psychiatric diagnosis C. Biomarkers strongly indicative of Alzheimer's disease or other neurodegenerative process

Appendix 3: Diagnostic criteria for svPPA and nfvPPA

Supplementary Table 3. Gorno-Tempini diagnostic criteria for svPPA and nfvPPA (Gorno-Tempini et al., 2011)

Level Diagnosis	nfvPPA	svPPA	lvPPA
I. Clinical	At least one of:	Both of:	Both of:
II. Core Features	1. Agrammatism in language production 2. Effortful, halting speech with inconsistent speech sound error and distortions (apraxia of speech)	1. Impaired confrontation naming 2. Impaired single-word comprehension	1. Impaired single-word retrieval in spontaneous speech and naming 2. Impaired repetition of sentences and phrases
III. Other Features	At least two of:	At least three of:	At least three of:
	1. Impaired comprehension of syntactically complex sentences 2. Spared single-word comprehension 3. Spared object knowledge	1. Impaired object knowledge, particularly for low-frequency or low-familiarity items 2. Surface dyslexia or dysgraphia 3. Spared repetition 4. Spared speech production (grammar and motor speech)	1. Speech (phonological) errors in spontaneous speech and naming 2. Spared single-word comprehension 3. Spared motor speech 4. Absence of frank agrammatism
IV. Imaging Supported	One or more of:	One or more of:	One or more of:
	1. Predominant left posterior fronto-insular atrophy on MRI 2. Predominant left posterior fronto-insular hypoperfusion or hypometabolism on SPECT or PET	1. Predominant anterior temporal lobe atrophy 2. Predominant anterior temporal hypoperfusion or hypometabolism on SPECT or PET	1. Predominant left posterior perisylvian or parietal atrophy on MRI 2. Predominant left posterior perisylvian or parietal hypoperfusion or hypometabolism on SPECT or PET
V. Pathologically Definite	Criterion I and II (above) or III (below)		
	1. Histopathological evidence of a specific neurodegenerative pathology (e.g. FTLD-tau, FTLD-TDP, AD, other) 2. Presence of a known pathogenic mutation		

Appendix 4: Musical background questionnaire (Hailstone et al., 2009)

Music Questionnaire

Name: _____

D.O.B. _____ **Age:** _____

Date of Test: _____

1. Have you ever had any musical training (music lessons at school, lessons on an instrument, etc)? YES/NO

1a. If Yes, what kind and for how long?
_____
_____

2. Have you ever played a musical instrument? YES/NO
If No, skip to question 6.

3. If Yes, which instrument(s)?
_____
_____
3a. How long did you play it (them) for?
_____
_____

3b. What standard did you reach (grade, etc)?
_____

4. Do you still play an instrument regularly? YES/NO
If No, skip to question 6.

5. If Yes, which instrument?

5a. Approx how many hours per week do you play?
_____

5b. Where do you play (at home, band, orchestra, etc)?
_____

6. Do you listen to music regularly? YES/NO

7. If Yes, approximately how many hours per week do you listen to music?
_____

8. What kind of music do you mainly listen to (pop, easy listening, jazz, classical, etc)?
_____
_____

9. Are you able to recognise a familiar tune without the help of the lyrics? YES/NO

10. Can you tell if you sing in tune? YES/NO

Appendix 5: Revised Barcelona Music Reward Questionnaire (BMRQ) (Mas-Herrero et al., 2013)

BARCELONA MUSIC REWARD QUESTIONNAIRE

1. S/he likes to listen to very tuneful music.

Completely disagree	Disagree	Either agree nor disagree	Agree	Completely agree
1	2	3	4	5

2. S/he likes to listen to very emotional music.

Completely disagree	Disagree	Either agree nor disagree	Agree	Completely agree
1	2	3	4	5

3. S/he doesn't like to dance, not even with music s/he likes.

Completely disagree	Disagree	Either agree nor disagree	Agree	Completely agree
1	2	3	4	5

4. S/he gets strong emotional reactions when listening to certain pieces of music (tears, laughs).

Completely disagree	Disagree	Either agree nor disagree	Agree	Completely agree
1	2	3	4	5

5. Music calms and relaxes him/her.

Completely disagree	Disagree	Either agree nor disagree	Agree	Completely agree
1	2	3	4	5

6. Music often makes him/her dance and/or sing.

Completely disagree	Disagree	Either agree nor disagree	Agree	Completely agree
1	2	3	4	5

7. S/he is very receptive to new music s/he is not familiar with.

Completely disagree	Disagree	Either agree nor disagree	Agree	Completely agree
1	2	3	4	5

Appendix 6: Revised Immediate Mood Scaler (Nahum et al. 2017)

MOOD QUESTIONNAIRE

Name:

DRC code:

D.O.B:

Age:

Date of test:

PLEASE CIRCLE THE SCORE THAT BEST CORRESPONDS TO YOUR CURRENT MOOD:

RELAXED	**1**	**2**	**3**	**4**	**5**	**ANXIOUS**
BORED	**1**	**2**	**3**	**4**	**5**	**INTERESTED**
SLEEPY	**1**	**2**	**3**	**4**	**5**	**ALERT**
SAD	**1**	**2**	**3**	**4**	**5**	**HAPPY**

Adapted from the Immediate Mood Scaler (Nahum et al. 2017)

Appendix 7: Modified Interpersonal Reactivity Index (Davis, 1983)

MODIFIED INTERPERSONAL REACTIVITY INDEX

Indicate how well each statement describes the subject's CURRENT behaviour. There are no right or wrong answers. We just want to get your impression of how you think the subject typically behaves.

		Does NOT describe well	←		→	Describes VERY well
1	The subject shows tender, concerned feelings for people less fortunate than him/her	1	2	3	4	5
2	The subject sometimes finds it difficult to see things from the "other person's" point of view	1	2	3	4	5
3	Sometimes the subject does NOT feel very sorry for other people when they are having problems	1	2	3	4	5
4	The subject tries to look at everybody's side of a disagreement before he/she makes a decision	1	2	3	4	5
5	If the subject sees somebody being taken advantage of, the subject feels kind of protective towards him/her	1	2	3	4	5
6	The subject is likely to try to understand others better by imagining how things look from their perspective	1	2	3	4	5
7	Other people's misfortunes do NOT usually disturb the subject a great deal	1	2	3	4	5
8	If the subject is sure he/she is right about something, he/she doesn't waste much time listening to other people's arguments	1	2	3	4	5
9	If the subject sees someone being treated unfairly, the subject doesn't feel much pity for him/her	1	2	3	4	5
10	The subject is often quite touched by things he/she sees happen	1	2	3	4	5
11	The subject believes that there are two sides to every question and tries to look at both of them	1	2	3	4	5
12	I would describe the subject as a pretty soft-hearted person	1	2	3	4	5
13	If the subject is upset at someone, the subject usually tries to put him/herself "in the other person's" shows for a while	1	2	3	4	5
14	Before criticizing me, the subject is likely to imagine how he/she would feel if he/she were in my place	1	2	3	4	5

Appendix 8: Audio files

Supplementary Table 4. Description of audio files

Track No.	File Name	Description
Chapters 3 and 4		
1	Audio file 3.1	No deviant *Symphony No 40 (Mozart)*
2	Audio file 3.2	Acoustic deviant *Twelve days of Christmas*
3	Audio file 3.3	Syntactic deviant *Für Elise (Beethoven)*
4	Audio file 3.4	Semantic deviant *God Save the Queen*
Chapter 5 and 6		
5	Audio file 5.1	'reward': expected consonant target chord *C major*
6	Audio file 5.2	'punishment': unexpected dissonant target chord *C major*
7	Audio file 5.3	'reward': expected consonant target chord *C minor*
8	Audio file 5.4	'punishment': unexpected dissonant target chord *C minor*

Appendix 9: Pilot study for Chapters 5 and 6

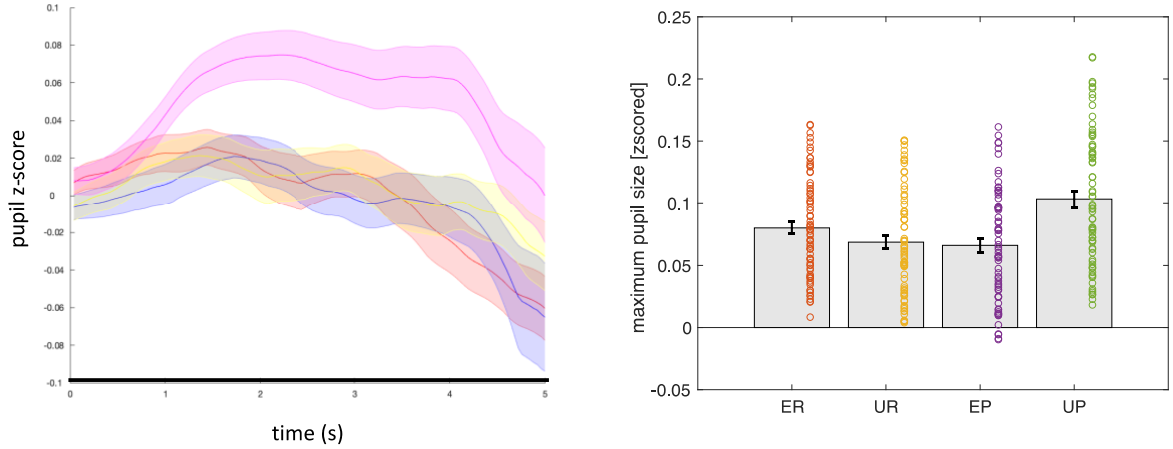

Supplementary Figure 1. Results of pilot study for Chapters 5 and 6. Eight young healthy individuals took part in this pilot study, aged 22 to 34 years old. Participants had to fixate a cross in the centre of the monitor screen while listening to a set of 120 musical stimuli played in randomized order. Pupil diameter was continuously measured (details in Methods chapter 2). From this set, four categories of stimuli were presented (30 trials per category): 'expected reward' (ER), comprising chord progressions with consonant target chords that resolved the progression (using a perfect or imperfect cadence); 'unexpected punishment'(UP), comprising chord progressions in which the target chord was dissonant; 'expected punishment' (EP) comprising chord progressions in which the three priming chords and the target chord were dissonant; and 'unexpected reward' (UR), comprising dissonant chord progressions in which the target chord was consonant. *Left panel*: Onset of the target chord is at time 0. To generate these pupil time series, trial-by-trial pupil time series from individual participants were first filtered, converted to z-scores based on the signal mean and standard deviation for that participant's dataset and baseline-corrected by subtracting the pre-deviant baseline (one-second interval prior to target chord onset); the plots show the mean normalised pupil time series flanked by error envelopes representing the standard deviation of the group pupillary response, for each experimental condition coded with colours as follows: pink = UP; Blue = UR; Yellow = EP; Red = ER. Right panel: the histograms show maximum pupil size (baseline-corrected and z-scored) extracted from the five seconds following the target chord; red circles are individual trials; error bars indicate standard error of the mean.

Appendix 10: Participant involvement by chapter

		CHAPTER			
ID	GROUP	3	4	5	6
1	Control	✓	✓		
2	Control	✓	✓		
3	Control	✓	✓		
4	Control	✓	✓		
5	Control	✓	✓	✓	✓
6	Control	✓	✓	✓	✓
7	Control	✓	✓		
8	Control	✓	✓		
9	Control	✓	✓	✓	✓
10	Control	✓	✓		
11	Control	✓	✓		
12	Control	✓	✓		
13	Control	✓	✓		
14	Control	✓	✓		
15	Control	✓	✓	✓	✓
16	Control	✓	✓		
17	Control	✓	✓	✓	✓
18	Control	✓	✓		
19	Control	✓	✓		
20	Control	✓	✓		
21	Control	✓	✓	✓	✓
22	Control	✓	✓		
23	Control	✓	✓	✓	✓
24	Control	✓	✓		
25	Control	✓	✓		
26	Control	✓	✓		
27	Control	✓	✓	✓	✓
28	Control	✓	✓	✓	✓
29	Control	✓	✓	✓	✓
30	Control	✓	✓		
31	Control	✓	✓		
32	Control	✓	✓		
33	Control	✓	✓	✓	✓
34	Control			✓	✓
35	Control			✓	✓
36	Control			✓	✓
37	Control			✓	✓
38	Control			✓	✓
39	Control			✓	✓
40	Control			✓	✓
41	Control			✓	✓
42	Control			✓	✓
43	Control			✓	✓
44	Control			✓	✓
45	Control			✓	✓
46	tAD	✓	✓		
47	tAD	✓	✓		
48	tAD	✓	✓		
49	tAD	✓	✓		
50	tAD	✓	✓		
51	tAD	✓	✓		
52	tAD	✓	✓		
53	tAD	✓	✓		
54	tAD	✓	✓		
55	tAD	✓	✓		
56	tAD	✓	✓		

57	tAD	✓	✓		
58	tAD	✓	✓		
59	tAD	✓	✓		
60	tAD	✓	✓		
61	tAD	✓	✓		
62	tAD	✓	✓		
63	tAD	✓	✓		
64	tAD	✓	✓		
65	bvFTD	✓	✓	✓	✓
66	bvFTD	✓	✓	✓	✓
67	bvFTD	✓	✓	✓	✓
68	bvFTD	✓	✓		
69	bvFTD	✓	✓	✓	✓
70	bvFTD	✓	✓	✓	✓
71	bvFTD	✓	✓		
72	bvFTD	✓	✓	✓	✓
73	bvFTD	✓	✓		
74	bvFTD	✓	✓	✓	✓
75	bvFTD	✓	✓	✓	✓
76	bvFTD	✓	✓	✓	✓
77	bvFTD	✓	✓	✓	✓
78	bvFTD	✓	✓		
79	bvFTD	✓	✓	✓	✓
80	bvFTD	✓	✓	✓	✓
81	bvFTD	✓	✓	✓	✓
82	bvFTD	✓	✓	✓	✓
83	bvFTD	✓	✓	✓	✓
84	bvFTD			✓	✓
85	bvFTD			✓	✓
86	bvFTD			✓	✓
87	bvFTD			✓	✓
88	bvFTD			✓	✓
89	svPPA	✓	✓		
90	svPPA	✓	✓		
91	svPPA	✓	✓		
92	svPPA	✓	✓		
93	svPPA	✓	✓		
94	svPPA	✓	✓		
95	svPPA	✓	✓		
96	svPPA	✓	✓		
97	svPPA	✓	✓		
98	svPPA	✓	✓		
99	svPPA	✓	✓		
100	svPPA	✓	✓		
101	nfvPPA	✓	✓		
102	nfvPPA	✓	✓		
103	nfvPPA	✓	✓		
104	nfvPPA	✓	✓		
105	nfvPPA	✓	✓		
106	nfvPPA	✓	✓		
107	nfvPPA	✓	✓		
108	nfvPPA	✓	✓		
109	nfvPPA	✓	✓		
110	nfvPPA	✓	✓		
111	nfvPPA	✓	✓		
112	nfvPPA	✓	✓		

Participants are ordered by group. The empty boxes indicate which patient groups were not recruited to the experimental cohort represented by the column heading. A tick denotes that the participant was recruited to that experimental cohort. ID numbers are not sequential and serve no other purpose than to differentiate between participants and display the extent of overlap between studies.

Appendix 11: Division of labour

The work described in this thesis was conducted by EB with assistance from other researchers based at the Dementia Research Centre (UCL), the Ear Institute, UCL and the Paris Brain Institute (Institut du Cerveau et de la Moelle Epinière). Contributors are detailed below.

Chapter 3: Behavioural, autonomic and neuroanatomical correlates of musical surprise processing

Experimental design: EB, JDW

Construction of tests: EB, JDW

Data collection: EB, HS, CJDH, RLB, LLR, CVG, MRK, JCSJ, AN

Data analysis: EB in consultation with SZ (pupillometry), JMN (statistics)

Chapter 4: Sensitivity to the statistical structure of melodies

Experimental design: EB, JDW

Construction of tests: EB, JDW

Data collection: EB, HS, CJDH, RLB, LLR, CVG, MRK, JCSJ, AN

Data analysis: EB in consultation with SZ (pupillometry), JMN (statistics)

Chapter 5: Musical reward processing in frontotemporal dementia: the exploration-exploitation dilemma

Experimental design: EB, JDW

Construction of tests: EB, JDW

Data collection: EB, HS, MRK, JCSJ, AN, CVG

Data analysis: EB

Chapter 6: Computational modelling of learning dynamics in a musical reinforcement-learning paradigm

Experimental design: EB, JDW

Construction of tests: EB

Data collection: EB, HS, MRK, JCSJ, AN, CVG

Data analysis: EB in consultation with AW (VBA toolbox)

Appendix 12: Publications

Publications arising as a direct result of the work conducted in this thesis

Chapter 4 - Disorders of music processing in dementia. In: Cuddy LL, Belleville S, Moussard A, editor(s). Music and the Aging Brain. Academic Press; 2020. p. 107–49
Benhamou E. *& Warren J D.*

Decoding expectation and surprise in dementia: the paradigm of music, *Brain communications, under review*
Benhamou E., *Zhao S., Sivasathiaseelan H., Russell LL., Johnson JCS., Rekena-Komuro MC., Bond RL., Hardy CJD., Rohrer JD., Warren JD*

Reward processing deficits in behavioural variant frontotemporal dementia: a musical reinforcement learning paradigm, *in preparation*
Benhamou E., *Wiehler A., Johnson JCS., Rekena-Komuro MC., Sivasathiaseelan H., Russell LL, Bond RL., Hardy CJD., Rohrer JD., Warren JD.*

Other substantial contributions

The critical circuit architecture of semantic memory: spectral dynamic causal modelling of a neurodegenerative proteinopathy, *Scientific Reports, 2020*
Benhamou E., *Marshall CR., Russell LL., Hardy CJD., Bond RL., Sivasathiaseelan H., Friston KJ., Rohrer JD., Warren JD., Razi A.*

Processing of degraded speech in brain disorders, *Neuroscience and Biobehavioral Reviews, in press*
Jiang J., ***Benhamou E.,*** *Johnson JCS., Warren JD., Hardy CJD.*

Impaired phonemic discrimination in logopenic variant primary progressive aphasia. *Ann Clin Transl Neurol (2020)*
Johnson JCS., Jiang J., Bond RL., ***Benhamou E.,*** *Requena-Komuro M., Russell L.L, Nelson A., Sivasathiaseelan H., Marshall CR., Volmer AP., Rohrer JD., Warren JD., Hardy CJD.*

Altered time awareness in dementia: clinical features and brain substrates, *Front Neurol (2020)*
Rekena-Komuro MC., Marshall CR., Bond RL., Russell LL., Greaves C., Moore KM., Agustus JL., ***Benhamou E.,*** *Sivasathiaseelan H., Hardy CJD., Rohrer JD., Warren JD.*

Rapid ocular responses are a robust marker for bottom-up driven auditory salience. *Journal of Neuroscience (2019)*
Zhao S., Yum NG., Benjamin L., ***Benhamou E.,*** *Furukawa S., Dick F., Slaney M., Chait M.*

Frontotemporal Dementia: A Clinical Review. *Semin Neurol* (2019)
Sivasathiaseelan H., Marshall CR., Agustus JL., ***Benhamou E.,*** *Bond RL. Leeuwen JEP., Hardy CJD., Rohrer JD, Warren JD.*

Findings of Impaired Hearing in Patients with Nonfluent/Agrammatic Variant Primary Progressive Aphasia. *JAMA Neurol* (2019).
Hardy CJD., Frost C., Johnson JCS., Sivasathiaseelan H., Agustus JL., Bond RL., ***Benhamou E.,*** *Russell LL., Marshall CR., Rohrer JD., Bamiou DE., Warren JD.*

Melody Processing Characterizes Functional Neuroanatomy in the Aging Brain. *Front. Neurosci. (2018).*
Agustus JL., Golden HL., Callaghan MF., Bond RL., ***Benhamou E.,*** *Hailstone JC., Weiskopf N, Warren JD.*